Spring 2015

Investigation of the Potential for Algaenan to Produce Hydrocarbon Based Fuels From Algae by Hydrous Pyrolysis

Wassim Adel Obeid
Old Dominion University

INVESTIGATION OF THE POTENTIAL FOR ALGAENAN TO PRODUCE HYDROCARBON BASED FUELS FROM ALGAE BY HYDROUS PYROLYSIS

by

Wassim Adel Obeid
B.S. Chemistry, June 2008, American University of Beirut, Lebanon

A Dissertation Submitted to the Faculty of
Old Dominion University in Partial Fulfillment of the
Requirements for the degree of

DOCTOR OF PHILOSOPHY

CHEMISTRY

OLD DOMINION UNIVERSITY
May 2015

Approved By:

Patrick G. Hatcher (Director)

Sandeep Kumar (Member)

Thomas Isenhour (Member)

James Lee (Member)

ABSTRACT

INVESTIGATION OF THE POTENTIAL FOR ALGAENAN TO PRODUCE HYDROCARBON BASED FUELS FROM ALGAE BY HYDROUS PYROLYSIS

Wassim Adel Obeid
Old Dominion University, 2015
Director: Dr. Patrick G. Hatcher

The use of algae as a feedstock for hydrous pyrolysis has a high potential for producing biofuels. The non-food nature of algae in addition to the various advantages associated with the hydrous pyrolysis process makes this combination for the production of biofuels of high interest. However, current results from algae processing have alluded to some challenges: byproducts arising from the thermal transformation of carbohydrates and proteins, which become incorporated in the oil fraction, result in high oxygen and nitrogen contents of the oil. Accordingly, this produces an oil of low quality for refineries. This dissertation investigates use of a pretreatment approach where only the energy-rich component of algae, called algaenan, is used as feedstock for hydrous pyrolysis, thus removing the carbohydrate and proteinaceous components prior to hydrous pyrolysis. This leads to the production of a higher quality oil with less oxygen and nitrogen content.

Algaenan from *Scenedesmus* spp. was isolated using the three most common chemical isolation protocols followed in the literature to investigate their effects on the algaenan structure. A new isolation protocol was proposed based on selecting the most effective chemical treatments, from each of the three procedures, which had the least effect on the algaenan structure. Algaenan isolated by an abbreviated isolation approach was then subjected to hydrous pyrolysis to investigate its potential to produce a

hydrocarbon-rich oil. Detailed analysis of the oil by advanced analytical techniques, including two dimensional gas chromatography coupled to time-of-flight mass spectrometry and electrospray ionization coupled to Fourier transform ion cyclotron mass spectrometry, revealed it to have hydrocarbon-rich and heteroatom-poor qualities similar to many Type I kerogen derived crude oils.

Results also showed that hydrous pyrolysis treatment can be used to effectively concentrate algaenan from algal cells by finding the optimum temperature and time parameters. A protocol is presented which outlines a stepwise process to reach the optimum algaenan isolation parameters. Such a need can be envisioned if one is to eventually commercialize the process.

From the results, a new two-step strategy is proposed to 1) isolate algaenan, by low temperature hydrous pyrolysis followed by 2) produce high quality oils from the isolated algaenan by high temperature hydrous pyrolysis. This strategy aimed to minimize the incorporation of heteroatoms into the oils by using hydrous pyrolysis to remove the carbohydrates and proteins prior to producing oils from algaenan. Detailed analysis of the produced oil with this approach shows that it is hydrocarbon-rich, heteroatom-poor and similar to that produced from the hydrous pyrolysis of the chemically isolated algaenan.

To my parents whose endless love and support made this a reality and to the soul of my grandfather, a man like no other.

ACKNOWLEDGMENTS

A large number of people are to thank because they each affected my time at ODU differently. Mostly I would like to thank my thesis advisor Dr. Patrick Hatcher for accepting me into his group, for the countless hours of guidance and for always believing in me. Thank you for everything. Second, I would like to thank Dr. Elodie Salmon who was always there to provide help and feedback when most needed.

I would also like to thank all the members of the hatcher group, for their valuable input and for their friendship. I would like to specifically mention Rajaa Mesfioui, who urged me to join the Hatcher group; Amanda Willoughby, for being the best cubicle neighbor; Derek Waggoner, who is the instrument guru in the lab and who is kinder than many give him credit for; and Blaine Hartman, for her help in the lab and for always telling you what's on her mind, a quality much needed and only few have.

The list would not be complete without mentioning Chelsea When, for her help in performing the experiments mentioned in brown coal chapter; Jason Collins, for all the times we spent at the library and at the gym and for whom the phrase "mind over matter" is forever engraved in my mind; Nardos Sori, who is my oldest friend at ODU; Hussam AbuAssi, who took me in his home in open arms when I first came to Norfolk; Hany SalahEldeen, my roommate and "partner in crime"; Dr. Joe El-khoury and Fadi Jradi, my friends from Lebanon and my academic companions since the days of undergrad. Last but not least, my undergraduate research advisor Dr. Najat Saliba, who was a mentor to me and whose guidance and inspiration is the reason I am here now.

NOMENCLATURE

HP	Hydrous pyrolysis
HTL	Hydrothermal liquefaction
HTG	Hydrothermal gasification
TAGs	Triacylglycerides
FFA	Free fatty acids
DAGs	Diacylglycerides
MAGs	Monoacylglycerides
AA	Amino acid
AAs	Amino acids
k_1	AA formation rate constant
k_2	AA decomposition rate constant
Bb	*Botryococcus braunii*
FTIR	Fourier Transform Infrared spectrometry
EA	Elemental Analysis
NMR	Nuclear magnetic resonance
^{13}C	Carbon-13
ssNMR	Solid state nuclear magnetic resonance spectrometry
Py-GC/MS	Flash pyrolysis coupled to gas chromatography mass spectrometry
TFA	Trifluoroacetic acid
CPMAS	Cross polarization magic angle spinning
CDS	Chemical Data Systems
GC-MS	Gas chromatography mass spectrometry

GC-FID	Gas chromatography flame ionization detection
GCxGC-TOFMS	Two-dimensional gas chromatography coupled to time-of-flight mass spectrometry
ESI-FTICR-MS	Electrospray ionization coupled to Fourier transform ion cyclotron mass spectrometry
T	Temperature
P	Pressure
V_w^T	Volume of waster at the experimental temperature
M_w	Mass of water added at room temperature
V_R	Volume of the reaction vessel
ρ_w^T	Density of water at the experimental temperature
ρ_v^T	Density of the water vapor (steam) at the experimental temperature
NaOH	Sodium hydroxide
KOH	Potassium hydroxide
CO_2	Carbon dioxide
HMF	Hydromethylfurfural
Sp.	Species (singular)
Spp.	Species (plural)
DCM	Dichloromethane
DPMAS	Direct polarization magic-angle-spinning
CDS	Chemical Data Systems
NSO	Nitrogenated, sulfurated, and oxygenated
TOF	Time-of-flight
THF	Tetrahydrofuran
AI_{mod}	Modified aromaticity index

DBE	Double bond equivalence
C.I. Algaenan	Chemically isolated algaenan
HHV	High heating value
m/z	Mass-to-charge ratio
S/N	Signal-to-noise ratio

TABLE OF CONTENTS

Page

LIST OF TABLES

LIST OF FIGURES

CHAPTER I

INTRODUCTION

1. WHY ALGAL BIOFUELS

The search for alternative fuels has greatly been expanded in recent years and has reached a level of environmental, economic, and strategic importance. The United States government passed the Energy Independence and Security Act in 2007 which mandates the production of 36 billion gallons of bio-derived fuels by 2022 (U.S.Congress, 2007). In addition, the United States Navy set up a goal to increase its use of alternative fuels to 50 % by 2020 (U.S.Navy, 2009). To meet this demand, there will be a need to accelerate the commercialization of alternative fuel production from multiple feedstock's, one of which includes algae.

The use of hydrous pyrolysis (HP) to produce oils from algae has been documented as early as the 1990's (Dote et al., 1994; Inoue et al., 1994). Recently, there has been an increasing interest in using hydrothermal liquefaction (HTL), which is similar to HP, to produce biofuels from algae (Biller and Ross, 2012). This interest is mainly focused on increasing the efficiency with which HP can extract algal triglycerides used commonly as feedstock for biofuels production. It is important to make a distinction between HP and HTL. Most biofuels applications employing HTL envision relatively short contact times with the intended purpose to extract algal oils that are chemically analogous to acyl glycerides.

This dissertation is formatted based on the journal *Organic Geochemistry*

This approach recognizes that water's properties at near-critical point conditions become more similar to those of organic solvents. Accordingly, short contact times are normally sufficient to extract the bio-oils. HP is viewed as being different in that the sub-critical heating must be conducted for a sufficient length of time to induce cracking (pyrolysis) of energy-rich algal components and the oils produced are degradation products of the process rather than merely extractives of existing oils within the algae. Unfortunately, this distinction has not been made in the HTL literature because the focus of studies have been on recovering maximal amounts of oils with the least amounts of expended energy and without focusing on the subtleties between extraction where carbon-carbon bonds are not broken and pyrolysis. It is well known that HTL involves mainly hydrolysis reactions (Garcia-Moscoso et al., 2013).

Algae's nature as an aquatic organism makes its processing with traditional dry thermochemical methods such as anhydrous pyrolysis and gasification less appealing as the need to pre-dry the algae increases the costs of the process (López Barreiro et al., 2013). Therefore, HP's use of water makes it ideal for processing feedstock such as algae. In addition, it has been shown that the aqueous phase following the thermal treatment contains organic and inorganic nutrients that can be recovered and reused as a fertilizer to regrow the algae (Levine et al., 2013). This reduces the net amount of fertilizer needed and thus decreases algae growing costs.

Most studies relating to the HTL of algae focus on either concentrating lipids in the residue so they can subsequently be converted into biodiesel or on liquefying the algae to produce the highest percent conversion to liquid biocrude (Savage, 2012; López Barreiro et al., 2013). Currently, direct HTL to biocrude is the economically more

favorable approach because it requires neither thermal drying of the residue, solvent extraction of the lipids, nor transesterification to biodiesel. Many studies have investigated the potential for HTL of various strains of algae such as (*Spirulina* sp., *Chlorella* sp., *Botryococcus braunii, Desmodesmus* sp., and others) at the whole range of temperatures for biofuel production (Dote et al., 1994; Brown et al., 2010; Garcia Alba et al., 2011; Jena et al., 2011). However, few if any studies have employed HTL for sufficient periods of time to allow for cracking reactions like those associated with HP.

Algae in the eyes of the biofuels community are generally thought to be made up of three major components that are of importance to biofuel production: Lipids, proteins, and carbohydrates. In some recent experiments, algae have been found to produce oils in abundance; however, these oils are rich in oxygen and nitrogen molecules, arising from the thermal transformation of carbohydrates and proteins, that require additional treatments involving catalytic upgrading to produce saturated hydrocarbons (Garcia Alba et al., 2011; Biller and Ross, 2012; Torri et al., 2012). Recent work by Garcia Alba et al. (2011) and Torri et al. (2012) have shown that *Desmodesmus* sp. algae readily yield hydrocarbon-rich oils but these contain an abundance of oxygenated and nitrogenated species whose existence is associated with carbohydrates and proteins contained in the algae (Garcia Alba et al., 2011; Torri et al., 2012). Ultimately, the aim of direct HP or HTL processing of algae is to produce a high yield of biofuel that has low heteroatom content and preferably resembles crude oils in its chemistry. However, the general trend in the algal biofuels literature has been to focus on the total quantitative yield of oil while dismissing the importance of the produced oils' chemical properties by invoking the need for downstream upgrading solutions. In this dissertation, I aim to describe a new

approach that utilizes pretreatment of algae to concentrate an energy-rich biopolymer called algaenan and then applying HP to produce a hydrocarbon-rich and heteroatom-poor bio-oil that is very similar to crude oils. Along the route to this aim, I examine and compare various chemical isolation methods and also examine ancient coal deposits thought to be derived from algae with the intention of understanding how natural maturation leads to production of oil.

2. DISSERTATION OBJECTIVES

The overarching hypothesis in this dissertation is that hydrous pyrolysis of algaenan from Chlorophyta algae, one of which is *Scenedesmus/Desmodesmus* spp., produces a hydrocarbon-rich bio-oil significantly reduced in the O and N-containing species. The dissertation is divided into several sub-hypotheses that collectively aim to answer the major hypothesis:

1. *Traditional chemical treatments used to isolate algaenan from freshwater Chlorophyta algal species alter the chemistry of the algaenan polymer (Chapter II).* The isolation of algaenan from its parent algae is the first step employed in the effort to characterize it. Three different protocols are the most followed in the isolation of algaenan. Because different structures have been proposed for algaenan from the same parent algae but isolated using different isolation protocols, we examined the possible effects the isolation procedure has on the algaenan chemistry. The structures are examined by flash pyrolysis coupled to gas chromatography mass spectrometry (py-GC/MS) and by carbon-13 (^{13}C) solid state nuclear magnetic resonance spectrometry (ssNMR) to compare their

chemical differences. A new procedure that combines chemical treatments which have the least effect on the algaenan structure is suggested.

2. *Hydrous pyrolysis of a low rank brown coal from the Moscow basin with high contributions from organic geo-biopolymers will succeed in artificially maturing the sample to produce a hydrocarbon-rich oil (Chapter III).* Previous palynological studies of coal from the Moscow basin report contributions from mainly algae, fungi, mosses and ferns (Krevelen and Schuyer, 1957). In addition, this coal has a unique property as it was never buried deeply to undergo significant maturation; temperatures are thought to have never risen above 25 °C. As a result, the coals in this basin never reached a temperature required for the formation of bituminous coals and thus are still in the stage of hard brown coals (Larsen and Chilingar, 1967). The sample is analyzed by multiple analytical techniques such as ^{13}C ssNMR and py-GC/MS. The expelled oils are analyzed by gas chromatography flame ionization detection (GC-FID), gas chromatography mass spectrometry (GC-MS), and two-dimensional gas chromatography coupled to time-of-flight mass spectrometry (GCxGC-TOFMS).
3. *Hydrous pyrolysis of algae from Scenedesmus/Desmodesmus* spp. *algae and its isolated algaenan will produce a hydrocarbon-rich oil (Chapters IV and V).* In Chapter IV, algae and isolated algaenan are subjected to HP to test if they will thermally mature similarly to ancient geo-biopolymer containing coal (i.e. Moscow coal). In addition, I aim to prove that the algaenan in the algae is the source of the majority of the hydrocarbons. To achieve this, samples of whole algae and chemical isolated algaenan were treated under hydrous pyrolysis

conditions. Following the treatment the fractions were collected and analyzed via multiple analytical techniques (Chapter IV). In Chapter V, detailed molecular analysis of the polar fraction in the produced oils is performed by electrospray ionization coupled to Fourier transform ion cyclotron mass spectrometry (ESI-FTICR-MS).

4. *A subset of the above central hypothesis is that a two-step hydrous pyrolysis can produce algaenan quality oil from algae directly without the need for chemical isolation of algaenan (Chapter VI).* A protocol is suggested for using low temperature and short contact time treatment of the whole algae, analogous to HTL, to isolate algaenan (first step). The low temperature HTL is investigated to evaluate its efficacy in removing the labile carbohydrates and proteins while leaving the algaenan intact. The second step is taking the solid residue from the first step and treating it at a higher temperature and under HP conditions that would crack the algaenan biopolymer into expelled oil. The removal of the proteins and carbohydrates from the first step HTL would prevent their highly oxygenated pyrolysis products from being incorporated in the oil fraction. Following the treatment the oil fraction is collected and analyzed via multiple analytical techniques, namely GC-FID, GC/MS, and ESI-FTICR-MS and compared with oils produced by HP of chemically-isolated algaenan.

3. BACKGROUND INFORMATION

3.1 Algae

Algae are a group of eukaryotic organisms that grow photoautotrophically and

lack complex cell and tissue types found in land plants such as: xylem, phloem, and stomata. Algae have evolved into many diverse forms (e.g., uni- and multi- cellular plants) and display characteristic varieties in size, shape, color, structure and composition and can also change these characteristics under different environmental stressors. These facts make it sometimes difficult to readily classify algae. Algae species are typically divided into macro- and micro- algae. Macroalgae, also known as "seaweeds" are multicellular plants growing in salt or fresh water and they constitute the classes: *Chlorophyta* (green seaweed); *Phaeophyta* (brown algae); and *Rhodophyta* (red algae). Microalgae are defined as microscopic algae growing in salt or fresh water and they typically constitute the classes: *Bacillariophyta* (diatoms); *Chlorophyta* (green algae); *Chrysophyta* (golden algae); *Cyanobacteria* (blue-green) (Anders S Carlsson, 2007). Algae are thought to have the highest potential for producing biofuels than any other biomass (Chisti, 2007; López Barreiro et al., 2013). Algae's uniqueness as a scalable and economic biofuel source stems from their ability to photosynthetically capture energy at high yields in controlled environments (Kumar et al., 2014), they are not used for food, do not need arable land to grow, and they have a higher oil production potential than other biomass feedstock for biofuels. Currently, a very popular process for the production of biofuels from algae is hydrothermal liquefaction which in the current study is better referred to as hydrous pyrolysis (HP).

3.2 HP process and water properties

HP, also known as HTL in the biofuels literature, is the process where a sample is heated in the presence of water and remains in contact with liquid water for the whole duration of the experiment at sub critical temperatures, i.e., those do not exceed the

critical point of water (T = 374 °C, P = 217.7 atm) (Lewan et al., 1979). HP experiments are typically conducted in closed system reactor vessels that are designed to handle high temperatures and pressures under which the experiments are performed. Typically, the amount of water added should be large enough to ensure that there remains some liquid water (not steam) covering the entire sample at the operating temperature. However, care should be taken to not add too much water as the thermal expansion of water can be dangerous if it expands to a higher volume than that of the reactor vessel. The volume of water at a specified temperature can be calculated using the following equation:

$$V_w^T = \frac{M_w - V_R \rho_v^T}{\rho_w^T - \rho_v^T} \quad (1)$$

Where V_w^T is the volume of water at the experimental temperature; M_w is the mass of water added at room temperature; V_R is the volume of the reaction vessel; ρ_w^T is the density of water at the experimental temperature; and ρ_v^T is the density of the water vapor (steam) at the experimental temperature.

At ambient conditions, water is the typical polar solvent having low miscibility to nonpolar compounds and gasses and having a high dielectric constant of 78.5, a density of 0.997 g/ml (Kruse and Dinjus, 2007), and a dissociation constant of near $1*10^{-14}$. As the temperature increases, water's properties change: its dielectric constant decreases, its density also decreases, and its dissociation constant increases (Figure 1).

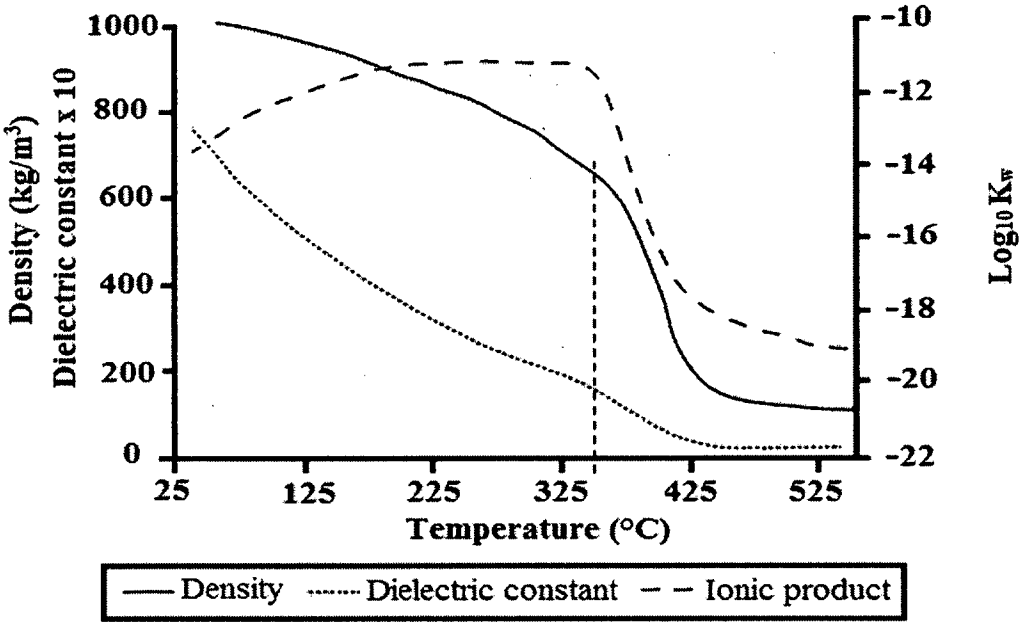

Figure 1. Properties of water at with increasing temperature: density, dielectric constant at 30 MPa, and logarithm of dissociation constant at 25 MPa. Vertical line denotes critical point. Redrawn with permission from Biller and Ross (2012).

At temperatures and pressures close to the critical point (T = 374 °C, P = 217.7 atm), the dielectric constant of water is around 10, which is close to that of methylene chloride. The decreasing trend for the dielectric constant (Figure 1) signifies that the water starts acting more as a nonpolar solvent as the temperature increases, has increasing solubility to nonpolar compounds and gases, and consequently less solubility for ionic salts. The change in the density of water with temperature is most intense near the critical point, for example between 200 °C and 300 °C the density changes from 0.864 g/ml to 0.712 g/ml. However, between 350 °C and 370 °C the density changes from 0.574 g/ml to 0.453 g/ml. These changes in density correlate with properties such as degree of hydrogen bonding, polarity, dielectric strength, diffusivity and viscosity (Peterson et al., 2008). In addition, at near critical point conditions, the dissociation constant has a value

of about 10^{-11}, three orders of magnitude greater than that of water at standard temperature and pressure. This enhances acid and base reaction potential of water since the hydroxide and hydronium ion concentrations are higher. At temperatures near and higher than the critical point, water has gas like properties such as a dramatic decrease in density, dissociation constant, and a slight decrease in the dielectric constant. In addition, reactions, such as radical reactions, become more prevalent. Consequently, hydrothermal gasification (HTG) of the samples, conducted at conditions above the critical point of water, becomes the main process decreasing in the yield of liquid products and increasing the yield of gasses. Since this dissertation is concerned with investigating the use of HP to produce liquid fuel from algae, the discussion in the section will be limited to investigations at subcritical conditions.

3.3 HP of lipids

Lipids in algae are considered to be in the forms of either triacylglycerides (TAGs) or free fatty acids (FFA). Reactions of lipids are heavily influenced by the properties of water at the various temperatures (Peterson 2008). As mentioned in the section above, the increasing temperature causes a decrease in the polarity of the water as a solvent which in turn causes lipids to become more soluble in the water and the water to become more soluble in the lipid fraction (Mills and Mcclain, 1949). The fact that both phases become soluble in each other until they become completely miscible has been observed to be the reason why the hydrolysis rate of TAGs to FFA and glycerol increases exponentially with temperature. Depending on the nature of the TAGs, complete miscibility has been observed at temperatures ranging from 293 °C to 339 °C (Mills and Mcclain, 1949; King et al., 1999). TAG hydrolysis to FFAs has been shown to proceed as

a stepwise reaction from the TAGs to the diacylglycerides (DAGs) to monoacylglycerides (MAGs) to glycerol, releasing a FFA at each step (Patil et al., 1988). The process has been shown to go almost to completion (97 % hydrolysis) at temperatures as low as 260 °C and 280 °C and at times as short at 15-20 min without the use of catalysts (Holliday et al., 1997).

Although TAG hydrolysis to FFA can be accomplished efficiently (>96 %), FFA decarboxylation to hydrocarbons is a bit more difficult and is not as effective at subcritical conditions without the use of catalysts. In addition, the decarboxylation mechanism in hydrothermal conditions can vary significantly depending on the general structure of the acid (e.g.; carbon length, saturated/unsaturated, branched/linear). Linear saturated carboxylic acids under hydrothermal conditions undergo decarboxylation in the 1) absence of base catalysis via a monomolecular cleavage of the α,β C–C bond to produce acetic acid and C_{n-2} alkane as the major product and 2) in the presence of base catalysts (i.e. NaOH and KOH) to produce CO_2 and the C_{n-1} alkene (Watanabe et al., 2006). Decarboxylation in mono unsaturated carboxylic acids has been shown to be also dependent on the bond type and group attached to the α-, β-, and γ-carbons (Wang and Poirier, 1994; Bach and Canepa, 1996; Li and Brill, 2002). For instance, it was shown that methyl substitution on the β-carbon position increased the decarboxylation rate while as a methyl substitution on the γ-carbon resulted in a decreased decarboxylation rate. These results suggest a synchronous reaction via a six membered cyclic transition state (Smith and Blau, 1964; Bigley and Thurman, 1967a, b; Wang and Poirier, 1994). Decarboxylation of FFA to hydrocarbon is of high value because it decreases the oxygen percentage thus increasing the quality of the biofuel. Catalysis of this reaction can be

achieved either in the form inorganic heterogeneous added minerals, surface catalysis of the reactor wall, or homogeneous soluble catalysts (Watanabe et al., 2006; Biller et al., 2011; Biller and Ross, 2011; Duan and Savage, 2011b). Bell et al. (1994) examined mineral catalysis and reactor wall effects on the rate of decarboxylation of acetate and found that depending on the type of material used in the reactor the rate of decarboxylation changed. For instance, stainless steel reactors were found to increase the rate of decomposition of acetic acid by six orders of magnitude at temperatures as low as 100 °C when compared to reactions performed in gold reactors (Kharaka et al., 1983; Bell et al., 1994). This is in agreement with other experiments examining the role of catalysts on the decarboxylation of FFA under subcritical conditions (Biller and Ross, 2010; Biller et al., 2011). In addition, Belsky et al. (1999) observed that at subcritical conditions the rate of decarboxylation can be enhanced by adding bases such as NaOH and KOH. This is because the base neutralizes the acidic proton of the acid leading to the prevalence of the ionic form of the FFA which is more soluble in water than that of the non-ionic acid form (Belsky et al., 1999).

3.4 HP of carbohydrates

Carbohydrates in algae are mostly in the form of cellulose, starch (glucose accounts for 80 % of total carbohydrate content (Pandey et al., 2011; Ho et al., 2013)), and other homologues such as small amounts of xylose and of mannose (Popper and Tuohy, 2010; Ho et al., 2013). Algae lack other biomolecules such as hemicellulose and lignin (Batista et al., 2014). The HP of carbohydrates does not yield direct biocrude oils (Laurens et al., 2012); however, they yield polar organic compounds soluble in the aqueous phase. When dealing with HP of carbohydrates, two main processes are in play,

hydrolysis and decomposition. Hydrolysis is the de-polymerization of polymeric carbohydrates into smaller oligomers or monomers in the presence of water. Decomposition, as a result of the thermal treatment, results in the formation of new molecules. Some examples of compounds formed from decomposition of glucose under HP conditions with no added catalysts are shown in Table 1.

Table 1. Glucose degradation products under HP conditions. Data modified from Peterson et al. (2008) with permissions.

Compounds	Study
Acetaldehyde	2
Acetic acid	1,2,4
Acetol (hydroxyl acetone)	4
Acetone	2
Propenoic acid	2
Arabinose	4
1,2,4-Benzenetriol	2
Dihydroxyacetone	1,2,3,4
Erythrose	1
Formic acid	1,2,4
Fructose	1,2,3,4
2-Furaldehyde (furfural)	2,3,4
Glyceraldehyde	1,2,3,4
Glycoaldehyde	1,2,3,4
Glycolic acid	2
5-Hydroxymethylfurfural (5-HMF)	1,2,3
Lactic acid	2
Levoglucasan	1,4
Manose	4
Pyruvaldehyde	1,2,3,4

[1]Kabyemela et al. (1999); [2]Srokol et al. (2004); [3]Bonn and Bobleter (1983); [4]Antal et al. (1990)

Both hydrolysis and decomposition of carbohydrates increase significantly with increasing time and temperature of the reaction in water. Cellulose is a polymer made up

of cellobiose monomers bound with β-(1, 4) glycosidic bonds. This type of linking causes cellulose to have strong intramolecular interactions making it a more rigid molecule (gives the molecule a more packed and crystalline structure). In addition, cellulose is more difficult to hydrolyze compared to other carbohydrates and requires special enzymes to break the β-(1,4) glycosidic bond. This rigidity and resistance are the main reasons cellulose is used as a structural building material for many plants and algae. Cellulose however can be hydrolyzed under HP conditions into smaller oligomers, and subsequently into cellobiose, glucose monomers, and other degradation products. Because of the strength of the cellulose β-(1,4) glycosidic bond, higher temperatures are needed to break down the cellulose polymer. In addition, it was observed that cellulose loses its crystallinity prior to degradation at about 320 °C (Deguchi et al., 2006). However, once the crystallinity is lost, the hydrolysis progresses rapidly. This suggests that the crystallinity of cellulose prevents its hydrolysis.

Starch, a polysaccharide that consists of mainly of glucose monomers found as 1) amylose (non-branched polymer consisting of α-D-glucose monomers bound with α-(1,4) linages) and 2) amylopectin (an amylose like branched polymer containing additional α-(1,6) branched glucose about every 24 to 30 glucose units). Starch can be easily hydrolyzed by HP to produce compounds such as glucose, maltose, fructose, 5-hydromethylfurfural (5-HMF), and furfural (Nagamori and Funazukuri, 2004). For example, Nagamori and Funazukuri (2004) showed that at 180 °C (5 min), the starch polymer hydrolyzes into smaller molecular weight soluble oligomers. In addition, no glucose or other products (fructose, maltose, 5-HMF, furfural, or gaseous products) were observed until a reaction time of greater than 40 min at 180 °C. Starch hydrolysis into

maltose and glucose was significantly increased at temperatures greater than 200 °C. For instance, starch hydrolysis into glucose (which can also isomerize to fructose under these conditions (Kabyemela et al., 1999)) was observed after 106 min, 50 min, 23 min, 10 min, and 5 min reaction times at 160 °C, 180 °C, 200 °C, 220 °C, and 240 °C respectively. Secondary decomposition to 5-HMF increased dramatically with temperature. Nagamori and Funazukuri (2004) report 5-HMF percentage of original starch conversion of 2 % (40 min, 180 °C), 12 % (200 °C, 40 min), 22 % (220 °C, 20 min), and 20 % (240 °C, 5 min).

3.5 HP of proteins

Proteins are macromolecules made up of amino acid (AA) building blocks. AAs have a similar backbone composed of a carboxyl group, an amine group, and a side chain group that is unique to every different amino acid. The amine group from one AA reacts with the carboxyl group from another forming a C–N bond called the peptide bond. Proteins are similar to carbohydrates in that they undergo both hydrolysis and degradation under HP conditions. Hydrolysis of proteins results in their de-polymerization to the individual AA monomers and smaller chain peptides. Typically, research involving protein HP aims to find the best conditions that result in the maximum yield of free AAs and lowest decomposition. Since most research in the area of HP of proteins focuses on maximizing the production of AAs, direct degradation kinetics of proteins are not readily available because of the difficulty of quantifying the remaining unaltered protein/peptides after the HP treatment. Therefore, AA formation (k_1) and subsequent degradation (k_2) kinetics are often the quantities that are measured via the following model (Qian et al., 1993; Rogalinski et al., 2005; Quitain et al., 2006;

Rogalinski et al., 2008):

$$Protein \xrightarrow{k_1} amino\ acid \xrightarrow{k_2} degradation\ product \quad (2)$$

These conditions are typically under 250 °C as decomposition becomes more favorable at higher temperatures. The reactions are also dependent on many factors, such as the sequence and length of the peptide and the pH of the solution. Table 2 shows some reaction rate constants for the degradation of albumin. Geiger and Clarke (1987) reported data for HP on a five-AA protein and Qian et al. (1993) reported data for HP on a two-AA protein. The calculated half-lives are as follows for examples of two and five AA peptides. A two-AA peptide example has the following half-lives: 4 days at 110 °C, 21 h at 160 °C, 12 h at 180 °C, 5 h at 225 °C, 3 h at 250 °C and 2 h at 275 °C (Qian et al., 1993). A five-AA peptide example has the following half-lives: 8 h at 110 °C, 8 min at 160 °C, 3 min at 180 °C, 20 s at 225 °C, 7 s at 250 °C and 3 s at 275 °C (Geiger and Clarke, 1987). It is reasonable that long chain proteins have a higher chance of hydrolysis and/or decomposition.

Table 2. Rate of decomposition of albumin based on Equation 2 above. Adapted with permissions from Brunner (2014).

T (°C)	k_1 (s^{-1})	Half-life 1 (s)	k_2 (s^{-1})	Half-life 2 (s)
110	3.8×10^{-6}	1.9×10^{5}	1.6×10^{-11}	4.4×10^{10}
160	5.6×10^{-5}	1.2×10^{4}	3.9×10^{-8}	1.8×10^{7}
180	1.4×10^{-4}	5.0×10^{3}	5.5×10^{-7}	1.3×10^{6}
225	8.4×10^{-4}	8.3×10^{2}	9.5×10^{-5}	7.3×10^{3}
240	1.4×10^{-3}	4.9×10^{2}	4.4×10^{-4}	1.6×10^{3}
250	2.0×10^{-3}	3.5×10^{2}	1.0×10^{-3}	6.9×10^{2}
275	4.3×10^{-3}	1.6×10^{2}	1.1×10^{-2}	63
290	6.7×10^{-3}	1.0×10^{2}	3.9×10^{-2}	1.89
310	1.1×10^{-2}	63	3.4×10^{-1}	2
330	2.0×10^{-2}	35	5.1×10^{-1}	1.4

AA decomposition characteristics are dependent mainly on temperature, type of AA, and show a complex dependence on pH (Walter et al., 1967; Li and Brill, 2003). Decomposition of the subsequently formed AAs can be a result of decarboxylation, deamination, or other decomposition reactions (Bada, 1991). AA decomposition can also produce different gaseous compounds (such as carbon dioxide, carbon monoxide, hydrogen, and methane), low alkanes and alkenes, alcohols (up to C_5), amides, aldehydes, and carboxylic acids (Walter et al., 1967; Abdelmoez et al., 2010) and is dependent on the identity of the AA. Examples of some products are shown in Table 3. Decarboxylation (Bada et al., 1978; Sohn and Ho, 1995) and racemization (Smith and Sivakua, 1983; Baum and Smith, 1986; Kawamura and Yukioka, 2001) reactions occur at lower temperatures than those required for deamination.

Table 3. Some amino acid degradation products observed under HP conditions. Edited with permissions from Abdelmoez et al. (2010).

Tested amino acid	Products		
	Amino acid	**Acids**	**Other**
Glycine	N/A	Acetic acid[3]; Carbonic acid[2]; Formic acid[1,2]; Glycolic acid[1,2]	Ammonia[1,2]; Formaldehyde[3]; Methane[3]; Methylamine[1,2,3]
Alanine	N/A	Lactic acid[1,2]; Formic acid[1,2]; Acetic acid[1,2]; Carbonic acid[2]; Pyruvic acid[1]; Propionic acid[1]	Ammonia[1,2]; Ethane[3]; Ethylamine[1,2]
Valine	N/A	Formic acid[2]; Carbonic acid[2]	Ammonia[2]
Leucine	N/A	Acetic acid[1,2]; Formic acid[1,2]; Carbonic acid[2]	Ammonia[1,2]; 3-Methyl-1-butene[3]
Isoleucine	N/A	Acetic acid[2]; Formic acid[2]; Carbonic acid[2]	Ammonia[2]
Methionine	N/A	Acetic acid[2]; Formic acid[2]; Carbonic acid[2]	Ammonia[2]
Phenylalanine	N/A	Acetic acid[1]; Formic acid[1,2]; Carbonic acid[2]	Ammonia[1,2]
Tyrosine	Glycine[2]	Formic acid[2]; Carbonic acid[2]	Ammonia[2]; Methylamine[2]
Serine	Glycine[1,2]; Alanine[1,2]	Acetic acid[2]; Formic acid[2]; Carbonic acid[2]; Pyruvic acid[1]; Lactic acid[1]; Glycolic acid[1]	Ammonia[2]; Ethanolamine[2]; Ethylamine[1]
Threonine	Glycine[2]	Acetic acid[2]; Formic acid[2]; Carbonic acid[2]	Ammonia[2]
Cysteine	Glycine[2]; Alanine[2]	Pyruvic acid[2], Acetic acid[2]	Ammonia[2]
Proline	N/A	Carbonic acid[2]	Ammonia[2]
Lysine	Valine[2]	Formic acid[2]; Carbonic acid[2]	Ammonia[2]
Histidine	Glycine[2]	Formic acid[2]; Carbonic acid[2]	Ammonia[2]; Methylamine[2]
Arginine	Proline[2]	Formic acid[2]; Carbonic acid[2]	Ammonia[2]
Aspartic acid	N/A	Acetic acid[1,3]; Maleic acid[1,2], Malic acid[1]; Succinic acid[1]; Pyruvic acid[1,2], Fumaric acid[1]; Lactic acid[1]; Formic acid[1]	Ammonia[1,2]; Ethane[3]; Ethanol[3]; Ethylamine[3]; 2-methyl-5-ethyl-pyridin[3]
Glutamic acid	N/A	Pyroglutamic acid[2]	N/A

[1]Sato et al. (2004); [2]Abdelmoez et al. (2010); [3]Walter et al. (1967)

Decarboxylation results in the formation of carbonic acid and amines. As mentioned earlier, decarboxylation occurs before deamination under HP conditions. Mechanistically, the zwitterion form of the AAs undergoes decarboxylation by involving hydrogen bonded water molecule as shown and by forming a five-coordinate carbon atom as shown in Figure 2. Decarboxylation rate is constant across the 3 – 8.5 pH range and becomes more complex and different for each AA outside this range; detailed discussion is outside the scope of this thesis and further discussion about pH and ionic strength effects on AA decarboxylation can be found in the articles by Li and Brill (2003), Li et al. (2002), and Li and Brill (2002). Typically, the half-life of AAs decarboxylation range from about (570 – $4.7x10^5$) days at 110 °C, (0.6 – 16) h at 225 °C, (7 – 112) min at 250 °C and (63 – 950) s at 275 °C depending on the AA. The half-life rates were calculated using data from Li and Brill (2003) and first order rate-law calculations.

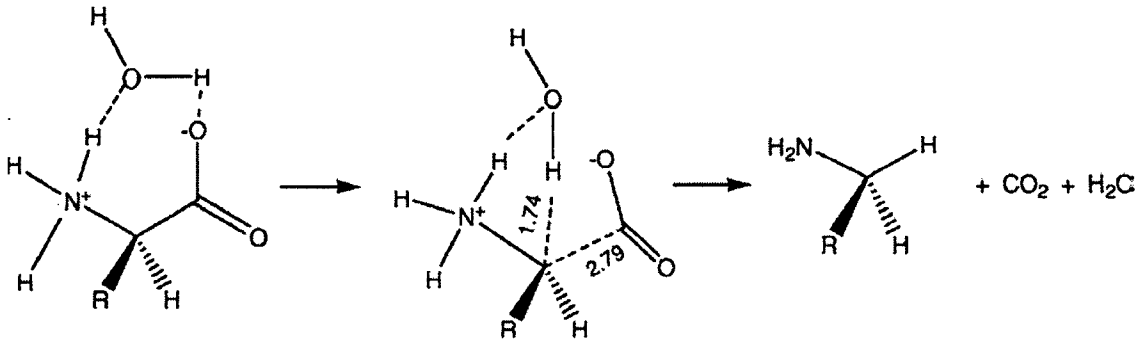

Figure 2. Mechanism for AA decarboxylation. Copied with permissions from Li and Brill (2003).

Although racemization is not the focus of this thesis, racemization has been used as a dating method to estimate the age of specimens in geology (Schroeder and Bada, 1976), archaeology (Griffin et al., 2009), paleontology (Poinar et al., 1996) , meteorology

(Cohen and Chyba, 2000), and other earth and planetary fields. Racemization has been studied under HP conditions to determine the mechanism and rate of the reaction. It has been shown that mechanistically, the rate determining step for AA racemization occurs during the proton abstraction step at the α-carbon forming the carbanion. A simplified scheme is shown in Figure 3. Half-lives of racemization for AA has range from (15–52) days at 110 °C, (250–950) s at 225 °C, (80–175) s at 250 °C, and (25–50) s at 275 °C depending on the AA.

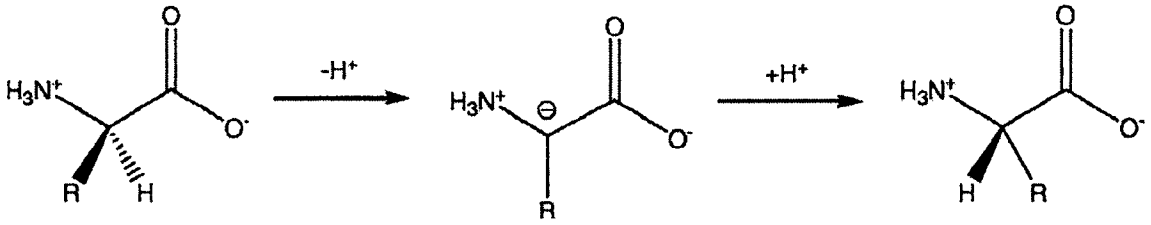

Figure 3. Mechanism for AA racemization. Copied with permissions from Li and Brill (2003).

Deamination of AAs results in the release of ammonia and organic acids while as ammonia can also be released from the side chains of amide groups of some AAs like asparagine and glutamine leading to the concentrations of ammonia to be larger than the concentration of the total AAs (Sohn and Ho, 1995). The released ammonia can then participate in other reaction forming nitrogen containing organic molecules such as pyrazines (Izzo and Ho, 1993a, b) and amide (Chiaberge et al., 2013) under HP conditions. Studies have suggested that deamination follows the following reaction (Abdelmoez and Yoshida, 2013):

$$Amino\ acid + H_2 \rightarrow carboxylic\ acid + NH_3 \quad (3)$$

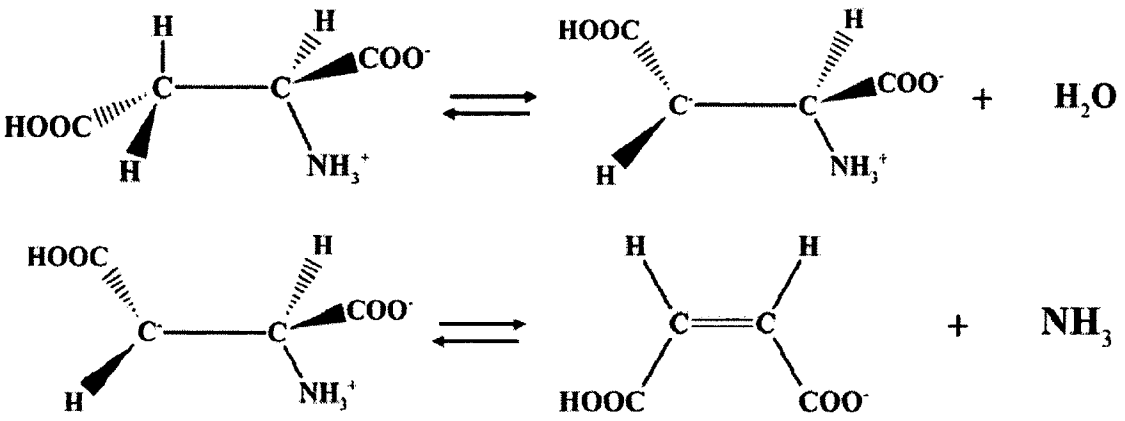

Figure 4. Mechanism for aspartic acid deamination (Bada and Miller, 1970).

Deamination is more favorable at temperatures higher than those required for decarboxylation for all amino acids except aspartic acid. Kinetics for the deamination of AAs are not readily available. In fact, at this time I am only aware of two studies that report deamination kinetics (Bada and Miller, 1970; Cox and Seward, 2007) that both investigate the deamination of aspartic acid. This is because most studies that focus on the deamination of AAs were performed at thermal conditions of interest to food chemists (T < 170 °C). At those conditions, deamination is not prevalent and is catalyzed by the reactor material. The mechanism for aspartic acid deamination has been shown to occur via the formation of a carbanion intermediate (Figure 4). Half-lives of aspartic acid deamination are calculated to be about: 34 days at 110 °C, 61 s at 225 °C, 11 s at 250 °C, and 2.3 s at 275 °C depending on the AA. These numbers are calculated by extrapolation of Arrhenius parameters from Bada and Miller (1970). It is worth noting that Cox and Seward (2007) determined the kinetics of aspartic acid under HP conditions to be highly complex, in contrast to previous studies which indicated almost exclusively deamination.

At lower temperatures (T < 170 °C), decarboxylation and polymerization are more prevalent than deamination. At higher temperatures (T > 170 °C), aspartic showed evidence indicating that it can simultaneously dimerize and cyclize, deaminate, and decarboxylate. Figure 5 shows some more degradation products of proteins from HP experiments.

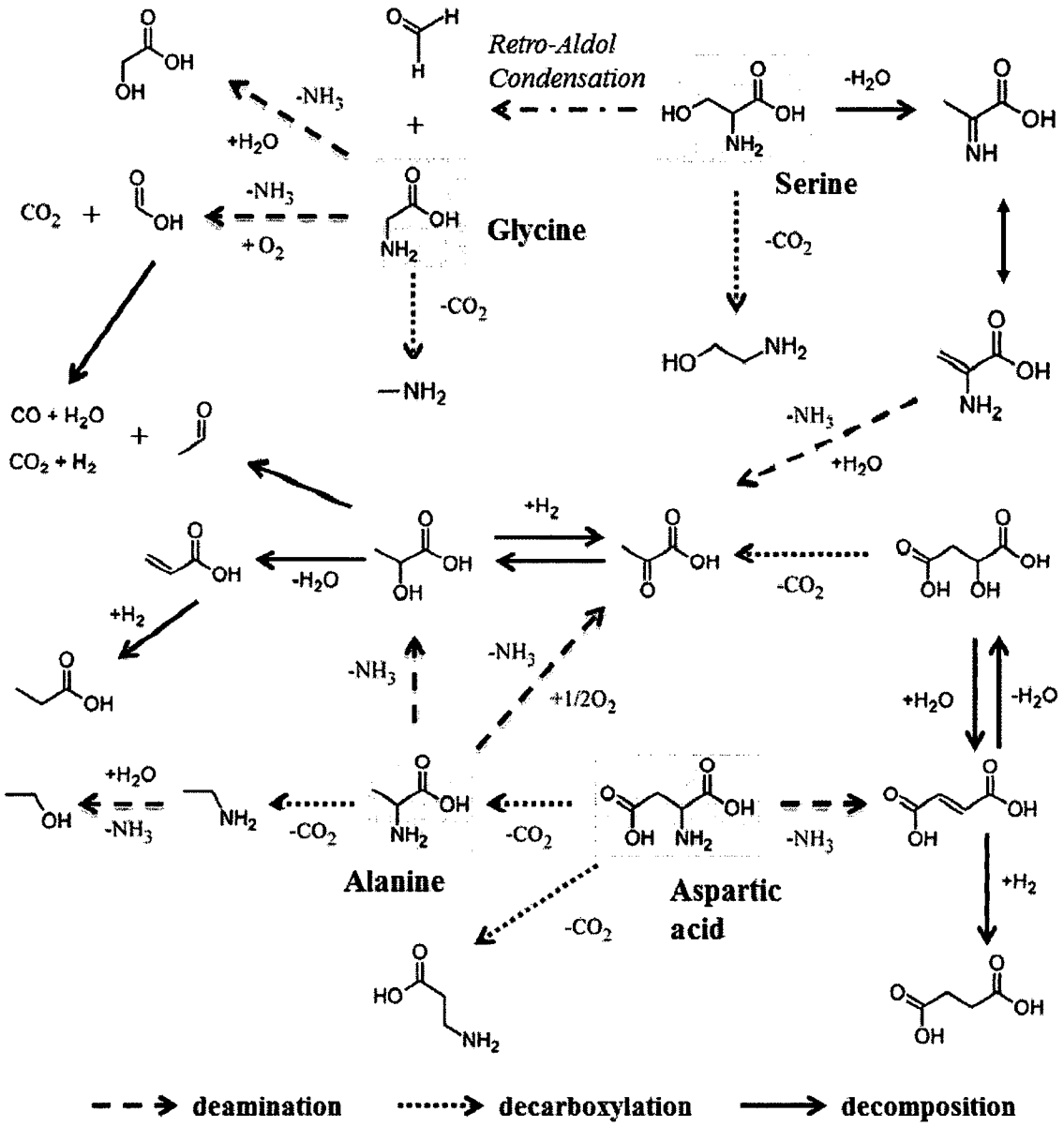

Figure 5. Reactions for decomposition of Glycine, Serine, Alanine, and Aspartic acid under HP conditions. Redrawn with permission from Sato et al. (2004).

3.6 Algaenan

Algaenan is the highly aliphatic, insoluble, non-hydrolyzable biopolymer component of the protective outer wall of algae (Berkaloff et al., 1983b; Tegelaar et al.,

1989b). Algaenan is not present in all algal species; it has been observed in some species of green algae, dinoflagellates, and eustigmatophytes (Versteegh and Blokker, 2004; De Leeuw et al., 2006; Kodner et al., 2009). The importance of algaenan stems from the observation that algaenan survives biological degradation and chemical transformation during sedimentary processes leading to its selective preservation during diagenesis (Largeau et al., 1986; Goth et al., 1988; Derenne et al., 1992b; Metzger and Largeau, 1994; Behar et al., 1995b; Allard et al., 1998; Metzger et al., 2007). In fact, algaenan from different species have been shown to persist throughout sedimentary deposition and become selectively enriched to make up a significant fraction of residual organic matter. In addition, algaenan has been shown to survive microbial enzymatic degradation (Zelibor et al., 1988) and chemical alterations from harsh acids and bases. Their polymethylenic structure renders them virtually immune to the natural processes that are known to affect other "labile" biopolymers such as lipids, proteins, and carbohydrates. Microscopic studies on kerogen samples reveal that the dominant species of algae composing them include *Botryococcus braunii* (Bb; races A, B and L), *Scenedesmus* spp., *Tetraedron* spp., and *Pediastrum* spp. or their extinct ancestors (Blokker et al. (1998) and references therein). Examples of algaenan containing algae are shown in Table 4.

The algaenan structures from different species are all characterized as having a highly aliphatic structure. However, there exist significant differences in the algaenan structures when comparing the nature of the aliphatic (i.e. whether straight chain or branched chain) and functional group connectivity (i.e. ester, ether, or aldehyde linked). For example, *Botryococcus braunii* are sub-classified into different races (A, B, and L) based on the aliphatic nature and connectivity of each respective algaenan. Algaenan

from race A is made up of alkadiene and alkatriene hydrocarbons having chain lengths from $C_{25} - C_{33}$ (Metzger et al., 1993). Algaenan from race B are made up of units called botryococcenes which are isoprenoids with chain length ranging from $C_{30} - C_{37}$ (Metzger et al., 1985). Algaenan from race L has been investigated more recently and is shown to be made of: 1) long polymethylenic hydrocarbon main chain (C_{32}) substituted by some aldehyde functional groups and connected to a 2) tetraterpenoid (C_{40}) side chain via an ester functional group (Salmon et al., 2009a).

Table 4. Algae species containing algaenan. Data modified from (Gelin et al., 1999) with permission.

Class and name	References
Chlorophycea	
Botryococcus braunii race A	Metzger et al. (1993)
Botryococcus braunii race B	Metzger et al. (1985)
Botryococcus braunii race L	Salmon et al. (2009a)
Chlorella emersonii	Allard and Templier (2001)
Chlorella minutissima	Allard and Templier (2000)
Chlorella pyrenosidosa (UTEX 1230)	Zelibor et al. (1988)
Chlorella vacuolatus	Derenne et al. (1992a)
Dunaliella tertiolecta	Zelibor et al. (1988)
Nanochlorum eucaryotum	Derenne et al. (1992a)
Scenedesmus armatus	Allard and Templier (2000)
Scenedesmus longus	Staehelin and Pickettheaps (1975)
Scenedesmus communis	Blokker et al. (1998)
Scenedesmus obliquus	Zelibor et al. (1988)
Scenedesmus pannonicus	Allard and Templier (2000)
Scenedesmus subspicatus	Blokker et al. (2000)
Tetraedron minimum	Goth et al. (1988); Allard and Templier (2001)
Prasinophyceae	
Gymnodinium catenatum	Gelin et al. (1999)
Lingulodinium polyedrum	Kokinos et al. (1998)
Eustigmatophyceae	
Nannochloropsis granulata	Gelin et al. (1999)
Nannochloropsis oculata	Gelin et al. (1999)
Nannochloropsis salina	Gelin et al. (1996a); Gelin et al. (1996b); Gelin et al. (1997c)
Nannochloropsis sp.	Gelin et al. (1996a); Gelin et al. (1996b); Gelin et al. (1997c)

The chemical structures of several algaenans have been suggested using different chemical isolation protocols from algal cultures. These protocols employed chemical and mechanical treatments to successively remove labile components present in algae, such as proteins, carbohydrates, and lipids (Hatcher et al., 1983; Nguyen et al., 2003) in different

order. Zelibor et al. (1988) proposed a procedure for the isolation of algaenan based on previously proposed methods (Schnitzer and Khan, 1972) for humic substances isolation from soil and sediments. Allard et al. (1998) proposed an improved isolation protocol after observing that the drastic basic and acidic hydrolysis steps employed by Berkaloff et al. (1983b) produce melanoidin like artifacts not intrinsic to the mycobacteria cell wall analyzed (Allard et al., 1997). Blokker et al. (1998) proposed a modified isolation protocol based on previous studies aimed at isolating algal cell walls (Burczyk and Loos, 1995). Since then, most methods of isolating algaenan have been adapted from those previous protocols in order to optimize the procedure and avoid the formation of melanoidin like artifacts into the purified algaenan samples (Allard and Templier, 2000; Kodner et al., 2009; Salmon et al., 2009a)

Due to algaenan's insolubility, methods of its identification have been established by integrating multiple pieces of information obtained from invasive and non-invasive methods which provide bulk chemical information; for instance, Fourier Transform Infrared spectrometry (FTIR), Elemental Analysis (EA), 1D and 2D ^{13}C Nuclear Magnetic Resonance spectrometry (NMR), and py-GC/MS (Gelin et al., 1997b; Bertheas et al., 1999; Zang, 2002; Salmon et al., 2009a). Different structures for algaenan have been proposed in the literature; for example, those for the different races of *Botryococcus braunii* which are distinguished based on the type of hydrocarbons they synthesize and use (Largeau et al., 1984; Kadouri et al., 1988; Derenne et al., 1989). Allard and Templier (2000) and Blokker et al. (1998) also investigated the structure of algaenan from *Scenedesmus communis* and suggested that they have some structural differences. Blokker et al. (1998) characterized the algaenan of *Scenedesmus communis* as having an

aliphatic structure linked by ester and ether linkages. Conversely, Allard and Templier (2000), who used the procedure outlined below, concluded that the contribution of ether bridges to the algaenan in their study is minor. It is interesting though, that the algaenan extracted from the same algae using different procedures has different characteristics when analyzed. It is important that the isolated algaenan represent, as much as possible, the algaenan found in the parent algae, otherwise conflicting conclusions regarding the algaenan structure could evolve. In Chapter II of this thesis, we investigate the effect that different isolation procedures have on structures of algaenan.

Ancient kerogens derived from algal remains have been shown to produce an abundance of paraffinic oil when pyrolyzed (Behar et al., 1995c) These algaenans are likely the precursors of kerogen in shales that yield paraffinic petroleum upon natural maturation (De Leeuw and Largeau, 1993). Moreover, when pyrolysis techniques are employed for studies of algaenan (Behar et al., 1995b; Blokker et al., 1998; Salmon et al., 2009a) formation of oils is observed. Previous investigations have shown that one can simulate the process by which this algaenan converts to petroleum-like hydrocarbons using pyrolysis approaches (Behar et al., 1995b; Salmon et al., 2009a)

Pyrolysis has been employed as a method to simulate the thermal maturation of organic matter in the geologic record (Lewan et al., 1979; Lewan, 1985; Behar et al., 1995b; Behar et al., 1995c; Ruble et al., 2001; Wilkins and George, 2002; Ruble et al., 2003; Stanton et al., 2005). Pyrolysis techniques are typically divided into two major types: open and closed pyrolysis. In open pyrolysis, the system works under close to atmospheric pressure conditions with an inert gas passing over the heated sample. The products released from the pyrolysis are removed thereby decreasing the chance for

further reaction. In closed pyrolysis, the reaction is occurring in an isolated system where the products stay in contact with the heated sample and the whole system operates at elevated pressures. Reactions in geologic conditions are likely to be happening under closed or semi-closed system conditions for the following reasons: 1) low flowing rates of fluid in the sediment, 2) possible saturation threshold before expulsion of hydrocarbons, and 3) the possible retention of part of the mobile phase either on the minerals or inside the kerogen network (Behar et al., 1995b). In addition, the oils produced from the closed system experiments more closely resemble crudes formed in nature. One reason is that *n*-alkenes, which are a major product of the open pyrolysis, are not a major product in neither the natural crudes nor in oils produced by closed pyrolysis.

Closed pyrolysis experiments for thermal maturation are usually conducted in one two different modes: anhydrous and hydrous. Anhydrous pyrolysis is a closed system pyrolysis in which the organic matter is heated in the absence of water. Hydrous pyrolysis is a closed system pyrolysis in which the organic matter is heated in the presence of water. Moreover, there are three main conditions that need to be met: 1) that liquid water exist at the highest temperature of pyrolysis, 2) that the sample be completely submerged under water at the highest temperature, and 3) that there is enough space above the liquid water surface to allow for free thermal expansion of water and the produced gasses.

Thermal cracking is thought to start by the homolytic cleavage of weaker bonds resulting in the generation of reactive radicals. The products henceforth generated depend on the environment where the radical exists. If hydrogen donor solvents are readily available, then the formation of aliphatics is favored but if they do not exist then the

radicals react with themselves and/or the sample and thus resulting in condensation products. Hoering (1984) has shown that the water provides a source of hydrogen that react with the radicals thus capping the reaction and preventing condensation; this was shown as a result of the incorporation of deuterium in the pyrolysis products when kerogen was pyrolyzed under heavy water. It has been suggested that under hydrous pyrolysis conditions, products from primary cracking of the organic matter is favored over the cross-linking reactions (Lewan, 1985; Behar et al., 2003). In addition, comparison between the two different closed pyrolysis methods of kerogen showed that hydrous pyrolysis has the potential to produce the most quantity of liquid oils under similar time and temperature conditions (Artok et al., 1998; Behar et al., 2003).

CHAPTER II

THE EFFECT OF DIFFERENT ISOLATION PROCEDURES ON ALGAENAN MOLECULAR STRUCTURE IN SCENEDESMUS GREEN ALGAE

PREFACE

The contents of this chapter were published in 2014 in Organic Geochemistry and are reformatted to fit this thesis. Below is the full citation. See Appendix B for the copyright permission.

> Obeid, W., Salmon, E., Hatcher, P.G., 2014. The effect of different isolation procedures on algaenan molecular structure in Scenedesmus green algae. Organic Geochemistry, 76, 259-269.

1. INTRODUCTION

Algaenan is the highly aliphatic, insoluble, non-hydrolyzable biopolymer component of the protective outer wall of algae (Berkaloff et al., 1983b; Tegelaar et al., 1989a). It has been shown that during sedimentary processes algaenan survives biological degradation and chemical transformation, leading to its selective preservation during diagenesis and thus ultimately becoming a part of kerogen (Largeau et al., 1986; Goth et al., 1988; Derenne et al., 1992b; Metzger and Largeau, 1994; Behar et al., 1995b; Allard et al., 1998; Metzger et al., 2007). Algaenan is not present in all algal species; it has been observed in some species of green algae, dinoflagellates, and eustigmatophytes

(Versteegh and Blokker, 2004; De Leeuw et al., 2006; Kodner et al., 2009). Microscopic studies on kerogen samples reveal that the dominant species of algae composing them include *Botryococcus braunii* (*Bb*; races A, B and L), *Scenedesmus* spp., *Tetraedron* spp., and *Pediastrum* spp. or their extinct ancestors (Blokker et al. (1998) and references therein).

The chemical structures of several algaenans have been suggested using different chemical isolation protocols from algal cultures. These protocols employed chemical and mechanical treatments to successively remove labile components present in algae, such as proteins, carbohydrates, and lipids (Hatcher et al., 1983; Nguyen et al., 2003) in different order. Zelibor et al. (1988) proposed a procedure for the isolation of algaenan based on previously proposed methods (Schnitzer and Khan, 1972) for humic substances isolation from soil and sediments. Allard et al. (1998) proposed an improved isolation protocol after observing that the drastic basic and acidic hydrolysis steps employed by Berkaloff et al. (1983b) produce melanoidin like artifacts not intrinsic to the mycobacteria cell wall analyzed (Allard et al., 1997). Blokker et al. (1998) proposed a modified isolation protocol based on previous studies aimed at isolating algal cell walls (Burczyk and Loos, 1995). Since then, most methods of isolating algaenan have been adapted from those previous protocols in order to optimize the procedure and avoid the formation of melanoidin like artifacts into the purified algaenan samples (Allard and Templier, 2000; Kodner et al., 2009; Salmon et al., 2009a)

Due to algaenan's insolubility, methods of its identification have been established by integrating multiple pieces of information obtained from invasive and non-invasive methods which provide bulk chemical information; for instance, FTIR, EA, 1D and 2D

^{13}C NMR, and py-GC-MS (Gelin et al., 1997b; Bertheas et al., 1999; Zang, 2002; Salmon et al., 2009a). Different structures for algaenan have been proposed in the literature; for example, those for the different races of *Botryococcus braunii* which are distinguished based on the type of hydrocarbons they synthesize and use (Largeau et al., 1984; Kadouri et al., 1988; Derenne et al., 1989). Allard and Templier (2000) and Blokker et al. (1998) also investigated the structure of algaenan from *Scenedesmus communis* and suggested that they have some structural differences. Blokker et al. (1998) characterized the algaenan of *Scenedesmus communis* as having an aliphatic structure linked by ester and ether linkages. Conversely, Allard and Templier (2000), who used the procedure outlined below, concluded that the contribution of ether bridges to the algaenan in their study is minor. It is interesting though, that the algaenan extracted from the same algae using different procedures has different characteristics when analyzed. It is important that the isolated algaenan represent, as much as possible, the algaenan found in the parent algae, otherwise conflicting conclusions regarding the algaenan structure could evolve. In this paper, we compare the detailed stepwise effect of different isolation techniques for algaenan from *Scenedesmus/Desmodesmus* algae sample, primarily using NMR techniques to follow the structural evolution brought about by each successive treatment.

2. MATERIALS AND METHODS

2.1 Sample Description

The sample was collected from the algal raceway water at the Old Dominion University algae farm in Spring Grove, Virginia USA. The raceway water sample was classified as a *Scenedesmus/Desmodesmus* complex containing minor amounts of

picoplankton. To address difficulties in identifying of the algal species arising from phenotypic plasticity effects, molecular sequencing was employed. The analysis showed that although the two populations appear to be morphologically different, they are likely the same species and are possibly identical.

2.2 The procedure by Zelibor et al. (1988)

The procedure (Table 5) begins by removal of lipids from freeze dried algae by Soxhlet extraction using a 1:1 (v:v) mixture of benzene:methanol overnight. The residue is treated with 0.5 N NaOH at room temperature overnight, followed by multiple washes with distilled water and acidification to pH 6 with HCl. The insoluble fraction is treated with sodium paraperiodate to remove the carbohydrates from the algae using the mild procedure adapted from Ritchie and Purves (1947) followed by a 1 h 1:1 (v:v) benzene:methanol extraction. The extracted residue is then refluxed with 6 M HCl for 18 h to remove proteinaceous material. The remaining algaenan is extracted again with 1:1 (v:v) benzene:methanol for 1 h and the resulting residue is freeze dried. This procedure is slightly modified from the original procedure to achieve optimum isolation of the algaenan. The reasoning behind each modification is detailed in the text.

Table 5. Summary of the Zelibor, Allard, and Blokker algaenan extraction techniques with a description of each step.

Zelibor et al. (1988)			**Allard et al. (1998)**			**Blokker et al. (1998)**		
Extraction Step	***Step description***	***Yield***	***Extraction Step***	***Step description***	***Yield***	***Extraction Step***	***Step description***	***Yield***
Benzene:MeOH 1:1 (v/v) [overnight]	Lipid extraction	78.7 %	$CHCl_3$ (30 min) $CHCl_3$:MeOH (24h)	Lipid extraction	80.0 %	Potter Homogenizing	Isolation of cell wall	87.3 %
0.5N NaOH (24h)	Basic treatment	71.3 %	TFA Treatment	Protein removal	37.7 %	α-amylase treatment	Carbohydrate removal	65.1 %
Paraperiodate [overnight]	Carbohydrate removal	27.8 %	6N HCl (18h)	Carbohydrate removal	10.7 %	MeOH, DCM, Hexane extractions	Lipid removal	42.4 %
6 N HCl (18 h)	Protein removal	11.9 % (Algaenan)	KOH/2-methoxyethanol (100 °C, 1 h)	Basic treatment	4.4 % (Algaenan)	2M H_2SO_4 (2h)/Basic treatment	Protein removal	4.7 % (Algaenan)

* Yields (% wt.) are based on initial weight (lyophilized algae)

2.3 The procedure by Allard et al. (1998)

The freeze dried algae is treated with $CHCl_3$ (30 min) and 2:1 (v:v) mixture of $CHCl_3$:MeOH (24 h) to remove lipids. The residue is then subjected to successive acid hydrolysis treatments with trifluoroacetic acid (TFA) [2 x 2 M TFA for 3h each, followed by 4 M TFA for 18 h]. After each hydrolysis step, the reflux solution and the wash water are tested by the colorimetric test for polysaccharide detection [Phenol (1 ml , 5 % wt. aqueous solution) and H_2SO_4 (5 ml, 18 M) are added to 1 ml of solution](Dubois et al., 1956). A positive test for residual carbohydrates is represented by the production of a yellow color. If the wash water has significant amounts of sugars, we continue to the next TFA extraction step; if not, we stop the TFA extractions and proceed to the next step. For our sample, the wash water gave a negative result for sugars after the 4 M, 18 h hydrolysis. The residue is refluxed with MeOH for 1 h, then rinsed with water and treated with 6 M HCl (18 h). The residue is then rinsed with water until the water has a neutral pH. The residue is then successively refluxed for 1h with water, MeOH, $CHCl_3$:MeOH, and a basic treatment [2-methoxyethanol (146 ml)/water(20 ml)/KOH(4 g)]. The residue recovered is washed successively for 1 h with water, MeOH, and $CHCl_3$ and freeze dried.

2.4 The procedure by Blokker et al. (1998)

The isolation begins by removing the cytoplasm of the algae cells using a Potter homogenizer. The residue was then subjected to a treatment using α-amylase in acetate solution to remove starch from the residue (Burczyk and Loos, 1995). The residue was then subjected to multiple washes with acetate buffer, saturated sodium chloride solution and deionized water (3x). The residue was then extracted ultrasonically with MeOH, MeOH/DCM (1:1, 2x), DCM/hexane (1:1, 2x) and hexane (1x). The obtained residue is

stirred with H_2SO_4 (12 M) for 1 h, subsequently washed with 10 ml double distilled water (3x). The residue was then suspended ultrasonically in H_2SO_4 (2 M) and refluxed for 2 h while stirring. The residue is then washed with deionized water (3x), MeOH (2x), DCM/hexane (1x) and finally with hexane (1x). The extracted material was refluxed in 7.5 ml KOH in MeOH (1 M, 4 % H_2O) for 1 h. The final residue was washed with MeOH (4x), DCM/hexane (2x) and hexane (1x) and then freeze dried.

2.5 Carbon-13 solid state NMR

^{13}C ssNMR spectra were collected using the Spinal 64 basic ramp cross polarization magic angle spinning (CPMAS) pulse program with decoupling, using a 400 MHz Bruker AVANCE II with ^{13}C resonating at 100 MHz and ^{1}H resonating at 400 MHz. Samples were placed in 4 mm NMR rotors and covered with a Kel-F cap and rotated with frequency of 13 kHz at the magic angle (54.7 °) with 1.5 ms contact time and 1 s recycle delay. Spectra were calibrated externally to glycine (176.03 ppm). Contact time and recycle delay were chosen to render the spectra as quantitative as possible. This was achieved by increasing the recycle delay to allow adequate T_1 relaxation of all the carbon atoms and by varying the contact time until the cross polarization spectrum was essentially identical to that of the spectrum obtained by direct polarization with magic angle spinning, an accepted quantitative technique.

2.6 Pyrolysis GC-MS

Pyrolysis-gas chromatography-mass spectrometry was performed with a Chemical Data Systems (CDS) pyrolysis system CDS 2000 Plus coupled to a Leco Pegasus II GC/MS system with the GC operating in the split mode (50:1). The source and transfer line temperatures were maintained at 200 °C and 280 °C respectively. Mass

spectra were collected at a rate of 20 spectra per second after a 30 s solvent delay. Masses were acquired at a range between 35 *m/z* and 500 *m/z*. The column used for GC separation has a 30 m x 0.25 mm i.d. with fused silica capillary column with a film thickness of 0.25 μm (5 % phenylpolysiloxane – 95 % methylpolysiloxane, Restek Rtx-5). Helium was used as the carrier gas, with flow rate of 1 ml/min. the oven temperature was programmed as follows: initial temperature was 50 °C, held for 1 min; then for a heating rate of 10 °C /min until the final temperature reaches 300 °C, held for 5 min. About 0.1 – 0.2 mg of samples were transferred to precombusted quartz tubes fitted with quartz spacers then covered with glass wool. The samples were placed in an auto sampler which transferred them to the pyrolysis chamber. The temperature of the pyrolysis chamber was held at 300 °C during the short period of sample injection. The samples were then rapidly (0.01 °C/ms) heated to a temperature of 650 °C, and held for 15 s as pyrolysis products were swept into the GC-MS system.

3. RESULTS AND DISCUSSION

3.1 Dried algae

Figure 6 shows the CPMAS ^{13}C ssNMR spectrum of the lyophilized algae. We observe peaks ranging from 10 to 40 ppm corresponding to aliphatic carbons (terminal CH_3, mid-chain -CH_2- and -CH-). We also observe a peak at 54 ppm, this corresponds to alpha carbons in proteins. The peaks at 62 and 72 ppm are characteristic of carbohydrate carbons having attached hydroxyl groups. The peak at 105 ppm corresponds to the anomeric carbon in carbohydrates. The spectrum also shows peaks at 130 ppm (protonated aromatic or olefinic carbons), 138 ppm (non-heteroatom non-protonated

aromatic carbons), and 159 ppm (O-substituted aromatic); the peak at 118 combined with that at 138 ppm suggest the existence of terminal olefinic carbons ($RC=C^*H_2$ and $RC^*=CH_2$ respectively). The large peak at 174 ppm corresponds to the carboxyl/amide carbons (from lipids and proteins). The overall spectrum is typical of algal biomass composed of proteins, carbohydrates, lipids, and algaenan (Zang et al., 2001).

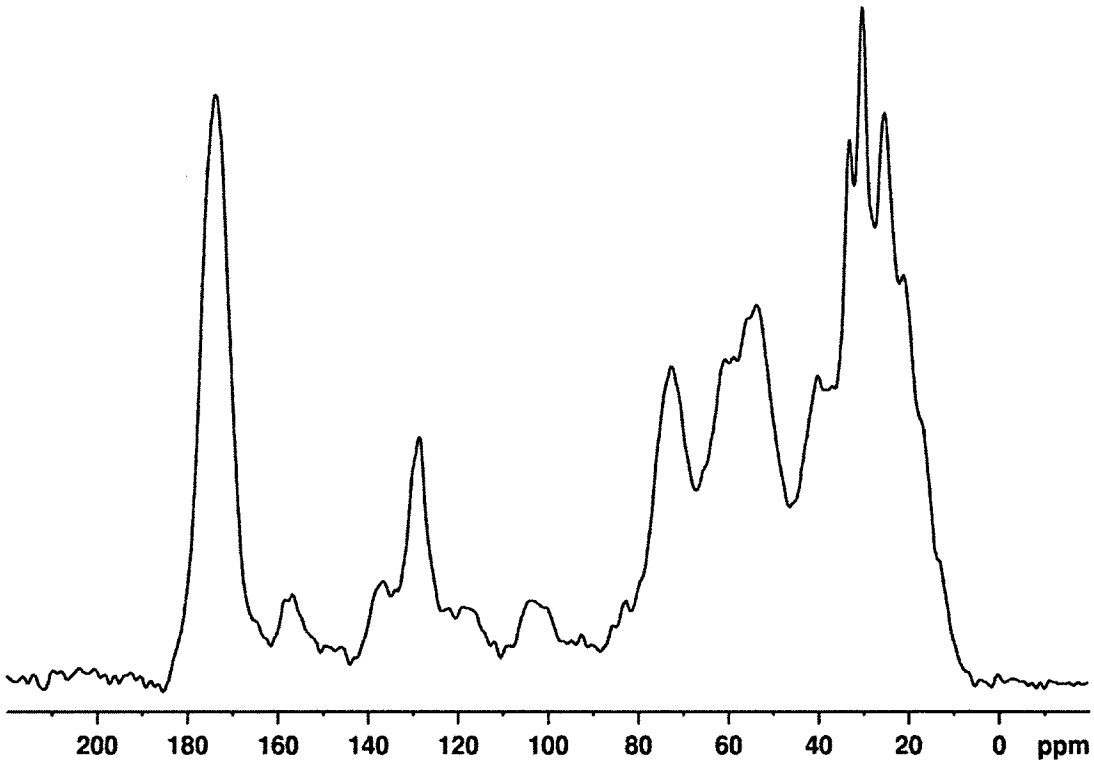

Figure 6. ^{13}C ssNMR for lyophilized algae.

3.2 Algaenan isolation procedure by the Zelibor et al. (1988) method

3.2.1 Carbon-13 solid state NMR

Figure 7 shows CPMAS ^{13}C NMR spectra obtained after each extraction step for

the Zelibor et al. (1988) procedure. The lipid portion constitutes around 21.3 % wt. of the dried algae biomass (Table 5). After the lipid extraction step (Figure 7A), we notice a decrease in the relative proportion of the aliphatic region 0 – 45 ppm from 40.6 % to 35.1 %. This change is expected as the lipids are being removed from the residue. In addition, we notice an increase in the signals at 174 ppm (carboxyl and amide groups) and between 45 and 60 ppm (α-carbon of proteins); this increase is the result of the relative enrichment of the amide groups in proteins as the lipids are removed from the algae. It is worth mentioning that proteins and carbohydrates appear to be minimally affected by this extraction extrapolating from the fact that their corresponding peaks are not significantly changed relative to each other. The peak areas only change in proportion to the loss of signal in the aliphatic region due to the loss of lipids extracted. The ratio of proteins to carbohydrates 95 – 110 ppm both before and after the Soxhlet extraction remains relatively constant (6.2 and 6.1, respectively). It is important to note that the losses mentioned above and in subsequent discussions are for the individual steps of each process condition. With increasing amount of processing there is a cumulative weight loss as shown in Table 5. One can examine the net change in NMR spectral areas normalized to the carbon loss that has occurred. We were not able to measure carbon losses directly but have weight losses that can also be used for this purpose, with admittedly less accuracy. The normalized cumulative areas for each step of the process are parenthetically shown in Table 6.

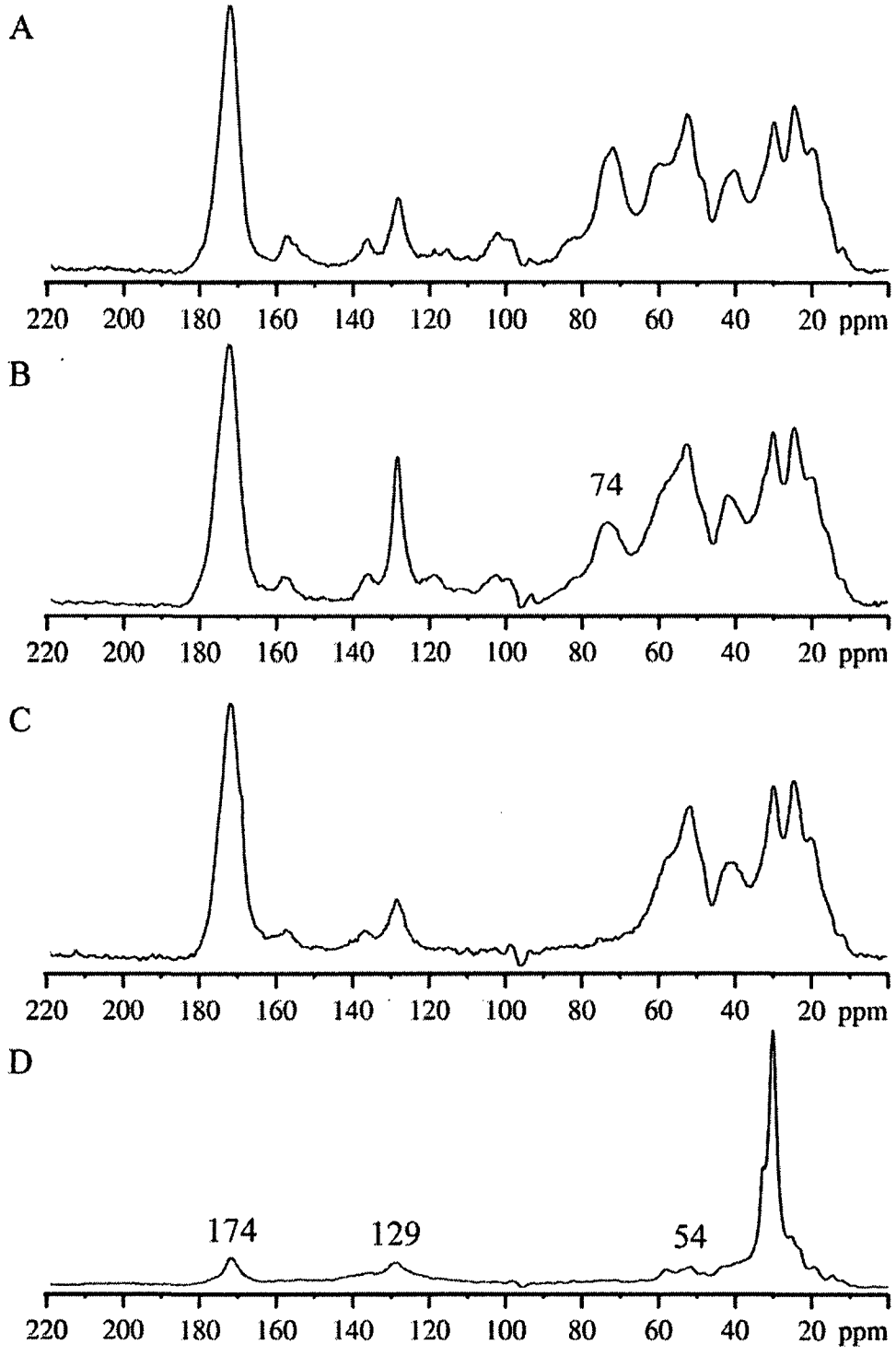

Figure 7. ^{13}C ssNMR of residues after each extraction step using Zelibor et al. (1988) procedure. A) After lipid extraction. B) After 0.5 N NaOH. C) After sodium paraperiodate treatment. D) After 18 h 6 N HCl treatment (algaenan).

Table 6. Area normalized to 100 % for different regions of ^{13}C ssNMR spectra after each isolation step [a]. Values in parenthesis are normalized to the weight % in Table 5 [b].

NMR Region (ppm)	*Dried Algae Biomass*	*After Soxhlet Extraction*	*After NaOH treatment*	*After Paraperiodate Treatment*	*After HCl treatment /Algaenan*
Zelibor et al. (1988)					
0 – 45	40.6	35.1 (27.6)	37 (26.4)	42.4 (11.8)	61.4 (7.3)
45 – 60	13.5	16.7 (13.1)	17.4 (12.4)	19 (5)	5.2 (0.6)
60 – 95	16.3	18.1 (14.2)	13.5 (9.6)	5.5 (1.5)	0.8 (0.1)
95 – 110	2.2	2.7 (2.1)	1.7 (1.2)	Bdl	1.4 (0.2)
110 – 150	8.7	6.5 (5.1)	9.2 (6.6)	5.8 (1.6)	17.8 (2.1)
150 – 164	1.7	1.7 (1.3)	0.9 (0.6)	1.1 (0.3)	3.4 (0.4)
164 – 190	16.4	19 (15)	20 (14)	26 (7.2)	8.7 (1)
190 – 220	0.8	Bdl [c]	Bdl	1 (0.3)	1.4 (0.2)

NMR Region (ppm)	*Dried Algae Biomass*	*After Lipid removal*	*After TFA Treatments*	*After HCl/ Before Basic Treatment*	*After Basic Treatment/ Algaenan*
Allard et al. (1998)					
0 – 45	40.6	34.6 (27.7)	46.4 (17.5)	69.8 (7.5)	73.7 (3.2)
45 – 60	13.4	15.4 (12.3)	5.3 (2)	5.4 (0.6)	4.1 (0.2)
60 – 95	16	19 (14)	26 (10)	1.8 (0.2)	2.8 (0.1)
95 – 110	2.2	2.7 (2.2)	5.9 (2.2)	1 (0.1)	1.4 (0.1)
110 – 150	8.7	7 (6)	9.7 (3.7)	13.8 (1.5)	12.9 (0.6)
150 – 164	1.7	2 (2)	1.4 (0.5)	2.4 (0.3)	2 (0.1)
164 – 190	16.4	18.6 (14.9)	3.9 (1.5)	4.4 (0.5)	2 (0.1)
190 – 220	0.8	0.7 (0.6)	1 (0.4)	1.4 (0.1)	1.2 (0.1)

NMR Region (ppm)	*Dried Algae Biomass*	*After Cell Wall Isolation*	*After amylase treatment*	*After Acid treatment*	*After Basic Treatment/ Algaenan*
Blokker et al. (1998)					
0 – 45	40.6	42.4 (37)	43.1 (28.1)	56 (24)	67.3 (3.2)
45 – 60	13.5	13.8 (12)	13.8 (9)	12 (5)	6.7 (0.3)
60 – 95	16	16 (14)	16 (10)	5.7 (2.4)	7.2 (0.3)
95 – 110	2.2	1.8 (1.6)	2.8 (1.8)	1.3 (0.6)	1.8 (0.1)
110 – 150	8.7	7.6 (6.6)	7.2 (4.7)	10.4 (4.4)	7.9 (0.4)
150 – 164	1.7	1.5 (1.3)	1.2 (0.8)	1.4 (0.6)	1.9 (0.1)
164 – 190	16.4	16.9 (14.8)	14.8 (9.6)	12.6 (5.3)	6.2 (0.3)
190 – 220	0.8	0.24 (0.21)	1.3 (0.8)	0.6 (0.3)	1.1 (0.1)

[a] Note: Maximum relative error was calculated for each spectral section as follows: 1) The error was assumed to be a result of the contribution of the area of the noise to the area of each region. 2) The area of each region was determined by integration (A_{region}). 3) A region of noise with the same spectral width as each corresponding region was integrated and its area determined (A_{noise}). The error was calculated to be A_{noise}/A_{region} * 100. Errors are as follows: 0-45 ppm (1 %); 45-60 ppm (5 %); 60-95 ppm (8 %); 95-110 ppm (10 %); 110-150 ppm (3 %); 150-164 ppm (14 %); 164-190 ppm (5 %); 190-220 (18 %).

[b] Normalized area values were included to more easily follow the losses. Weight % was used as a proxy for carbon.

[c] Bdl: below detection limit.

The original Zelibor et al. (1988) procedure includes an additional step between the lipid removal and the weak base extraction; it involves the extraction of the residue by a 0.01 N HCl solution. Originally this step was used to isolate the low molecular weight compounds in soil samples as part of the process for the isolation of humin. Inspection of the NMR spectrum (not shown) of the residue after this step showed no significant changes in the structure of the algae residue. This led us to believe that this step could be omitted without affecting our extraction.

The next step is the overnight treatment with 0.5 N NaOH at room temperature (Figure 7B). In the Zelibor et al. (1988) procedure, the basic extraction step occurs at an earlier stage than that in either the Allard et al. (1998) and Blokker et al. (1998) procedures. Its intent is to isolate humic acids, compounds soluble in basic solutions but not in acid solutions, from soil and sediment samples. Unlike the Allard et al. (1998) and Blokker et al. (1998) procedures that use a strong base under reflux, this step is performed at room temperature. After the base extraction, we observe multiple changes. The extracted fraction constitutes around 7.4 % wt. of the original algae (Table 5). While the carbohydrates seem to relatively decrease (peaks at 105 and 73 ppm), peaks corresponding to proteins (peak at 53 ppm and amide at 174) slightly increase. This could be a result of the solubility of some carbohydrates in the basic media. The concentrations of protein characteristic peaks after this treatment relatively increase. This suggests that either they are not affected by this treatment or that they are removed less readily than carbohydrates.

The next step (Figure 7C) is treatment with sodium paraperiodate used for the removal of carbohydrates, (Ritchie and Purves, 1947). The paraperiodate complexes with

vicinal diols, breaks the C-C bond between them and oxidizes them to aldehydes resulting in smaller, more soluble carbohydrate moieties. The removal of the carbohydrates is clearly observed by the disappearance of the carbohydrate characteristic peaks (72 and 105 ppm) following this treatment. The residue left is 27.8 % wt. of the original dried algae which suggests that the carbohydrates constitute approximately 43.5 % wt. of the original lyophilized sample.

The final step in the algaenan extraction is to remove the proteins; this is accomplished through a strong acid hydrolysis (Figure 7D). In the original Zelibor et al. (1988) procedure, the hydrolysis was for 2 h. After the 2 h hydrolysis, we notice that the protein characteristic peaks at 54 and 174 ppm have not disappeared completely (data not shown). Total loss of the peak at 174 ppm is not expected because we have determined that ester functionalities exist in the algaenan and these resonate at this same chemical shift. It is clear that either the 2 h hydrolysis is not sufficient for the complete removal of proteins from the algaenan structure and/or that the algaenan is shielding the proteins from hydrolysis. Zang et al. (2001) and Nguyen et al. (2003) have suggested that the algaenan incorporates or encapsulates the proteins and shields them from hydrolysis and degradation. To test this, we increased the hydrolysis time stepwise at 2 hours intervals and monitored the changes. The protein content in the algaenan decreased as hydrolysis time increased to about 8 hours. Further, hydrolysis failed to remove more of the proteins, even after 18 h of hydrolysis as evident from the peak at 54 ppm which has not been removed (Figure 7D). This leads us to consider that there are some proteinaceous materials remaining encapsulated in the paraffinic algaenan structure shielded from HCl hydrolysis. The algaenan remaining from this extraction constitutes around 11.9 % wt. of

the original lyophilized algae. This leads us to deduce that the algae sample contains around 15.9 % wt. proteins that can be removed by HCl hydrolysis. NMR analysis shows that the final algaenan isolated by the Zelibor et al. (1988) procedure is highly aliphatic with 61.4 % of the carbons in aliphatic form. It is interesting to see both peaks at 30 and 33 ppm which have been shown to correspond to the amorphous and crystalline polymethylene groups in other aliphatic biopolymers such as cutan (Sachleben et al., 2004), respectively. The crystalline polymethylene groups assume a crystalline structural arrangement when the successive methylene groups are oriented in an *all-trans* configuration. Mixtures of *trans* and *gauche* configurations lead to amorphous character. NMR analysis of residues after each successive HCl treatment shows an increase in the ratio of amorphous to crystalline methylene groups as the reaction time increases. This behavior is typical of polymers that are exposed to temperatures higher than the transition temperature (T_g) of the polymer and is readily observed in cuticular polymers (Sachleben et al., 2004). The bifurcation of the polymethylene peak was not observed previously by Zelibor et al. (1988) because the NMR field strength was insufficient to resolve the subtle chemical shift change.

3.2.2 Pyrolysis GC-MS on Algaenan

Pyrolysis of the algaenan extracted with the modified Zelibor et al. (1988) procedure (Figure 8A) shows a strong dominance of an *n*-alkane/*n*-alkene homologous series (C_6 – C_{33}) across the chromatogram. The distribution of peaks shows three characteristics; for C_8 – C_{15} compounds the peak intensities increase systematically, for C_{15} – C_{23} the peak intensities remain relatively constant, and for C_{23} – C_{33} the intensities decrease systematically. It is typical of algaenan to produce such a distribution of peaks.

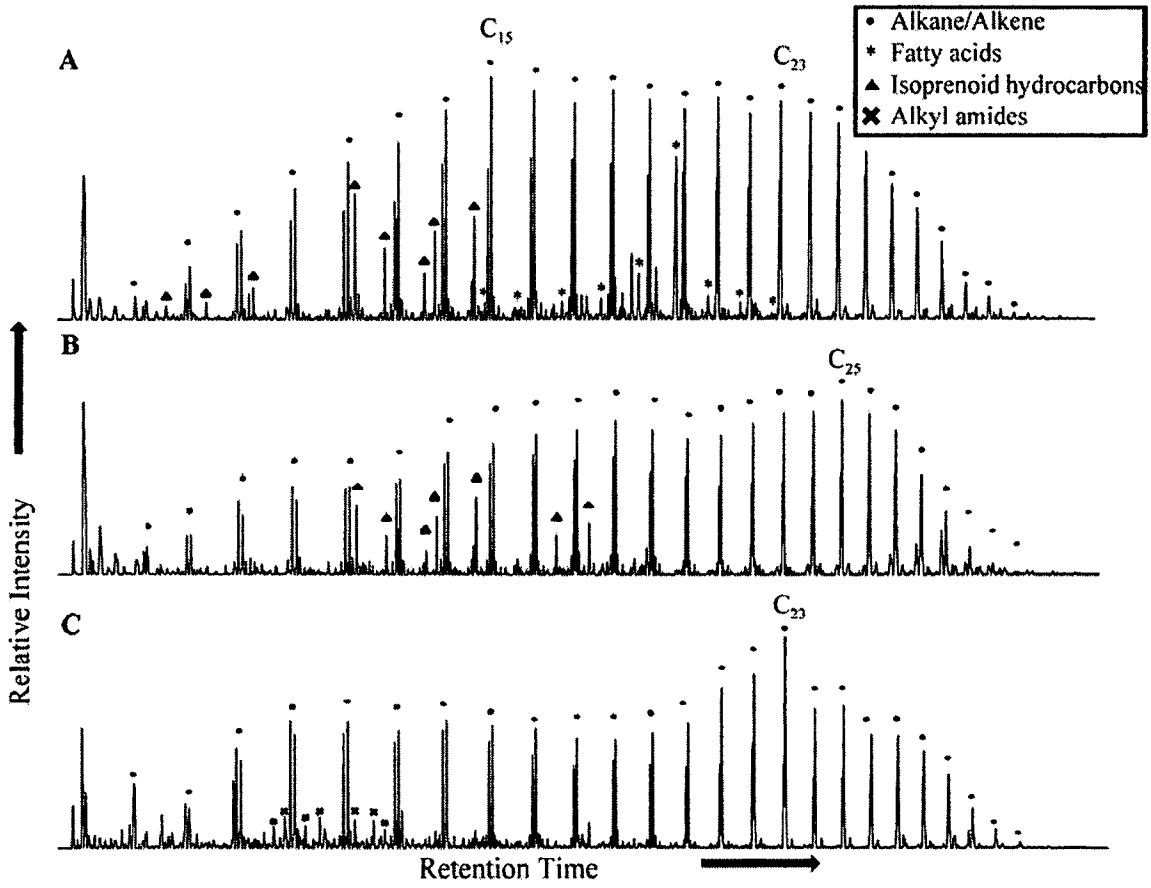

Figure 8. GC chromatogram of pyrolyzed algaenan extracted by A) Zelibor et al. (1988) B) Allard et al. (1998) C) Blokker et al. (1998). Annotations are explained in the legend and *n*-alkane/alkene carbon numbers listed above selected peaks. The small peaks that are not assigned in the chromatogram could not be identified with confidence.

We also observe the presence of isoprenoid alkanes with chain distributions from C_{11} – C_{18} and two monounsaturated isoprenoids; however, they are less dominant than linear hydrocarbons. We also observe a homologous series of fatty acids (73 *m/z*) in the pyrolyzate (C_{11} – C_{24}) with C_{16} being the dominant peak. In order to determine if those fatty acids originated from the algaenan base structure or if they were from free fatty acids that are released as a result of the HCl hydrolysis procedure, we performed a 1 h 2:1

(v:v) $CHCl_3$:MeOH extraction and pyrolyzed again. We observed no change in the pyrolyzate chromatogram. This, in addition to evidence from NMR (the peak at 174 ppm remains unchanged after multiple extractions) indicates that the fatty acids released result from the cleavage of ester linkages in the algaenan produced by the Zelibor et al. (1988) method (Bailey and Turek, 1956; Bailey and Bird, 1977). For long-chain esters, the cleavage occurs between the carbon-oxygen bond forming the acid and an olefin by a concerted mechanism and a quasi-six-membered ring intermediate. The olefin produced can undergo further free radical decomposition forming shorter chain paraffins and olefins.

3.3 Algaenan isolation by the Allard et al. (1998) procedure

3.3.1 Carbon-13 solid state NMR

Figure 9 shows CPMAS ^{13}C NMR spectra obtained after each treatment step for the Allard et al. (1998) procedure. After the lipid extraction step (Figure 9A), we notice similar effects as the Zelibor et al. (1988) procedure, a decrease in the aliphatic peaks while peaks for carbohydrates and proteins proportionally unchanged relative to each other (Table 6). After the extraction of the lipids, the residue remaining constitutes around 80 % wt. of the original lyophilized algae. This means that 20 % wt. of the algae is removed by this step. Although the procedure uses different solvents to remove the lipids, it solubilizes approximately the same portion of lipids as that of Zelibor et al. (1988). The small discrepancy is probably due to the higher efficiency of Soxhlet extraction.

The next step is the treatment with multiple TFA extractions (Figure 9B). The residue remaining constitutes 37.7 % wt. of the original algae. The portion removed by

the TFA treatment is around 42.3 % wt. of the original algae. From NMR data (not shown) we observe that the protein characteristic peak (53 ppm) along with the peak at 174 ppm (carboxyl and amide groups) decreases sequentially as we increase the concentration and reaction time for the TFA. In the final residue (treated with both 2 M and 4 M TFA) we observe only a small residual of proteins as shown by the presence of a relatively small signal at 53 and 175 ppm. Even though the test for determining when to stop increasing the TFA concentrations and terminate the treatment is when the water wash yields negative assays for carbohydrates, the final residue indicates the presence of some residual carbohydrates that are not released and solved. This is also highlighted by the fact that after the TFA treatments, the carbohydrate characteristic peaks are relatively enriched in the residue. Perhaps the TFA could not effectively access some of the carbohydrates in the algaenan. It is important to note that peaks for carbohydrates are rather well resolved and contain resonances observed only in pure crystalline cellulose (88 ppm and 65 ppm) (Earl and Vanderhart, 1981). Perhaps the TFA is ineffective because crystalline cellulose is less accessible to the TFA.

The next step is to treat the TFA-extracted residue with 6 M HCl for 18 h, after which the carbohydrates nearly complete eliminated (Figure 9C). The residue remaining is 10.7 % wt. of the original residue, a yield comparable to that obtained using the Zelibor et al. (1988) procedure. The peak at 54 ppm remains relatively unchanged with this treatment indicating that the proteins are unaffected by hydrolysis and are perhaps shielded from the HCl hydrolysis by the structure of the algaenan. This is the same observation made for the algaenan isolated by the Zelibor et al. (1988) procedure.

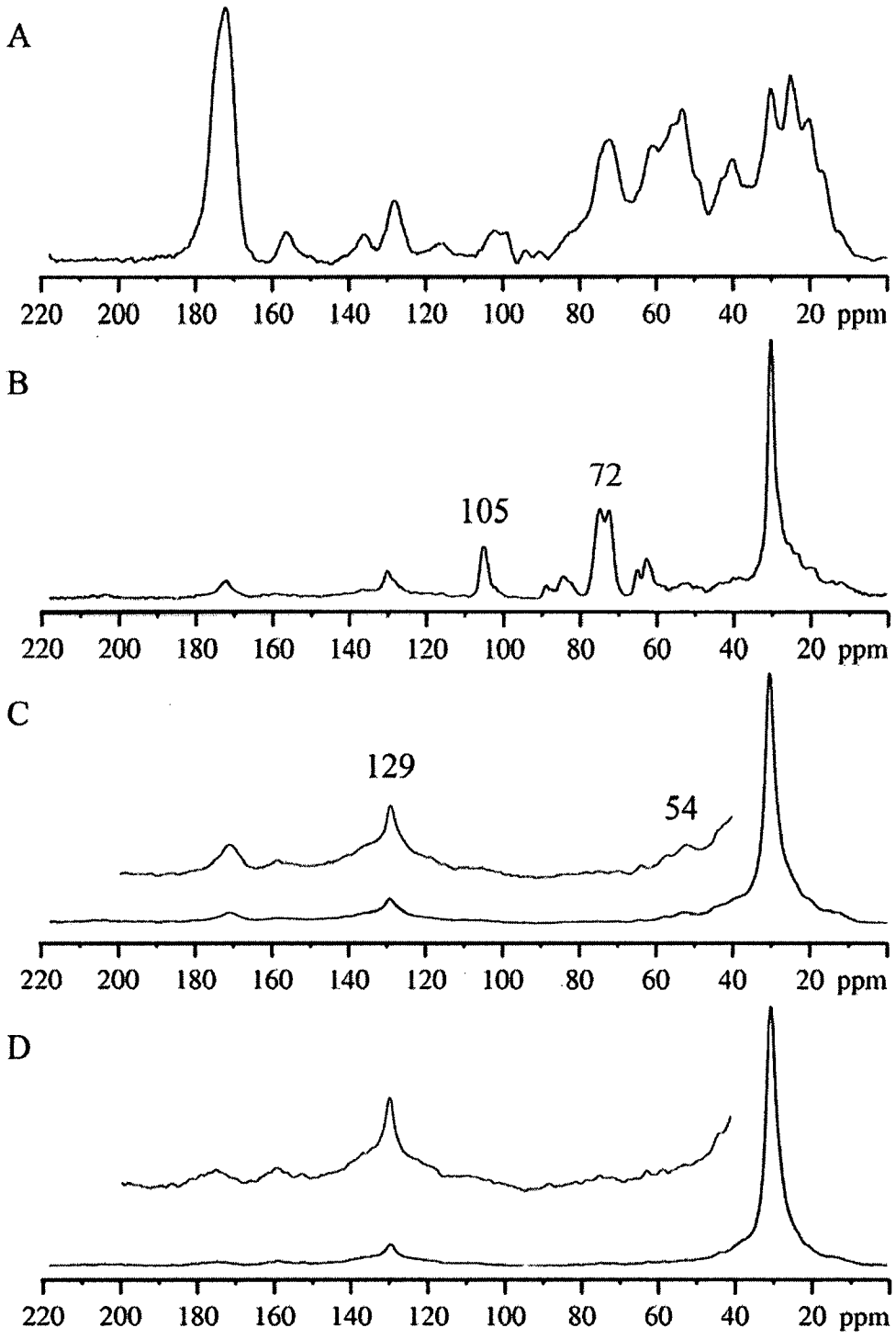

Figure 9. ^{13}C ssNMR of residues after each extraction step using Allard et al. (1998) procedure. A) After lipid extraction. B) After total TFA extractions. C) After 18 h 6 N HCl treatment. D) After 2-methoxyethanol/KOH basic extraction.

Next, we subject the acid-hydrolyzed residue to a 2-methoxyethanol/KOH base extraction for 1h under reflux. The residue remaining from this extraction (algaenan) is 4.4 % wt. of the original lyophilized algae. This treatment removed an additional 6.4 % wt. (relative to the lyophilized algae) compared to the previous residue. Following the extraction, we notice a disappearance in the peak at 54 ppm and a decrease for that at 174 ppm (Figure 9D), indicating that there are no encapsulated proteins remaining. The presence of 2-methoxyethanol during treatment with a strong base in the Allard procedure opens the possibility for the formation of the 2-methoxyethyl ester (R-COO-CH_2-CH_2-OCH_3). The possible transesterification as well as the strong base would effectively cleave the ester functionalities that are possible linkages in algaenan. This alteration of the long chain intramolecular esters could expand the structure of the algaenan and could relax the encapsulation of proteins within the algaenan matrix. The small peak at 73 ppm and a smaller peak at 65 ppm may correspond to signals from carbons associated with methoxyethyl groups. Moreover, the ester peak is shifted downfield slightly (178 ppm) compared with esters prior to treatment (174 ppm), strongly suggestive that transesterification/base hydrolysis has occurred. Finally the algaenan is washed with multiple solvents whereupon no significant changes in the NMR spectra are observed. This remaining residue is labeled final algaenan.

3.3.2 Pyrolysis GC-MS on Algaenan

The pyrolysis of the final algaenan extracted by the Allard et al. (1998) procedure (Figure 8B) shows a strong predominance of the *n*-alkane/*n*-alkene homologous series that ranges from $C_6 - C_{33}$ with a bimodal distribution at C_{15} and at C_{25}. We also observe the same isoprenoid distribution (between C_{12} to C_{15}) as that for the algaenan extracted

with the Zelibor et al. (1988) procedure but with different intensities. The intensities for these isoprenoids are higher for the algaenan isolated by the Allard et al. (1998) procedure. One difference in the isoprenoid distributions is the absence of the first three isoprenoids (between C_8 and C_{11}) that were identified in the Zelibor et al (1988) chromatogram but not in the Allard et al (1998). These isoprenoids still appear in the Allard et al. (1998) chromatogram but are very small and could not be confidently identified by their fragmentation pattern despite having the same retention time. The similar situation can be observed with the higher homologues (between C_{16} and C_{18}) that appear in the Allard et al. (1998) chromatogram but not the Zelibor et al. (1988). The compounds are there but they are very weak. Another noticeable difference is that the pyrolyzate of the algaenan extracted from the Allard et al. (1998) procedure did not contain fatty acids. This could result from the presumed 2-methoxyethanol/KOH transesterification which can destroy the long ester chain and form the 2-methoxyethyl ester. To test our hypothesis, we pyrolyzed a sample of the Allard algae before the basic treatment. We noticed that before the basic extraction, the pyrolyzate contained fatty acid peaks. In fact, the pyrolyzate had the same distribution of fatty acids as that of the algaenan extracted with the Zelibor et al. (1988) procedure (not shown). This result is consistent with the NMR data showing that transesterification with 2-methoxyethanol/KOH destroys ester functionalities in the algaenan structure. Considering the fact that esters are the likely cross-links for algaenan, loss of encapsulated proteinaceous substances, which were entrapped within the algaenan structure, would be expected as these cross-link points are eliminated and the algaenan structure opens up.

3.4 Algaenan isolation by the Blokker et al. (1998) procedure

3.4.1 Carbon-13 solid state NMR

Figure 10 shows CPMAS ^{13}C ssNMR spectra obtained after each treatment step for the Blokker et al. (1998) procedure. The solid residue following the Potter homogenation constitutes 87.3 % of the total algae mass. This residue consists mainly of the fully separated cell walls from the cytoplasm so that only the cell walls are subjected to chemical treatments later on. ^{13}C ssNMR on the residue (Figure 10A) shows no drastic differences in the peaks with that of the original algae. Alternatively, when comparing the relative area percentages we see some slight differences. The areas of the peaks between 0 – 60 ppm and 160 – 190 ppm relatively increase compared with those of the rest of the spectra. This increase is only about 2.1 % (Table 6) and hence shows that there is no significant change in the chemistry of the residue. One noticeable difference between this spectrum and those of the solvent extraction residues of the two previous methods is the survival of the peak at 33 ppm. The first organic solvent extraction step in the Blokker et al. (1998) procedure comes after the Potter homogenation step. This extraction differs from the two other procedures in that it is performed ultrasonically and without external heating of the solvents. This may be a key factor for preserving the crystallinity of this algaenan structure. Hot organic solvents used in the Zelibor et al. (1988) and the Allard et al. (1998) procedures could be swelling the algaenan structural component and transforming crystalline carbons into amorphous carbons. It is well known that crystalline polymers can be transformed to their non-crystalline state by use of solvents at elevated temperatures (Scheirs, 2000).

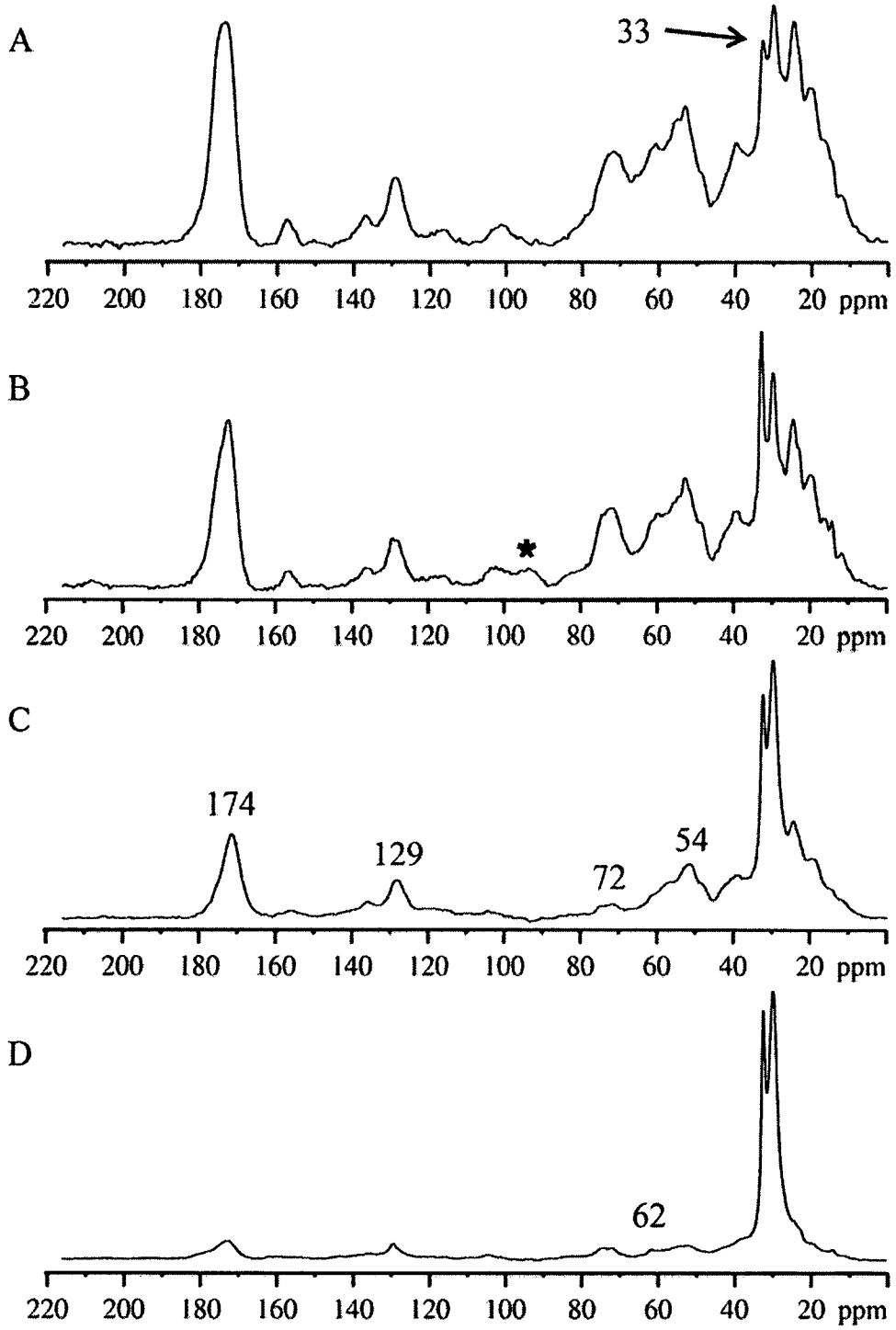

Figure 10. ^{13}C ssNMR of residues after each extraction step using Blokker et al. (1998) procedure. A) After Potter homogenation. B) After α-amylase treatment. Sample was spun at 8 kHz (* denotes spinning side band). C) After H_2SO_4 treatment. D) After methanol/KOH basic extraction.

The next step is the treatment with α-amylase enzyme to remove the carbohydrates that are in the algal residue. The ^{13}C ssNMR spectrum of the residue did not show very significant changes in the peaks 72 – 105 ppm characteristic of carbohydrates (Figure 10B). The results lead us to deduce that the treatment is ineffective in removing all carbohydrates that reside in the *Scenedesmus* cell wall matrix. The α-amylase enzyme has the ability to hydrolyze α-(1,4) glycosidic bonds in some types of carbohydrate molecules such as starch and glycogen to break them into their monomers (Stenesh, 1998). Although *Scenedesmus* cell walls contain starch, they mostly contain cellulose (Lee, 2008) that is not hydrolyzable by the α-amylase enzyme causing it to remain in the residue. Table 5 shows that, following the treatment with α-amylase, the remaining residue is 22.2 % lighter; while as that from the paraperiodate treatment in the Zelibor et al. (1988) process resulted with a residue that is 43.5 % lighter. This result gives us reason to believe that, for *Scenedesmus*, the paraperiodate treatment is more effective.

The next step in the Blokker et al. (1998) procedure is the removal of the soluble lipid portion from the algae by a series of organic solvents MeOH, MeOH/DCM (1:1, 2x), DCM/hexane (1:1, 2x) and hexane (1x) with decreasing polarity. The remaining residue is 22.7 % lighter following the extractions. This result compares very favorably to lipid extractions from the Zelibor et al. (1988) and the Allard et al. (1998) which the organic solvent extractions resulted in a removal of 22.4 % and 20.0 % of the weight respectively.

Figure 10C shows the ^{13}C ssNMR spectrum of the residue after the 2 M H_2SO_4 reflux for 2 h. Following the treatment, we notice a decrease in the areas between (45 – 60 ppm) corresponding to proteins, it is interesting to see that there still remains a

significant amount of proteins following the treatment. Although we saw proteins survive an acid reflux treatment with both the Zelibor et al. (1988) and Allard et al. (1998) treatments, the amount of proteins remaining in the residue is significantly more in the Blokker et al. (1998) treatment. This seems to suggest that 2 hours of reflux is not sufficient to hydrolyze all the accessible proteins, analogous to the observations made with the Zelibor et al. (1988) and the Allard et al. (1998) procedures. We also notice a decrease in the areas between (72 – 105 ppm) characteristic of carbohydrates with the Blokker et al. (1998) procedure. When comparing with the Zelibor et al. (1988) and the Allard et al. (1998) procedures where no peaks are observed in the carbohydrate region after acid hydrolysis, the Blokker et al. (1998) procedure is not as effective in removing carbohydrates. Blokker et al. (1998) identify those peaks as carbons connected via ether oxygen which normally resonate in the same region. However, the existence of a ^{13}C ssNMR peak at 72 ppm and an additional peak at 105 ppm for the anomeric carbon of carbohydrates seems to suggest that these peaks correspond to unhydrolyzed carbohydrate peaks.

The last step in the algaenan isolation is the reflux of the solid residue with KOH in MeOH for 1h. Figure 10D shows the ^{13}C ssNMR of the remaining residue. Following the treatment, the remaining residue is of highly aliphatic nature with the major peaks being at 30 and 33 ppm representing the amorphous and crystalline polymethylene structures. In the NMR spectrum presented by Blokker et al. (1998), the amorphous and crystalline peaks are not resolved due to the lower resolving power of the spectrometer used. The spectrum shown in Figure 4D shows some important changes compared with the spectrum of Figure 10C. First, we notice that the peaks at 174 and 54 ppm have

diminished significantly; this is similar to what is observed in the respective spectrum from the Zelibor et al. (1988) procedure for the removal of proteins. It is expected that the protein peaks would be completely removed following the base treatment, similar to the effect observed following the base extraction in the Allard et al. (1998) procedure; however, the existence of residual protein signals (peaks at 54 and 174 ppm) suggests that the base is not as effective as expected in the removal of proteins and could result in the formation of alkyl amides as observed with pyrolysis (see section below). Allard et al. (1997) noted that the existence of carbohydrates and proteins under basic conditions of hydrolysis could produce artifacts. Considering the fact that some carbohydrates and proteins remain in the residue prior to base hydrolysis suggests that there is a possibility that the Blokker et al. (1998) procedure could introduce artifacts. The existence of residual carbohydrate peaks at 70 – 80 ppm and 105 ppm indicates that these survive the treatment.

3.4.2 Pyrolysis GC-MS of Algaenan

The pyrolysis of the final algaenan extracted by the Blokker et al. (1998) procedure (Figure 8C) shows a strong predominance of the *n*-alkane/*n*-alkene homologous series that ranges from $C_6 - C_{32}$ with a bimodal distribution maximizing at C_{12} and C_{23}. The *n*-alkane/*n*-alkene pattern is only slightly different than the ones observed for the algaenans from each of the other isolation procedures. Contrary to what is observed with the Zelibor et al. (1988) and the Allard et al. (1998) isolated algaenans, isoprenoid hydrocarbons and the fatty acids are not found in the pyrolyzate. When we examined the residue before the base reflux treatment, we observed fatty acids and isoprenoids in the pyrolyzate. This is similar to the changes observed with the pyrolyzate

of the residues from before and after the base treatments with the Allard et al. (1998) process. One noticeable difference with the chromatogram of the Blokker et al. (1998) algaenan is the appearance of some pyrolysis peaks identified as alkyl amides ranging from C_8 to C_{10}. These are not present in the chromatograms of the algaenan samples from the other two procedures. The amides observed are likely to be artifacts considering that they are only observed in algaenan isolated by the Blokker et al. (1998) procedure that utilizes a strong alkaline hydrolysis under reflux as the final treatment to remove residual proteinaceous materials. We suggest that this alkaline reflux along with the occurrence of proteins could be releasing ammonia which reacts with esters to form alkyl amides through an amidation reaction (McKee and Hatcher, 2010). The Allard et al. (1998) procedure also uses an alkaline reflux in the workup but our NMR spectra show that proteinaceous materials are not present in the residue subjected to the alkaline hydrolysis. Thus, the release of ammonia is avoided. The production of amides from an amidation reaction partly explains the observed lack of isoprenoids only in the algaenan isolated by the Blokker et al. (1998) procedure. Salmon et al. (2009a) showed that algaenan from another algae (*Botryococcus braunii*) contains a C_{40} isoprenoid that is ester-linked to the main algaenan backbone. If the algaenan from *Scenedesmus* contains isoprenoids linked in a similar fashion, then amidation will rupture the ester and release the isoprenoid from the algaenan. It is also likely that the alkaline hydrolysis alone is able to rupture the ester linkage to remove isoprenoids from the algaenan.

4. CONCLUSIONS

The three different procedures by Zelibor et al. (1988), Allard et al. (1998), and

Blokker et al. (1998) employ the use of chemical techniques that remove biologically labile compounds (lipids, proteins and carbohydrates). The chemical treatments employed in the Zelibor et al. (1988) procedure first removed lipids, then carbohydrates, finally the proteins; and yielded a higher percentage of algaenan (11.9 %), and did not seem to result in the hydrolysis of the ester linkages of the algaenan structure as their byproducts could be detected by pyrolysis. In addition, there seemed to be some proteins encapsulated in the algaenan structure. The chemical treatment employed by the Allard et al. (1998) protocol acted similarly to those in the Zelibor et al. (1988) procedure in removing the labile components of the algae except for two differences: First the order of labile compound removal was different, lipids, proteins, then carbohydrates. To prevent the formation of artifacts it seems that removing proteins first then carbohydrates is preferable. Second, the Allard et al. (1998) procedure included a 2-methoxyethanol/KOH reflux step which led to the transesterification of the ester functionalities that are thought to link the algaenan structure together and appeared to produce the 2-methoxyethyl ester and a final yield of 4.4 % algaenan. The chemical treatment employed by Blokker et al. (1998) first employed the use of a Potter homogenizer to remove the cytoplasm content followed by an enzymatic treatment to remove the carbohydrates. While the mild solvent extraction step apparently preserved the crystallinity of the algaenan polymer, the enzymatic attack did not seem to be successful in removing all the carbohydrates, as it is ineffective in hydrolyzing cellulose. The final procedure was to use methanol/KOH which, in the presence of proteins, resulted in the breaking of esters and formation of alkyl amides. The algaenan yield is also similar to that of Allard et al. (1998) at 4.7 % and both procedures yield a lower quantity of algaenan than that of Zelibor et al. (1988).

This could be due to the use of base hydrolysis at elevated temperatures.

This study shows that the methodology used to extract algaenan from algae has an effect on the structure of the algaenan but all three procedures generally produce an algaenan polymer with more-or-less similar characteristics (e.g., presence of carboxyls, olefinic carbons, and polymethylenic carbons). The macromolecular network of the algaenan structure is very difficult to define since the utilization of any isolation procedures is altering the macroscopic network of the algaenan (e.g. crystallinity of the algaenan polymer, and the nature of oxygenated cross-links). Moreover, we recognize that each isolation method has some advantages and disadvantages. If we accept the aspects that are advantageous for each process and combine them, it is possible to suggest a new procedure for algaenan isolation. Below we suggest an ideal procedure that could be employed in future work.

The first step is to remove the cytoplasm of the algae cell by using a Potter homogenizer to provide the following chemical treatment more access to the isolated cell wall increasing treatment efficiency. Following this we suggest that the Potter homogenized material be extracted with 1:1 (v:v) benzene:methanol for 24 h in a Soxhlet extractor to remove free lipids. The residue is then treated with sodium paraperiodate to remove the carbohydrates from the algae using the mild procedure adapted from Ritchie and Purves (1947). The residue from this treatment is then washed with deionized water and the wash tested for residual carbohydrates using a colorimetric methods [Phenol (1 ml , 5 % wt. aqueous solution) and H_2SO_4 (5 ml, 18 M) are added to 1 ml of solution (Dubois et al., 1956)]. A positive test for residual carbohydrates is represented by an absorbance at 485 nm. If positive, the paraperiodate treatment should be repeated. The

carbohydrate-free residue is then extracted by a 1 h 1:1 (v:v) benzene:methanol extraction. The extracted residue is then refluxed with 6 M HCl for 8 h to remove proteinaceous material. The remaining algaenan is extracted again with 1:1 (v:v) benzene:methanol for 1 h and the resulting residue is freeze dried. Following this procedure, the resulting algaenan would most likely have the least altered structure. It is also likely to contain some encapsulated proteins as it does not seem possible to remove them without employing a base hydrolysis step. We avoid the use of base in this proposed procedure because this approach was found to cleave ester linkages that are part of the integral structure of the algaenan and also can produce artifacts.

CHAPTER III

CONVERSION OF BROWN COAL TO HYDROCARBON BASED OIL BY HYDROUS PYROLYSIS AT SUBCRITICAL CONDITIONS

PREFACE

The majority of the contents in this chapter were published on 2013 in proceedings to the 14th International Conference on Coal Science & Technology. Below is the full citation

Obeid, W., Hatcher, P.G. "Conversion of brown coal to hydrocarbon based oil by hydrothermal liquefaction at subcritical conditions." Proceedings to the 14th International Conference on Coal Science & Technology, October 2013.

It is included in this thesis because of reports in the literature suggesting that a significant portion of the coal is derived from algae. However, more recent literature suggests other sources are more important, even though algae probably contributed to the organic matter at deposition. If algae are the dominant components, then the sample would be an ideal one for study of the propensity of ancient algaenan accumulating in an economically large region to produce oil. The deposit from which the sample originated is geologically extensive.

1. INTRODUCTION

HP, also known as HTL, is growing in interest as a method for production of liquid fuels (Biller and Ross, 2010; Savage, 2012). Major advantages in the use of

hydrothermal liquefaction include the lack of the need for dewatering samples before processing and the lack of necessity for catalysts; eliminating expensive dewatering and catalyst costs. Moreover, the use of water at high temperatures and pressures has been shown to be successful in simulating the natural maturation of organic material in the formation of petroleum (Lewan, 1985; Ruble et al., 2001; Ruble et al., 2003). In effect, such a process, if transformed to become economically viable, could be used on a large scale to produce petroleum-like liquid fuels from organic matter.

Low-rank coals, such as lignite coals, are ideally suited for use as feedstock for HP to produce hydrocarbon based fuels. One advantage is the fact that they are cheaper to use than other types of coals (20 dollars per short ton vs. 80 dollars per short ton for anthracite coal in the U. S. in 2012) (EIA, 2013). This is because they cannot be used in traditional boilers in coal-fired power plants, which are optimized to process high-rank coals, making them less favorable for electricity generation. In fact, only about 8 % of the coals mined for power production in the U.S. are lignites (EIA, 2013). Their high moisture content poses no issues in HP because HP uses water. In addition, their low nitrogen and oxygen content, compared to other types of biomass typically used as feedstock in HP, also makes them ideal for HP. Another advantage for using low rank coals is the fact that they are not thermally mature and typically have a higher proportions of hydrocarbon-producing aliphatic groups than more thermally matured coals, making their potential higher or producing hydrocarbon like fuels

In this manuscript we investigate the use of a brown coal sample from the Moscow basin as a starting material for HP. Previous palynological studies of coal in that region report contributions from algae, fungi, mosses and ferns (Krevelen and Schuyer,

1957). In addition, this coal has a unique property as it was never buried deeply to undergo significant maturation; temperatures are thought to have never risen above 25 °C. As a result, the coals in this basin never reached a temperature required for the formation of bituminous coals and thus are still in the stage of hard brown coals (Larsen and Chilingar, 1967). Thomas and Meyen (1984) have investigated coal samples from the Lower Carboniferous sections of the Moscow basin. They noted large contributions from on type cuticle from stems of a small lycophyte named *Eskdalia*. Certain highly aliphatic biopolymers found in plant material, such as cutan and suberan, have been shown to survive diagenesis and be incorporated in sedimentary deposits and coals (McKinney et al., 1996; Hatcher and Clifford, 1997b; Schouten et al., 1998). Collinson et al. (1994) isolated an *Eskdalia* lycophyte stem cuticle from a Moscow brown coal sample and analyzed it with flash pyrolysis. They noticed that the pyrolyzate were very similar to that of cuticle isolated from *Agave americana*. Both pyrolyzates were dominated by a homologous *n*-alkane/*n*-alkene series typically indicating the presence of the bio-macromolecule cutan in the Moscow brown coal.

We employ the use of multiple analytical techniques to characterize the starting material and the expelled oils. The Moscow brown coal and solid residues were analyzed by ^{13}C ssNMR and py-GC-MS. The expelled oils were analyzed by GC-FID and GCxGC-TOFMS. GCxGC-TOFMS is a powerful tool for separating complex mixtures such as oils. The uniqueness of GCxGC-TOFMS stems from the fact that is adds a second dimension of separation when compared to one dimension gas chromatography techniques. The compounds that coelute in the one dimensional GC chromatogram are separated based on their polarity in the second dimension; increasing polarity results in

an increasing retention in the second dimension. This provides a kind of chemical logic to the separation. With a combination of retention times from two dimensions and a mass spectral analysis, a large number of compounds can be identified and grouped into separate classes.

2. MATERIALS AND METHODS

2.1 Sample description

The sample was collected from the Kimovsk region about 200 km south of Moscow (Figure 11). The sample is from the southern limb of the Moscow basin which is characterized as having shallow carboniferous deposits (Alekseev et al., 1996). The Moscow basin has a north to south extent of about 600 km and an east to west extent of about 1000 km. Alekseev et al. (1996) reported the Moscow basin having a sedimentary thickness more than 2 km in the depocenter. The brown coal of the Moscow basin was formed during the Lower Carboniferous period and is thought to have originated 350 million years ago.

2.1 Carbon-13 solid state NMR

NMR spectra were acquired via a direct polarization magic-angle-spinning (DPMAS) pulse sequence using a 400 MHz Bruker AVANCE II with 1H resonating at 400 MHz and ^{13}C at 100 MHz. The dried solid sample (ca. 80 mg) was placed in a 4 mm NMR rotor and sealed with a Kel–F cap. Samples were spun at the magic angle (54.7°) with a frequency of 13 kHz and a recycle delay of 30s to allow for full T_1 relaxation. All solid state spectra were externally calibrated to the glycine standard (176.03 ppm). More details concerning the conditions are described by Dria et al. (2002).

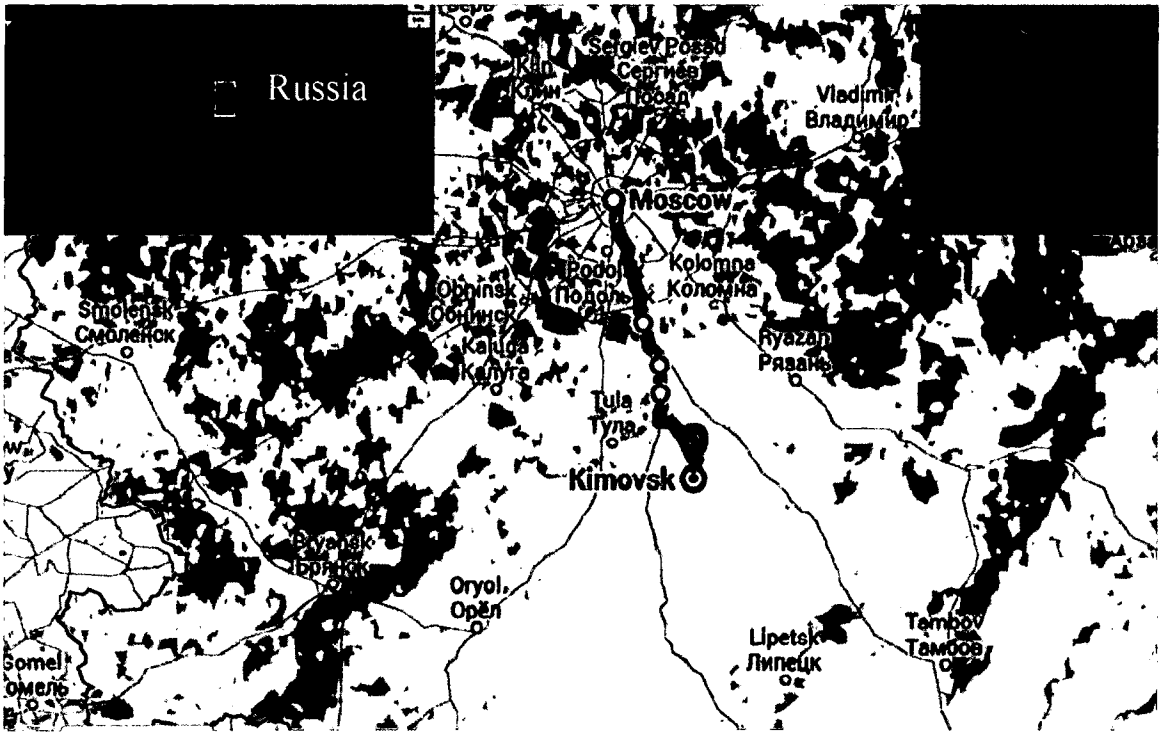

Figure 11. Map showing the Kimovsk region where the sample was collected.

2.3 Hydrothermal treatment

In short, carburized 24 mL stainless steel reactors were filled each with 1 g of brown coal, and 8 mL of distilled water. A 1 mm Cr–Ni screen was placed on top of the solid to prevent it from floating during the progress of the experiment. Sample volume (based on an approximate sample density), reactor volume, and amount of added water were calculated to ensure that the sample remained submerged in a liquid water phase throughout the experiment. The reactor was then flushed with nitrogen gas. Artificial maturation was achieved by isothermal heating of the samples at 360 °C for 24 h, 48 h and 72 h.

2.4 Gas chromatography-flame ionization detection

GC-FID analysis was performed with a Hewlett-Packard HP 6890 series GC system equipped with an HP 6890 injector. The oil samples were injected neat with the GC operating in the split mode (400:1). The FID detector was set at 250 °C and the inlet temperature was held constant at 280 °C throughout the analysis. The signal was measured at a rate of 20 spectra per second. The column used for GC separation has a 30 m x 0.25 mm i.d. with fused silica capillary column with a film thickness of 0.25 μm (5 % phenylpolysiloxane - 95 % ethylpolysiloxane, Agilent J&W DB-5). Helium was used as the carrier gas, with flow rate of 1 ml/min. the oven temperature was programmed as follows: initial temperature was 50 °C, held for 1 min; then for a heating rate of 10 °C /min until the final temperature reaches 300 °C, held for 5 min. Peak identifications were performed by gas chromatography coupled to mass spectrometry.

2.5 Pyrolysis-GC/MS

Py-GC/MS was performed with a Chemical Data Systems (CDS) pyrolysis system 2000 plus coupled to a Leco Pegasus II GC/MS system with the GC operating in the split mode (50:1). The source and transfer line temperatures were maintained at 200 °C and 280 °C respectively. Mass spectra were collected at a rate of 20 spectra per second after a 30 s solvent delay. Masses were acquired at a range between 35 *m/z* and 500 *m/z*. The column used for GC separation has a 30 m x 0.25 mm i.d. with fused silica capillary column with a film thickness of 0.25 μm (5 % phenylpolysiloxane – 95 % methylpolysiloxane, Restek Rtx-5). Helium was used as the carrier gas, with flow rate of 1 ml/min. the oven temperature was programmed as follows: initial temperature was 50 °C, held for 1 min; then for a heating rate of 10 °C /min until the final temperature

reaches 300 °C, held for 5 min. About 0.1 – 0.2 mg of samples were transferred to precombusted quartz tubes fitted with quartz spacers then covered with glass wool. The samples were placed in an auto sampler which transferred them to the pyrolysis chamber. The temperature of the pyrolysis chamber was held at 300 °C during the short period of sample injection. The samples were then rapidly (0.01 °C/ms) heated to a temperature of 650 °C, and held for 15 s as pyrolysis products were swept into the GC-MS system.

2.6 Two-dimensional gas chromatography - time of flight - mass spectrometry

GCxGC-TOFMS was performed using an Agilent 6890 series GC system (Palo Alto, CA, USA) equipped with a secondary oven, a non-moving quad-jet dual-stage thermal modulator and coupled to a Leco Pegasus 4D time-of-flight (TOF) mass analyzer. The oil samples were diluted in dichloromethane and 1μL was injected in split mode (20:1) in the injector at 280 °C. The primary column used for GC separation has a 30 m x 0.25 mm i.d. with fused silica capillary column with a film thickness of 0.25 μm (low polarity phase; Crossbond® 1,4-bis(dimethylsiloxy)phenylene dimethyl polysiloxane, Restek Rxi-5Sil MS). The secondary column has a 1 m x 0.1 mm i.d. with fused silica capillary column with a film thickness of 0.1 μm (5 % phenylpolysiloxane – 95 % methylpolysiloxane, Restek Rtx-5). The GC conditions are as follows: Helium was used as the carrier gas at a corrected constant flow rate of 1.0 mL/min. The primary oven temperature was initially set to 40 °C with a hold time of 0.5 min; followed by a heating rate of 3 °C/min until the final temperature reached 290 °C, held for 40 min. The secondary oven was set at a +10 °C offset from the primary oven temperature program. The modulator offset was +15 °C relative to the primary oven temperature program. The modulation period was 4 s with 1.3 s hot pulse. Mass spectrometer conditions were as

follows: Ion source was set at 200 °C and in electron ionization mode at -70eV. The spectra were collected for a mass range of 40 *m/z* to 400 *m/z* at an acquisition rate of 100 spectra/second. The transfer line temperature was set at 280 °C and the solvent delay was 360 s. Data was processed using ChromaTOF version 4.50.8.0 .

3. RESULTS AND DISCUSSION

3.1 Starting material

EA of the Moscow brown coal and the residues is shown in Table 7. The original sample had H/C of the sample was 1.5 which is consistent with the sample being a brown coal and hints to and highly aliphatic nature. Figure 12 shows the ssNMR spectrum of the Moscow basin coal sample. The aliphatic region dominates the spectrum (75.0 %) and shows three peaks at 14.8 ppm (terminal methyl groups; $-CH_3$), 30.3 ppm (amorphous polymethylenic chains; $-CH_2-$), and 42.6 ppm (methylene carbon α to quaternary carbon; $-\underline{C}H_2-CR_4$). The high aliphatic content combined with low contribution from the aromatic region (17.2 %) in the solid is typical of this type of immature coal.

Table 7. Elemental analysis of samples. Ash corrected.

	Yield (%)	C (%)	H (%)	N (%)	S+O (%)	Ash (%)	H/C
Original sample	–	74.0	9.2	0.9	15.9	19.5	1.5
Residue after 24 h	80.4	72.5	9.3	0.6	17.6	43.9	1.5
Residue after 48 h	58.0	69.2	4.9	0.6	25.4	44.8	0.9
Residue after 72 h	53.8	68.3	4.1	0.4	27.2	45.1	0.7
Oil after 24 h	0[a,b]	ND	ND	ND	ND	ND	ND
Oil after 48 h	27.7[a]	71.5	10.5	BDL	18.8	ND	1.7
Oil after 72 h	31.1[a]	80.3	11.4	BDL	8.3	ND	1.7

[a] Based on original carbon in brown coal. [b] No expelled oil, small amount of oil formed on the side of reactor and was not collected. ND: not determined. BDL: below detection limit.

The aromatic region contains small peaks at 115 ppm (H-substituted aromatic carbon olefinic carbons), 130 ppm (C-substituted aromatic carbon), and 150 ppm (O-substituted aromatic carbon), in addition to a broad peak from 61 to 90 ppm (heteroatom substituted aliphatic carbon). This distribution of peaks in the aromatic region is characteristic of contribution from lignin (Hatcher and Clifford, 1997a). However, the small peak areas in combination with the absence of lignin by-products from py-GC-MS of the coal and in the GC-FID (see section 3.3 below) of the expelled oil suggest minimal contribution from lignin. The spectrum also shows peaks at 177 ppm (carbon from carboxyl functional group) and 210 ppm (carbon from carbonyl functional group). The fact that the carbon in the coal has survived for a long time period is evidence of its resistivity.

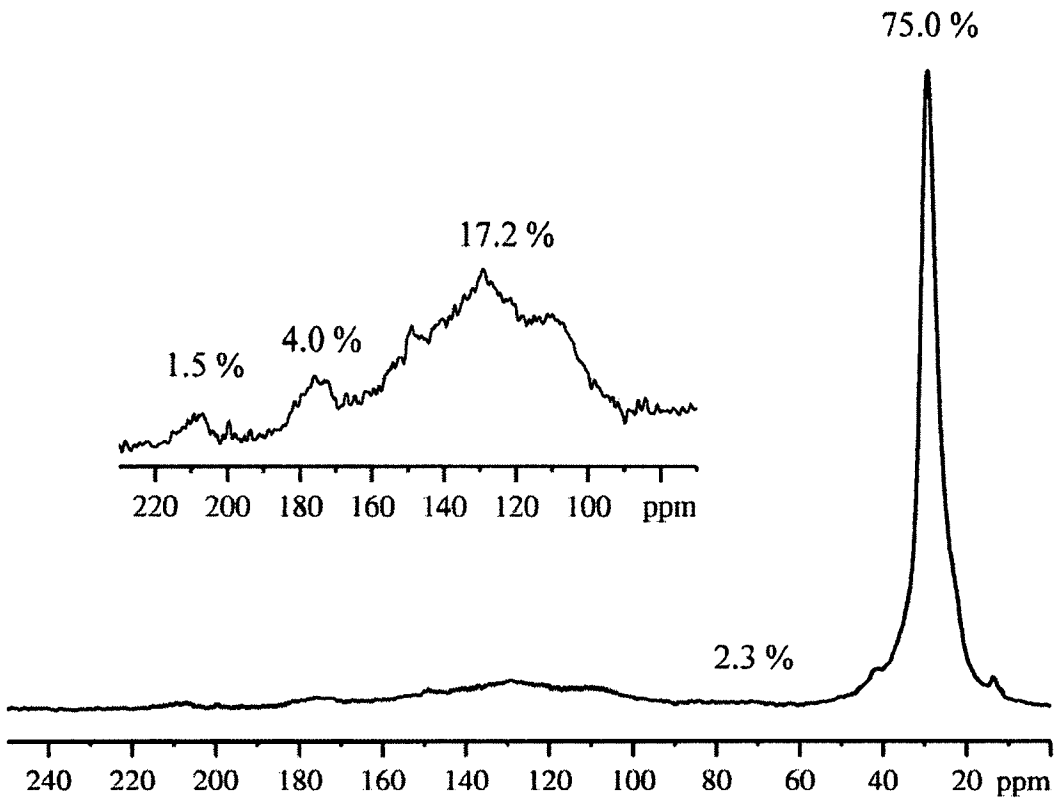

Figure 12. DP-MAS ^{13}C ssNMR spectrum of untreated coal.

Flash pyrolysis chromatogram of the Moscow brown coal sample is shown in Figure 13. The chromatogram shows a major contribution from C_8 to C_{32} *n*-alkane/*n*-alkene homologous series peaks. These products show a non-symmetric tri-modal distribution with three local maxima at C_{11}, C_{17}, and C_{25}. There are no noticeable branched alkanes and alkenes in the pyrolyzate. The fact that branched alkanes don't appear in the pyrolyzate in combination with what was shown with NMR confirms the straight chain aliphatic nature of Moscow brown coal. There are also some minor contributions from the alkyl benzenes and alkyl naphthalene compounds in the pyrolyzate which can originate from either cracking of some of the aromatic components of the coal or from aromatization reactions that occur during pyrolysis. In addition, the

chromatogram shows a fatty acid chain series with carbon numbers ranging from C_8 to C_{23}. The existence of this fatty acid series in addition to evidence of carboxyl group in NMR suggests that the brown coal contains ester linkages within its structure.

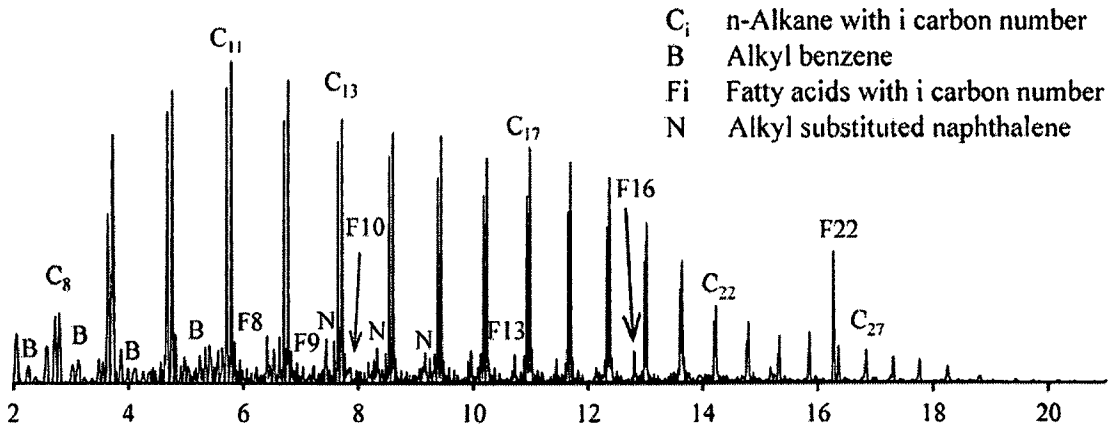

Figure 13. Py-GC/MS chromatogram of Moscow brown coal. Time in minutes.

When combining data from NMR and flash pyrolysis, it seems that the coal sample contains at least three distinctive linked straight-chain aliphatic resistive polymers. There are three known straight chain biologically derived geopolymers that could be responsible for such a distribution: cutan, suberan, and algaenan. Collinson et al. (1994) observed a similar distribution to Figure 12 in the pyrolyzate of fossilized cuticles morphologically identified as *Alethopteris lesquereuxi* pinnule cuticles from the Carboniferous age. The pyrolyzate of the fossilized cuticle showed an *n*-alkane/*n*-alkene distribution with maxima at C_{11}, C_{18}, and C_{24} which they attributed to originating from the pyrolysis of preserved cutan. The strong peak in the chromatogram labeled as F_{22} is not a straight chain fatty acid, its mass spectrum seems to suggest a C_{22} fatty acid with one unsaturation; however, its relative retention time does not fit with that of an aliphatic

fatty acid. Turner et al. (2013) observed a similar high abundance C_{22} compound in the pyrolyzate of suberan, which they identified as the C_{22} lactone (docosanolide). The compound's mass spectrum clearly shows the molecular ion peak at 338 *m/z* along with the $(M-18)^+$ fragment at 330 *m/z* from the loss of water, both having similar percent abundances. In addition, the mass spectrum lacks a dominant peak at 73 *m/z* which indicates that it is not a fatty acid. The existence of the docosanolide is indicative of the existence of suberan in the Moscow brown coal.

3.2 Solid residues

Figure 14 shows ^{13}C ssNMR of the residue following the three HP treatments. The major change observed overall is the relative decrease in the intensity of the aliphatic region compared to that of the aromatic/olefinic region as the heating times increase.

After treatment for 24 h, the aliphatic peak (0 – 50 ppm) area decreases by 12 %. In addition, the peaks at 150 ppm (O-substituted aromatic), 177 ppm (carboxyl), and 210 ppm (carbonyl) disappear. The aliphatic region also shows the same peaks at 14.8 ppm and 30.3 ppm as those for the untreated coal. One difference can be observed however, and that is the appearance of a sharp peak at 22.9 ppm (methylene carbon α to terminal methyl, CH_3-$\underline{C}H_2$-). In the NMR spectrum for the untreated coal it seems that this peak exists but is not as resolved as that for the residue after treatment. This suggests that the aliphatic portion of the residue remaining after the HP treatment is either more mobile or has less variability in its chain length structure.

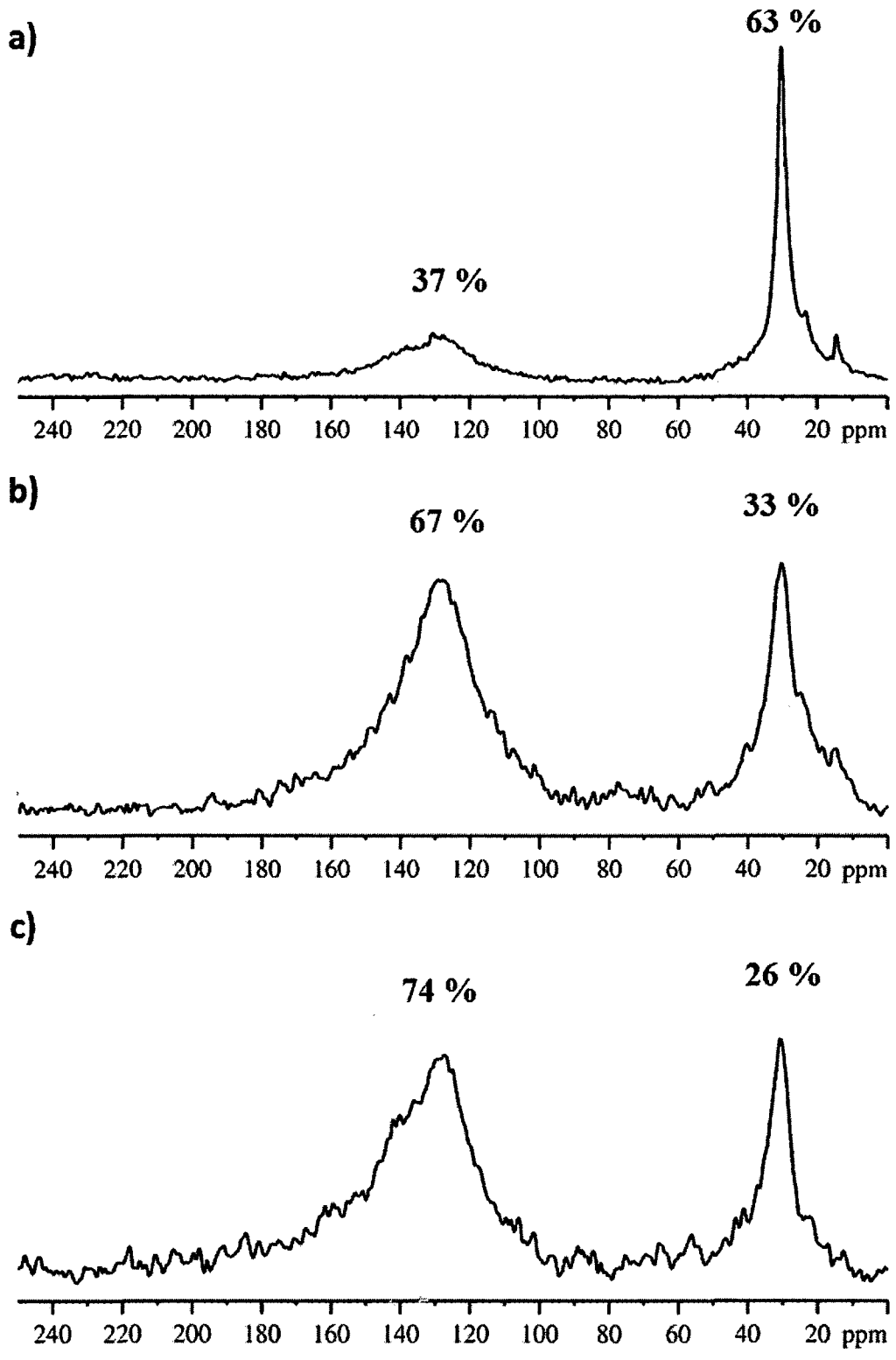

Figure 14. DP-MAS ^{13}C ssNMR spectrum of coal residue after HP at 360 °C for a) 24 h, b) 48 h, and c) 72 h.

Finally, there is a relative increase in the peak at 142 ppm (non-heteroatom non-protonated aromatic carbon). This suggests that there exists a process of aromatization in addition to that of cracking to smaller compounds. This is consistent with the elemental analysis data (Table 7) showing a decrease in the H/C value (1.5 – 1.4).

After treatment for 48 h, the aliphatic region further decreases by 32 % which is coupled by an increase in that of the aromatic region. There is a significant change between the intensities of the peaks at 30.3 ppm, 22.9 ppm, and 14.8 ppm relative to each other. This suggests that the aliphatic portion in the coal sample is cracking and possibly hints to a decrease in its average chain length. Elemental analysis data shows a further decrease in the H/C ratio to a value of 0.9. The decrease in H/C ratio is expected with increasing thermal maturation, as more of the aliphatics are cracking into oils and condensing. Following the treatment for 72 h, the aliphatic region area further decreases by 5 % coupled by a relative increase in the aromatics. Elemental analysis on the remaining residue also shows a further decrease in the H/C ratio to a value of 0.7. The fact that some aliphatic component survived the treatment speaks of its resistivity and of possibility for further conversion. The efficiency of cracking the remaining aliphatic component remains to be further investigated.

3.3 HP data and GC-FID of produced oil

Following HP of the coal, the vessels were vented and the floating oil was collected through a Pasteur pipette. The expelled oils were clear, had a light yellow/brown color, and were spread thin on the surface of the water. This allowed for their direct collection without solvent extraction. The neat oils were analyzed by GC-FID and GC-MS for identification of the produced products. It is worth mentioning that the 24

h experiment did not produce enough floating oil to be collected for neat oil analysis. However, we did notice a small oil ring form on inside of the reactor, but that film was too small to collect.

Since the gas fraction was not collected, the amount of carbon converted to hydrocarbons was estimated (Table 8) by combining carbon balance data from elemental analysis and carbon distribution data from quantitative ^{13}C ssNMR. The following assumptions were taken into account: 1) the cracking of the aromatic carbons into oil and gas is negligible compared to that from the cracking of the aliphatic carbons. 2) The increase in the amount of aromatic carbons is from aromatization of aliphatic carbons. 3) Because of the absence of oxygen in the vessel, oxidation of aliphatic and aromatic carbon to carbon dioxide is negligible. 4) The only contribution to carbon dioxide and carbon monoxide came from cracking of carboxyl and carbonyl carbons. 5) The cracked aliphatic carbons that did not aromatize were the sole contributors to the produced hydrocarbons.

Table 8. Hydrocarbon transformation calculation using assumptions in section 3.3.

	Original sample	**24 h**	**48 h**	**72 h**
Carbon (%)[a]	59.6	40.7	38.1	37.5
Solid (%)	100[b]	80.4[c]	58.0[c]	53.8[c]
Carbon in remaining solid (%)	59.6	32.7	22.1	20.2
Aliphatic remaining (% of C)[d]	44.7	20.2	7.3	5.3
Aromatic remaining (% of C)[d]	10.3	12.5	14.8	14.9
Total aliphatic transformed (% of C)[e]		24.5	37.4	39.4
Total aromatic increase from original sample (% of C)[f]		2.2	4.5	4.6
Total hydrocarbon conversion (% of C)[g]		22.7	32.9	34.8

[a] Not ash corrected.
[b] Moscow brown coal loaded in reactor before HP.
[c] Residue recovered after HP.
[d] Calculated by using NMR percentages Figure 12 for original sample and Figure 14 for the remaining residues.
[e] Calculated by subtracting remaining aliphatic from aliphatic in original sample. Includes aliphatics transformed into hydrocarbons (elute) and aromatics (residue).
[f] Calculated by subtracting remaining aromatic from aromatic in original sample.
[g] Calculated by subtracting aromatic increase from total aliphatic transformed.

There are multiple trends that can be observed from the data in Table 8 and Figure 15. The first trend is a decrease in the normalized aliphatic carbons percent remaining in the residue as the HP time increases. This decrease in the aliphatic carbons is coupled by an increase of the aromatic carbons. After 24 h of treatment, the aliphatic carbons decrease by 24.5 % of which 2.2 % are transformed into aromatic carbons. Following treatment for 48 h, an additional 12.9 % of the aliphatic carbons are lost from the residue of which 2.4 % of them are transformed into aromatics. After 72 h, the decrease (compared to 48 h) is an additional 2.0 % of the aliphatic carbons in the residue coupled to a minor conversion to aromatics (0.1 %).

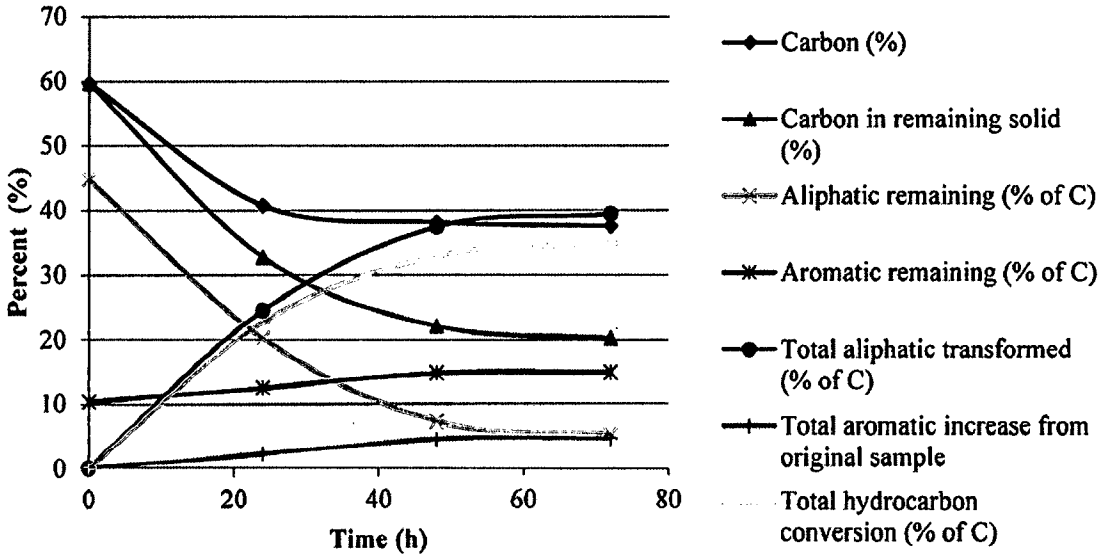

Figure 15. Evolution curves for reactants and products from HP of Moscow brown coal. Data from Table 8.

The trends for the different fractions show either an exponential decay of the carbon percentages in the residue and the aliphatic portion. These decreases are coupled by a negative exponential function-type increase in the total hydrocarbon conversion and the formed aromatics. From the graph, we can estimate at what time the contribution of the coal becomes less important to the total increase of hydrocarbons. It seems that between 55 h and 72 h of reaction time the cracking of the solid residue is not efficient and does not contribute to significant increases in the total expelled hydrocarbons. However, if we assume that the major source of the heteroatom containing compounds in the oil if from the coal then between 55 h and 72 h the major process taking place could be the cracking of the NSO into hydrocarbon oils and not the formation of the NSO's.

Figure 16 shows one-dimensional GC-FID chromatograms for the expelled oils form the 48 h and 72 h HP experiments. The oil chromatograms exhibit very high

similarity to one another. The 48 h oil shows a distribution of *n*-alkanes extending from C_8 to C_{34}. This dominance of *n*-alkane in the expelled oil fraction is consistent with what is expected from hydrothermally maturing a coal sample having the NMR and flash pyrolysis propertied discussed above. In addition, the expelled oil looks similar to those obtained from HP of low-rank lignite coals (Behar et al., 2003; Hartman and Hatcher, 2014). The oils also show a lack of branched alkanes similar to what was observed in the pyrolyzate from flash pyrolysis. In addition, the oils also show some contributions from alkylbenzenes, cycloalkanes, and alkylnaphthalenes. Contrary to the pyrolyzates from flash pyrolysis, the expelled oils do not show evidence of fatty acids in the chromatogram.

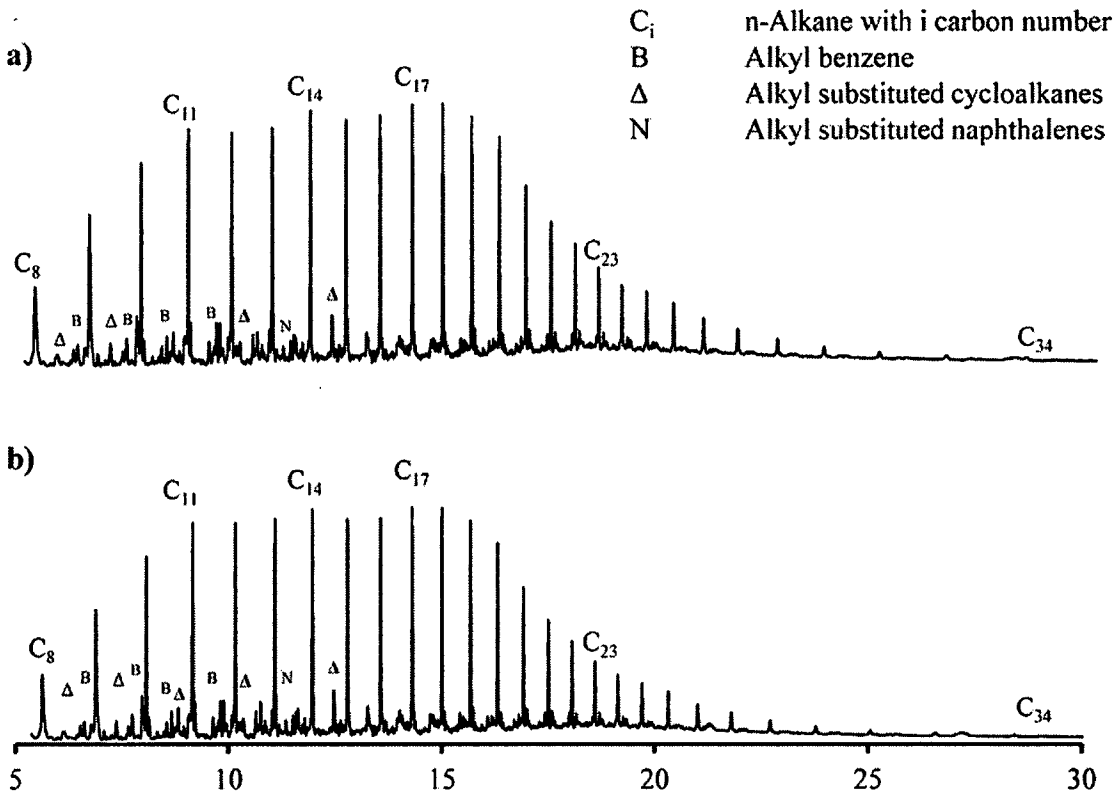

Figure 16. GC-FID chromatogram of oil produced by HP of Moscow brown coal at 360 °C for a) 48 h and b) 72 h. Identification of peaks was done with GC-MS. Time in minutes.

One major difference between the two produced oils is in their elemental composition (Table 7). The expelled oil from the 72 h experiment has significantly less heteroatom (8.3 % vs. 18.8 %), higher carbon (80.3 % vs. 71.5 %), and higher hydrogen (11.4 % vs. 10.5 %) content. This "upgrading" effect is expected in hydrous pyrolysis experiments as longer heating times have shown to decrease the heteroatom content of oils. However, increasing heating time did not have any effect on the H/C molar ratio (1.7 %) suggesting a minimal effect of heating time on the oil's overall aliphatic nature. Behar et al. (2008) investigated the role of NSO's in the formation of hydrocarbon expelled oils

from thermal maturation of lignite coals. They determined that the primary cracking in the kerogen produces mainly NSO (nitrogenated, sulfurated, and oxygenated) compounds and is minimally responsible for the production of hydrocarbons. The majority of the hydrocarbons are produced from the secondary cracking of the NSO into hydrocarbons and smaller NSO compounds. At temperatures as high as 360 °C, Behar et al. (2008) observed a decrease in the NSO fraction of the oils with thermal maturation time which is similar to our observation.

3.4. GCxGC- TOFMS of produced oils

Figures 17 and 18 the GCxGC-TOFMS chromatograms of the oils from the 48 h and 72 h experiments. Table 9 shows the different classes of compounds that were identified in the chromatograms. The GCxGC analysis shows a strong predominance of the *n*-alkanes/isoalkane homologous series that ranges from $C_7 - C_{32}$. The oil expelled at 48 h shows a slightly higher percentage of *n*-alkane/isoalkanes than that for 72 h (51.8 % vs. 52.9 % total peak areas). In addition, the *n*-alkane/isoalkanes in the 48 h and 72 h oils accounts for 17 % and 16 % of total peak numbers respectively.

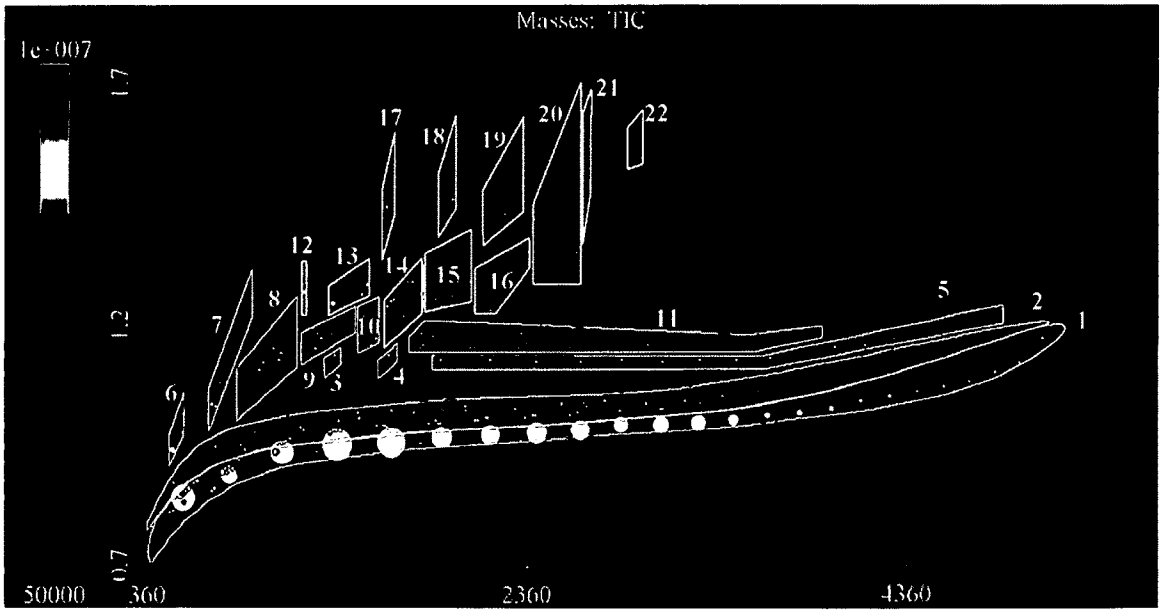

Figure 17. GCxGC-TOFMS chromatogram of 48 h oil produced from HP of Moscow brown coal.

In general, the distributions for *n*-alkanes are very similar to those obtained from GC-FID analysis for both oils. The isoalkanes in the oils are much less abundant than the *n*-alkanes, do not contain isoprenoids and are present only as monomethyl-*n*-alkanes substituted at the 2, 3, or 4 carbon. The lack of isoprenoid hydrocarbons is consistent with observations from GC-FID and py-GC-MS and is indicative of the lack of isoprenoid-like geo-biopolymers in the Moscow brown coal. The methyl-*n*-alkane series ranged in length from $C_7 - C_{18}$ in both oils. It is possible that the brown coal contains some branching that could lead to the formation of methyl-*n*-alkanes; however, because of their low abundance, it is more likely that they result from methyl shifts during cracking. It is also worth mentioning that the oils contain some mono unsubstituted *n*-alkyl-1-enes, *n*-alkyl-2-enes, and *n*-alkyl-3-enes. However, they are more abundant in the oil from the 48 h than from the experiment at 72 h. Leif and Simoneit (2000) have observed that during

hydrous pyrolysis of kerogens *n*-alkyl-1-enes are produced and isomerize (with acid catalysis enhanced in the presence of sulfur) to form mid-chain monoalkenes. These monoalkenes can eventually be reduced to form the alkanes with further thermal maturation.

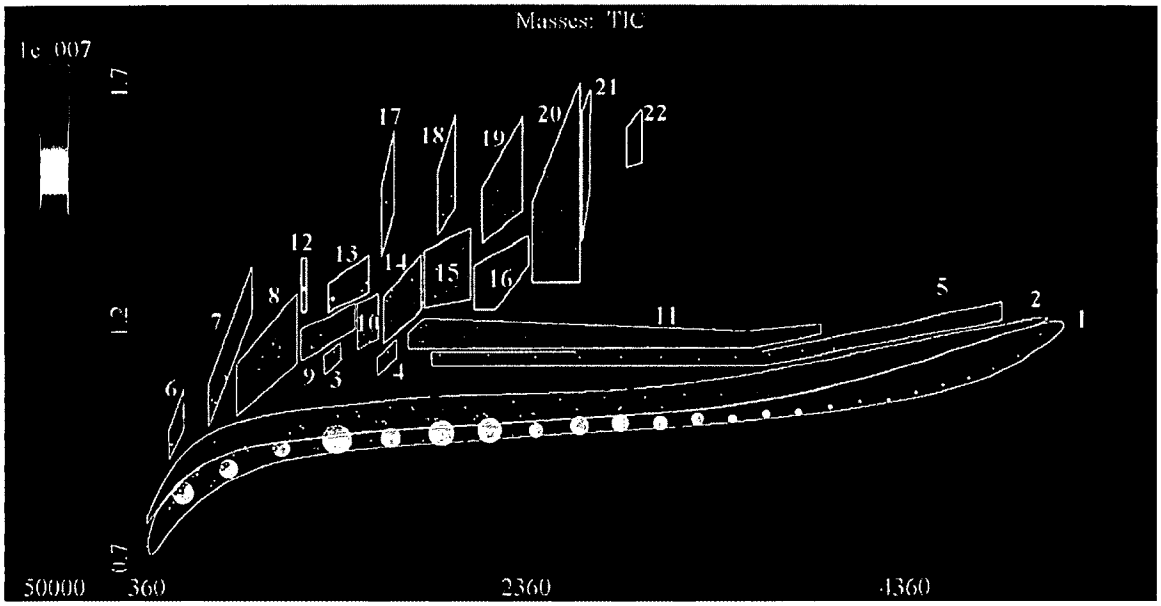

Figure 18. GCxGC-TOFMS chromatogram of 72 h oil produced from HP of Moscow brown coal.

The second most dominant species in the oils are the alkylcyclopentanes ($C_i$cy(5)) and alkylcyclohexanes ($C_i$cy(6)). In contrast to the *n*-alkanes/isoalkanes fraction, the cylopentanes and cyclohexanes are more dominant in the 48 h oil than in the 72 h oil suggesting that they are more readily produced by cracking at lower stress. The $C_i$cy(5)/$C_i$cy(6) can be divided into two groups: mono-*n*-alkyl substituted cycloalkanes and multi-substituted cycloalkanes. Mono-*n*-alkyl substituted cycloalkanes in the oils range from C_4-C_{16}cy(6) and from C_5-C_{17}cy(5). The cyclohexane products are more

abundant than the cyclopentanes in both oils, this could be due to hindrance in the cyclization step. Kissin (1990) suggested that the formation of the mono-*n*-alkylcyclohexanes and cyclopentanes in the crude oils are the result of a thermoradical mechanisms resulting from the breaking of long chain *n*-alkanes into mixtures of long and short *n*-alkanes and olefins followed by the cyclization of olefin radicals into the mono-*n*-alkyl substituted cyclohexane products. Multi-substituted cycloalkanes are less abundant than the mono-*n*-alkyl substituted cycloalkanes in both oils and they are found as predominantly as 1-methy-2-alkylcyclohexanes and 1-methyl-3-alkylcyclohexanes. Mango (1990) investigated the source of multi-substituted cyclohexanes and suggested that they are most likely a result of the cyclization of branched alkanes.

Table 9. Identification and quantification of GCxGC-TOFMS chromatograms.

No	Description	Abbreviation	Expelled oil (48 h)		Expelled oil (72 h)	
			Area (%)	*Count (%)*	*Area (%)*	*Count (%)*
1	*n*-Alkanes/isoalkanes	$C_8 - C_{32}$	51.8	17.0	52.9	16.0
2	Alkylcyclopentane + Alkylcyclohexane[a]	$C_5 - C_{17}$cy(5) + $C_4 - C_{16}$ cy(6)	22.8	26.4	20.6	23.8
3	C9 Ketones	C_9K	0.2	0.2	0.3	0.5
4	C10 Ketones	$C_{10}K$	0.3	0.5	0.3	0.5
5	Greater than C10 Ketones	$>C_{10}K$	2.5	5.5	2.3	4.8
6	Toluene + C1 Alkylthiophenes	T C_1Th	0.9	1.2	0.8	0.9
7	C2 Alkylbenzenes + C2 Alkylthiophenes	C_2B C_2Th	2.4	2.1	2.7	1.8
8	C3 Alkylbenzenes + C3 Alkylthiophenes	C_3B C_3Th	2.4	3.6	3.1	3.9
9	C4 Alkylbenzenes+ C4 Alkylthiophenes	C_4B C_4Th	1.4	4.3	1.6	4.1
10	C5 Alkylbenzenes	C_5B	1.1	4.3	1.1	4.4
11	Greater than C5 Alkylbenzenes	$>C_5B$ $>C_5Th$	1.3	8.6	1.5	8.9
12	Indane	I	0.5	0.2	0.6	0.2
13	C1 Indanes	C_1I	2.0	1.2	2.2	1.3
14	C2 Indanes	C_2I	1.7	3.8	1.4	3.0
15	C3 Indanes[b]	C_3I	1.3	4.8	1.4	4.5
16	C4 Indanes[b]	C_4I	0.4	2.9	0.4	2.8
17	Naphthalene + Benzothiophene	N BTh	0.3	0.5	0.3	0.7
18	C1 Alkylnaphthalenes C1 Alkylbenzothiophene	C_1N C_1BTh	0.6	1.2	0.7	1.1
19	C2 Alkylnaphthalenes C2 Alkylbenzothiophene	C_2N C_2BTh	0.5	2.4	0.6	3.2
20	C3 Alkylnaphthalenes	C_3N	0.2	2.4	0.4	3.4
21	Biphenyl	$C_0 - C_1Biph$	0.3	1.0	0.4	1.1
22	C1 Fluorene + C2 Biphenyl	C_1Flu C_2Biph	0.2	0.7	0.2	0.9
	Unclassified		4.9	5.2	4.6	8.2
	Sum		100	100	100	100

[a] includes mono-alkenes. [b] includes C_{i-1} 4-hydronaphthalene

Alkylketones (C_iK) are formed in both oils, those at 48 h and those at 72 h, and their concentration is greater in the 72 h expelled oil maximizing at $C_{11}K$. The ketones are predominantly *n*-alkan-2-ones and minor amounts of *n*-alkan-3-ones. Acyclic ketones from hydrous pyrolysis have been shown to be a result of oxidation of existing acyclic alcohols and/or mono-unsaturated alkenes, especially under long reaction times (Leif and

Simoneit, 2000). Leif et al. (2000) has shown, using model compounds, that kerogens under hydrothermal conditions produce *n*-alkan-2-ones by a series of reaction steps starting by the cracking of the kerogen into *n*-alk-1-enes (minor product from cracking of kerogen under hydrous pyrolysis) followed by hydration to *n*-alkan-2-ol and further oxidation into the *n*-alka-2-ones.

Alkylbenzenes (C_iB) in the oils range from $C_1 - C_{15}B$. They are more abundant in the 72 h oil but they show the same distribution in both samples maximizing at C_3B. Alkylbenzenes in both samples are found as mono-, di-, and trialkyl benzenes with the alkyl side chains being either straight chain or branched. The distribution in alkylbenzenes for both samples is the same: mono- > di- > trialkyl benzenes and alkylbenzenes with straight side chains being more abundant that their branched counterpart. Alkylbenzenes in oils possibly originate either from cracking of the coal or aromatization reactions of cyclic alkanes produced during HP. However, it is less likely that the alkylbenzenes (especially *n*-alkylbenzenes) are produced as a result of the primary cracking of the coals. There are two pieces of evidence that support this concept, 1) the aromatic fraction stays mostly constant in the residue with increasing reaction time from 48 h to 72 h (Table 8); 2) there is decrease in the *n*-alkylcyclohexane fraction with increasing reaction time. It is interesting that we did not observe the formation of any phenolic or alkyl phenolic compounds in the oils. Hartman and Hatcher (2014) observed the occurrence of phenols when they analyzed the expelled oils from HP of Wyodak Anderson coal (a low volatile bituminous coal). They attribute the occurrence of these phenols as a result of HP of lignin-derived aromatic structures in their original coal. The lack of phenolic compounds in the expelled oils is also an indication of the lack of lignin-

containing plant contributions when the coal was formed.

Alkylthiophenes (C_iTh) in sedimentary rocks are thought to be have formed by the incorporation of reduced inorganic sulfur into functionalized or unsaturated geo-biopolymers during early diagenesis (Brassell et al., 1986; Damste et al., 1989). This incorporation is thought to increase the stability of the biopolymers thus rendering them less susceptible to biodegradation and thermal degradation. Alkylthiophenes are more abundant in the 72 h oil sample. This is expected as they are the result of thermal cracking of the coal. Alkylthiophenes in both oils samples are found as two types: 2-*n*-alkylthiophenes and 2-methyl-5-*n*-alkylthiophenes. The 2-*n*-alkylthiophenes range from $C_1 - C_4$ in the 48 h oil sample and $C_1 - C_9$ in the 72 h oil and the 2-methyl-5-*n*-alkylthiophenes range from $C_1 - C_3$ in the 24 h oil and $C_1 - C_8$ in the 72 h.

Alkylnaphthalenes (C_iN) have been identified in both oils. Their concentration is higher in the 72 h oil than the 42 h oil. Alkylnaphthalenes maximize at C_1N for both samples. It has been noted that the occurrence of alkylnaphthalenes in crude oils is indicative of high thermal maturity (Peters et al., 2005). Benzo[b]thiophene (C_iBTh) is thought to form as a result of aromatization of the produced thiophenes (Nikonov and Senning, 1989). In addition, the oils contain minor amounts of acenaphthene, biphenyl (Biph), and C_1fluorene (C_1Flu). The origin of these compounds has been found to be thermal alteration of biological precursors (McCollom et al., 1999) and secondary thermal aromatization of primary pyrolysis products such as indanes (Fahim et al., 2009).

4. CONCLUSIONS

This work focuses on the characterizing the non-polar volatile fraction of expelled

oils from HP of the Moscow brown coal. HP is a very promising technique to simulate natural thermal maturation of coals into expelled oils. HP's advantage as a tool for production of oils is twofold as it not only cracks the coal into liquid oils but also results in the oil's upgrading by simultaneously lowering the heteroatom content with increasing reaction time. The Moscow brown coal's highly aliphatic structure, as deduced by ssNMR and py-GC/MS, is critical to its viability as a HP feedstock to produce oils that resemble highly aliphatic crude oils. HP treatment is effective in transforming the aliphatic structures of the Moscow brown coal to produce an aliphatic oil by breaking the C-C bonds and favoring the formation of alkanes. Py-GC-MS and palynological studies of coal show evidence of geo-biopolymers (e.g. suberan, cutan, and possibly algaenan) surviving in the Moscow brown coal. Our results, in addition to evidence from the literature, also show that these geo-biopolymers are the key ingredient that gives the coal this aliphatic-oil producing quality. It is therefore logical to deduce that HP of any of the multitude of plant-based aliphatic geo-biopolymers will result in the production of a hydrocarbon based fuel oil. The GCxGC analyses show that the oil produced by HP is one that is mainly composed of *n*-alkanes, alkyl aromatics, and alkylcycloalkanes making it a very high quality oil to be used as a feedstock for fuel production.

Considering the fact that 34% of the whole coal is converted to these oils, I can estimate a yield of 2.9×10^3 barrels of crude oil per 1000 tons of coal. The basin is estimated to contain 12 billion tons of this coal (Lamer, 1957) and would yield 3.5×10^{10} barrels of oil when subjected to HP in a commercial operation.

CHAPTER IV

HYDROUS PYROLYSIS OF *SCENEDESMUS* ALGAE AND ALGAENAN.

PREFACE

The contents of this chapter were accepted for publication in *Organic Geochemistry on March 2nd 2015.*

1. INTRODUCTION

The search for alternative fuels has greatly been expanded in recent years and has reached a level of environmental, economic, and strategic importance. The United States government passed the Energy Independence and security act in 2007 which mandates the production of 21 billion gallons of bio-derived fuels by 2022 (U.S.Congress, 2007). In addition, the United States Navy set up a goal to increase its use of alternative fuels to 50 % by 2020 (U.S.Navy, 2009). To meet this demand, there will be a need to accelerate the commercialization of alternative fuel production from multiple feedstock, one of which includes algae. The U. S. Department of Energy has identified algae as an important non-food feedstock for conversion to hydrocarbon fuels and has proposed that one attractive process for conversion is hydrothermal liquefaction. The use of hydrothermal liquefaction, also known as hydrous pyrolysis, on algae has been documented as early as the 1990's (Dote et al., 1994; Inoue et al., 1994) with efforts focusing mainly on using the process for extracting the hydrocarbons naturally produced

by *Botryococcus braunii.* The recent increased interest in using hydrous pyrolysis to produce biofuels from algae (Biller and Ross, 2012; Savage, 2012) have been mostly motivated by the advantages it poses over other conversion techniques. These include eliminating the need for drying the algae before treatment, suitability of algae as a feed stock, and the high energy efficiency of the hydrothermal process.

In some recent experiments, algae have been found to produce oils in abundance; however, these oils were rich in oxygen and nitrogen molecules that require additional treatments involving catalytic upgrading to produce saturated hydrocarbons (Garcia Alba et al., 2011; Biller and Ross, 2012; Torri et al., 2012). Garcia-Alba et al. (2011) and Torri et al. (2011) have shown that *Desmodesmus* sp. algae readily yield hydrocarbon-rich oils upon hydrous pyrolysis, but these contain an abundance of oxygenated and nitrogenated species whose existence is associated with the thermal decomposition of carbohydrates and proteins contained in the algae (Garcia Alba et al., 2011; Torri et al., 2012). In their work, hydrocarbons with high boiling points (greater than 350 °C) and alkylbenzenes, both produced at high temperature, were attributed to algaenan-derived products, shown previously by Hatcher and Salmon (2009) to be abundantly produced at near critical point temperatures of water. Algaenan is an aliphatic polyethylene biopolymer found in the cell walls of some groups of green algae, eustigmatophytes, and dinoflagellates (Berkaloff et al., 1983a; De Leeuw and Largeau, 1993; Blokker et al., 1998; Versteegh and Blokker, 2004; Kodner et al., 2009). It is most abundant and diverse in green algae from the genera *Scenedesmus, Tetraedron, Chlorella, Botryococcus and Haematococcus* (Kodner et al., 2009). Barreiro et al. (2013) has highlighted the fact that algaenan potential is still not fully understood when employing hydrothermal liquefaction (López Barreiro et al.,

2013). In this current study we propose that chemically isolated algaenan from whole algae will behave similar to kerogen, producing a hydrocarbon-based oil that is significantly reduced in O and N-containing species under hydrous pyrolysis or hydrothermal liquefaction conditions. The underlying reason for this is that algaenan isolates are composed mainly of C and H atoms and generally devoid of significant amounts of heteroatomic species (O and N).

Algaenan is a recalcitrant material that is insoluble and non-hydrolyzable. It has been shown that the algaenan may be selectively preserved in sediments and is thought to be converted into petroleum as it matures over geological time (Philp and Calvin, 1976; Tegelaar et al., 1989c; Derenne et al., 1991; Derenne et al., 1997). Previous studies have shown that one can simulate the process by which this algaenan converts to petroleum-like hydrocarbons using closed system anhydrous pyrolysis (Behar et al., 1995a; Salmon et al., 2009b). When pyrolyzed, algaenan produces a suite of hydrocarbons with chain lengths from 6 to 37 carbons, not unlike many petroleum hydrocarbons. These algaenans are likely the precursors of Type I kerogen in shales that yield paraffinic petroleum upon natural maturation (De Leeuw and Largeau, 1993). Ancient kerogens derived from algal remains have been shown to produce an abundance of paraffinic oil when they underwent thermal treatment (Behar et al., 1995a) particularly in the presence of water (Ruble et al., 2001).

In this study, algae from *Scenedesmus/Desmodesmus* spp. was subjected to hydrous pyrolysis as described by Lewan (1993). We further treated the microalgae with an abbreviated algaenan isolation procedure to concentrate the algaenan and then subjected the algaenan-enriched residue to hydrous pyrolysis along with the whole algae

for comparison. To our knowledge, this is the first time isolated algaenan is investigated as a feedstock to hydrous pyrolysis.

The strategy in this experiment was to first verify our belief that the hydrothermal treatment would produce substantial quantities of hydrocarbons from wet algae and algaenan charged into an aqueous medium as a test bed for biofuels production strategies. The large reactor allowed for processing of a large amount of algae which should produce a significant amount of oil. This allows for collection the oil physically without the use of any organic solvents which reduces the possibility of partitioning of water soluble compounds into the oil fraction and losing the volatiles after removing the solvent. Previous studies employing either analytical flash pyrolysis (Kodner et al., 2009) or closed tube pyrolysis (Salmon et al., 2009a) show that hydrocarbons are readily produced from dried algaenan. The former approach yields hydrocarbons that are a mixture of alkanes and alkenes extending across a carbon number range from C_6 to C_{32}, and the latter yields mainly saturated hydrocarbons with a similar carbon number distribution. The second part of our strategy was to analyze the oils that were produced by this process to investigate their molecular characteristics by utilizing two-dimensional gas chromatography to investigate the volatile nonpolar fraction of the oil.

2. MATERIALS AND METHODS

2.1 Sample information

Algae harvested from the Old Dominion University algal farm near Hopewell, Virginia. The main algal forms in the demonstration open raceway pond system are *Scenedesmus/Desmodesmus* spp. with subordinate *Oocystis* spp. also present.

2.2 Abbreviated algaenan isolation

Lipids were removed by extracting the algae with 1:1 (v/v) benzene:methanol for 24 h using a Soxhlet extraction apparatus. The majority of carbohydrates and proteins were afterwards removed by treatment of the dried residue with 2 N sodium hydroxide at 60 °C for 2 h. The efficacy of removal was evaluated by use of ^{13}C ssNMR spectroscopy described below. The solid was then washed excessively with deionized water to remove the residual sodium hydroxide and treated with Dowex 50W-x8 cation exchange resin to exchange any residual sodium. The solid was given a final rinse with deionized water. Final yield was about 27 %.

2.3 Hydrothermal treatment

A detailed description of hydrothermal treatment experiments is given by Lewan (1993). In short, carburized 1 liter Hastelloy-C276 reactors were filled each with 50 g of whole algae or 45 g of algaenan, and 450 g of distilled water. A 1 mm Cr–Ni screen was placed on top of the solid to prevent it from floating during the progress of the experiment. Sample volume (based on an approximate sample density), reactor volume, and amount of added water were calculated to ensure that the sample remained submerged in a liquid water phase throughout the experiment. The reactor was then evacuated and filled with 25 psia of helium. Artificial maturation was achieved by isothermal heating of the samples at 260 °C, 310 °C, and 360 °C for 72 h. The temperatures were continuously monitored during the experiments at 30 s intervals with type J thermocouples. Standard deviations of temperature were between 0.2 and 0.7 °C for the experiments. Upon completion of the heating, the reactors were left to cool to room temperature overnight. The reason 72 h was chosen as the reaction time is because

the amount of expelled oil from source rocks does not increase significantly after the 72 h. The algaenan recalcitrant structure was assumed to behave similarly.

2.4 Fraction collection

After cooling to room temperature overnight, the gas pressure and temperature were recorded and gas samples were collected in 30 cm^3 stainless steel cylinders. The reactors were then opened to quantitatively collect the remainder of the fractions. The samples generated an expelled oil which was collected by pipetting from the surface of the water and transferring to previously tared glass vials. The water recovered from the reactor was filtered (0.45 μm) and an aliquot analyzed for pH and Eh at room temperature. The reactor walls, reactor head and thermowell were rinsed with benzene to recover any adsorbed oil films. The benzene was later evaporated at room temperature and placed in a separate container and weighed. The remaining solid residue was removed from the reactor and left to air dry in a hood.

2.5 Oil fraction-separation

Following collection, the expelled oil was separated into saturates, aromatics, and NSO's by liquid chromatography using silica gel columns eluted successively with *n*-pentane, 15:85 (v/v) pentane/DCM, and 50:50 (v/v) DCM/methanol. Quantification for the *n*-pentane and the 15:85 (v/v) pentane/DCM fractions was attained with chromatography-flame ionization detection and calibrating via external calibration with a hydrocarbon calibration standard (Part No: 5080-8716) purchased from Agilent. For the 50:50 (v/v) DCM/methanol fraction, quantification was achieved by drying an aliquot of the fraction at room temperature and under nitrogen gas flow followed by weighing the residue.

2.6 Gas chromatography-flame ionization detection

Gas chromatography coupled to flame ionization detection (GC-FID) analysis was performed with a Hewlett-Packard HP 6890 series GC system equipped with an HP 6890 injector. The oil samples were injected neat with the GC operating in the split mode (400:1). The FID detector was set at 250 °C and the inlet temperature was held constant at 280 °C throughout the analysis. The signal was measured at a rate of 20 spectra per second. The column used for GC separation has a 30 m x 0.25 mm i.d. with fused silica capillary column with a film thickness of 0.25 μm (5 % phenylpolysiloxane - 95 % ethylpolysiloxane, Agilent J&W DB-5). Helium was used as the carrier gas, with flow rate of 1 ml/min. the oven temperature was programmed as follows: initial temperature was 50 °C, held for 1 min; then for a heating rate of 10 °C /min until the final temperature reaches 300 °C, held for 5 min. Peak identifications were performed by gas chromatography coupled to mass spectrometry.

2.7 Gas chromatography - mass spectrometry

GC-MS analysis was performed with a Hewlett-Packard HP 6890 series GC system coupled to a Leco Pegasus III time-of-flight (TOF) mass analyzer. Samples were injected in split mode at a split ratio of 400:1 for neat oil injections. The GC conditions, column type, and temperature program were the same as those for GC-FID. The source and transfer line temperatures were maintained at 200 °C and 280 °C respectively. Mass spectra were collected at a rate of 20 spectra per second after a 240s solvent delay. Masses were acquired at a range between 35 *m/z* and 500 *m/z*.

2.8 Carbon-13 solid state NMR methods

NMR spectra were acquired via a direct polarization-magic-angle spinning (DPMAS) pulse sequence using a 400 MHz Bruker AVANCE II with ^{1}H resonating at 400 MHz and ^{13}C at 100 MHz. The dried solid sample (ca. 80 mg) was placed in a 4 mm NMR rotor and sealed with a Kel–F cap. Samples were spun at the magic angle (54.7°) with a frequency of 13 kHz and a recycle delay of 30s to allow for full T_1 relaxation. All solid state spectra were externally calibrated to the glycine standard (176.03 ppm). More details concerning the conditions are described by Dria et al. (2002).

2.9 Elemental analysis

Elemental carbon, hydrogen, and nitrogen, and sulfur compositions for the solid residue, oil, and soluble organic content in the water fraction were determined using a CE Flash EA 1112 elemental analyzer. All measurements were performed in triplicate for consistency.

2.10 Standard oil samples

Oil samples (crude set # 2) were purchased online from ONTA geology company, www.onta.com. The set included nine different oil samples with different properties: Extra-Light Crude Oil (Appalachian basin, USA; sweet, paraffinic), Light Crude Oil (South Louisiana, USA; sweet, paraffinic), Light Medium Crude Oil (Qua Iobe, Nigeria; sweet, waxy, paraffinic), Medium Crude Oil (North Slope Alaska, USA; sweet, paraffinic naphthenic), Medium-Heavy Crude Oil (Texas, USA; sour, naphthenic), Medium-Heavy Crude Oil (Arabian, Saudi Arabia; sour, aromatic-intermediate), Heavy Crude Oil (Vasconia, Colombia; sour, aromatic-naphthenic), Heavy Crude Oil (Oriente, Ecuador;

sour, aromatic-asphaltic), Extra-Heavy Crude Oil (Merey, Venezuela; sour, aromatic-asphaltic).

2.11 Simulated Distillation

Simulated distillation analysis was performed following the ATSM D 2887 standard method. Briefly, 0.1uL of neat oil samples were injected into an Aglilent 7890A gas chromatograph (GC) equipped with a flame ionization detector. The column used for GC separation has a 10 m x 0.53 mm i.d. with fused silica capillary column with a film thickness of 2.65 μm (100 % dimethylpolysiloxane, Agilent J&W DB-1). Helium was used as the carrier gas, with flow rate of 20 mL/min. The oven temperature was programmed as follows: initial temperature was 40 °C; then a heating rate of 20 °C /min until the final temperature reaches 350 °C, held for 4 min for a total run time of 19.5 min. Boiling point calibration standards (Part No: 5080-8716) were purchased from Agilent. Simulated distillation analysis of the resulting chromatograms was done by the Agilent Technologies SimDis software version A.02.02.

2.12 Two-dimensional gas chromatography - mass spectrometry

GCxGC-TOFMS was performed using an Agilent 6890 series GC system (Palo Alto, CA, USA) equipped with a secondary oven, a non-moving quad-jet dual-stage thermal modulator and coupled to a Leco Pegasus 4D time-of-flight (TOF) mass analyzer. The oil samples were diluted in dichloromethane and 1μL was injected in split mode (20:1) in the injector at 275 °C. The primary column used for GC separation has a 30 m x 0.25 mm i.d. with fused silica capillary column with a film thickness of 0.25 μm (low polarity phase; Crossbond® 1,4-bis(dimethylsiloxy)phenylene dimethyl polysiloxane, Restek Rxi-5Sil MS). The secondary column has a 1.1 m x 0.15 mm i.d.

with fused silica capillary column with a film thickness of 0.15 μm (midpolarity Crossbond® phase, Restek Rxi-17Sil MS). The GC conditions are as follows: He was used as the carrier gas at a corrected constant flow rate of 1.0 mL/min. The primary oven temperature was initially set to 40 °C with a hold time of 0.5 min; followed by a heating rate of 3 °C/min until the final temperature reached 290 °C, held for 40 min. The secondary oven was set at a +10 °C offset from the primary oven temperature program. The modulator offset was +25 °C relative to the primary oven temperature program. The modulation period was 4 s with 1.3 s hot pulse. Mass spectrometer conditions were as follows: Ion source was set at 200 °C and in electron ionization mode at -70eV. The spectra were collected for a mass range of 40 *m/z* to 400 *m/z* at an acquisition rate of 100 spectra/second. The transfer line temperature was set at 300 °C and the solvent delay was 220 s. Data was processed using ChromaTOF version 4.50.8.0 .

2.13 GCxGC-TOFMS semi quantification

In addition, semi-quantitative measurements of the various compounds can be obtained by combining quantification data from GCxGC-TOFMS and simulated distillation. Vendeuvre et al. (2007) found that GCxGC-TOFMS peak intensities can be used to estimate simulated distillation data obtained by the ATSM D2887 standard method. This was done using the following rational: since simulated distillation (ASMS D2887) calculates the percent mass of oil that that is distilled at specified boiling temperatures up to 475 °C based on *n*-alkane calibrations, we can extend the assumption to GCxGC-TOFMS integration data since the elution of the compounds in GCxGC-TOFMS are also governed mainly by boiling point. Percent area integrations can be incorporated with the simulated distillation to calculate percent mass for each compound

or compound class as follows:

$$X_{compound} \approx \%mass_{(SimDis)} \times \%area_{(GCxGC-TOFMS)} \quad (4)$$

Where X is the % mass of the compound of group of compounds in the whole oil; $\%mass_{(SimDis)}$ is the percent of the oil that is observable by simulated distillation/ eluted and detected by the GC; $\%area_{(GCxGC\text{-}TOFMS)}$ is the percent of total intensity of the compound.

2.14 Lipid analysis

Lipid analysis was performed using a modified tetramethylammonium hydroxide (TMAH) method proposed by (Woo and Kim, 1999) to convert lipids to fatty acid methyl esters (FAMEs). Briefly, freeze dried algae was Soxhlet extracted with 1:1 (v:v) benzene:methanol for 24 h. The extract was then dried and weighed. A small (1 mg) sample was transferred to a glass reaction tube and TMAH (25 % wt. in methanol), purchased from Sigma-Aldrich (PN: 334901), and connected to a vacuum line where most methanol was removed. The tubes were flame sealed while under vacuum and placed in an oven at 250 °C for 2 h. After the tubes cooled to room temperature, they were opened and the samples were taken up with ethyl acetate and filtered to remove any solid particulates. The FAMEs were identified and quantified by comparison to a FAME standard mixes purchased from Sigma-Aldrich (GLC-40 [PN:1895], GLC-50 [PN:1894], GLC-90 [PN:1896]).

3. RESULTS AND DISCUSSION

3.1 Starting material

The two samples, whole algae and algaenan isolate, are initially examined by

elemental analysis with the data shown in Table 10. Following the chemical isolation of the algaenan from algae, we notice a decrease in the % N (10.1 % to 4.7 %) and % O (30.5 % to 27.3 %) and an increase in the % C (52.3 % to 58.4 ^{13}C ssNMR on both the algae and isolated algaenan (Figure 19) indicate that the algae and algaenan spectra are typical of algal biomass and its corresponding algaenan (Zelibor et al., 1988). The spectrum of whole algae shows peaks ranging from 10 to 45 ppm corresponding to aliphatic carbons (terminal CH_3, mid chain -CH_2- and -CH-) which mainly originate from the remaining fatty acids or algaenan that are part of the algae biomass.

Table 10. Analysis (ash corrected) of solid residue (% daf).

	C (%)	H (%)	N (%)	O[a] (%)
Algae	51.3	8.1	10.1	30.5
Algaenan	58.4	9.6	4.7	27.3

[a] Calculated by difference

The spectrum also shows a peak at 54 ppm which is characteristic to the α-carbon in proteins. The peaks at 63 and 74 ppm are attributed to hydroxyl substituted carbohydrate carbons. The peak at 105 ppm corresponds to the anomeric carbon in carbohydrates. The spectrum also shows peaks at 129 ppm (protonated aromatic or olefinic carbons), 156 ppm (O-substituted aromatic), and 173 ppm (carboxyl carbon from fatty acids or amide). The NMR spectrum for algaenan comparatively shows a relative diminution of peaks characteristic for proteins, carbohydrates, and lipids and a relative enhancement of long-chain aliphatic carbons that are the characteristic signature of algaenan. The treatment is more effective in removing proteins than carbohydrates from the algae; this is also evident in the fact that the nitrogen content decreased more than that

of the oxygen. Although the carbon and the oxygen content of the algaenan isolate are high, NMR shows that the base treatment was successful in concentrating the algaenan in the residue.

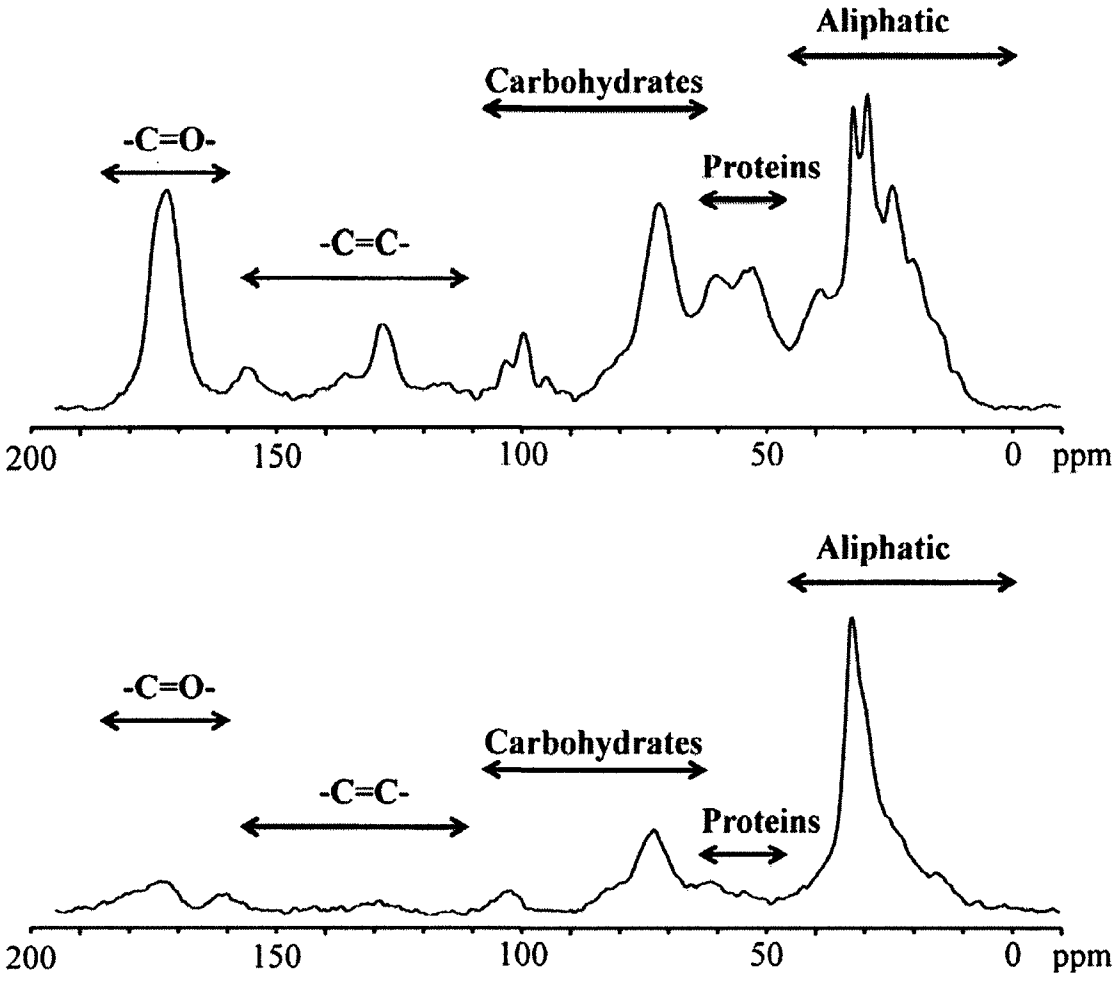

Figure 19. Quantitative ^{13}C ssNMR spectra of whole algae (upper) and the algaenan concentrate (lower) with chemical shift regions of component structural entities in algae shown.

3.2 Overview of hydrothermal treatment results

The distribution of products from hydrothermal treatment of the algae and the algaenan are depicted in Figure 20. The yields of products are reported on a carbon normalized basis to more appropriately represent the transformation of the organic fraction of algae and algaenan. As the temperature increases, the amount of carbon associated with recovered residue and water soluble organic matter decreases. In contrast, the amount of oil, gas, and dissolved CO_2 species increase with increasing temperatures. Conversion of the algae biomass carbon to the different fractions other than the insoluble residue is 58 % at 260 °C, 74 % at 310 °C, and 89 % at 360 °C. This increase is expected as higher reaction temperature prompts more cracking of the algal biomass organic matter to volatile and extractable products. The carbon percentages for the gas increase with increasing temperatures (8 %, 11 %, and 22 % at 260 °C, 310 °C, and 360 °C) and oil fractions (21.4 %, 33.5 % and 49 % at 260 °C, 310 °C, and 360 °C). The water-soluble fraction shows opposite behavior with carbon percentages decreasing with increasing temperature. The sharp decrease in the water-soluble carbon percentages at 360 °C is interesting and suggests that pyrolysis for extended periods of time at such high temperature significantly decomposes that fraction. The decomposition of the water-soluble fraction is a source of nitrogenated and oxygenated compounds that can end up in the oil fraction, lowering its quality. In a recent study conducted at low hydrothermal severity and short contact times, we show that both proteinaceous and carbohydrate-like material dissolves in the aqueous phase, so it is likely that heating at higher thermal severity will impact this component of the reaction medium (Garcia-Moscoso et al., 2013).

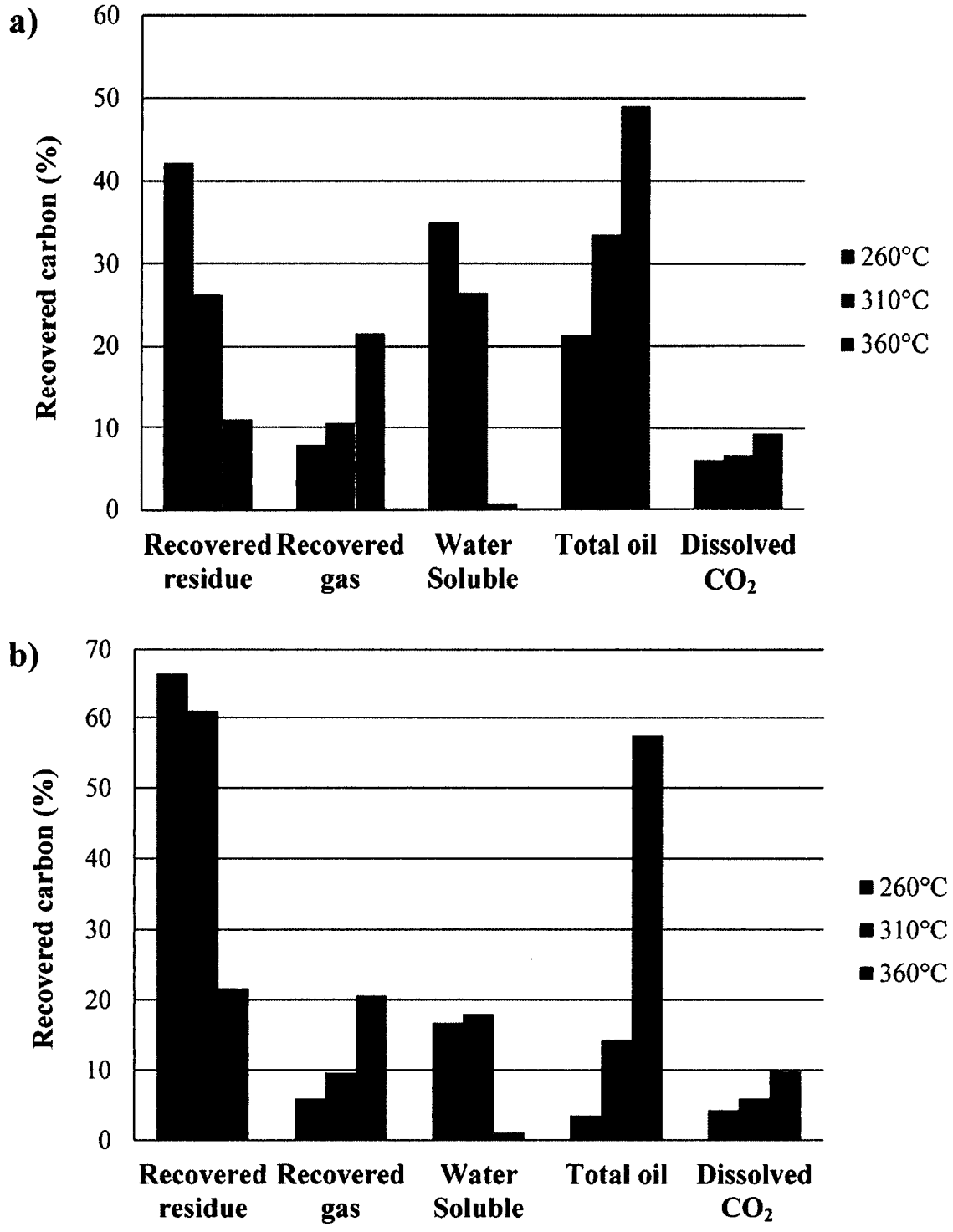

Figure 20. Carbon percent distribution for each fraction after each HTL for a) algae and b) algaenan.

Algaenan transformation shows similar trends with increasing temperature as those of algae for all the fractions. However, lower carbon conversion percentages (33 %, 39 %, and 78 % conversion for 260 °C, 310 °C, and 360 °C respectively) are observed. This is expected as the algaenan isolate contains lesser quantities of thermally labile components. An increase in temperature from 260 °C to 310 °C leads to only a 6 % increase in conversion while as increasing the temperature to 360 °C leads to an additional 39 % conversion. This shows that the algaenan polymethylenic structure can resist cracking at temperatures up to 310 °C, but not at 360 °C. The carbon yields for gas increase with increasing temperatures (6 %, 10 %, and 21 % at 260 °C, 310 °C, and 360 °C) and oil fractions (4 %, 14 % and 58 % at 260 °C, 310 °C, and 360 °C). It is interesting, when comparing the oil fraction between algae and algaenan isolate liquefaction at similar temperatures, that the liquefaction of algae produces more oil at 260 °C (21 % vs. 4 %) and 310 °C (34 % vs. 14 %) but at 360 °C, the algaenan produces more oil (49 % vs. 58 %). The water-soluble fraction does not change significantly when increasing the temperature from 260 °C to 310 °C (17 % to 18 %) suggesting that the compounds in this fraction are more stable than those formed from the algae at similar conditions. At 360 °C, the water fraction decreases significantly (1 %) similar to that in the algae liquefaction.

3.3 Recovered residue

A more detailed insight on the chemical transformations of the algae recovered residue can be assessed with ^{13}C ssNMR of the residues following each hydrothermal treatment step (Figure 21). Following whole algae reaction at 260 °C, the peaks corresponding to proteins (54 ppm) and carbohydrates (63 and 74 ppm) have

disappeared. This is a clear indication that the subcritical conditions at this low level of heating hydrolyzed the products making them more soluble into the aqueous phase. A similar phenomenon has been observed with subcritical heating of terrestrial plant biomass at similar temperatures (Savage, 1999). It is also noteworthy that, at a lower temperature (260 °C) virtually no expelled oil formation is observed (all the oil comes from the benzene rinse of the reactor wall and thermal well). In fact, the algae char spectrum resembles that of algaenan but with an increased portion of aromatic carbons (129.7 ppm). This suggests that the algaenan can sustain thermal stress with some aromatization taking place. The aliphatic section of the char shows peaks at 12.2 ppm, 14.7 ppm, 20.7 ppm, 23.1 ppm, 30.2 ppm, 32.7 ppm, 37.7 ppm. The 14.7 ppm and 23.1 ppm correspond to terminal methyl ($-CH_3$) and methylene groups alpha to methyl groups. In addition, peaks corresponding to 30.2 ppm and 32.7 ppm correspond to the amorphous and crystalline arrangements of the long chain methylene groups ($-CH_2-$). The shoulder peak at 37.7 ppm corresponds to the alpha carbon to the carbonyl group. It is interesting to observe that there are two small peaks at 12.2 ppm and 20.7 ppm; these peaks correspond to terminal methyl ($-CH_3$) and methylene groups alpha to methyl groups that are for shorter chain lengths than those for 14.7 ppm and 23.1 ppm. At 310 °C, the residue shows a 6 % decrease of the aliphatic proportion in the sample. In addition, only minor changes between the relative distributions of the aliphatic carbon peaks are observed such as a slight decrease in peak areas for peaks at 14.7 ppm and 23.1 with respect to that of 30.2 ppm.

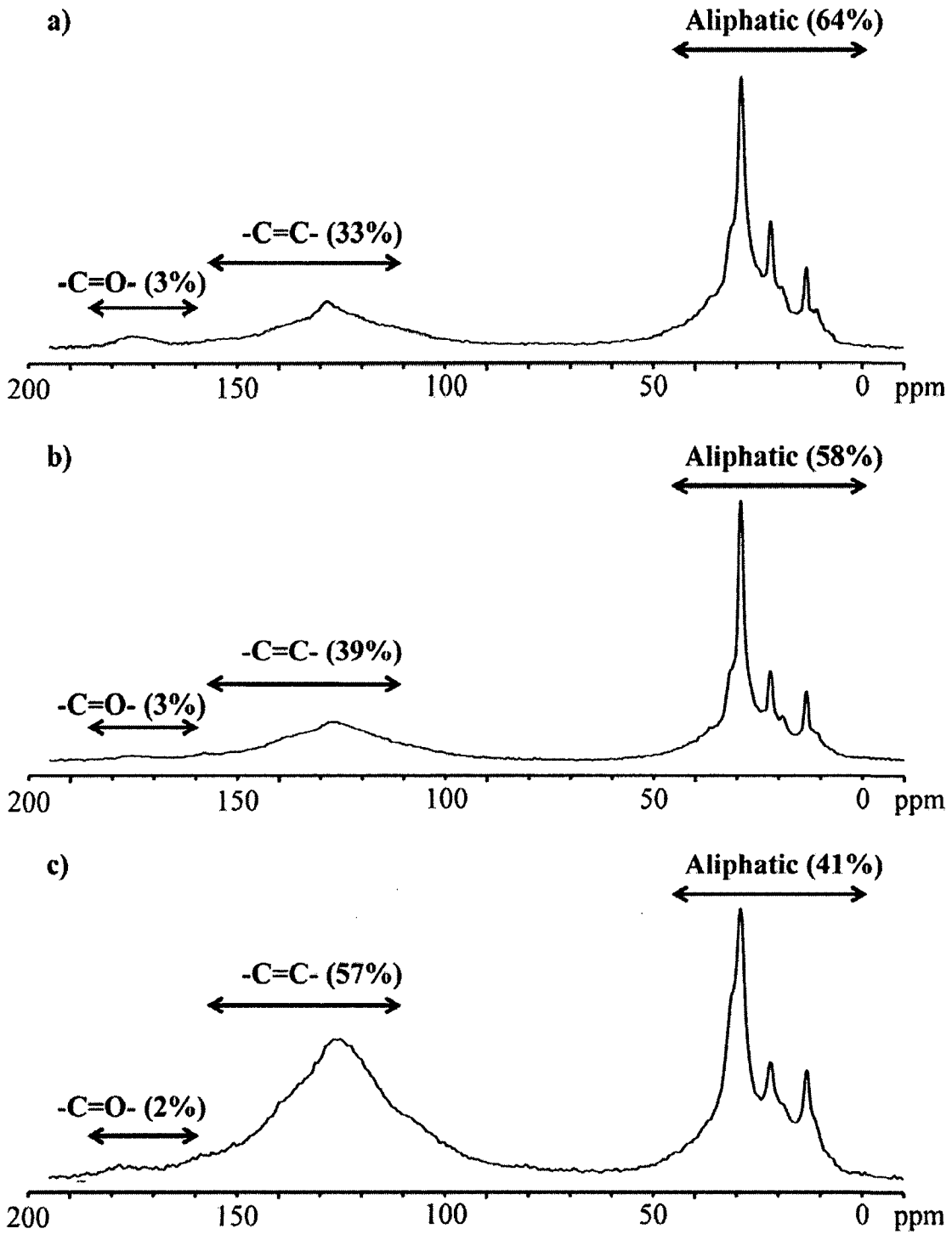

Figure 21. Quantitative ^{13}C ssNMR spectra for the insoluble residues obtained at each of three hydrothermal treatment temperatures of whole algae at a) 260 °C, b) 310 °C, and c) 360 °C.

The high aliphatic content of the remaining residue hints at capacity of this aliphatic portion in cracking to gas and oil at higher temperatures. At 360 °C, the amount of the carbon in the recovered residue decreases even further to account for only 20 % of the total carbon. In addition, the chemistry of the char changes to mainly aromatic (57 %) with only (41 %) residual aliphatic nature. It is likely that the residual aliphatic material could be converted to additional oil and gas by extending the heating time beyond 72 h. This was not verified due to the lack of sample. We also analyzed the algaenan solid residue after each treatment, however the NMR spectra were distorted and we were not able to get representative information from them. We hypothesize that there might have remained some sodium in the residue from the isolation procedure that entered the reactor vessel. The fact that the untreated algaenan residue did not show any distortion suggests that the sodium is only causing distortion in the NMR spectra after the hydrothermal treatment. The case could be that sodium is causing some iron from the reactor to solubilize (C.M. , 1988) and mix with the residue thus contaminating it and causing that distortion.

3.4 Oil fraction

3.4.1 General information

The maximum yield of oil products for both samples was at 360 °C where a clear biphasic solution (aqueous and oil) was observed upon cooling of the reactors. The oil generated from both samples contributed to a low-density phase found floating on the water. In the case of the algaenan concentrate, this phase existed as a waxy material and its carbon-normalized yield was 57.5 % of the carbon-based charge in the reactor. Such a waxy matrix is common to experiments conducted on Type I kerogens known to generate

waxy oils (Lewan, 1985; Ruble et al., 2001). In contrast, whole algae yielded liquid oil (carbon-based yield of 49 %), and its physical state suggests that a larger proportion of low-molecular-weight components constituted this oil compared with the algaenan.

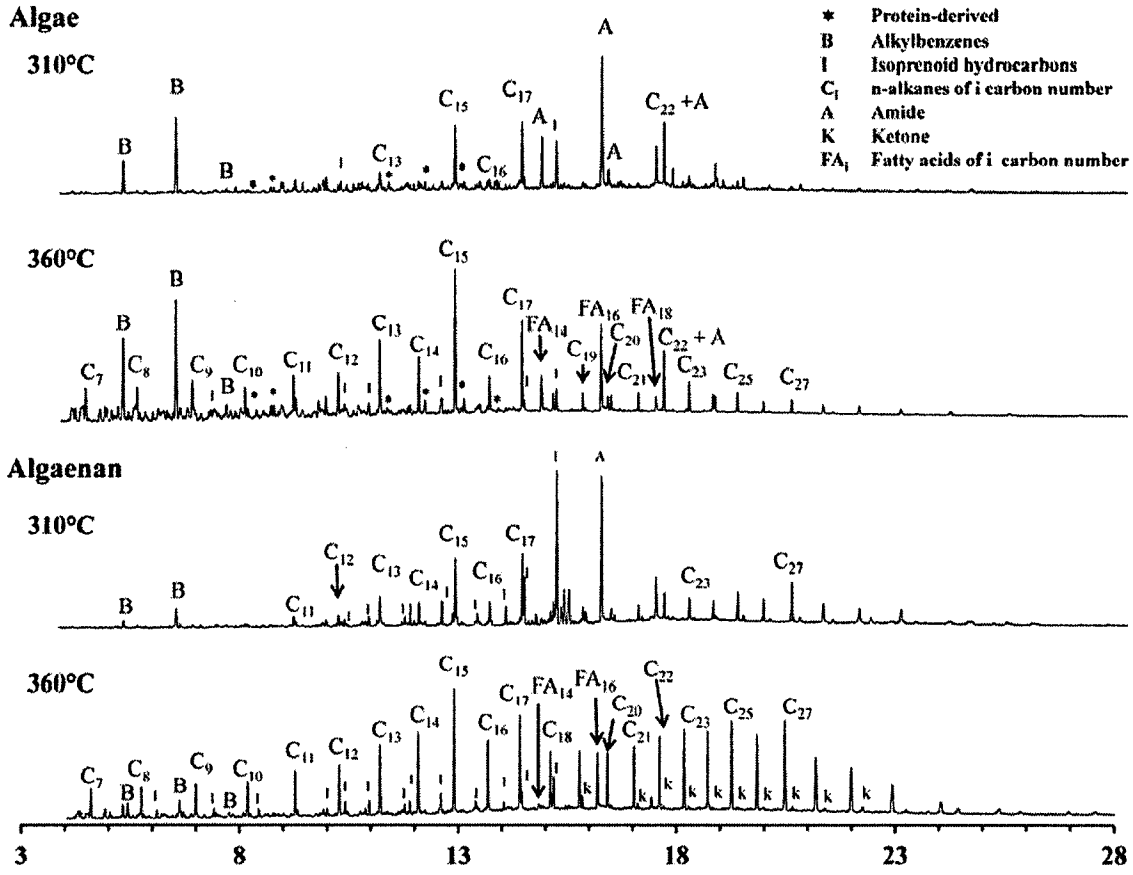

Figure 22. Gas chromatographic traces for recovered oil samples. Time in minutes.

Figure 22 shows one-dimensional GC-FID analysis of the oils from whole algae and the algaenan at 310 °C and 360 °C. It is worth mentioning that at 260 °C, neat oil samples were not collected because not enough oil was floating on the aqueous surface. The chromatogram of the algae oil at 310 °C shows the existence of alkylbenzenes (toluene, xylene, and propylbenzene), protein derived products such as amides (C_{14}AA,

C_{16}AA), pyridines, quinolones, quinoxalines, and indoles (Not identified specifically in GC-FID, see GCxGC section). In addition, the hydrocarbon abundance is very minimal except for the C_{13}, C_{15}, and C_{17} *n*-alkanes. This distribution is likely due to the decarboxylation of the C_{14}, C_{16}, and C_{18} fatty acids in the algae. Indeed, the C_{14}, C_{16}, and C_{18} fatty acids are the most abundant in the whole algae sample (Table 11). The same FA distribution was also found by Makulla (2000) for *Scenedesmus Obliquus*. Biller et al. (2011) observed that saturated lipids were more abundant following the hydrothermal process. This explains the fact that we do not see the C_{15} or C_{17} alkenes from the decarboxylation of the $C_{16:1}$ and $C_{18:1}$ fatty acids. The chromatogram of the algaenan oil at 310 °C is similar to that of the algae oil at 310 °C for the lower boiling point fraction up to C_{17} alkane. Some differences include a lower concentration on alkylbenzenes, lack of identifiable protein-derived compounds, and the appearance of some longer chain *n*-alkanes (C_{19} – C_{33}). The appearance of the longer chain alkanes suggests a start to the cracking of the algaenan. It is worth noting that the paucity of alkanes in the oils formed at 310 °C for both the algae and the algaenan is further evidence of the resistance of algaenan to cracking.

Table 11. Quantification of total fatty acid content in *Scenedesmus* algae.

	Fatty acid (FA)							
	13:0	14:0	15:0	16:0	16:1	17:0	18:0	18:1
Weight (mg FA/g algae)	BDL	0.65	0.56	6.38	0.93	0.85	0.91	1.61

BDL: Below detection limit

At 360 °C, the chemistry of the oil changes significantly for both the algae and

the algaenan. The algae oil shows a distribution of *n*-alkanes extending from *n*-C_7 to *n*-C_{33} and maximizing at *n*-C_{15} with a slight predominance of odd-numbered *n*-alkanes, especially in the range of *n*-C_{13} to *n*-C_{17}. The predominance is greatest with the whole algae, reflecting the fact that it had not been treated with solvents that would extract free lipids and contained fatty acids which generated the *n*-alkanes. The *n*-alkane predominance for *n*-C_{13}, *n*-C_{15}, and *n*-C_{17} suggests that the *n*-alkane distribution includes a component that derives from the simple decarboxylation of the pre-existing free fatty acids or triglyceryl fatty acids in the sample. It is also interesting to see the evolution of *n*-alkanes larger than C_{19} in the algae fraction. The lack of the larger chain length hydrocarbons in the 310 °C oils suggests a non-lipid origin. Indeed studies performed on hydrous pyrolysis of lipids do not show the evolution of alkanes with longer chain length than the parent lipid in the absence of a catalyst (Biller et al., 2011). In addition, the more dominant suite of *n*-alkanes derives from cracking of the algaenan structure in such a manner as to produce a rather smooth distribution of the homologous series of *n*-alkanes.

The chromatogram of the algaenan oil at 360 °C is significantly different from that at 310 °C. The first difference that can be seen is the major increase in the *n*-alkane hydrocarbons (C_7 to C_{34}). We also see the evolution of C_{14} and C_{16} fatty acids that were not in the 310 °C chromatographic trace. The algaenan isolate was treated with strong base which can be expected to hydrolyze triglyceryl esters of fatty acids and extracted with organic solvent to remove these and free fatty acids from the sample. Thus, the algaenan is expected to contain fewer fatty acid components than the whole algae, consistent with the fact that the *n*-alkanes generated from decarboxylation of these acids are not as dominant as in oil from whole algae. The observation that some of the peaks in

the chromatogram are from fatty acids is evidence that not all fatty acids are decarboxylated under conditions of hydrothermal treatment. Some of these fatty acids could exist as esters within the algaenan and be liberated as acids upon thermal decomposition. A similar observation was made using flash pyrolysis experiments on algaenan isolated from the same algae (Obeid et al., 2014). The general distribution of *n*-alkanes in the algaenan isolate at 360 °C matches that observed in the whole algae, suggesting that it is the algaenan present in whole algae that gives rise to the majority of the hydrocarbons during hydrothermal treatment. There are some notable differences, however, aside from the abundance of fatty acids noted above. Most apparent is the presence of alkylbenzenes observed in whole algae oil and in much lesser quantities in the oil from algaenan (Figure 22). This is an indication that the majority of these derive from the non-algaenan component of whole algae, probably the proteins which contain aromatic amino acids. Likewise, the alkylamides found only in the whole algae oil are derived from non-algaenan components (GCxGC-TOFMS analysis, section 3.4.2, shows some are also detected in the algaenan oil), probably alkylamides incorporated into the algae from amidation reactions, e.g., reactions of ammonia with triglycerides (McKee and Hatcher, 2010; Chiaberge et al., 2013). Also notable is the distribution of methyl ketones observed in the algaenan isolate and present in only trace amounts in the whole algae. These are clearly associated with the algaenan in the algae, probably reflecting the presence of mid-chain ketones or ether cross-links in the macromolecular structure of algaenan (Gelin et al., 1997a).

What is most significant about the traces shown in Figure 22 is the overall distribution of *n*-alkanes and isoprenoid alkanes which resemble somewhat the

distribution commonly observed for algal-derived kerogen samples subjected to hydrous pyrolysis (Ruble et al., 2001). Unlike flash pyrolysis data for algaenan isolates (Kodner et al., 2009) which are dominated by both *n*-alkanes and *n*-alkenes, only *n*-alkanes are present in the oil from hydrous pyrolysis, similar to what is observed for kerogens. Moreover, the oils also resemble some crude oils in their distributions of hydrocarbons.

Simulated distillation experiments indicate that algae and algaenan oils distillation patterns are comparable to those observed for a number of well-known crude oils (Figure 23). A bar graph of the simulated distillation results is plotted based on four boiling point fraction cuts: Initial Boiling Point (IBP) to 200 °C, 200 °C to 350 °C, 350 °C to 475 °C and greater than 475 °C, representative of the Naphtha, Kerosene and gas oil, light and mid-heavy vacuum gas oil, and vacuum residue respectively (Behrenbruch and Dedigama, 2007). The algaenan oil compares favorably with that of paraffinic-naphthenic crude oil having medium density from North Slope (Alaska). The algae oil compares favorably to that of the paraffinic crude oil sample having light-medium density from Qua Iobe (Nigeria). This is consistent with the fact that the NSO fraction of the algae oil is 12 % wt. greater than that of the algaenan oil.

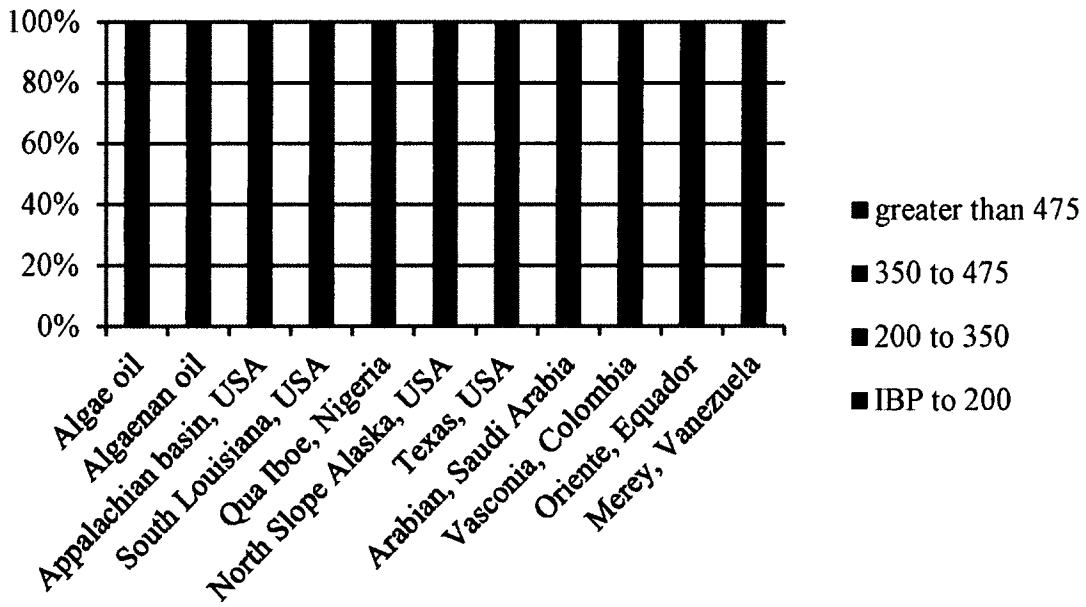

Figure 23. Plot for algae oil samples and some common petroleum samples. Data obtained from analysis of crudes by simulated distillation. Appalachian basin, USA (Paraffinic, Extra light density); South Louisiana, USA (Paraffinic, Light density); Qua Iobe, Nigeria (Paraffinic, Light-Medium density); North Slope Alaska, USA (Paraffinic-Naphthenic, medium density); Texas, USA (Naphthenic, medium-heavy density); Arabian, Saudi Arabia (Aromatic-Intermediate, medium-heavy density); Vasconia, Colombia (Aromatic-Naphthenic, heavy density); Oriente, Ecuador (Aromatic-Asphaltic, heavy density); Merey, Venezuela (Aromatic-Asphaltic, extra heavy density).

Elemental analysis of the crudes along with their calculated High Heating Values (HHV) are shown in Table 12. It is well known that the higher the oxygen content of the oil, the lower the lower its HHV and thus its quality. The High Heating Value (HHV) of typical liquid fuels ranges between 35 and 48 MJ/kg (Channiwala and Parikh, 2002). The whole algae oil contains 16 % oxygen and has a HHV of 35 MJ/kg. This is comparable to

recent studies on hydrous pyrolysis of different algae strains reporting crudes with oxygen contents between 9 % to 19 % and HHVs between 32 and 37 MJ/kg (Biller et al., 2012). The algaenan oil, however, contains less oxygen (6 %) and has a HHV of 41 MJ/kg making it a much higher quality crude oil.

Table 12. CHNSO compositions of recovered oil from hydrothermal liquefaction experiments as determined by elemental analysis.

	C (%)	H (%)	N (%)	S (%)	O (%)	HHV* (MJ/kg)
Algae (360 °C)	69.6 ± 2.7	10.6 ± 0.6	3.5 ± 0.5	BDL	16.3 ± 2.8	35.0 ± 1.2
Algaenan (360 °C)	81.4 ± 0.1	11.2 ± 1.5	1.4 ± 0.1	BDL	6.0 ± 1.5	41.0 ± 1.8

BDL: Below Detection Limit.* calculated by the Boie formula (Boie, 1953)

To be useful as a quality feedstock for refining operations, crude oil needs to display a low proportion of NSO compounds that represent complex heteroatomic molecules within the crude, and values of less than 20 % of the total crude oil by weight are common among most crude oils (Peters et al., 2007). The distribution of aliphatic, naphthenic/aromatic, and NSO-containing molecules in the algae oil is shown in Table 13. Polar NSO-type compounds constitute 43.1 % and 31.8 % of the total oil recovered from whole algae and algaenan oil, respectively. While these levels of NSOs are generally higher than most crude oils (Peters et al., 2007), they are not as abundant as in oils derived from other biomass sources such as woody or terrestrial plant biomass (Oasmaa and Czernik, 1999; Wildschut et al., 2009). Moreover, they are also not as abundant as in oils derived from hydrous pyrolysis of whole algae (Patil et al., 2008) which require upgrading to produce useful fuels. This is mainly because the algae is relatively rich in algaenan that yields predominantly *n*-alkanes, and these overwhelm the

polar hydrous pyrolysis products that one obtains from non-algaenan components of whole algae which dominate other algal strains lacking algaenan.

Table 13. Weight percentages of oil components in the recovered oil from hydrothermal liquefaction experiments as determined by column chromatography on silica gel.

	Aliphatics and Naphthenic (Saturates)	Aromatics	NSOs
Algae	38.4 %	17.2 %	43.1 %
Algaenan	35.4 %	31.8 %	31.8 %

3.4.2 GCxGC-TOFMS

Figures 24 and 25 show the GCxGC-TOFMS chromatograms of the algae and the algaenan oils. GCxGC-TOFMS is a powerful tool for separating complex mixtures such as oils. The compounds that coelute in the one dimensional GC chromatogram are separated based on their polarity in the second dimension; increasing polarity results in an increasing retention in the second dimension. This combination provides a kind of chemical logic to separation and thus with a combination of retention times from two dimensions and a mass spectral analysis, a large number of compounds can be identified and grouped into separate classes (Table 14).

The GCxGC analysis shows a strong predominance of the *n*-alkanes/isoalkane homologous series that ranges from C_6-C_{37}. The algaenan oil showed a higher percentage of *n*-alkane/isoalkanes than that of algae oil (41.4 % wt. vs. 38.5 % wt.). In general, the distributions for *n*-alkanes are very similar to those obtained from GC-FID analysis for both the algae oil and the algaenan oil. The isoalkanes can be divided into two groups: isoprenoid derivatives and 2-methyl-alkanes. As their name suggests, the first group of

isolakanes exhibit structures that would be expected from isoprenoid hydrocarbons. These isoprenoids are found to range from C_6-C_{20}. It is interesting that their concentration increases with increasing carbon number and maximizes at C_{20} (phytane: 2,6,10,14-Tetramethylhexadecane) suggesting that they arise from the cracking of the phytane into smaller molecules. Their existence in the algaenan oil suggests that some of the chlorophyll must have remained in the algaenan residue since the *Scenedesmus* algaenan is thought to be aliphatic in nature (Blokker et al., 1998; Obeid et al., 2014). The second group consists of 2-methyl-*n*-alkane series ranging in length from C_7-C_{28}. These are less abundant than the other isoalkanes and since their distribution extends to higher than C_{20}, this suggests a different origin for those compounds, and we suspect that they arise from a methyl shift that could occur during the cracking of the aliphatic algaenan structure. It is also worth mentioning that we do observe mono unsubstituted *n*-alkyl-1-enes and mono unsubstituted isoprenoids, but their concentration is very small in the total oil compared to the *n*-alkanes. Leif et al. (2000) have suggested that these are important intermediates in hydrous pyrolysis of kerogens (Leif and Simoneit, 2000).

The second most dominant species in the oils are the alkylcyclopentanes ($C_i$cy(5)) and alkylcyclohexanes ($C_i$cy(6)). In contrast to the *n*-alkanes/isoalkanes fraction, the cylopentanes and cyclohexanes are more dominant in the algae oil than in the algaenan oil (17.86 % wt. vs. 10.85 % wt.). The $C_i$cy(5)/$C_i$cy(6) can also be divided into two groups: mono-*n*-alkyl substituted cycloalkanes and multi-substituted cycloalkanes. Mono-*n*-alkyl substituted cycloalkanes in the algae oil range from C_1-C_{13}cy(6) and from C_2-C_{14}cy(5) and in algaenan oil range from C_1.C_{18}cy(6) and from C_2-C_{16}cy(5). Both the algae oil and the algaenan oil *n*-Cicy(6) exhibit a bimodal distribution maximizing at

C_1cy(6) and C_9cy(6).

The cyclohexane products are more abundant than the cyclopentanes in both oils, this could be due to hindrance in the cyclization step. It has been suggested (Kissin, 1990) that the formation of the mono-*n*-alkyl cyclohexanes and cyclopentanes in the crude oils are the result of a thermoradical mechanisms resulting from the breaking of long chain *n*-alkanes and fatty acids into mixtures of long and short *n*-alkanes and olefins followed by the cyclization of olefin radicals into the mono-*n*-alkyl substituted cyclohexane products. With that in mind, it stands to reason that the C_9cy(6) would be a major product as it could be formed from the cracking of the C_{16} fatty acids or the C_{16} algaenan ester linkages forming the intermediate olefin. It is worth mentioning that previous studies reporting hydrothermal treatment on similar algae (Torri et al., 2012) and algal lipid extract (Biller et al., 2011) did not note the formation of these mono-*n*-alkyl substituted cycloalkanes.

It is possible that the long heating times in this study compared to the short times of other studies is responsible for their higher concentration. Multi-substituted cycloalkanes are less abundant than the mono-*n*-alkyl substituted cycloalkanes in both the algae and algaenan oil. It has originally been thought that their origin in crude oils is from ring opening reactions of steranes at elevated temperatures. This belief was later shown to not likely be the case as steranes were shown to have high thermal stability (Kissin, 1990; Mango, 1990) noting that the sources of these cyclohexanes are most likely cyclization of branched alkanes and isoprenoid hydrocarbons. This is likely the case with hydrothermal treatment as similar compounds are shown to form like 1-methy-2-alkylcyclohexanes and 1-methyl-3-alkylcyclohexanes. In addition the alkyl side chains in the 2 and 3 positions

on the cyclohexane ring were found to exist either as *n*-alkyl or as a branched alkyl. The branched form was more abundant in the algae oil than in the algaenan oil.

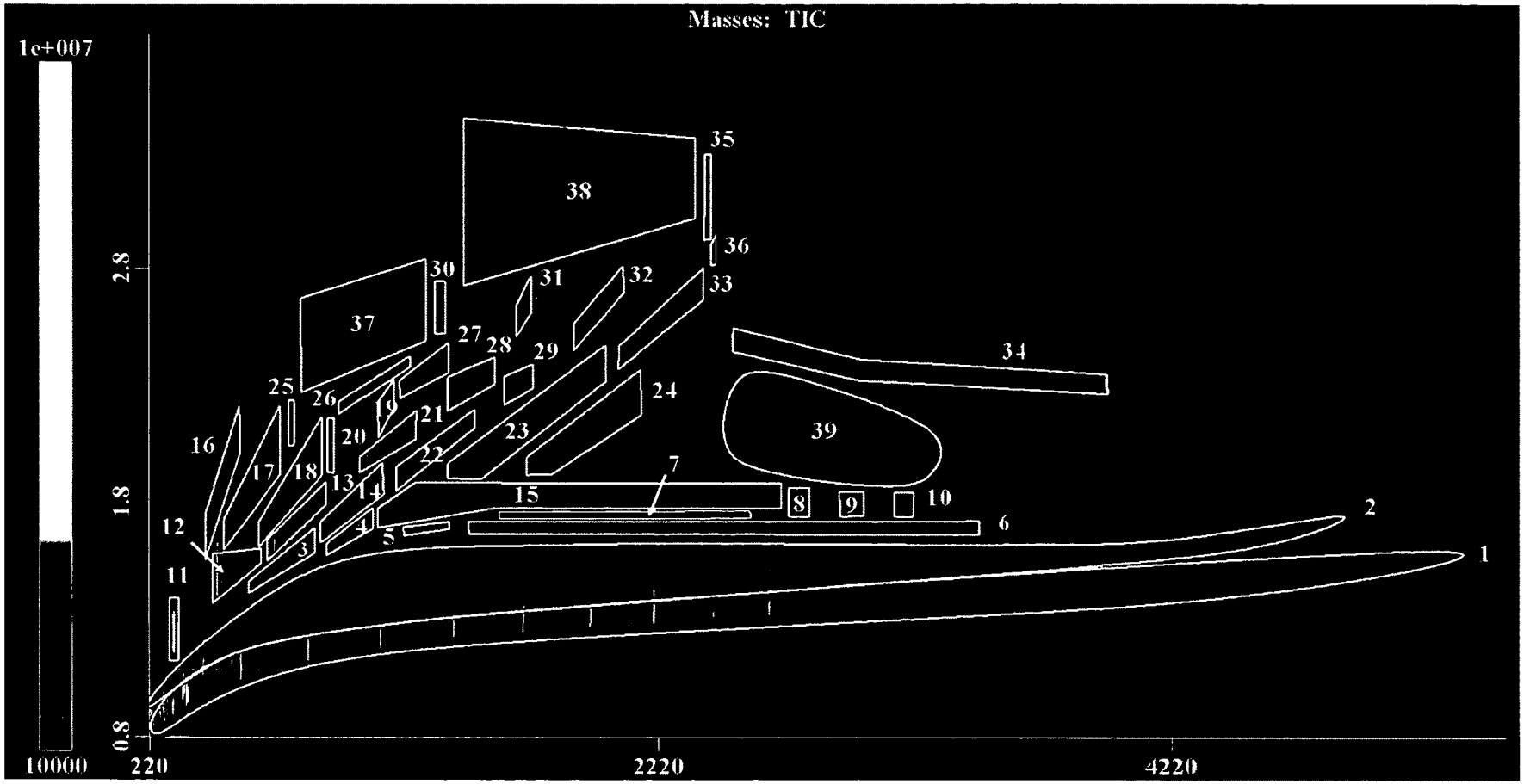

Figure 24. GCxGC-TOFMS chromatogram of algae (360 °C) oil.

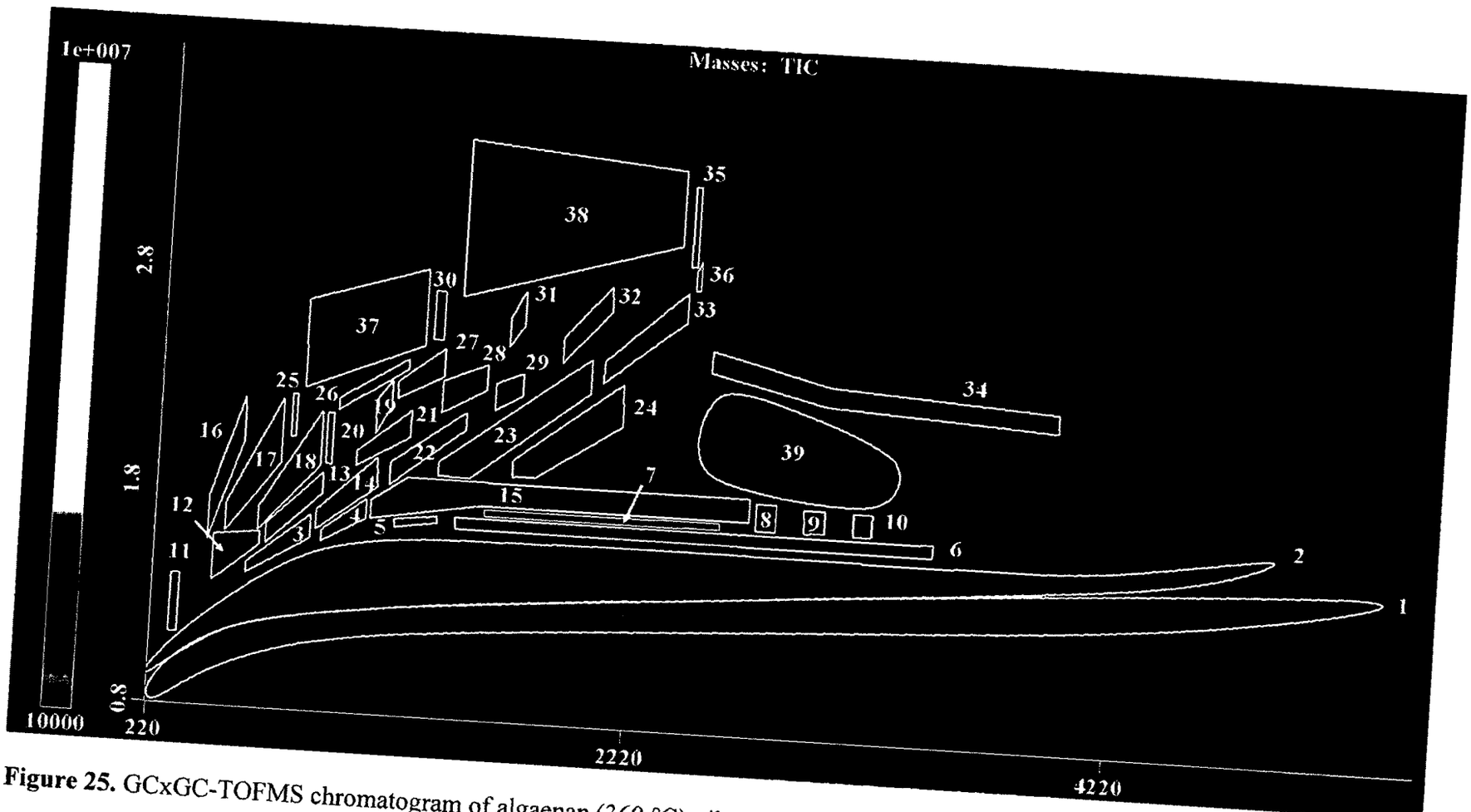

Figure 25. GCxGC-TOFMS chromatogram of algaenan (360 °C) oil.

Alkylketones (CiK) are formed in both the algae and algaenan oils but their distribution differs significantly between both samples. In the algae oil, the ketones exist in both branched and straight chain forms. It is worth mentioning that the branched ketones are only detectable up to $C_{10}K$ while as the straight chain ketones are detectable up till $C_{20}K$. The ketones in the algae oil are found mostly as straight chain (predominantly *n*-alkan-2-ones and a minor amount of *n*-alkan-3-ones) and have a bimodal distribution maximizing at C_9K and at $C_{15}K$. The reason that Table 14 shows C_8K being more abundant is that the value represents the total ketones (branched + straight). In the algaenan oil, the predominant ketones are the straight chain ketones (also *n*-alkan-2-ones and a minor amount of *n*-alkan-3-ones) with almost no detectable branched ketones. The straight-chain ketones also range from $C_7K - C_{22}K$ with maximum concentration at $C_{17}K$. Acyclic ketones from hydrous pyrolysis have been shown to be a result of oxidation of existing acyclic alcohols and/or mono-unsaturated alkenes, especially under long reaction times (Leif and Simoneit, 2000). Branched ketones are most likely the result of the oxidation of branched acyclic alcohols found in the whole algae. Leif et al. (2000) has shown that kerogens under hydrothermal conditions produce *n*-alkan-2-ones by a series of reaction steps starting by the cracking of the kerogen into *n*-alk-1-enes (minor product from cracking of kerogen under hydrous pyrolysis) followed by hydration to *n*-alkan-2-ol and further oxidation into the *n*-alka-2-ones. A similar mechanism can be envisioned to be occurring with the algaenan biopolymer under these similar conditions to produce a series of *n*-alkan-2-ones. For example, the cleavage of ester functionalities, α to the carbonyl, and possibly ethers, would produce the 1-alkene followed by an OH addition to form the 2-alkanol and then the 2-ketone.

Table 14. Identification and quantification of GCxGC-TOFMS chromatograms.

No	Description	Abbreviation	Algae oil	Algaenan oil
1	*n*-Alkanes/isoalkanes	$C_8 - C_{37}$	38.46	41.38
2	Alkylcyclopentane + Alkylcyclohexane	$C_1 - C_{19}$cy(5) + $C_1 - C_{18}$ cy(6)	17.86	10.85
3	C8 Ketones	C_8K	0.21	0.05
4	C9 Ketones	C_9K	0.10	0.02
5	C10 Ketones	C_{10}K	0.04	0.05
6	Greater than C10 Ketones	>C_{10}K	0.24	0.63
7	*n*-C9 – C13 Fatty acids	$C_9 - C_{13}$FA	0.14	0.02
8	*n*-C14 Fatty acid	C_{14}FA	0.16	0.06
9	*n*-C15 Fatty acid	C_{15}FA	0.00	0.01
10	*n*-C16 Fatty acid	C_{16}FA	0.17	0.31
11	Toluene (C1 Alkylbenzene)	T	1.92	0.62
12	Ethylbenzene/C2 Alkylbenzenes	C_2B	3.41	1.33
13	C3 Alkylbenzenes	C_3B	0.99	0.25
14	C4 Alkylbenzenes	C_4B	0.87	0.25
15	Greater than C4 Alkylbenzenes	>C_4B	1.09	0.39
16	C1 Alkylcyclopentanone + C1 Alkylpyridines[a]	C_1cy(5k) + C_1Py	0.13	0.04
17	C2 Alkylcyclopentanone + C2 Alkylpyridines[a]	C_2cy(5k) + C_2Py	0.50	0.05
18	C3 Alkylcyclopentanone + C3 Alkylpyridines[a]	C_3cy(5k) + C_3Py	0.32	0.02
19	C4 Alkylcyclopentanone + C4 Alkylpyridines[a]	C_4cy(5k) + C_4Py	0.08	0.02
20	Indane	I	0.27	0.19
21	C1 Indanes	C_1I	0.62	0.34
22	C2 Indanes	C_2I	1.03	0.34
23	C3 Indanes	C_3I	1.30	0.41
24	C4 Indanes	C_4I	0.53	0.07
25	Phenol	P	0.15	0.23
26	C1 Alkylphenols	C_1P	0.37	0.05
27	C2 Alkylphenols	C_2P	0.64	0.10
28	C3 Alkylphenols	C_3P	0.34	0.06
29	C4 Alkylphenols	C_4P	0.22	0.05
30	Naphthalene	N	0.08	0.03
31	C1 Alkylnaphthalenes	C_1N	0.15	0.08
32	C2 Alkylnaphthalenes	C_2N	0.18	0.11
33	C3 Alkylnaphthalenes	C_3N	0.06	0.02
34	C11 – C18 Alkylamides	$C_{11} - C_{18}$AA	0.19	0.09
35	Biphenyl	Biph	0.03	0.01
36	C1 Fluorene	C_1Flu	0.01	<0.01
37	Group A[b]	Group A	0.37	0.08
38	Group B[c]	Group B	0.45	0.17
39	Steranes	Ste	0.33	1.34
	Unclassified		3.41	1.18
	Sum		77.41	61.30

[a] Alkylpyridines not observed in algaenan oil. [b] Includes: mono-, di-, and tri-methyl substituted 2-cyclopenten-1-ones, phenyl ketones, and phenyl ketones. [c] Includes: C_1-C_2Quinolines, C_2-Quinoxaline, and C_0-C_3 Indoles.

Analysis of the fatty acid by 2D-GCxGC-TOFMS did not provide any new insights from what was mentioned in the sections above.

Alkylbenzenes (C_iB) in the algae and algaenan oils range from C_1-C_9B. They are more abundant in the algae oil than in the algaenan oil but they show the same distribution in both samples maximizing at C_2B with ethylbenzene being the most abundant isomer followed by *p*-xylene. Alkylbenzenes in both samples are found as mono-, di-, and trialkyl benzenes with the alkyl side chains being either straight chain or branched. The trend in these samples seems to be mono- > di- > trialkyl benzenes and that alkylbenzenes with straight side chains being more abundant that their branched counterpart. These general trends seem to be the same in both oil samples. It has been suggested that alkylbenzenes in oils can originate from aromatization reactions of thermal decomposition products of lipids and proteins (Higman et al., 1970). In addition, it has also been suggested that alkylbenzenes could be a byproduct of thermal decomposition of algaenan (Torri et al., 2012). This seems like a valid hypothesis as it is evident that alkylbenzenes are in the algaenan oil. However, it is unlikely that the alkylbenzenes (especially *n*-alkylbenzenes) are produced as a result of the primary cracking of the algaenan, as flash pyrolysis studies on chemically isolated algaenan shows no or minor contribution of alkylbenzenes in the pyrolyzate (Obeid et al., 2014). It is more likely that the alkylbenzene contribution to the algaenan oil is the result of aromatization of cycloalkanes produced during the hydrothermal process.

Protein pyrolysis products such as Alkylpyridines (C_iPy), alkylphenols (C_iP), alkylamides (C_iAA), C_1-Quinolines, C_2-Quinoxaline, and C_i alkylindoles were identified in the algae oil. In the algaenan oil only alkylphenols, alkylamides and indoles were

observed, this is probably due to the low initial concentration of proteins in the algaenan sample. Alkylpyridines range from C_1Py – C_5Py (mono-, di-, and tri- substituted pyridines) and maximize at C_2Py and C_3Py in the algae oil with the highest species being the (di- and tri-) methyl substituted followed by the ethyl substituted. Alkylpyridines are thought to be produced by a one-step condensation of amino acids and sugars (Hwang et al., 1995) (i.e., melanoidin decomposition). Alkylphenols range from P – C_4P in both algae and algaenan oils but are more prevalent in the algae oil than in the algaenan oil. They maximize at C_2P in algae oil and P in algaenan oil. Alkylindoles range from C_0-C_3 and maximize at C_1 and C_2 alkylindoles (mono- and di-methyl substituted indole and isomoers) in both algae and algaenan oils. It is thought that both alkylphenols and alkylindoles form as a result of cracking of protein side chains during the thermal treatment, e.g., tyrosine and tryptophan, respectively (Chiavari and Galletti, 1992). Alkylamides (C_iAA) range from *n*-C_{11}AA – *n*-C_{18}AA and are more abundant in the algae oil than in the algaenan oil. In contrast to one-dimensional GC-MS, GCxGC-TOFMS was able to detect the same series of alkylamides as those found in the algae oil. Alkylamides maximize at *n*-C_{16}AA for both the algae and algaenan oil. As mentioned above, we believe that alkylamides are incorporated into the algae from amidation reactions of ammonia with triglycerides (McKee and Hatcher, 2010; Chiaberge et al., 2013). The algae oil in addition contains small amounts of C_1-C_2 quinolines (various isomers) and C_2-quinoxaline. To our knowledge these compounds were not noted to form during subcritical conditions, however they were noted to form in oils formed under supercritical treatment of algae (Duan and Savage, 2011a).

Alkylcyclopentanones ($C_i$cy(5k)) in the algae and algaenan oils range from C_1 –

C_4cy(5k). They are more abundant in the algae oils but are still found in the algaenan oil due to the presence of some residual carbohydrates after the treatment to isolate algaenan. The majority of the cyclopentanoes are mono-, di-, tri- , and tetramethyl cyclopentanones. Biller and Ross (2011) have shown that cyclopentanone was observed to form as thermal decomposition products of glucose. It is also worth mentioning that other carbohydrate derived products have been observed in minor quantities in the algae and algaenan oils such as C_1 – C_2 cyclohexanones, tetra-methyl-2-cyclopenten-1-ones, and 1,4-cyclohexanedion (Kuhlmann et al., 1994). The oils also show furans which are typically found in oils from whole algae. Seven furan compounds were identified with 4-methyl-2-propyl-furan and 2-ethyl-5-methyl-furan being the major products (0.15 %wt. of algae oil). Alkylnaphthalenes (CiN), biphenyl (Biph), and C_1fluorene (C_1Flu) have been identified in the algae and algaenan oils. Their concentration is higher in algae than the algaenan oils. Alkylnaphthalenes maximize at C_2N for both samples. It has been noted that the occurrence of alkylnaphthalenes in crude oils is indicative of high thermal maturity (Peters et al., 2005). In addition, the algae oil contained a minor amount of anthracene, phenanthrene, and acenaphthene. The origin of these compounds has been found to be thermal alteration of biological precursors (McCollom et al., 1999) and secondary thermal aromatization of primary pyrolysis products such as indanes (Fahim et al., 2009).

4. CONCLUSIONS

Hydrothermal treatment of *Scenedesmus/Desmodesmus* spp. algae and its algaenan concentrate produce oil that physically fractionates from the aqueous phase and

that show a predominance of hydrocarbons similar to those found in some fossil crude oils (Peters et al., 2005). Most of the hydrocarbons produced in the hydrous pyrolysis of whole algae appear to originate from algaenan that is an abundant component of the algae. This could be a hint that algaenan containing algae are more suitable to be used as feedstock to hydrous pyrolysis to produce a hydrocarbon rich biofuel.

The algaenan showed resistance to thermal degradation at temperatures as high as 310 °C but showed evidence of cracking at 360 °C. This was shown to be the case for both the whole algae and isolated algaenan. The decrease of the aliphatic region of the ^{13}C ssNMR in addition to the evolution of a much higher concentration of *n*-alkanes from GC-FID provided evidence for this. Simulated distillation showed that the algae oil compares favorably with an example paraffinic crude oil sample having light-medium density from Qua Iobe (Nigeria). The algaenan oil compares favorably with a paraffinic-naphthenic crude oil having medium density from the North Slope (Alaska).

Most importantly, algaenan oil contains much less nitrogen and oxygen (1.4 % and 6 %) than the oil from whole algae (3.5 % and 16,3 %) and has a higher high heating value (41 MJ/Kg vs. 35 MJ/Kg). These bulk characteristics are important considerations for the development of conversion strategies in algal bio refineries, considering the fact that increased heteroatom contents for algal oils will most likely lead to higher cost expenditures for refinement of oils into usable fuels.

GCxGC-TOFMS was instrumental in allowing for detailed analysis of molecular information about the non-polar volatile fraction of both oils. The algae oil showed a much higher concentration of protein and carbohydrate pyrolysis products, compounds that render the oil more oxygenated and decrease its overall value. The algaenan oil

showed a higher potential fuel value than whole algae oil with contributions from compounds such as *n*-alkanes (short and long chain), 2-methyl-*n*-alkanes with carbon numbers greater than C_{20}, and long chain *n*-alkylcycloalkanes.

CHAPTER V

HYDROUS PYROLYSIS OF *SCENEDESMUS* ALGAE AND ALGAENAN: FTICR-MS OF PRODUCED OILS

PREFACE

In this chapter, we present some of the data and analysis that were not discussed in Chapter IV and were not included in the publication because they address mostly the polar compounds and these were not the focus of Chapter IV. This chapter is meant to provide an in-depth analysis of the polar constituents in the hydrous pyrolysis (HP) oils by Fourier transform ion cyclotron mass spectrometry (FTICR-MS).

1. INTRODUCTION

HP of algae has shown the most promise as a technique to produce biologically derived liquid biofuels (Elliott and Baker, 1989; Elliott, 2007; Duan and Savage, 2011b, c; López Barreiro et al., 2013). Typically, algal derived biofuels have high heteroatom contents (4 – 7) % N and (5 – 19) % O which in turn translates to having oils with a high polar fraction. In fact, in Chapter IV I have observed that 43.1 % wt. of the algae derived oil and 31.8% of the algaenan derived oil are part of the NSO (Nitrogen-, Sulfur-, and Oxygen-containing compounds) fraction that is too high boiling and polar to be analyzed by traditional gas chromatography. Torri et al. (2012) performed HP on *Desmodesmus* sp. and observed that less than 10 wt. % elutes through a silica column by a mixture less polar than Dichloromethane/Ethylacetate (1:1 v/v). This suggests that a significant

fraction of oils produced from HP of algae is polar and this means that much of this fraction remains uncharacterized.

NSOs are typically major pyrolysis products of kerogen, coals, and more recently algae. Lewan (1997) observed that oils produced by HP of immature coals have a larger NSO fraction than those formed from non-hydrous closed system pyrolysis. The importance of NSO compounds in the formation of petroleum has been suggested for sometime (Nikonov and Senning, 1989) (Tissot and Welte, 1984). More recently, Behar et al. (2008) investigated the role of NSOs in the primary cracking of kerogen. They observed that high molecular weight polar NSOs recovered from DCM (named DCM NSOs) constituted the largest fraction of products formed during primary cracking of kerogen. At higher thermal severity, the DCM NSOs undergo further cracking to produce nonpolar and polar hydrocarbons.

Due to their insolubility, NSOs do not lend themselves well to traditional analysis by gas chromatography. Electrospray ionization coupled to Fourier transform ion cyclotron mass spectrometry (ESI-FTICR-MS) is ideal for analysis of NSO compounds (Salmon et al., 2011; Kamga et al., 2014). Electrospray's soft ionization coupled to the high resolving power ($m/\Delta m_{50\%} \geq 400{,}000$ broadband) of the ion cyclotron analyzer and detector allows for calculation of exact molecular formulas (Sudasinghe et al., 2014). ESI-FTICR-MS has been successfully used to identify many compounds in petroleum (Marshall and Rodgers, 2008; Hockaday et al., 2009; Salmon et al., 2011). Schenk et al. (2008) analyzed HP produced oils from *Nannochloropsis salina* by ESI-FTICR-MS and were successful in identifying many classes of compounds. In this Chapter, I seek to characterize the oils produced from HP of *Scenedesmus/Desmodesmus* spp. as a whole

and from the HP of isolated algaenan. In Chapter IV, I showed that the oils from whole algae appeared to contain compounds that were generally more polar than those produced from algaenan. That study was limited to volatile species. Here I examine the nonvolatile polar fraction.

2. MATERIALS AND METHODS

2.1 Sample information

Algae and algaenan sample preparation information and HP conditions are found in Chapter IV, section 2. The expelled oils produced from HP of whole algae and algaenan at two temperatures (310 °C and 360 °C) were selected for analysis.

2.2 ESI-FTICR-MS sample preparation and parameters

Algae and algaenan oils were diluted in a mixture of THF:MeOH (1:1 v/v) to a final concentration of about 30 ppm carbon. The samples were continuously infused into an Apollo II ESI ion source of a Bruker Daltonics 12 Tesla Apex Qe FTICR-MS instrument. Samples were introduced via syringe pump operating at 2 μL/min. Ions were accumulated in the hexapole for 2.0 s before being transferred to the ICR cell. Shield and capillary voltages were adjusted for each sample for negative mode analysis. The spectra were acquired for 300 scans in broad-band mode from 200-1200 *m/z* collected with a 4 M Word time domain for the FID, which resulted in a total experiment time of 30 min per sample. The summed FID signal was zero filled once and Sine-Bell apodized prior to fast Fourier transformation and magnitude calculation using the Bruker Daltonics Data Analysis software. Prior to analyzing the sample, the mass analyzer was externally calibrated using a polyethylene glycol standard sample. Internal calibration of the

acquired spectra was performed on each of the samples using a homologous series of fatty acids that were observed across all the samples (also evident to exist from GC analysis) (Sleighter et al., 2008). Only *m/z* values with S/N > 3 were considered for further processing. Elemental formulas were calculated using a Matlab program developed by me (Appendix C) with an accuracy of less than 1.0 ppm, and final assignment choices were aided using a series of conservative rules inserted into a program developed using Matlab (v. 7.4.0, The Mathworks Inc., Natick, MA).

The designed program uses a modified brute force approach to match *m/z* data with masses fitting the criteria: $^{12}C_{0-\infty}$, $^{1}H_{5-100}$, $^{16}O_{1-30}$, $^{14}N_{0-5}$, $^{32}S_{0-10}$, $^{31}P_{0-1}$ and having an accuracy of < 1 ppm. In addition, the program identifies salt adduct and 13C isotopic peaks and eliminates them from further analysis. Peaks identified as solvent contaminants in the solvent blank were also subtracted from the sample spectra. Peak lists were drafted using only *m/z* values with signal to noise > 4. The resulting formulas were then selected based on integer number double bond equivalents (DBE) and the following constraints correspond to the standard range of atomic composition for natural organic matter (Stubbins et al., 2010): O/C $\leq$ 1.2, H/C $\leq$ 2.25, H/C $\geq$3, H < ((2*C)+ 2), N/O <1; N/C $\leq$ 0.5, O < (C+2), S/C $\leq$ 0.2, (S+P)/C < 0.2, P/C $\leq$ 0.1, O > 4*P, (N + 4*P + 4*S) < O.

3. RESULTS AND DISCUSSION

Figure 26 shows the ESI-FTICR-MS spectra of the oils from the algae and algaenan at the different reaction temperatures. The overall spectra show peaks ranging from 200 to 900 *m/z* for all the samples. All four samples are dominated by the same seven most intense peaks (256.240230 *m/z*, 284.271530 *m/z*, 340.334130 *m/z*, 368.35430

m/z, 396.396730 *m/z*, 424.428030 *m/z*, 452.459330 *m/z*). These peaks are atributed to even *n*-fatty acids (C_{16}, C_{18}, C_{22}, C_{24}, C_{26}, C_{28}, C_{30}) having the formula $C_nH_{2n}O_2$ (see discussion below). As the temperature increases, the C_{16} and C_{18} fatty acid magnitudes decrease in the samples and the rest of the fatty acids' increase maximizing at C_{24} fatty acid in the algae oil and C_{28} for the algaenan oils. It is important to note that having the C_{18} fatty acid in all the samples be at a higher concentration than the C_{16} fatty acid contrasts with what was shown in the Chapter IV (Table 11) where I show that the C_{16} fatty acids are abundant in the algae. This lack of correspondence is a combined result of contamination from the solvent which contained a high amount of C_{18} fatty acid and the fact that gas chromatography of underivatized fatty acids is not the best approach for evaluating their respective concentrations. Therefore, for the purposes of this Chapter, the C_{16} fatty acid is assumed to be higher in concentration than C_{18} fatty acid. More detailed analysis of the fatty acid distribution is discussed later in the Chapter. In addition, as the temperature increases, a high molecular weight series of compounds having masses between 600 to 850 *m/z* also increases in the sample (see insert to Figure 26). This effect results from having more energy to crack the long polymeric algaenan structure at higher temperature.

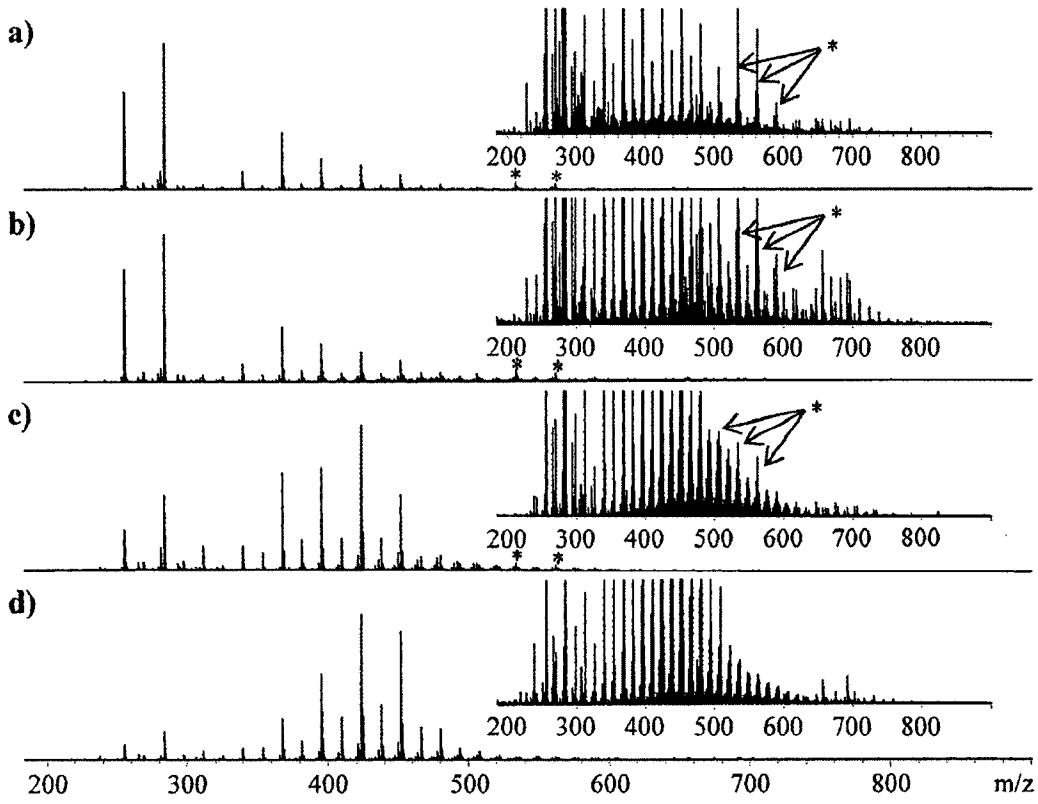

Figure 26. ESI-FTICR-MS spectra of the oils from algae at a) 310 °C, b) 360 °C and algaenan at c) 310 °C, d) 360 °C. Insert shows the expanded spectra. Asterisks denote CHON peaks.

The total number of peaks are shown in Table 15. The total number of peaks for the algae oils are greater than those for the algaenan oils. Between 80 % and 93 % of all the detected peaks were identified using the selection criteria as either ^{12}C monoisotopic unique formulas or ^{13}C isotopic peaks. The mass difference between the ^{12}C monoisotopic peak and that of one ^{13}C isotope is 1.00335 *m/z* indicating that compounds are singly-charged.

Table 15. Number of formulas.

	Total peaks	Assigned peaks	Isotopic peaks	Unknown peaks	Total identified	
						%
Algae						
310 °C	3118	2321	568	229	2907	93.2
360 °C	2250	1515	471	264	1986	88.3
Algaenan						
310 °C	2918	1871	650	397	2521	86.4
360 °C	1843	1054	430	359	1484	80.5

The identified molecular formulas were plotted on a van Krevelen diagram for better visualization (Figure 27). In a van Krevelen diagram (Kim et al., 2003), formulas are plotted on a scatter plot based on their hydrogen to carbon ratio (y-axis) and oxygen to carbon ratio (x-axis). The plot is further divided into separate areas which correspond to different H/C and O/C of different natural products such as lignin, tannin, protein, lipid, and unsaturated hydrocarbons (Hockaday et al., 2009). This is possible because the major biomolecules plot in specific areas on the van Krevelen diagram. Peaks that plot in overlapping areas are further differentiated based on their N/C ratio and AI_{mod} (modified aromaticity index) (Koch and Dittmar, 2006; Sleighter et al., 2008). This allows for better visualization of the data and for characterization of the molecules, as shown for the boxed areas in Figure 27, based on their plot location. It is worth mentioning that a formula that plots in a specific area, for example lignin, does not necessary mean it derives from lignin. In fact, lignin is a polymer found in wood and is absent in algae. However, a formula having the same atomic H/C, O/C, N/C, and AI_{mod} as that of lignin will most probably have a structure that is similar to that of lignin. This is the same for the rest of the aforementioned classes (Kim et al., 2003). The terminology is used in the dissolved

organic matter literature to distinguish the different areas in the van Krevelen plot (Sleighter et al., 2008; Hockaday et al., 2009; Zhong et al., 2011) and is adapted here to simplify the discussion.

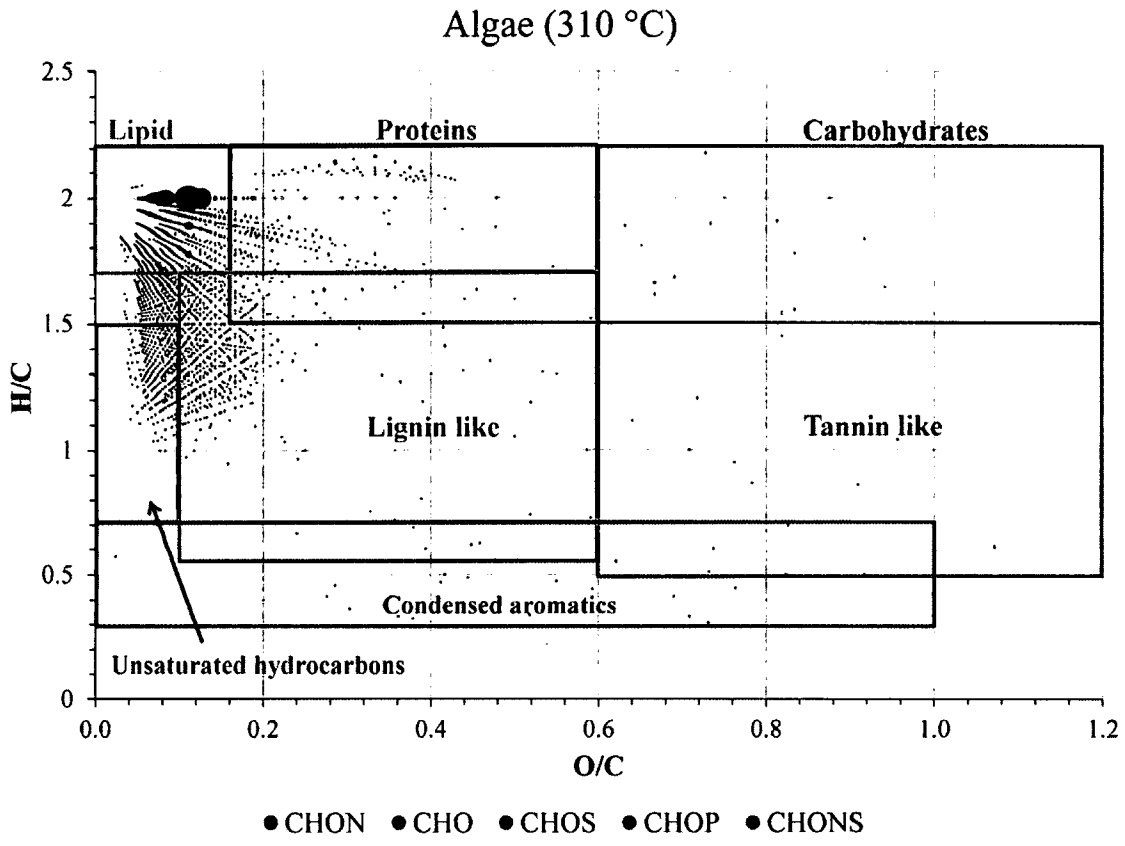

Figure 27. Van Krevelen diagram for all the assigned peaks in the expelled oil from HP algae at 310 °C. The size of the bubble for each data point is proportional to the peak magnitude (P). Peak magnitudes in the figure were linearly normalized ($Poriginal_{max}$ / $Poriginal_{min}$ = 10000 normalized to $Pfinal_{max}$ / $Pfinal_{min}$ = 100) for better visualization. Boxed areas in the plot represent molecules classified based only on H/C and O/C molecular ratios.

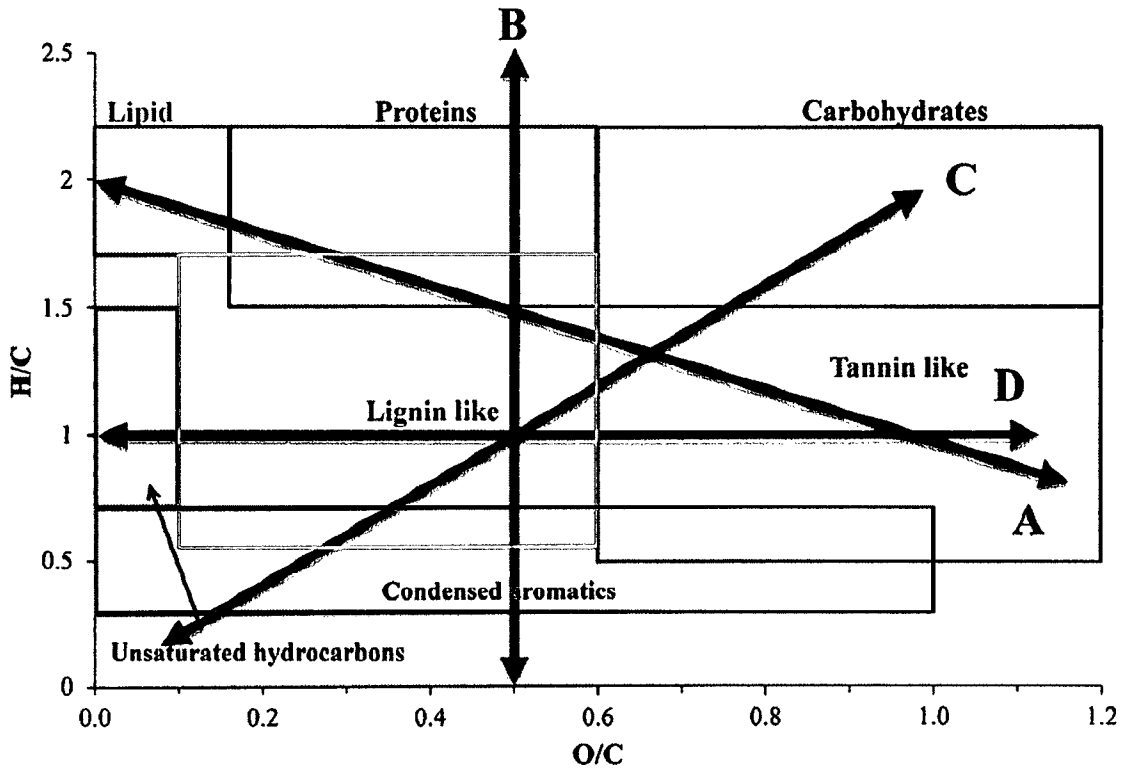

Figure 28. A van Krevelen diagram showing compound classifications (boxes) and arrows denoting the trend lines for molecules subjected to chemical reactions: (A) methylation/demethylation, or decarboxylation; (B) hydrogenation/dehydrogenation (including aromatization); (C) hydration/condensation; and (D) oxidation / reduction (Kim et al., 2003).

Kim et al. (2003) showed how compounds in complex samples can be related to different chemical transformations such as: methylation/demethylation, hydrogenation/dehydrogenation, hydration/condensation, oxidation/reduction, etc. This chemical logic is useful in analyzing complex mixtures such as oils produced from pyrolysis products. That being the case, changes in the location of where the peaks plot on a van Krevelen diagram between oils treated at different temperatures can also denote

the type of chemical reactions that can take place. For example, if a molecule undergoes hydrogenation, the location of its elemental formula on the van Krevelen should change vertically towards a higher H/C and in the opposite direction if undergoing dehydrogenation. There are two important notes to keep in mind when relating changes in areas to chemical reaction. First, the chemical reactions mentioned above are not an exhaustive list of reactions. However, they include most of the well-known reactions that can occur under HP conditions (Winters et al., 1983; Lewan, 1985; Leif and Simoneit, 2000). Second, it is possible that a change in a formula location is the result of multiple and sequential reactions.

Table 16. Quantification of % of total peak numbers and % of total peak magnitude belonging to a certain classification.

		Lipids	Protein	Carbohydrate like	Lignin like	Tannin like	Unsaturated hydrocarbons	Condensed aromatics	others
Magnitude									
	Algae								
	310 °C	72.9	0.2	0.4	10.9	0.2	11.8	0.1	3.5
	360 °C	83.7	0.3	0.4	5.2	0.1	2.2	0.0	7.9
	Algaenan								
	310 °C	88.3	0.2	0.0	3.4	0.1	4.2	0.1	3.7
	360 °C	94.2	0.1	0.0	2.4	0.1	1.8	0.1	1.2
Peak number									
	Algae								
	310 °C	28.1	0.8	0.8	32.7	0.9	29.8	0.6	6.4
	360 °C	39.2	2.2	1.0	20.3	1.4	12.9	0.3	22.7
	Algaenan								
	310 °C	40.1	1.0	0.4	24.2	1.5	24.3	0.4	8.2
	360 °C	52.0	0.8	1.2	15.5	2.4	18.3	1.0	8.8

Lipids: $0 < O/C \leq 0.2$; $1.7 < H/C \leq 2.2$
Protein: $0.2 < O/C < 0.6$; $1.5 < H/C \leq 2.2$; $N/C \geq 0.05$
Carbohydrate like: $0.6 \leq O/C \leq 1.2$; $1.5 < H/C \leq 2.2$
Lignin: $0.1 < O/C < 0.6$; $0.5 \leq H/C \leq 1.7$; AImod < 0.67
Tannin: $0.6 \leq O/C \leq 1.2$; $0.5 \leq H/C \leq 1.5$; AImod < 0.67
Unsaturated Hydrocarbons: $0.0 < O/C \leq 0.1$; $0.7 < H/C \leq 1.7$
Condensed Aromatic: $0.0 < O/C \leq 1.0$; $0.3 \leq H/C \leq 0.7$; AImod ≥ 0.67
Others: Any formula that does not fit into the other classifications

Table 16 shows the % of total peak intensities and % of peak numbers belonging to a certain classification for all four samples. Lipids, unsaturated hydrocarbons, and lignin-like formulas make up more than 90 % of the total peak numbers and more than 90% of the total intensities for both the algae and algaenan oil samples. As the temperature increases from 310 °C to 360 °C, the lignin-like and unsaturated hydrocarbons compounds decrease in number and magnitude. This is coupled with an increase in those for lipids, carbohydrate-like, tannin-like in both the algae and algaenan oils. Compounds that form as a product of HP of algae and plot in the lignin-like region likely have structures that are a combination of oxygenated aromatic and alicyclic compounds that have functional group substitutions such as alkylesters, acids, ethers, and alkylethers. Because lignin is not present in algae, it is very unlikely that the peaks in this region are derived from lignin which is a biopolymeric component of higher plants only. Hill Bembenic and Burgess Clifford (2013) investigated the stability of some lignin model compounds: aromatic ethers (dibenzyl ether), aromatic aldehydes (vanillin and syringaldehyde), and aromatic ketones (acetovanillone and acetosyringone) under HP conditions. They found that the functional groups for those compounds cleave at high temperatures (365°C) via hydrolysis, replacing the original methoxyl groups with hydroxyl groups. It is possible that this is also the reason why the tannin-like formulas increase also. The increase in lipid formulas with temperature is expected as the macromolecular algaenan structure cracks releasing free fatty acids into the oils (see CHO compound discussion below). The increase in carbohydrate-like formulas at increased temperature can be attributed to increase in the hydration of the double bonds of the alkanes formed from the hemolytic cleavage of the algaenan (Leif and Simoneit,

2000). The increase in the protein-like formulas with temperature for the algae oils can be attributed to the hydrolysis of proteins which leads to the incorporation of nitrogen into the oils to form neutral and non-basic nitrogenated species that can be detected by (-)-EST-FTICR-MS such as amides (McKee and Hatcher, 2010; Chiaberge et al., 2013) and pyrrole-like homologues (Qian et al., 2001; Hughey et al., 2002; Sudasinghe et al., 2014).

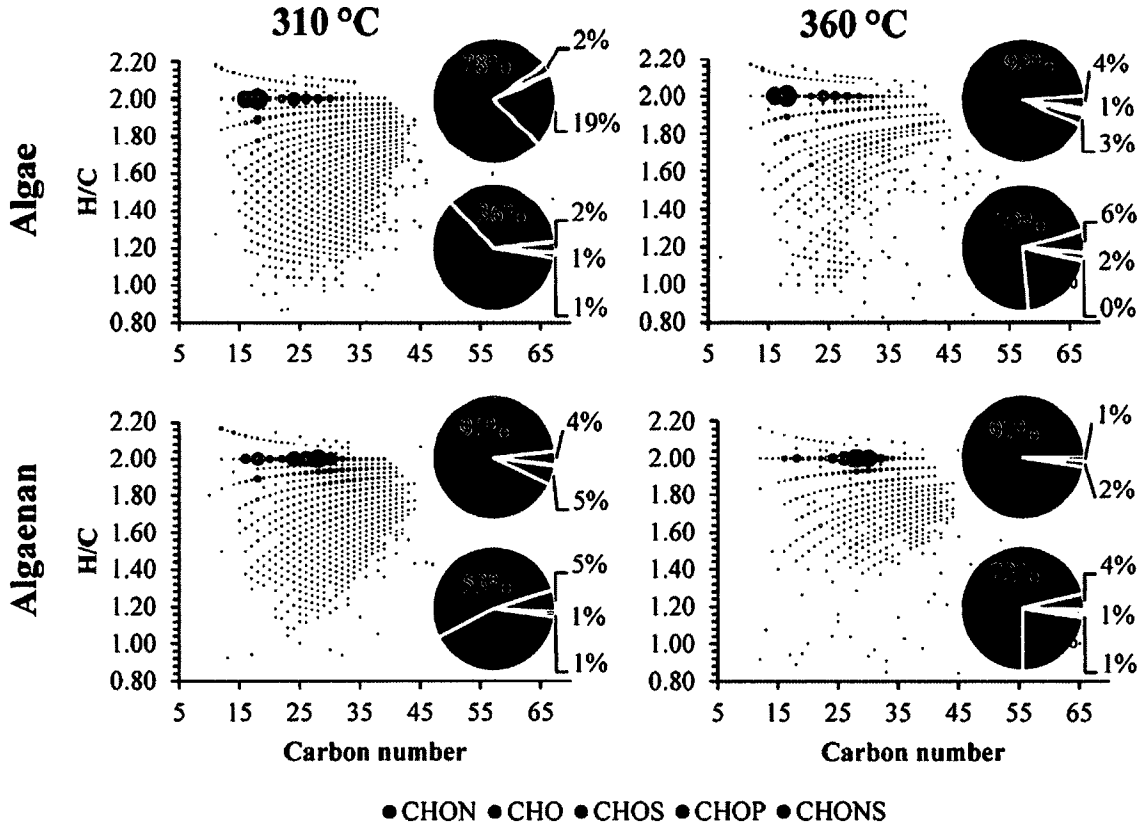

Figure 29. H/C vs. Carbon number diagrams for all the assigned peaks in the expelled oils. Pie charts display the percent of the total peak magnitude (top) and number (bottom) belonging to each molecular formula type for each sample. The size of the bubble is proportional to the peak height (P) except for C_{16} and C_{18} at H/C = 2 (see discussion). Peak heights in the figure (not pie charts) were linearly normalized ($Poriginal_{max}$ / $Poriginal_{min}$ = 10000 normalized to $Pfinal_{max}$ / $Pfinal_{min}$ = 100) for better visualization.

Greater than 95 % of the total peak intensities and 90 % of total peak numbers (Figure 29) for all the samples can be attributed to CHO and CHON compounds. Therefore, the discussion is focused on the changes in CHO and CHON molecules. The CHO compounds account for 36 % of the total identified peaks and 78 % of the total magnitude in the algae oil at 310 °C. The CHO compounds in the algae oil at 310 °C display about 11 different homologous series having multiple degrees of unsaturation ($C_nH_{2n}O_x$, $C_nH_{2n-2}O_x$ to $C_nH_{2n-20}O_x$) and ranging between C_{12} to C_{45}. The overwhelming magnitude belongs to the $C_nH_{2n}O_2$ series with high values at n = 16, 18, 22, 24, 26, 28, 30, and 32 (Figure 30). These compounds are interpreted to be the saturated free fatty acid series with the maxima for $C_{16}H_{32}O_2$ and $C_{24}H_{48}O_2$ fatty acids. This identification is confirmed when considering complementary data provided from Chapter IV in Table 11 (C_{16} fatty acid is the more abundant in *Scenedesmus* algae than C_{18} fatty acid). The peaks for unsaturated and di-unsaturated C_{18} fatty acids ($C_nH_{2n-2}O_2$ and $C_nH_{2n-4}O_2$) are possibly from the solvent contamination. CHON compounds in the algae oil at 310 °C are the major class of molecular formulas. They make up about 60 % of the total identified molecular formulas and they account for 19 % of the total magnitude for algae oil at 310 °C. Typically, hydrocarbons containing basic nitrogen atoms (pyridinic compounds) do not ionize well with negative mode ESI-FTICR-MS (Hughey et al., 2002). However it has been shown that compounds with weakly acidic nitrogen atoms (pyrrole benzologues) (Hughey et al., 2002), and oxygenated nitrogen containing compounds (Qian et al., 2001) can be observed in oils. We observe many types of series for CHO_xN_y with x = 1 – 10 and y = 1 – 5 with the highest peak magnitude belonging to the N_1O_3 series. Sudasinghe et al. (2014) observed the same N_1O_3 series as having the largest

nitrogen peak magnitude and they attributed them to likely belonging to pyrrole, indole and carbazole derivatives with oxygenated functional groups.

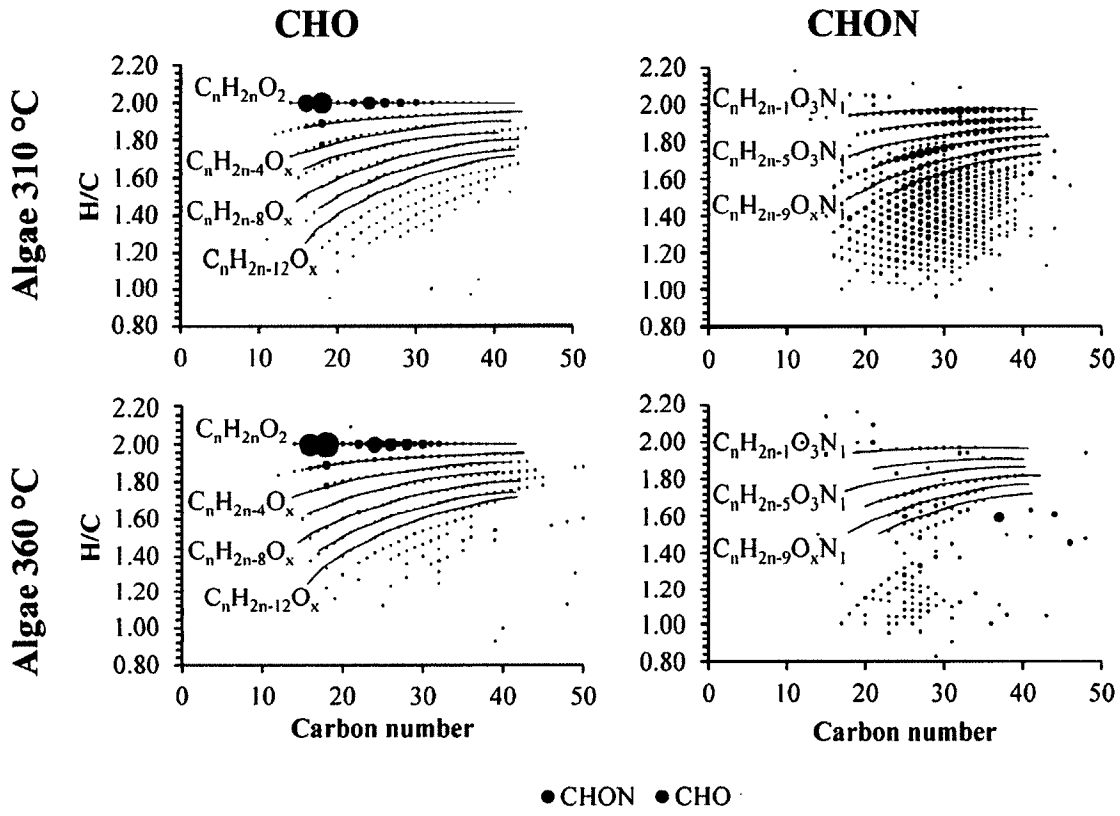

Figure 30. H/C vs. Carbon number diagrams of the CHO and CHON compounds in algae oils produced at 310 °C and 360 °C. The size of the bubble is proportional to the peak magnitude except for C_{16} and C_{18} at H/C = 2 (see discussion). No renormalization is applied to ease in the visualization of the CHON peaks. "x" denotes a series of 1 – 4 oxygen atoms.

The algae oil produced at 360 °C shows a similar distribution for the CHO compounds as those produced from the oil at 310 °C. The CHO compounds' contribution increases to account for 72 % of the total peak number and 92 % of the total magnitude.

The most significant change is the increase of the relative magnitude of the $C_nH_{2n}O_2$ series at carbon numbers n = 24, 26, 28, 30, and 32 (Figure 30) also maximizing at C_{24}. The evolution of more of these fatty acids is attributed to the increase in the degree of cracking of algaenan's intramolecular ester linkages and releasing them to into the oil. It is interesting to note that even though the GC-FID chromatogram of the algae oil at 310 °C (Figure 22 of Chapter IV) shows a small C_{23} *n*-alkane peak, presumably produced by decarboxylation of the C_{24} fatty acid during HP and cracking of the algaenan structure, the parent C_{24} *n*-fatty acid peak is observed with ESI-FTICR-MS (at 310 °C). At 360 °C, the GC-FID shows a large increase in the C_{23} *n*-alkane. This suggests that the lower temperature of 310 °C is sufficient to crack the algaenan, but not sufficient to induce decarboxylation of the fatty acids into hydrocarbons. At higher temperature, there is sufficient energy to decarboxylate and produce an abundance of *n*-C_{23} alkanes. Another interesting observation is the increase of the diacid series ($C_nH_{2n-2}O_4$) at carbon numbers n = 24, 26, 28, 30. It has been suggested (Kamga, personal communication) that, similar to even carbon numbered monoacids which undergo decarboxylation to form the odd carbon numbered *n*-alkanes, the even diacids can undergo decarboxylation of both carboxyl groups to form even *n*-alkanes. The data in Chapter IV indicate that the predominance of odd over even-numbered *n*-alkanes decreases with increasing thermal severity. This is consistent with the production of even-numbered alkanes from even-numbered diacids.

The CHON compounds in the algae oil at 360 °C decrease to account for 20% of the total identified peaks and 3 % of the total peak areas. Many of the higher carbon numbers (greater than 30 and H/C ratio less than 1.5) are removed. Comparison of the

total CHON formulas for the 310 °C and 360 °C treatments (Figure 31) shows that 82 % of the total number of CHON formulas are labile at 360 °C. However, about 10 % of the total formulas seem to be resilient to the conditions and exist in both oils.

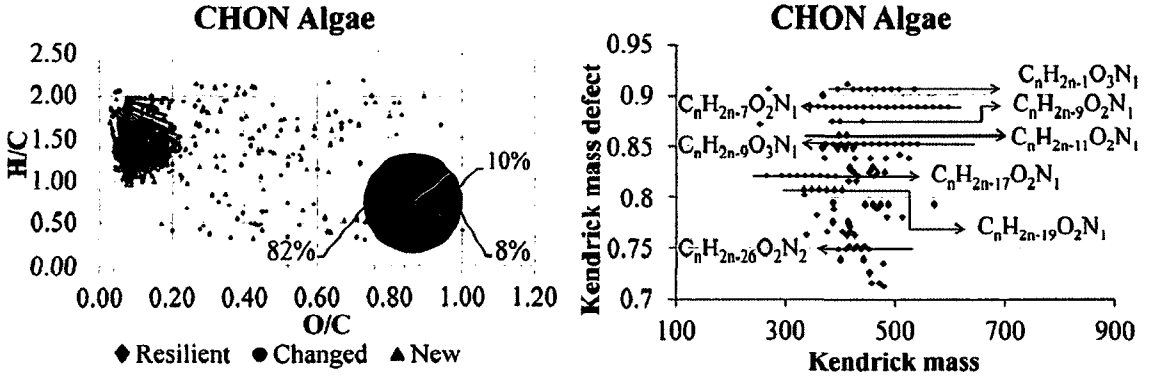

Figure 31. Van Krevelen diagram showing the CHON formulas of both the 310 °C and 360 °C algae oils (left). Changed: In the 310 °C, oil but not in 360 °C; resilient: in both the 310 °C and 360 °C; new: not in 310 °C but in 360 °C. Kendrick mass plot showing the CH_2 series of only the resilient CHON formulas (right).

The van Krevelen diagram of the CHON in algae oils at 310 and 360 °C shows that the resistant formulas (Figure 31 left, black dots) can be separated into two groups using the criteria utilized in Figure 27 and Table 16. The first group consists of CHON compounds that have a 1.5 – 2.0 H/C ratio and a 0 – 0.2 O/C which can be classified as lipid-like resistive CHONs. The second group consists of CHON compounds that have a 1.0 – 1.5 H/C ratio and a 0 – 0.2 O/C which can be classified as alicyclic-like resistive CHONs. Using a Kendrick mass plot, the multiple CHON homologous series become obvious. The first group series have the following molecular formulas: $C_nH_{2n-1}O_3N_1$ (DBE = 2), $C_nH_{2n-7}O_2N_1$ (DBE = 5), $C_nH_{2n-9}O_2N_1$ (DBE = 6), $C_nH_{2n-11}O_2N_1$ (DBE = 7),

and $C_nH_{2n-9}O_3N_1$ (DBE = 6). The second group series have the following molecular formulas: $C_nH_{2n-17}O_2N_1$ (DBE = 10), $C_nH_{2n-19}O_2N_1$ (DBE = 11), $C_nH_{2n-26}O_2N_2$ (DBE = 15). The most obvious relationship is that the $C_nH_{2n-7}O_2N_1$ (DBE = 5), $C_nH_{2n-9}O_2N_1$ (DBE = 6), $C_nH_{2n-11}O_2N_1$ (DBE = 7), $C_nH_{2n-17}O_2N_1$ (DBE = 10), $C_nH_{2n-19}O_2N_1$ (DBE = 11) all seem to be part of a series that increases in DBE. Although two missing series "$C_nH_{2n-13}O_2N_1$ (DBE = 8) and $C_nH_{2n-15}O_2N_1$ (DBE = 9)" that are not noted in Figure 31 appear to exist. However, those series don't appear to have sufficient peaks in their family to be called a series, possibly due to the threshold setting for peak detection. The high abundance of the N_1 compounds is interesting. Fu et al. (2006) have shown that N_1 series compounds are more resistive than other nitrogen containing compounds to hydrothermal treatment when they analyzed hydrothermally upgraded petroleum oils. In addition, the $C_nH_{2n-26}O_2N_2$ (DBE = 15) series could be diketopiperazines arising from the pyrolysis of peptides (Chiavari and Galletti, 1992; Sudasinghe et al., 2014).

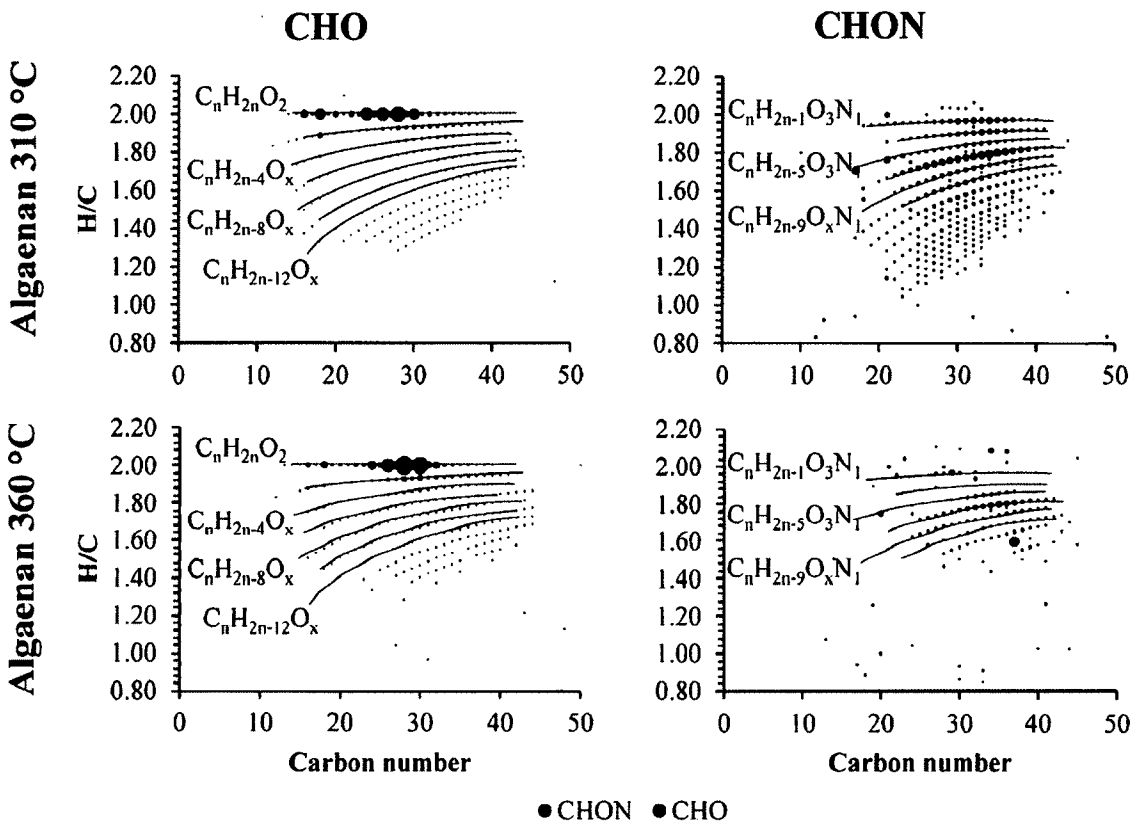

Figure 32. H/C vs. Carbon number diagrams of the CHO and CHON compounds in algaenan oils produced at 310 °C and 360 °C. The size of the bubble is proportional to the peak height except for C_{16} and C_{18} at H/C = 2 (see discussion). No renormalization is applied to ease in the visualization of the CHON peaks. "x" denotes a series of 1 – 4 oxygen atoms.

The CHO compounds in the algaenan oil at 310 ° C account for 53 % of the total identified peaks and 91 % of the total magnitude (Figure 30). The CHO compounds display the same 11 homologous series and carbon range (n = 12 – 45) as the ones in the algae oil at 310 °C. The overwhelming peak magnitude also belongs to the $C_nH_{2n}O_2$ series with high intensities at n = 16, 18, 22, 24, 26, 28, 30, and 32 (Figure 32). The major difference between algaenan and algae oils is that the fatty acid magnitudes shift to

those between C_{22} – C_{30} and maximize at C_{28} fatty acid in the algaenan oils. This is in contrast to the CHO compounds of algae oil at 310 °C which maximize at C_{24} fatty acid. The evolution of the *n*-alkane series in the GC-FID of the algaenan oil at 310 °C (Figure 22) maximizing at C_{15} and C_{27} is consistent which what is expected from the decarboxylation of the fatty acids to the alkanes. The CHON compounds in the algaenan oil at 310 °C account for 40 % of the total peak number and 5 % of the total magnitude. The distribution of the CHON molecular formulas in the algaenan oil at 310 °C is very similar to that of the algae at 310 °C. We know from elemental analysis (Table 10) and ^{13}C ssNMR (Figure 19) that the algaenan isolate contains some proteins that are not removed by the treatment. Therefore, the incorporation of nitrogen into the NSO from the algaenan is expected in our case. The content of N is much lower in algaenan, so I expect that algaenan oil should have fewer CHON compounds.

CHO compounds in the algaenan oil at 360 °C account for 72 % of the total identified peaks 97 % of the total magnitude (Figure 30). The most significant increase due to increased temperature is an increase in relative magnitude of the $C_nH_{2n}O_2$ series at carbon numbers n = 24, 26, 28, 30, and 32 (Figure 30), maximizing at C_{28}. In the algae oil at 360 °C, the main fatty acid is the n = 24 but in the algaenan oil the main fatty acid is the one with n = 28. The diacid series ($C_nH_{2n-2}O_4$) at carbon numbers n = 24, 26, 28, 30 is similar to that from the algae, however, the series is more prominent than in the whole algae. It is possible that this is why the magnitude ratios of odd over even *n*-alkanes is smaller in the algae oil at 360 °C than in the algaenan oil at 360 °C. This could suggest that the contribution of the even *n*-alkanes in the algae oils is affected by the concentration of the diacids which originate from the algaenan structure.

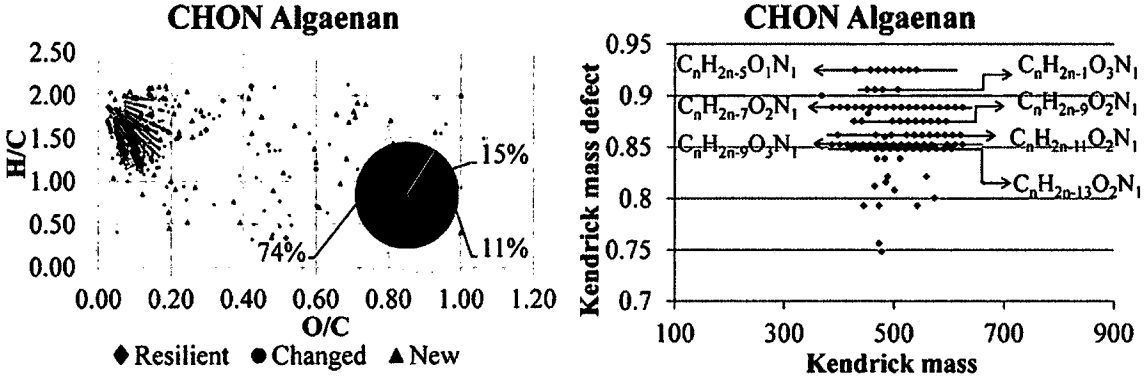

Figure 33. Van Krevelen diagram showing the CHON formulas of both the 310 °C and 360 °C algaenan oils (left). Changed: In the 310 °C, oil but not in 360 °C; resilient: in both the 310 °C and 360 °C; new: not in 310 °C but in 360 °C. Kendrick mass plot showing the CH_2 series of only the resilient CHON formulas (right).

CHON compounds for the algaenan oil at 360 °C make up 22 % of the total number of peaks and 2 % of the total magnitude. This decrease in comparison with the 310 °C oils is expected and is similar to what is observed with the algae oil. However, the main difference is that in the algaenan oil the CHON compounds, which plot between H/C 1.0 – 1.5, decompose, while in the algae oil these compounds persist. The resilient CHON compounds plot between 1.5 – 2.0 H/C and 0 – 0.2 O/C which is the lipid-like area of the van Krevelen diagram (Figure 33 left). About 74 % of the total CHON compounds are removed from the algae and about 15 % of the total CHON formulas are found in both algaenan oils. Figure 33 (right) shows the Kendrick mass plot of the resilient formulas in the oils. What is interesting is that the resilient formulas only belong to group one series that were observed in the algaenan oil. There are two additional formulas $C_nH_{2n-5}O_1N_1$ (DBE = 4) and $C_nH_{2n-13}O_2N_1$ (DBE = 8). The $C_nH_{2n-5}O_1N_1$ (DBE = 4) series could be attributed to aromatic amides. Typically, amides are not expected to

ionize efficiently in with (-) ESI-FTICR-MS (it is possible for them to ionize however). However, it is possible for aromatic amides to ionize with negative ESI and form the negatively charged carboxamide since their ionization can be stabilized by resonance from the aromatic ring (Chiu and Lo, 2000). The $C_nH_{2n-13}O_2N_1$ (DBE = 8) compound is part of the series $C_nH_{2n-9}O_2N_1$ (DBE = 6) and $C_nH_{2n-11}O_2N_1$ (DBE = 7). These compounds could be identified as a series of oxygenated alkylpyrrols.

4. CONCLUSION

ESI-FTICR-MS is uniquely suited to provide detailed molecular formula analysis of complex samples such as hydrothermally produced biofuels. Analysis of the algae and algaenan oils gives a more understanding to what is the composition of their NSO fractions. The major compounds in both oils at 310 °C and 360 °C are the CHO and CHON containing formulas. As the temperature increases from 310 °C to 360 °C, the concentration of CHO compounds increase dramatically to become the major components in both the algae and the algaenan oils. The CHO compounds are mainly found as mono unsaturated fatty acids homologous series with an even over odd carbon number predominance which undergo decarboxylation to produce *n*-alkanes homologous series having an odd over even predominance. Another major CHO series that is observed is the even numbered diacids. These compounds could undergo decarboxylation of both carboxyl groups to produce even numbered *n*-alkanes. In addition, these compounds' relative amount with respect to the sample is observed to increase at 360 °C but not 310 °C. This suggests that these diacids are part of the algaenan structure and are released into the oils by the thermal cracking of the algaenan at 360 °C. The CHON are

produced in significant amounts in the algae oil at 310 °C. However, they display different reactivity at different temperatures and whether they are found in the algae or the algaenan oils. CHON compounds in the bio oils behave similar to those in the petroleum oils in that those having a more aromatic and condensed core are more labile under HP (Zhang et al., 2013).

The survival of the CHON compounds in the algae and algaenan oils after heating for 72 hours at 360 °C is indicative of their high resistivity of thermal degradation. It seems that even small amounts of proteins remaining in the algaenan leads to nitrogen incorporation into the NSO fraction of oils which resists non-catalytic hydrothermal treatment up to 72 hours at 360 °C. This results in degrading the quality of the oils and them requiring further upgrading by other techniques. It is evident that to prevent the formation of resistive CHON, nitrogen needs to be removed before the cracking of the algaenan into oils.

CHAPTER VI

TWO-STEP PRODUCTION OF HYDROCARBON BASED FUELS FROM *SCENEDESMUS* ALGAE

1. INTRODUCTION

Nitrogen and oxygen contents in algal bio-oils are important in determining the quality of the produced oils. Although technologies that lower the heteroatom content of oils (upgrading technologies) exist (Castañeda et al., 2014), they typically employ the use of catalysts, long reaction times, and thus add additional costs to the whole process. The fundamental challenge facing the algal biofuels community is that algae contain proteins and carbohydrates which form degradation products with hydrous pyrolysis (HP) and these N-and O-containing byproducts are incorporated in the oils. Treatment of whole algae, with the purpose of producing a low heteroatom oil directly involves two basic strategies: 1) Use of a low temperature reaction to minimize thermal decomposition but of sufficient energy to release hydrocarbons and lipids from the algae or 2) treatment at high temperature to induce cracking and maximize bio-oil formation. The first will result in either insufficient thermal energy to induce decarboxylation of the high energy lipids, as reviewed in Chapter I, and the main purpose is to release low-heteroatom lipids. The second treatment, unfortunately leads to pyrolysis byproducts from proteins, carbohydrates, and lipids reacting with each other incorporating heteroatoms into the oils. For instance, protein pyrolysis byproducts can undergo condensation to form other resilient compounds such as diketopiperazines (Chiavari and Galletti, 1992) and can form

alkyl amides when they react with fatty acids within the same media (Chiaberge et al., 2013). In fact, alkyl amides are observed by GCxGC-TOFMS in the volatile fraction of whole algae oil (Chapter IV, Figure 24). In addition, ESI-FTICR-MS of whole algae and concentrated algaenan oils (Chapter V, Figures 31 and 33) show a series of CHON formulas. These CHON formulas evolve from the HP process (300 °C) and are resilient in the oils (up to 360 °C). The aliphatic nature of these formulas and their existence in both the algae and algaenan oils suggest that the reaction of the ammonium ion (formed as the result of protein pyrolysis) with the fatty acids or triglycerides can occur. Therefore, it seems that the removal of proteins and carbohydrates prior to HP of algae could be an important strategy to prevent the formation of heteroatom rich oils.

Algaenan isolated from whole algae has the potential to produce a heteroatom-poor hydrocarbon-rich biofuel (Chapter IV). Several chemical techniques have been proposed that outline different steps to isolate the algaenan from its parent algae (Allard et al., 1998; Blokker et al., 1998; Zelibor et al. 1988; Chapter I). The common strategy of those methods is the use of successive chemical treatments to remove labile components of algae, namely lipids, proteins, and carbohydrates without altering the algaenan structure. However, using chemical techniques to isolate sufficient amounts of algaenan is not feasible economically and requires significant amounts of chemicals, time, and effort. In addition, it is counter intuitive to the undertaken efforts to simplify the process.

In Chapter IV, I noticed that the ^{13}C ssNMR of the solid residue from HP of whole algae at 260 °C for 72 h (Figure 21a) has a dominant aliphatic region and appears very similar to the NMR spectrum of algaenan. Moreover, no significant amount of oil was generated suggesting minimal algaenan cracking. However, the aromatic region of

the NMR spectrum in the solid residue is enriched compared to that of chemically isolated algaenan (C.I. Algaenan) suggesting some alteration to the algaenan structure. Bobleter (1994) has shown that hydrous pyrolysis has the ability to hydrolyze carbohydrate biopolymers at low thermal severity into their individual monomer units making them soluble in water. Therefore, it seems possible that one can control the isolation and cracking of algaenan with HP by varying the temperature or heating for a short period of time (Garcia-Moscoso et al., 2013).

In this Chapter, I seek to investigate the minimum HP temperature and time conditions required to remove the maximum carbohydrates and proteins while minimizing decomposition of the algaenan. The criteria I will use to evaluate the optimal condition is based on which combination of temperature and time conditions gives an algaenan that matches chemically-isolated algaenan when analyzed by py-GC/MS, elemental analysis, and ^{13}C ssNMR. Once isolated by optimal treatment, the algaenan will be subjected to HP at 360 °C for 72 h to ensure maximum oil production and to produce a high quality oil. This oil will be examined by EA, GC-FID, GC-MS, and ESI-FTICR-MS to evaluate its quality.

2. MATERIALS AND METHODS

2.1 Sample information

Algae harvested from the Old Dominion University algal farm near Hopewell, Virginia. The main algal forms in the demonstration open raceway pond system are *Scenedesmus/Desmodesmus* spp. with subordinate *Oocystis* spp. also present.

2.2 Hydrothermal treatment

Carburized 24 mL stainless steel reactors were filled each with 1 g of freeze dried algae, and 8 mL of distilled water. A 1 mm Cr–Ni screen was placed on top of the solid to prevent it from floating during the progress of the experiment. Sample volume (based on an approximate sample density), reactor volume, and amount of added water were calculated to ensure that the sample remained submerged in a liquid water phase throughout the experiment. The reactor was then flushed with nitrogen gas and place in a furnace oven and heated isothermally. Experimental temperatures and times were varied between 180 – 260 °C and 1 h – 22 h respectively.

2.3 Pyrolysis GC/MS

Py-GC/MS was performed with a Chemical Data Systems (CDS) pyrolysis system CDS 2000 Plus coupled to a Leco Pegasus II GC/MS system with the GC operating in the split mode (50:1). The source and transfer line temperatures were maintained at 200 °C and 280 °C respectively. Mass spectra were collected at a rate of 20 spectra per second after a 30 s solvent delay. Masses were acquired at a range between 35 *m/z* and 500 *m/z*. The column used for GC separation has a 30 m x 0.25 mm i.d. with fused silica capillary column with a film thickness of 0.25 μm (5 % phenylpolysiloxane – 95 % methylpolysiloxane, Restek Rtx-5). Helium was used as the carrier gas, with flow rate of 1 ml/min. the oven temperature was programmed as follows: initial temperature was 50 °C, held for 1 min; then for a heating rate of 15 °C /min until the final temperature reaches 300 °C, held for 10 min. About 0.1–0.2 mg of samples were transferred to precombusted quartz tubes fitted with quartz spacers then covered with glass wool. The samples were placed in an auto sampler which transferred them to the

pyrolysis chamber. The temperature of the pyrolysis chamber was held at 300 °C during the short period of sample injection. The samples were then rapidly (0.01 °C/ms) heated to a temperature of 650 °C, and held for 15 s as pyrolysis products were swept into the GC-MS system.

2.4 Elemental analysis

Elemental carbon, hydrogen, and nitrogen, compositions for the solid residue, oil, and soluble organic content in the water fraction were determined using a CE Flash EA 1112 elemental analyzer. All measurements were performed in triplicate for consistency.

2.5 Carbon-13 solid state NMR methods

NMR spectra were acquired via a multiple cross polarization (magic angle spinning (multiCPMAS) pulse sequence using a 400 MHz Bruker AVANCE II with ^{1}H resonating at 400 MHz and ^{13}C at 100 MHz. The dried solid sample (ca. 80 mg) was placed in a 4 mm NMR rotor and sealed with a Kel–F cap. Samples were spun at the magic angle (54.7°) with a frequency of 14 kHz. The time between CP pulses, T_z , was optimized by varying the time between 0.2 – 0.7 ms and comparing the resulting spectra with ones obtained by Direct Polarization Magic Angle Spinning (DPMAS). The optimum value was found to be T_z = 0.5 s. All solid state spectra were externally calibrated to the glycine standard (176.03 ppm). More details concerning the pulse program and conditions are described by (Johnson and Schmidt-Rohr, 2014)

2.6 Gas chromatography-flame ionization detection

Gas chromatography coupled to flame ionization detection (GC-FID) analysis was performed with a Hewlett-Packard HP 6890 series GC system equipped with an HP

6890 injector. The oil samples were injected neat with the GC operating in the split mode (400:1). The FID detector was set at 250 °C and the inlet temperature was held constant at 280 °C throughout the analysis. The signal was measured at a rate of 20 spectra per second. The column used for GC separation has a 30 m x 0.25 mm i.d. with fused silica capillary column with a film thickness of 0.25 μm (5 % phenylpolysiloxane - 95 % ethylpolysiloxane, Agilent J&W DB-5). Helium was used as the carrier gas, with flow rate of 1 ml/min. the oven temperature was programmed as follows: initial temperature was 50 °C, held for 2 min; then for a heating rate of 15 °C /min until the final temperature reaches 300 °C, held for 15 min. Peak identifications were performed by gas chromatography coupled to mass spectrometry.

2.7 Gas chromatography - mass spectrometry

Gas chromatography coupled to mass spectrometry (GC-MS) analysis was performed with a Hewlett-Packard HP 6890 series GC system coupled to a Leco Pegasus III time-of-flight (TOF) mass analyzer. Samples were injected in split mode at a split ratio of 400:1 for neat oil injections. The GC conditions, column type, and temperature program were the same as those for GC-FID. The source and transfer line temperatures were maintained at 200 °C and 280 °C respectively. Mass spectra were collected at a rate of 20 spectra per second after a 240s solvent delay. Masses were acquired at a range between 35 *m/z* and 500 *m/z*.

2.8 ESI-FTICR-MS sample preparation and parameters

The oil was diluted in a mixture of THF:MeOH (1:1 v/v) to a final concentration of about 30 ppm carbon. The sample was continuously infused into an Apollo II ESI ion source of a Bruker Daltonics 12 Tesla Apex Qe FTICR-MS instrument and was

introduced via syringe pump operating at 2 μL/min. Ions were accumulated in the hexapole for 2.0 s before being transferred to the ICR cell. Shield and capillary voltages were adjusted for each sample for negative mode analysis. The spectra were acquired for 300 scans in broad-band mode from 200-1200 *m/z* collected with a 4 M Word time domain for the FID, which resulted in a total experiment time of 30 min per sample. The summed FID signal was zero filled once and Sine-Bell apodized prior to fast Fourier transformation and magnitude calculation using the Bruker Daltonics Data Analysis software. Prior to analyzing the sample, the mass analyzer was externally calibrated using a polyethylene glycol standard sample. Internal calibration of the acquired spectra was performed on each of the samples using a homologous series of fatty acids that were observed across all the samples (also evident to exist from GC analysis) (Sleighter et al., 2008). Only *m/z* values with S/N > 3 were considered for further processing. Elemental formulas were calculated using a Matlab program that I developed (Appendix C) with an accuracy of less than 1.0 ppm, and final assignment choices were aided using a series of conservative rules inserted into a program developed using Matlab (v. 7.4.0, The Mathworks Inc., Natick, MA).

The designed program uses a modified brute force approach to match *m/z* data with masses fitting the criteria: $^{12}C_{0-\infty}$, $^{1}H_{5-100}$, $^{16}O_{1-30}$, $^{14}N_{0-5}$, $^{32}S_{0-10}$, $^{31}P_{0-1}$ and having an accuracy of < 1 ppm. In addition, the program identifies salt adduct and ^{13}C isotopic peaks and eliminates them from further analysis. Peaks identified as solvent contaminants in the solvent blank were also subtracted from the sample spectra. Peak lists were drafted using only *m/z* values with signal to noise > 4. The resulting formulas were then selected based on integer number double bond equivalents (DBE) and the following constraints

correspond to the standard range of atomic composition for natural organic matter (Stubbins et al., 2010): O/C ≤ 1.2, H/C ≤ 2.25, H/C ≥3, H < ((2*C)+ 2), N/O <1; N/C ≤ 0.5, O < (C+2), S/C ≤ 0.2, (S+P)/C < 0.2, P/C ≤ 0.1, O > 4*P, (N + 4*P + 4*S) < O.

3. RESULTS AND DISCUSSION

3.1 Step 1: HP isolation of algaenan

The ultimate aim was to find the HP conditions (temperature and time) that give a solid algaenan residue having the following characteristics considered to be optimal for the cracking to hydrocarbons: 1) high H/C, 2) low N/C, 3) py-GC/MS chromatograms with algaenan-like hydrocarbon-rich compound distribution, and 4) ^{13}C ssNMR spectrum showing high aliphatic, low aromatic, and low heteroatom signals. Table 17 shows the HP experimental parameters and the elemental analysis data of the recovered residues.

Table 17. Experimental parameters for algae HP treatment and elemental analysis on the recovered residues. Not ash corrected.

Sample	Temperature (°C)/Time (h)	C (%)	H (%)	N (%)	H/C[a]	N/C[b]
Original	N/A	38.5 ± 0.6	6.1 ± 0.1	7.5 ± 0.3	1.9	0.17
a	160/1	32.9 ± 1.7	2.9 ± 0.0	4.1 ± 0.2	1.1	0.11
b	180/1	35.4 ± 2.3	3.9 ± 0.8	5.1 ± 0.7	1.3	0.12
c	240/1	33.9 ± 1.2	3.7 ± 0.2	3.2 ± 0.4	1.3	0.08
d	240/2	19.7 ± 0.3	1.4 ± 0.1	1.0 ± 0.1	0.85	0.04
e	240/5	20.1 ± 0.2	1.4 ± 0.2	0.8 ± 0.2	0.84	0.03
f	240/22	21.3 ± 0.4	1.5 ± 0.1	1.0 ± 0.2	0.85	0.04
g	250/2	19.8 ± 0.1	1.3 ± 0.0	1.0 ± 0.1	0.79	0.04
h	260/0.5	32.5 ± 0.9	4.4 ± 0.6	1.5 ± 0.2	1.6	0.04

Propagation of error was found to be a) between 0.2 – 1.2 % and b) between 5.0 – 18 %

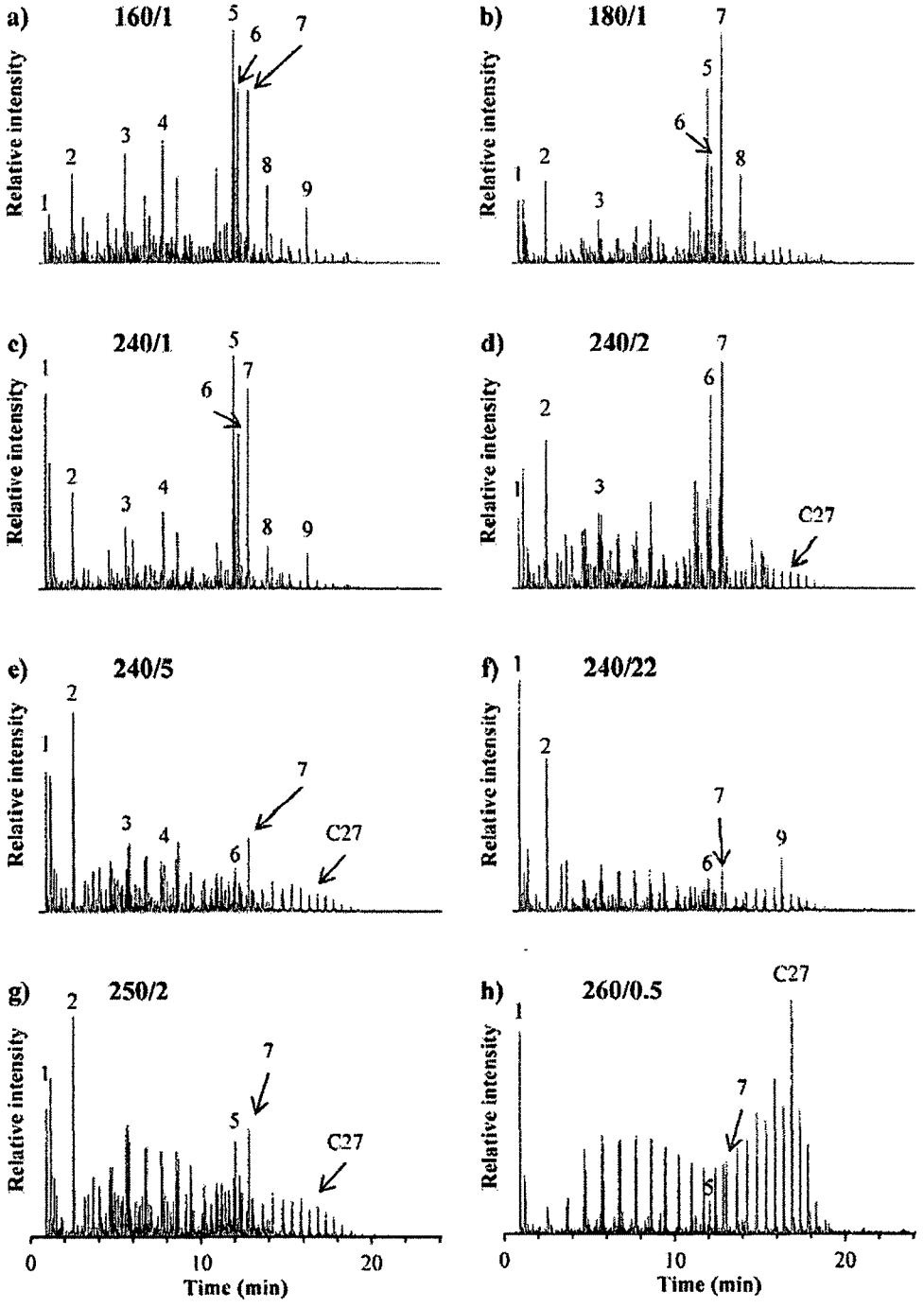

Figure 34. Py-GC/MS chromatograms of residues from different HP reactions. Letters correspond to conditions in Table 17. 1) CO_2, 2) toluene, 3) methyl phenol, 4) Indole, 5) phytane, 6) phytol, 7) *n*-hexadecanoic acid, 8) *n*-octadecanoic acid, 9) *n*-C22 fatty acid. C27 denotes the *n*-alkane/*n*-alkene C_{27} hydrocarbon peaks.

The general trend for the residues is a decrease in the H/C and N/C ratios as the temperature and reaction time increase or the severity of the thermal degradation increases. HP at 160 °C for 1 h resulted in a decrease in the H/C ratio from 1.9 to 1.1 and in the N/C ratio from 0.17 to 0.11 when compared to that of the original algae. However, HP at 180 °C for 1 h leads to an increase in the H/C ratio from 1.1 to 1.3 and in the N/C ratio from 0.11 to 0.12 compared to HP at 160 °C for 1h. Carbohydrates have faster decomposition kinetics than proteins at 160 °C and 180 °C. In fact, carbohydrates have a half-life of about 106 min and 50 min at 160 °C and 180 °C respectively (extrapolated data from Nagamori and Funazukuri (2004) listed in Chapter I, section 5 in this dissertation). At 160 °C and 180 °C, proteins have a half-life of about 200 min and 83 min, respectively, [extrapolated data from (Brunner, 2014) also listed in Chapter I, Table 4 in this dissertation]. Since the reaction time for samples (a) and (b) is 1 h, I hypothesize that the slight increase in the N/C ratio between samples a and b could be because of the faster removal of the carbohydrates with respect to the proteins in the 1 h timeframe. Flash pyrolysis chromatograms of samples (a) and (b) (Figure 34) show major peaks corresponding to pyrolysis of chlorophyll (phytane and phytol) and lipids (*n*-hexadecanoic acid, *n*-octadecanoic acid, and n-C_{22} fatty acid). In addition, the chromatograms show large peaks corresponding to toluene, methyl phenol, and Indole which are known to be pyrolysis products of proteins (Zang et al., 2001).

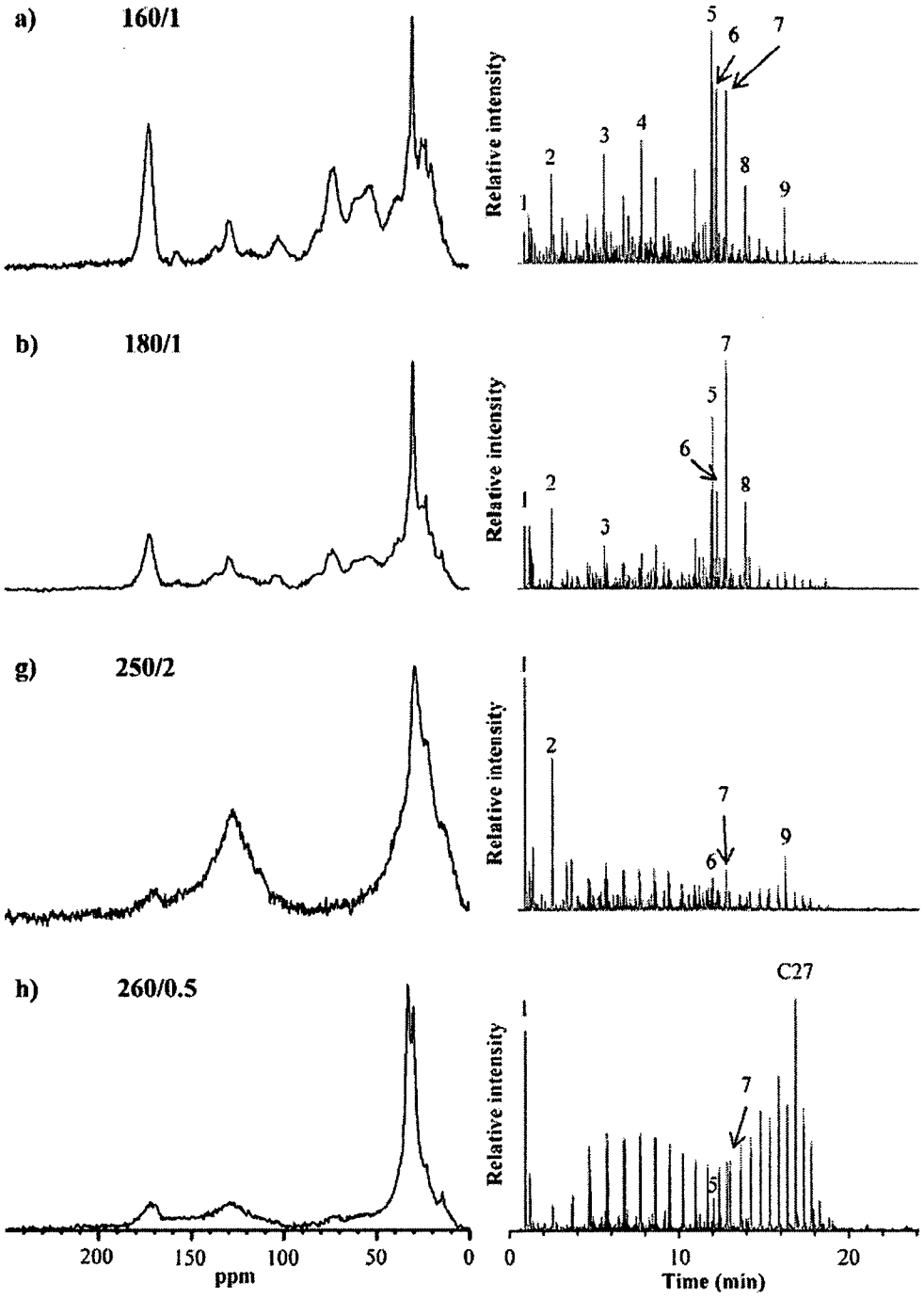

Figure 35. ^{13}C ssNMR spectra (left) and py-GC/MS chromatograms (right) of select samples. Labels correspond to experimental conditions outlined in Table 17. 1) CO_2, 2) toluene, 3) methyl phenol, 4) Indole, 5) phytane, 6) phytol, 7) *n*-hexadecanoic acid, 8) *n*-octadecanoic acid, 9) *n*-C_{22} fatty acid. C27 denotes the *n*-alkane/*n*-alkene C_{27} hydrocarbon peaks.

The ^{13}C ssNMR spectra of samples (a) and (b) (Figure 35) show a decrease in the peaks corresponding to proteins (54 and 174 ppm) and carbohydrates (62, 72, and 105 ppm) with increasing reaction temperature compared to those of original algae (Chapter II, Figure 6).

A major change in the N/C ratio occurs between samples (b) and (c), 0.12 and 0.8 respectively, when the temperature increases from 180 °C to 240 °C at a constant reaction time of 1 h. This change is due to the increase in the protein dissociation kinetics which have a half-life of 8 min (Chapter 1, Table 4) compared to that of carbohydrates which have a half-life of 5 min at 240 °C. Although the N/C ratio is lower, there remains a significant amount of proteins in the residue of sample (c). This is evident from the fact that the residue still contains 3.2 % N (Table 17) and that the py-GC/MS chromatogram of sample (c) shows a large contribution from toluene, methyl phenol, and indole (Figure 34c). HP of algae at 240 °C for 2 h results in a further decrease in the H/C and N/C ratios to values of 0.85 and 0.04 respectively. Interestingly, the large decrease in the H/C ratio suggests aromatization might be taking place in the residue. In addition, the py-GC/MS of the residue (Figure 34d) shows that there still remains some major contributions from chlorophyll and protein pyrolysis products. However, the chromatogram shows the evolution of an *n*-alkane/*n*-alkene homologous series ranging from $C_8 - C_{33}$ carbons. The $C_{20} - C_{33}$ series can be more easily observed at the later end of the chromatogram eluting between 13 min – 22 min (Figure 34d). The evolution of the *n*-alkane/*n*-alkene homologous series, markers for algaenan as shown in Chapter IV, is evidence for a higher percentage of algaenan in the residue. Increasing the reaction time to 5 h, while keeping the temperature at 240 °C, results in further decreasing of the carbon percent of the

residue. Nonetheless, the H/C and the N/C decrease slightly to 0.84 and 0.03 respectively. There is also a significant decrease in the peaks corresponding to chlorophyll pyrolysis products (Figure 34e). HP at 240 °C for 22 h results in continued diminution of the carbon percent and increase in the nitrogen percent in the residue. In addition, the H/C and N/C ratios increase slightly to 0.85 and 0.04. This increase could be due to the polymerization of protein pyrolysis products into insoluble solids at increased reaction times (Cox and Seward, 2007). Although increasing the reaction time results in an increase in the nitrogen content of the residue, the py-GC/MS chromatogram shows a significant decrease in peaks corresponding to protein pyrolysis products. HP at 250 °C for 2 h results in a residue with H/C of 0.79. This decrease in the H/C value is consistent with the ^{13}C ssNMR data which show an increase in the aromatic content of the residue (Figure 35g). Although the py-GC/MS of the residue shows a homologous *n*-alkane/*n*-alkane series characteristic of algaenan, the magnitude of the summed peaks is low in the chromatogram. This is consistent with the increase of the aromatic content of the residue which leads to a diminution of aliphatic carbons that are primarily responsible for bond rupture to form the $C_8 - C_{33}$ alkane series. Table 18 summarizes the results after each experiment and lists experimental logic for the strategy taken to find optimal conditions.

Table 18. Summary of results and actions taken after each step.

Sample	Temperature (°C) /Time (h)	Result	Action taken
a	160/1	High N/C, low quality py-GC/MS	Increase temperature
b	180/1	High N/C, low quality py-GC/MS	Increase temperature
c	240/1	Decrease in N/C, appearance of algaenan peaks in py-GC/MS	Increase reaction time
d	240/2	Decrease in N/C, too low H/C, slight decrease in protein peaks in py-GC/MS	Increase reaction time
e	240/5	Decrease in N/C, too low H/C, slight decrease in protein and chlorophyll peaks in py-GC/MS	Increase reaction time
f	240/22	Increase in N/C, too low H/C, too long reaction time, disappearance of protein and chlorophyll peaks in py-GC/MS	Increase temperature + decrease time
g	250/2	Decrease in N/C, too low H/C, too high aromatic carbons in NMR, disappearance of protein and chlorophyll peaks in py-GC/MS, too low magnitude of algaenan hydrocarbons in py-GC/MS	Increase temperature + decrease time
h	260/0.5	Low N/C, High H/C, algaenan-like py-GC/MS and NMR	optimal

HP treatment of the algae at 260 °C for 0.5 h resulted in a solid that is closest to chemically isolated algaenan (C.I. Algaenan). The residue has a high H/C value of 1.6 and a low N/C value of 0.04. Py-GC/MS of the residue (Figure 34h) shows a large magnitude of *n*-alkane/*n*-alkene homologous series characteristic of algaenan ranging from $C_8 - C_{33}$ with a bimodal distribution maximizing at C_{13} and C_{27}. The py-GC/MS also shows a predominance of the odd carbon numbers *n*-alkane/*n*-alkene homologs at C_{11}, C_{13}, C_{23}, C_{25}, and C_{27}. The ^{13}C ssNMR spectrum of the solid residue (Figure 35h) is very similar to that of algaenan (Chapter II, Figure 7) in that it shows high magnitude of aliphatic carbons (0 – 50 ppm) and a low contribution from protein, carbohydrate, and aromatic carbons. Moreover, the aliphatic peak is split into a doublet representing the presence of both amorphous and crystalline phases found to be so characteristic of well-preserved algaenan (Chapter II). The yield of the solid residue after HP of algae at 260 °C

and 0.5 h was 40 % wt. The residue from HP of algae at 260 °C for 0.5 h is chosen as a feedstock for the second step.

3.2 Step 2: HP of isolated algaenan to produce hydrocarbon based oil

The residue from the HP of algae at 260 °C for 0.5 h is collected and washed with deionized water. After washing, the residue (about 60 % wt.) is then loaded into a reactor and treated with HP at 360 °C for 72 h to ensure maximum oil generation. Following the treatment, the reactor is opened and the oil layer, existing as a waxy matrix, floating on the surface of the water is observed and is collected for analysis. Such a waxy matrix is common to experiments conducted on Type I kerogens known to generate waxy oils (Lewan, 1985; Ruble et al., 2001). In addition, the waxy consistency of the expelled oil is similar to that observed from the HP of chemically isolated algaenan (Chapter IV). The hydrothermal treatment yields expelled oil accounting for of 9 % wt. of original dry algae and 20 % wt. carbon. It is worth mentioning that this oil only accounts for the expelled oil and does not include any oil that is adsorbed to the surface of the remaining residue.

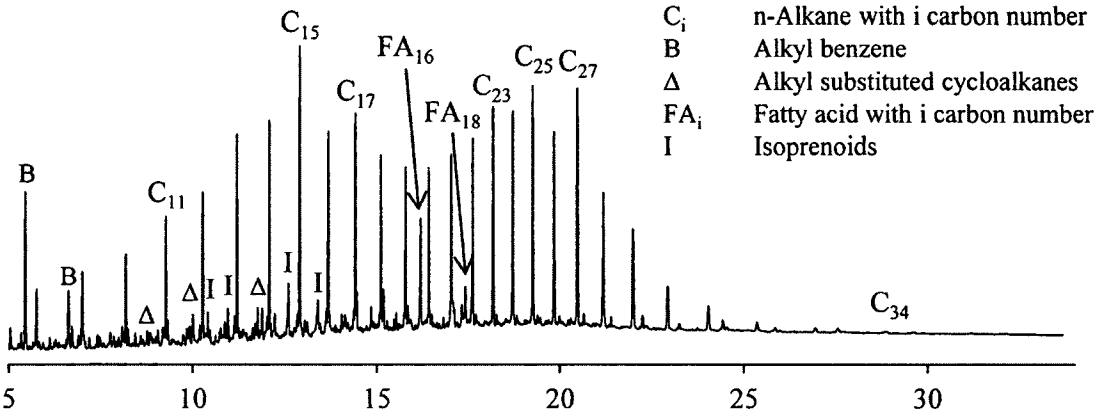

Figure 36. GC-FID of the expelled oil after second step HP. Identification of the peaks was achieved by parallel analysis of the oil with GC/MS.

Figure 36 shows one-dimensional GC-FID chromatogram of the expelled oil formed after the second step HP of isolated algaenan. The chromatogram is remarkably similar to that of oil from HP of C.I. algaenan at 360 °C (Chapter IV, Figure 22). The oil shows a long series *n*-alkanes extending from *n*-C_8 to *n*-C_{34} and having a bimodal distribution maximizing at *n*-C_{15} and C_{27}. In addition, the oil shows a slight predominance of odd-numbered *n*-alkanes such as C_{17}, C_{23}, and C_{27}. The maximization at C_{15} and C_{17} is consistent with observations of C_{16} and C_{18} fatty acids in the oil. These fatty acids can undergo decarboxylation to produce the n-1 alkane. Some of these fatty acids could exist as esters within the algaenan and be liberated as acids upon thermal decomposition. A similar observation was made using flash pyrolysis experiments on algaenan isolated from the same algae (Obeid et al., 2014).

The chromatogram of the oil shows the presence of C_1 – C_4 *n*-alkylbenzenes (toluene and xylene) which were absent in the py-GC/MS chromatogram (Figure 34f). Similar distributions of *n*-alkylbenzenes are observed in the oils from HP of chemically isolated algaenan (Chapter IV, Figure 25). It has been suggested that alkylbenzenes in oils can originate from aromatization reactions of thermal decomposition products of lipids and proteins (Higman et al., 1970). In addition, it has also been suggested that alkylbenzenes could be a byproduct of thermal decomposition of algaenan (Torri et al., 2012). This seems like a valid hypothesis as it is evident that alkylbenzenes are in the algaenan oil. However, it is unlikely that the *n*-alkylbenzenes are produced as a result of the primary cracking of the algaenan, as flash pyrolysis studies on HP isolated algaenan (Figure 34h) and chemically isolated algaenan shows no or minor contribution of alkylbenzenes in the pyrolyzate (Obeid et al., 2014). It is more likely that the

alkylbenzene contribution to the algaenan oil is the result of aromatization of cycloalkanes produced during the hydrothermal process.

Table 19. CHNSO composition of expelled oil from HP after Step 2 compared to those of whole algae and chemically isolated algaenan HP oils.

	C (%)	H (%)	N (%)	S (%)	O[a] (%)	HHV* (MJ/kg)
Whole algae oil	69.6 ± 2.7	10.6 ± 0.6	3.5 ± 0.5	BDL	16.3 ± 2.8	35.0 ± 1.2
Chemically isolated algaenan	81.4 ± 0.1	11.2 ± 1.5	1.4 ± 0.1	BDL	6.0 ± 1.5	41.0 ± 1.8
Step 2 oil	81.6 ± 0.7	11.4 ± 0.4	1.3 ± 0.0	BDL	5.7 ± 0.8[b]	41.3 ± 0.5[b]

[a] Value calculated by difference. [b] Error by propagation of error equation. BDL: Below Detection Limit.* calculated by the Boie formula (Boie, 1953)

Elemental analysis of the Step 2 expelled oil is shown along with the calculated High Heating Value (HHV) in Table 19. The elemental values for the expelled oil are very comparable to those for oil produced from HP of chemically isolated algaenan. The step 2 oil, however, contains slightly less oxygen (5.7 %) and nitrogen (1.3 %) and has a HHV of 41.3 MJ/kg. The High Heating Value (HHV) of typical liquid fuels ranges between 35 and 48 MJ/kg (Channiwala and Parikh, 2002) making the step 2 a high quality fuel.

3.1 ESI-FTICR-MS analysis of produced oil

Figure 37 shows the ESI-FTICR-MS spectra of the step 2 expelled oil. The overall spectrum shows peaks ranging from 200 to 700 *m/z*. All four samples are dominated by the same four most intense peaks (368.35430 *m/z*, 396.396730 *m/z*, 424.428030 *m/z*, 452.459330 *m/z*) which are attributed to the even *n*-fatty acids (C_{24}, C_{26}, C_{28}, C_{30}) having the formula $C_nH_{2n}O_2$.

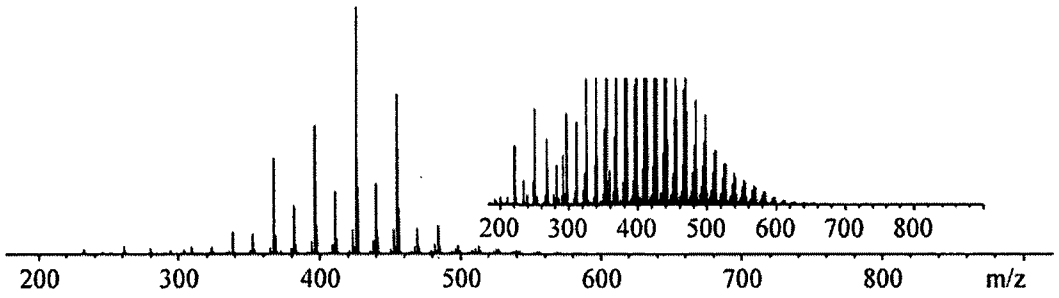

Figure 37. ESI-FTICR-MS spectra of the step 2 oil. Insert shows the expanded spectra.

The fatty acid distribution is very simillar to that of oil from HP of chemically isolated algaenan at 360 °C between 300 to 600 *m/z* (Chapter V, Figure 26d). The distributoion of the even numberd fatty acids in the ESI-FTICR-MS spectra maximizating at C_{28} is consistent between both oil samples (Chapter V, Figure 26d; and Figure 37). In addition, the fatty acid distribution explains the predominance of odd-over-even C_{21} – C_{28} *n*-alkanes in the GC-FID chromatograms and their maximization at C_{27}. (Chapter IV, Figure 22; and Figure 36).

The mass spectrum of step 2 oil lacks the high C_{16} and C_{18} fatty acid abundance that is observed in the mass spectrum of the oil from the chemically isolated algaenan. It is not clear why the their magnitude in the step 2 sample is low inspite of the predominance of their decarboxylation products (C_{15} and C_{17} *n*-alkanes) in the GC-FID chromatogram of the oil (Figure 36).

Table 20. Number of formulas.

	Total peaks	Assigned peaks	Isotopic peaks	Unknown peaks	Total identified	
						%
Step 2 oil	1389	767	354	268	1121	80.7

About 81 % of all the detected peaks were identified using the selection criteria as either ^{12}C monoisotopic unique formulas or ^{13}C isotopic peaks. In addition, the total number of peaks in the step 2 oil are lower than those in the oil form HP of chemically isoated algaenan (Chapter V, Table 15).

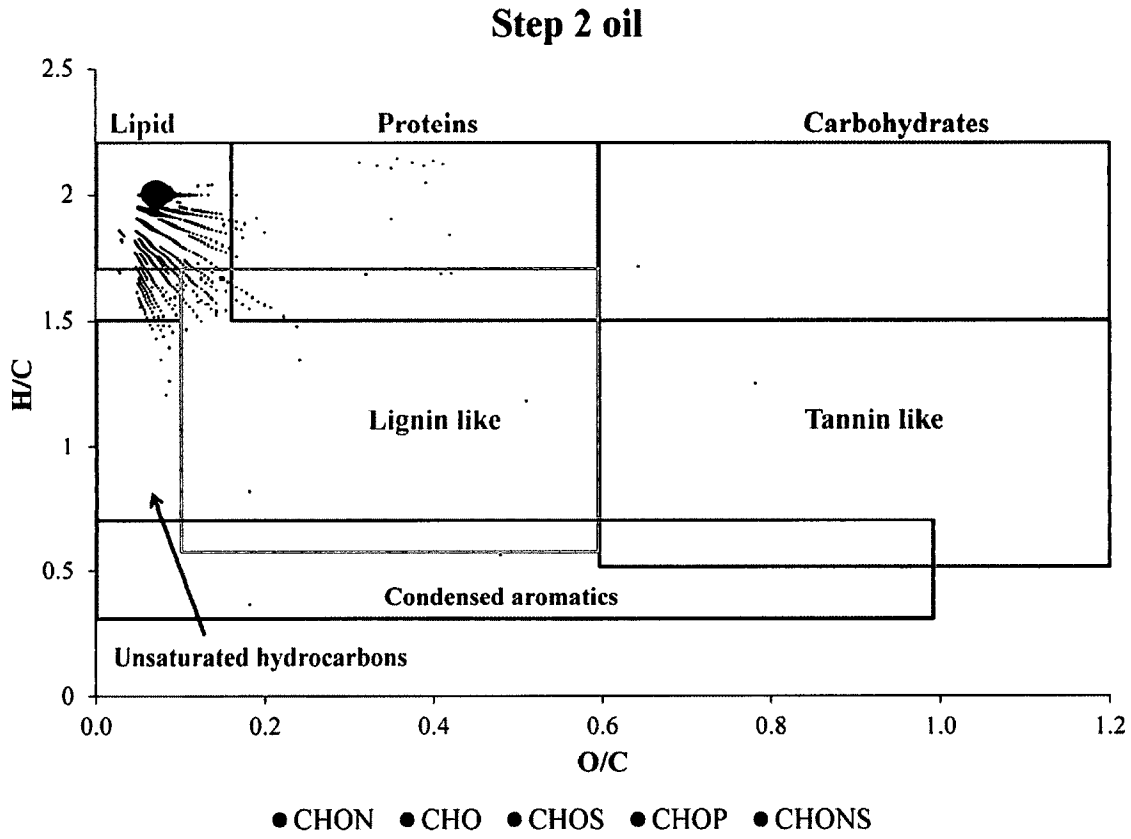

Figure 38. Van Krevelen diagram for all the assigned peaks in the step 2 expelled oil. The size of the bubble for each data point is proportional to the peak magnitude (P). Peak magnitudes in the figure were linearly normalized ($Poriginal_{max}$ / $Poriginal_{min}$ = 1000 normalized to $Pfinal_{max}$ / $Pfinal_{min}$ = 100) for better visualization. Boxed areas in the plot represent molecules classified based only on H/C and O/C molecular ratios.

The identified molecular formulas were plotted on a van Krevelen diagram for

better visualization (Figure 38). Details describing the significance of the van Krevelen diagram and the overlaid areas shown in Figure 38 are described in Chapter V and Hockaday et al. (2009). Briefly, the van Krevelen diagram allows for comparison of large data points in a simpler manner based on their O/C and H/C ratios. The diagram is further divided into separate areas which correspond to different H/C and O/C ratios of different natural products such as lignin, tannin, protein, lipid, and unsaturated hydrocarbons (Hockaday et al., 2009). Peaks that plot in a specific area have H/C and O/C values that are similar to where natural products such as lignin, tannin, protein, lipid, and unsaturated hydrocarbons would plot and thus they are named lignin-like, tannin-like, protein, lipid, and unsaturated hydrocarbons. It is worth reiterating that that a formula that plots in a specific area, for example lignin, does not necessary mean it derives from lignin. In fact, lignin is a polymer found in wood and is absent in algae. However, a formula having the same atomic H/C, O/C, N/C, and AI_{mod} as that of lignin will most probably have a structure that is similar to that of lignin. This is the same for the rest of the aforementioned classes (Kim et al., 2003). The terminology is used in the dissolved organic matter literature to distinguish the different areas in the van Krevelen plot (Sleighter et al., 2008; Hockaday et al., 2009; Zhong et al., 2011) and is adapted here to simplify the discussion.

Table 21. Quantification of % of total peak numbers and % of total peak magnitude belonging to a certain classification in Figure 38.

	Lipids	Protein	Carbohydrate like	Lignin like	Tannin like	Unsaturated hydrocarbons	Condensed aromatics	others
Magnitude								
C.I. Algaenan	94.2	0.1	0.0	2.4	0.1	1.8	0.1	1.2
Step 2	98.2	< 0.1	0.0	0.6	< 0.1	1.0	< 0.1	0.1
Peak number								
C.I. Algaenan	52.0	0.8	1.2	15.5	2.4	18.3	1.0	8.8
Step 2	61.7	0.6	0.2	13.7	0.2	21.4	0.1	2.1

Criteria for classification is in footnote Chapter V, Table 16

Quantification of the total number of peaks and their total intensities belonging to different classes is shown in Table 21. The peak magnitude of the lipids in the step 2 oil (98.2 %) is larger than that for the C.I. Algaenan oil (94.2 %). In addition, the peak magnitudes of all the other classes are lower for the step 2 oil than for the C.I. Algaenan. In addition, lipids also account for the most identified peak numbers (61.7 %) followed by unsaturated hydrocarbons (21.4 %) and lignin-like (13.7 %). This distribution order is similar to that for the C.I. Algaenan (lipids > unsaturated hydrocarbons > lignin-like). However, the lignin-like compounds are less in the step 2 oil than in the C.I. Algaenan oil (13.7 % vs. 15.5 %) and the unsaturated hydrocarbons are more in the step 2 oil than in the C.I. Algaenan oil (21.4 % vs. 18.3 %). Compounds that plot in the lignin-like region likely have structures that are a combination of oxygenated aromatic and alicyclic compounds that have functional group substitutions such as alkylesters, acids, ethers, and alkylethers. Compounds that plot in the unsaturated hydrocarbons can be thought of having aromatic and alicyclic structures that lack significant oxygen atom percentages in their formulas. ^{13}C ssNMR analysis of the HP solid feedstock, step 1 residue (Figure 35h)

and C.I. Algaenan solid Chapter IV (Figure 19), show the latter having significantly less C-O peak intensity. Upon HP of the feedstock, less oxygenated aromatic and alicyclic compounds are expected to form in the Step 2 oil (i.e. formation of relatively less lignin-like and more unsaturated hydrocarbons) than in the C.I. Algaenan oil (i.e. formation of relatively more lignin-like and less unsaturated hydrocarbons).

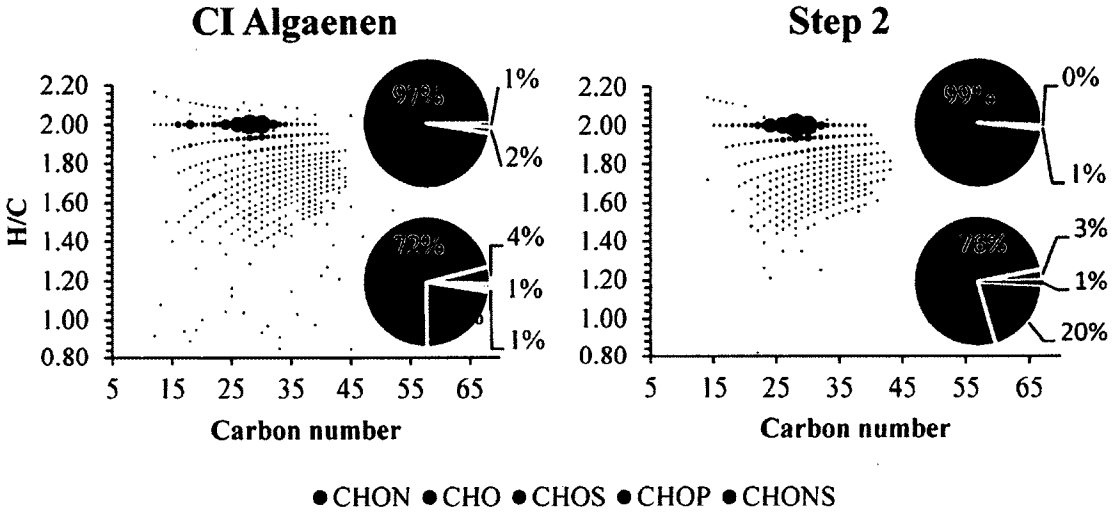

Figure 39. H/C vs. Carbon number diagrams for all the assigned peaks in the expelled oils. Pie charts display the percent of the total peak intensity (top) and number (bottom) belonging to each molecular formula type for each sample. The size of the bubble is proportional to the peak height (P). Peak heights in the figure (not pie charts) were linearly normalized ($Poriginal_{max}$ / $Poriginal_{min}$ = 1000 normalized to $Pfinal_{max}$ / $Pfinal_{min}$ = 100) for better visualization.

Greater than 99 % of the total peak intensities and 96 % of total peak numbers for the step 2 oil is attributed to CHO and CHON compounds (Figure 39). Therefore, the discussion in this section is focused on the changes in CHO and CHON compounds and

how they compare with those for C.I. Algaenan oil. The CHO compounds account for 76 % of the total identified peaks and 99 % of the total magnitude in the step 2 oil. This is higher than in the C.I. Algaenan oil (72 % of the total identified peaks and 97 % of the total magnitude). The CHO compounds display about 9 different homologous series having multiple degrees of unsaturation ($C_nH_{2n}O_x$, $C_nH_{2n-2}O_x$ to $C_nH_{2n-16}O_x$) and ranging between C_{12} to C_{45}. The highest magnitude belongs to the $C_nH_{2n}O_2$ series with highest values at n = 24, 26, 28, 30, and 32 (Figure 40). These compounds are interpreted to be the saturated free fatty acid series with the maxima at $C_{28}H_{56}O_2$ fatty acid. Figure 40 also shows the diacid series ($C_nH_{2n-2}O_4$) at carbon numbers n = 24, 26, 28, and 30, similar to the ones observed in the C.I. Algaenan oil. As mentioned in Chapter V, even carbon numbered monoacids ($C_nH_{2n}O_2$) undergo decarboxylation to form the odd carbon numbered alkanes ($C_{n-1}H_{2n}$). The even diacids ($C_nH_{2n-2}O_4$) can undergo decarboxylation of both carboxyl groups to form even *n*-alkanes ($C_{n-2}H_{2n-2}$).

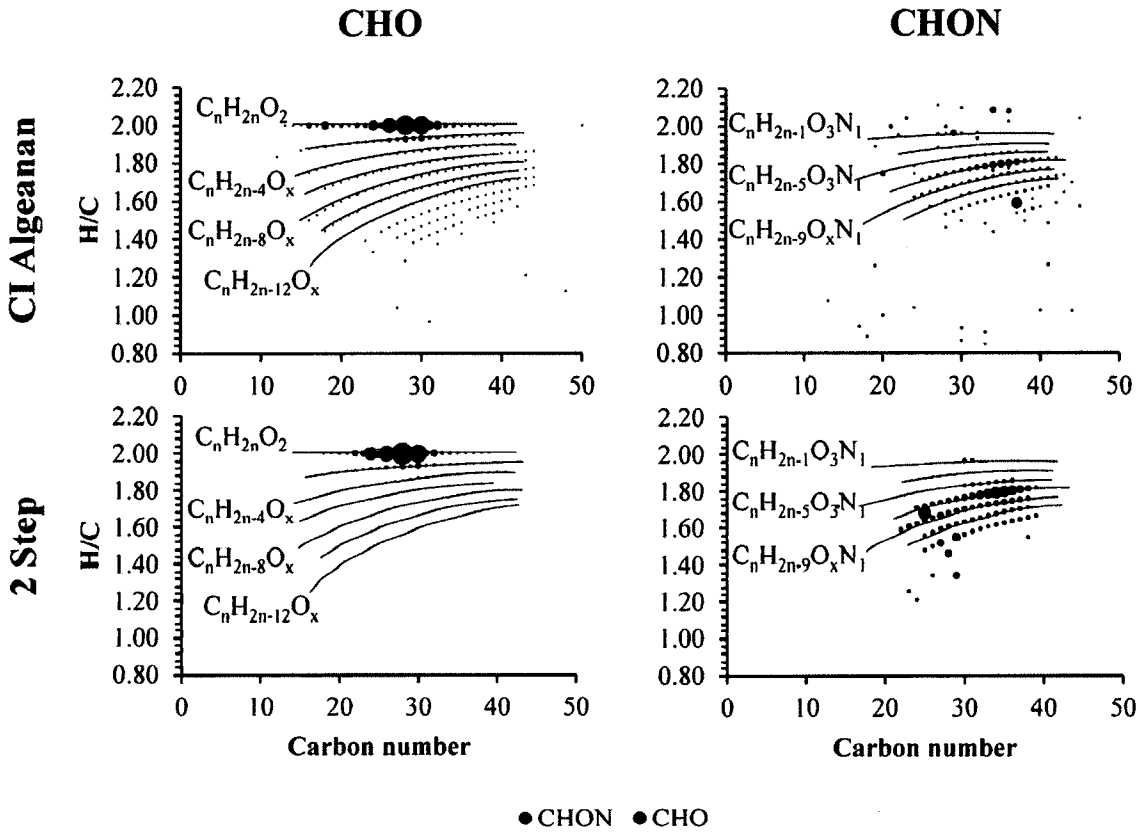

Figure 40. H/C vs. Carbon number diagrams of the CHO and CHON compounds in the expelled oils. The size of the bubble is proportional to the peak magnitude. No renormalization is applied to ease in the visualization of the CHON peaks. "x" denotes a series of 1 – 4 oxygen atoms.

CHON compounds in the step 2 oil make up 20 % of the total number of peaks and less than 1 % of the total magnitude. The values are very similar to those of the CHON compounds in the C.I. Algaenan oil. Despite employing the two step approach, CHON formulas still constitute 20 % of the total identified peaks in the step 2 oil. To investigate these formulas, all the CHON compounds from the C.I. Algaenan oil and the step 2 oil are plotted on a van Krevelen diagram (Figure 41,left). The common peaks plot between 1.5 – 2.0 H/C and 0 – 0.2 O/C which outline in the lipid-like area of the diagram.

About 33 % of the CHON formulas are found in both oils. Figure 41 (right) shows the Kendrick mass plot of the common formulas in the oils.

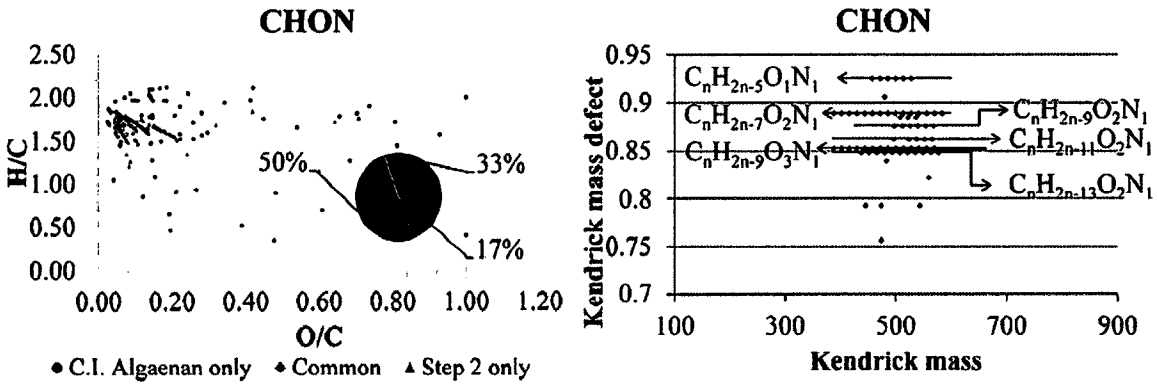

Figure 41. Van Krevelen diagram showing the CHON formulas of both the C.I. Algaenan oil and the step 2 oils (left). Kendrick mass plot showing the CH_2 series of only the common CHON formulas (right).

What is interesting is that the common formulas compare very favorably to those that were identified in the C.I. Algaenan oils (Chapter V, Figure 33). The series have the following molecular formulas: $C_nH_{2n-7}O_2N_1$ (DBE = 5), $C_nH_{2n-9}O_2N_1$ (DBE = 6), $C_nH_{2n-11}O_2N_1$ (DBE = 7), $CnH_{2n-13}O_2N_1$ (DBE = 8), $C_nH_{2n-9}O_3N_1$ (DBE = 6), and $C_nH_{2n-5}O_1N_1$ (DBE = 4). The same relationship is also observed in the step 2 oil between the $C_nH_{2n-9}O_2N_1$ (DBE = 6), $C_nH_{2n-11}O_2N_1$ (DBE = 7), and $C_nH_{2n-13}O_2N_1$ (DBE = 8). Our results confirm the observation by Fu et al. (2006) about the N_1 series compounds being more resistive than other nitrogen containing compounds to hydrothermal treatment. These series appears in both the C.I. Algaenan and step 2 oil and it is possible that they form early in the HP process (possibly at lower temperatures). However, that remains to be investigated. In addition, the $C_nH_{2n-26}O_2N_2$ (DBE = 15) series attributed to

diketopiperazines, arising from the pyrolysis of peptides followed by their product's polymerization (Chiavari and Galletti, 1992; Sudasinghe et al., 2014), is not detected. This could suggest that the 2 step process decreases the likelihood of polymerization N-containing byproducts into insoluble solids. The $C_nH_{2n-5}O_1N_1$ (DBE = 4) series could be attributed to aromatic amides or negatively charged carboxamide [Chapter V and Chiu and Lo (2000)]. The $C_nH_{2n-13}O_2N_1$ (DBE = 8) compound is part of the series CnH2n-9O2N1 (DBE = 6) and $C_nH_{2n-11}O_2N_1$ (DBE = 7). These compounds could be identified as a series of oxygenated alkylpyrroles (Chapter V).

4. CONCLUSION

The objective is to remove the labile proteins and carbohydrates from the algal matrix prior to liquefaction at high temperature. A two-step approach to HP of algae for biofuel production yields a hydrocarbon-rich oil that is very similar to that produced from HP of chemically isolated algaenan. In the first step, HP treatment is used to concentrate algaenan from algal cells by finding the optimum temperature and time parameters. The protocol suggested in this Chapter outlines a stepwise process to reach the optimum algaenan isolation parameters by utilizing analytical techniques such as EA, py-GC/MS, and ^{13}C ssNMR to analyze the algae HP residue. The residue is checked to for the following properties: 1) high H/C, 2) low N/C, 3) py-GC/MS chromatograms with algaenan-like hydrocarbon-rich compound distribution, and 4) ^{13}C ssNMR spectrum showing high aliphatic, low aromatic, and low heteroatom signals. Once reached, the highly aliphatic and heteroatom-poor residue can then be used as a feedstock for the second step HP. The optimum conditions for algaenan isolation from *Scenedesmus* sp. by

HP are found to be 260 °C for 30 min. It is possible for these parameters to be similar for different algae species; however this remains to be investigated.

The GC-FID chromatogram shows that the two step process successfully produces high quality oil similar to that produced from HP of algaenan isolated by harsh chemicals. Elemental analysis of the oil showed that it had low heteroatom content (1.3 % N and 5.7 % O) with a high heating value of 41.3 MJ/Kg which is comparable to many crude oils (Channiwala and Parikh, 2002).

ESI-FTICR-MS allows for the analysis of the NSO fraction of the oil. The NSO fraction of the oil shows a significant decrease in the magnitude and number of formulas that plot in the tannin, protein, and condensed aromatic regions. The CHO compounds are mainly found as mono unsaturated fatty acids homologous series with an even over odd carbon number predominance.

The same predominance is found in the oil from C.I. Algaenan HP. The fatty acids undergo decarboxylation to produce *n*-alkanes homologous series having an odd over even predominance. Even numbered diacids were also observed in the algaenan suggesting that they are part of the algaenan structure and could be a source for even numbered *n*-alkanes. A decrease in the magnitude of the CHON formulas is observed, however the decrease in their peak number was not as expected. The survival of the CHON compounds in the algae and algaenan oils after heating for 72 hours at 360 °C is indicative of their high resistivity of thermal degradation. It seems that even small amounts of proteins remaining in the algaenan leads to nitrogen incorporation into the NSO fraction of oils. However, the peak for diketopiperazine was not observed in the step 2 oil. This could suggest that the two step process decreases the chance of N-

compound polymerization by removing the proteins at low energy (260 °C) prior to high energy cracking (260 °C).

CHAPTER VII

CONCLUSIONS AND FUTURE WORK

1. CONCLUSIONS

This study set out to investigate the potential of algaenan as a feedstock for hydrous pyrolysis. The motivation behind this work was largely driven by two facts: 1) the importance of algae as a future biomass feedstock for fuels and 2) the fact that the current research focuses on producing heteroatom-rich oils from HP of whole algae and relying on upgrading the these oils downstream of the process to produce heteroatom-free oils that can be used in refineries. In my opinion, this approach is cost ineffective, involves multiple steps, and is not the optimum method to obtain high quality crude-oil like bio-oil. Therefore, this dissertation attempts to provide a new approach whereby the energy-producing components of algae, mainly algaenan and lipids, are first isolated and then treated under conditions that are analogous to those of long-term burial in the geological subsurface to yield "clean" hydrocarbon based oils that resemble petroleum.

The investigation commences with application of the three most commonly used protocols in the literature for chemically isolating algaenan from whole algae. The intention of this study was to isolate algaenan that could be uniquely recognized. Applying those protocols led me to observe that each of the different chemical techniques resulted in a different final isolated algaenan. These differences are mainly observed by flash pyrolysis and solid state ^{13}C NMR and thus explain some of the discrepancies in algaenan assigned structures in the literature. Each chemical isolation step from each of

the different procedures was then examined to determine their effects on the algaenan structure. From this, I was able to suggest a new algaenan isolation protocol which uses the most advantageous chemical protocols form each process and combine them. The selection criteria are based on which process is most successful in removing the proteins, carbohydrates, and lipids while leaving the algaenan intact as a residue. As was suggested subsequently, the chemical isolation protocols are time-consuming and most likely ineffective from a cost consideration.

The investigation continued to test if an ancient coal sample, collected from the Moscow basin and thought to be mainly derived from algae and other plant contributions, produces a high quality oil when subject to HP. In addition, this coal has a unique property as it was never buried deeply to undergo significant maturation; temperatures are thought to have never risen above 25 °C and the primary chemical modification through diagenetic reactions was removal of geochemically labile components such as carbohydrates, proteins, and lipids. As a result, the coals in this basin never reached a temperature required for the formation of bituminous coals and thus are still in the stage of hard brown coals. The results show that HP treatment is effective in transforming the aliphatic structures of the Moscow brown coal to produce an aliphatic oil by breaking the C-C bonds and favoring the formation of alkanes. This shows that to produce a crude-oil like quality oil, not only is the absence of the carbohydrates and proteins in the starting material important, but also the aliphatic nature of that material plays an important role as it facilitates cracking of the oil to hydrocarbons. From that, we can conclude that algaenan is ideally suited to produce the high quality oils.

The next step was actually testing the overarching hypothesis and subjecting

Scenedesmus/Desmodesmus sp. whole algae and its isolated algaenan to HP. Hydrothermal treatment of the algae and its algaenan, concentrated in large enough quantities for testing by an abbreviated chemical isolation procedure, produced oils that physically fractionate from the aqueous phase and that showed a predominance of hydrocarbons similar to those found in some fossil crude oils. Most of the hydrocarbons produced in the hydrous pyrolysis of whole algae appear to originate from algaenan that is an abundant component of the algae. The algaenan showed resistance to thermal degradation at temperatures as high as 310 °C but showed evidence of cracking at 360 °C and 72 h of treatment. This was shown to be the case for both the whole algae and isolated algaenan. Simulated distillation showed that the algae oil compared favorably with an example paraffinic crude oil sample having light-medium density from Qua Iobe (Nigeria). The algaenan oil compared favorably with a paraffinic-naphthenic crude oil having medium density from the North Slope (Alaska). Most importantly, algaenan oil contained much less nitrogen and oxygen (1.4 % and 6 %) than the oil from whole algae (3.5 % and 16.3 %) and had a higher high heating value (41 MJ/Kg vs. 35 MJ/Kg). These bulk characteristics are important for the development of conversion strategies in algal bio refineries, considering the fact that increased heteroatom contents for algal oils will most likely lead to higher cost expenditures for refinement of oils into usable fuels.

Detailed molecular analysis on the non-polar volatile fraction of the oils was performed using GCxGC-TOFMS. The algae oil showed a much higher concentration of protein and carbohydrate pyrolysis products, compounds that render the oil more oxygenated and decrease its overall value. The algaenan oil showed a higher potential fuel value than whole algae oil with contributions from compounds such as *n*-alkanes

(short and long chain), 2-methyl-*n*-alkanes with carbon numbers greater than C_{20}, and long chain *n*-alkylcycloalkanes. In addition, detailed analysis of the polar non-volatile fraction of the oils performed by ESI-FTICR-MS showed that as the temperature increases from 310 °C to 360 °C the concentration of CHO-containing formulas increase dramatically. They are mainly found as mono unsaturated fatty acids homologous series with an even-over-odd carbon number predominance. These fatty acids undergo decarboxylation to produce *n*-alkanes homologous series having an odd-over-even predominance. Another major CHO series that was observed is the even numbered diacids. These compounds could undergo decarboxylation of both carboxyl groups to produce even numbered *n*-alkanes. These diacids are part of the algaenan structure and are released into the oils by the thermal cracking of the algaenan at 360 °C. The alkyl CHON compounds that were produced at 310 °C were more resistant to thermal degradation or upgrading than were the aromatic CHON at 360 °C. This suggests that products from protein pyrolysis could be resistant to HP upgrading.

Although the chemically isolated algaenan oil was both hydrocarbon-rich and heteroatom-poor, the tedious chemical treatment to isolate algaenan presents a challenge to possibly expanding the HP process for biofuel production.

The final goal in this thesis was to test a two-step HP process in which 1) proteins and carbohydrates are removed using a low temperature HP to concentrate algaenan followed by 2) a high temperature HP treatment at 360 °C for 72 h to crack the algaenan into low heteroatom oil. To achieve this, a new algaenan isolation protocol was suggested. The procedure sought to find the best HP time and temperature parameters that yield a residue with 1) high H/C, 2) low N/C, 3) py-GC/MS chromatograms with

algaenan-like hydrocarbon-rich compound distribution, and 4) ^{13}C NMR spectrum showing high aliphatic, low aromatic, and low heteroatom signals. The oil produced from the second step was strikingly similar to that produced from HP of chemically isolated algaenan. The step 2 oil contained nitrogen and oxygen (1.3 % and 5.7 %) in amounts that were very similar to the oil from chemically isolated algaenan (1.3 % and 5.7 %) and had a higher high heating value of 41.3 MJ/Kg compared to 41 MJ/Kg for chemically isolated algaenan. The step 2 process is very favorable because we can produce the same quality of oil from whole algae as that achieved from HP of chemically isolated algaenan without the need to use any of the time- and energy-consuming chemical isolation techniques.

2. FUTURE WORK

There are multiple logical research directions towards which this research can be expanded. First, it would be very informative to actually perform the detailed proposed chemical isolation protocol described in Chapter II on a whole algae sample to isolate its algaenan. The impact of having a unified algaenan isolation method would benefit the community greatly as it would eliminate any variability in the algaenan isolation procedure and could lead to less variability in the proposed structures.

Second, testing the structure of the algaenan obtained after HP isolation and comparing it to that from chemical isolation using high resolution magic-angle-spinning solid state ^{13}C two dimensional NMR techniques would provide additional insights into algaenan structure and the impact of isolation strategies. With high resolution solid state ^{13}C two dimensional NMR, I can have a better insight of structural connectivities for

functional groups in the algaenan structure and if the HP isolation procedure has any molecular effects that were not observed from one dimensional solid state ^{13}C NMR.

Third, another aspect of research interest would be to measure the kinetics of algaenan cracking by HP. In this dissertation 360 °C for 72 h is used for maximum oil production based on kinetics for Type I kerogen HP cracking. Although I expect the kinetics to be similar, a detailed analysis of the reaction kinetics will be very valuable in further optimizing the HP process to produce oil from algaenan.

REFERENCES

Abdelmoez, W., Yoshida, H., 2013. Production of Amino and Organic Acids from Protein Using Sub-Critical Water Technology. International Journal of Chemical Reactor Engineering 11, 369-384.

Abdelmoez, W., Yoshida, H., Nakahasi, T., 2010. Pathways of Amino Acid Transformation and Decomposition in Saturated Subcritical Water Conditions. International Journal of Chemical Reactor Engineering 8, 1542-6580.

Alekseev, A.S., Kononova, L.I., Nikishin, A.M., 1996. The Devonian and Carboniferous of the Moscow Syneclise (Russian Platform): Stratigraphy and sea-level changes. Tectonophysics 268, 149-168.

Allard, B., Templier, J., 2000. Comparison of neutral lipid profile of various trilaminar outer cell wall (TLS)-containing microalgae with emphasis on algaenan occurrence. Phytochemistry 54, 369-380.

Allard, B., Templier, J., 2001. High molecular weight lipids from the trilaminar outer wall (TLS)-containing microalgae Chlorella emersonii, Scenedesmus communis and Tetraedron minimum. Phytochemistry 57, 459-467.

Allard, B., Templier, J., Largeau, C., 1997. Artifactual origin of mycobacterial bacteran. Formation of melanoidin-like artifact macromolecular material during the usual isolation process. Organic Geochemistry 26, 691-703.

Allard, B., Templier, J., Largeau, C., 1998. An improved method for the isolation of artifact-free algaenans from microalgae. Organic Geochemistry 28, 543-548.

Anders S Carlsson, J.B.v.B., Ralf Möller and David Clayton, 2007. Micro- and macro-algae: Utility for industrial applications, in: Bowles, D. (Ed.), EPOBIO: Realising the Economic Potential of Sustainable Resources - Bioproducts from Non-food Crops. University of York, UK.

Antal, M.J., Mok, W.S.L., Richards, G.N., 1990. Kinetic-Studies of the Reactions of Ketoses and Aldoses in Water at High-Temperature .1. Mechanism of Formation of 5-(Hydroxymethyl)-2-Furaldehyde from D-Fructose and Sucrose. Carbohydrate Research 199, 91-109.

Artok, L., Schobert, H.H., Nomura, M., Erbatur, O., Kidena, K., 1998. Effects of Water and Molecular Hydrogen on Heat Treatment of Turkish Low-Rank Coals†. Energy & Fuels 12, 1200-1211.

Bach, R.D., Canepa, C., 1996. Electronic Factors Influencing the Decarboxylation of β-Keto Acids. A Model Enzyme Study. The Journal of Organic Chemistry 61, 6346-6353.

Bada, J.L., 1991. Amino-Acid Cosmogeochemistry. Philosophical Transactions of the Royal Society of London Series B-Biological Sciences 333, 349-358.

Bada, J.L., Miller, S.L., 1970. Kinetics and Mechanism of Reversible Nonenzymatic Deamination of Aspartic Acid. Journal of the American Chemical Society 92, 2774-&.

Bada, J.L., Shou, M.Y., Man, E.H., Schroeder, R.A., 1978. Decomposition of Hydroxy Amino-Acids in Foraminiferal Tests - Kinetics, Mechanism and Geochronological Implications. Earth and Planetary Science Letters 41, 67-76.

Bailey, W.J., Bird, C.N., 1977. Pyrolysis of Esters .27. Pyrolysis of Lactones. Journal of Organic Chemistry 42, 3895-3899.

Bailey, W.J., Turek, W.N., 1956. Synthesis and Purification of Fatty Acids by the Pyrolysis of Esters. Journal of the American Oil Chemists Society 33, 317-319.

Batista, A.P., Moura, P., Marques, P.A.S.S., Ortigueira, J., Alves, L., Gouveia, L., 2014. Scenedesmus obliquus as feedstock for biohydrogen production by Enterobacter aerogenes and Clostridium butyricum. Fuel 117, Part A, 537-543.

Baum, R., Smith, G.G., 1986. Systematic Ph Study on the Acid-Catalyzed and Base-Catalyzed Racemization of Free Amino-Acids to Determine the 6 Constants, One for Each of the 3 Ionic Species. Journal of the American Chemical Society 108, 7325-7327.

Behar, F., Derenne, S., Largeau, C., 1995a. Closed Pyrolyses of the Isoprenoid Algaenan of Botryococcus-Braunii, L Race - Geochemical Implications for Derived Kerogens. Geochimica Et Cosmochimica Acta 59, 2983-2997.

Behar, F., Derenne, S., Largeau, C., 1995b. Closed pyrolysis of the isoprenoid algaenan of Botryococcus braunii, L race: geochemical implications for derived kerogens. Geochimica Et Cosmochimica Acta 59, 2983-2997.

Behar, F., Lewan, M.D., Lorant, F., Vandenbroucke, M., 2003. Comparison of artificial maturation of lignite in hydrous and nonhydrous conditions. Organic Geochemistry 34, 575-600.

Behar, F., Lorant, F., Lewan, M., 2008. Role of NSO compounds during primary cracking of a Type II kerogen and a Type III lignite. Organic Geochemistry 39, 1-22.

Behar, F., Vandenbroucke, M., Teermann, S.C., Hatcher, P.G., Leblond, C., Lerat, O., 1995c. Experimental simulation of gas generation from coals and a marine kerogen. Chemical Geology 126, 247-260.

Behrenbruch, P., Dedigama, T., 2007. Classification and characterisation of crude oils based on distillation properties. Journal of Petroleum Science and Engineering 57, 166-180.

Bell, J.L.S., Palmer, D.A., Barnes, H.L., Drummond, S.E., 1994. Thermal-Decomposition of Acetate .3. Catalysis by Mineral Surfaces. Geochimica Et Cosmochimica Acta 58, 4155-4177.

Belsky, A.J., Maiella, P.G., Brill, T.B., 1999. Spectroscopy of hydrothermal reactions - 13. Kinetics and mechanisms of decarboxylation of acetic acid derivatives at 100-260 degrees C under 275 bar. Journal of Physical Chemistry A 103, 4253-4260.

Berkaloff, C., Casadevall, E., Largeau, C., Metzger, P., Peracca, S., Virlet, J., 1983a. Hydrocarbon Formation in the Green-Alga Botryococcus-Braunii .3. The Resistant Polymer of the Walls of the Hydrocarbon-Rich Alga Botryococcus-Braunii. Phytochemistry 22, 389-397.

Berkaloff, C., Casadevall, E., Largeau, C., Metzger, P., Peracca, S., Virlet, J., 1983b. Hydrocarbon formation in the green alga Botryococcus braunii. Part 3. The resistant polymer of the walls of the hydrocarbon-rich alga B. braunii. Phytochemistry 22, 389-397.

Bertheas, O., Metzger, P., Largeau, C., 1999. A high molecular weight complex lipid, aliphatic polyaldehyde tetraterpenediol polyacetal from Botryococcus braunii (L race). Phytochemistry 50, 85-96.

Bigley, D.B., Thurman, J.C., 1967a. On Transition State for Decarboxylation of Beta-Keto Acids and Betagamma-Unsaturated Acids. Tetrahedron Letters, 2377-&.

Bigley, D.B., Thurman, J.C., 1967b. Studies in Decarboxylation .V. Kinetic Isotope Effects in Gas-Phase Thermal Decarboxylation of 2,2-Dimethyl-4-Phenylbut-3-Enoic Acid. Journal of the Chemical Society B-Physical Organic, 941-&.

Biller, P., Riley, R., Ross, A.B., 2011. Catalytic hydrothermal processing of microalgae: Decomposition and upgrading of lipids. Bioresource Technology 102, 4841-4848.

Biller, P., Ross, A.B., 2010. Potential yields and properties of oil from the hydrothermal liquefaction of microalgae with different biochemical content. Bioresource Technology 102, 215-225.

Biller, P., Ross, A.B., 2011. Potential yields and properties of oil from the hydrothermal liquefaction of microalgae with different biochemical content. Bioresource Technology 102, 215-225.

Biller, P., Ross, A.B., 2012. Hydrothermal processing of algal biomass for the production of biofuels and chemicals. Biofuels 3, 603-623.

Biller, P., Ross, A.B., Skill, S.C., Lea-Langton, A., Balasundaram, B., Hall, C., Riley, R., Llewellyn, C.A., 2012. Nutrient recycling of aqueous phase for microalgae cultivation from the hydrothermal liquefaction process. Algal Research 1, 70-76.

Blokker, P., Schouten, S., de Leeuw, J.W., Damste, J.S.S., van den Ende, H., 2000. A comparative study of fossil and extant algaenans using ruthenium tetroxide degradation. Geochimica Et Cosmochimica Acta 64, 2055-2065.

Blokker, P., Schouten, S., van den Ende, H., de Leeuw, J.W., Hatcher, P.G., Sinninghe Damste, J.S., 1998. Chemical structure of algaenans from the fresh water algae Tetraedron minimum, Scenedesmus communis and Pediastrum boryanum. Organic Geochemistry 29, 1453-1468.

Bobleter, O., 1994. Hydrothermal degradation of polymers derived from plants. Progress in Polymer Science 19, 797-841.

Boie, W., 1953. General diagrams for fuels. Technik 8, 305-309.

Bonn, G., Bobleter, O., 1983. Determination of the Hydrothermal Degradation Products of D-(U-C14) Glucose and D-(U-C-14) Fructose by Tlc. Journal of Radioanalytical Chemistry 79, 171-177.

Brassell, S.C., Lewis, C.A., Deleeuw, J.W., Delange, F., Damste, J.S.S., 1986. Isoprenoid Thiophenes - Novel Products of Sediment Diagenesis. Nature 320, 160-162.

Brown, T.M., Duan, P., Savage, P.E., 2010. Hydrothermal liquefaction and gasification of Nannochloropsis sp. Energy & Fuels 24, 3639-3646.

Brunner, G., 2014. Chapter 8 - Processing of Biomass with Hydrothermal and Supercritical Water, in: Gerd, B. (Ed.), Supercritical Fluid Science and Technology. Elsevier, pp. 395-509.

Burczyk, J., Loos, E., 1995. Cell Wall-Bound Enzymatic-Activities in Chlorella and Scenedesmus. Journal of Plant Physiology 146, 748-750.

C.M. , S., 1988. Alloy Selection for Caustic Soda Service. Nickel Development Institute, USA.

Castañeda, L.C., Muñoz, J.A.D., Ancheyta, J., 2014. Current situation of emerging technologies for upgrading of heavy oils. Catalysis Today 220–222, 248-273.

Channiwala, S.A., Parikh, P.P., 2002. A unified correlation for estimating HHV of solid, liquid and gaseous fuels. Fuel 81, 1051-1063.

Chiaberge, S., Leonardis, I., Fiorani, T., Bianchi, G., Cesti, P., Bosetti, A., Crucianelli, M., Reale, S., De Angelis, F., 2013. Amides in Bio-oil by Hydrothermal Liquefaction of Organic Wastes: A Mass Spectrometric Study of the Thermochemical Reaction Products of Binary Mixtures of Amino Acids and Fatty Acids. Energy & Fuels 27, 5287-5297.

Chiavari, G., Galletti, G.C., 1992. Pyrolysis—gas chromatography/mass spectrometry of amino acids. Journal of Analytical and Applied Pyrolysis 24, 123-137.

Chisti, Y., 2007. Biodiesel from microalgae. Biotechnology Advances 25, 294-306.

Chiu, F.C.K., Lo, C.M.Y., 2000. Observation of amide anions in solution by electrospray ionization mass spectrometry. Journal of the American Society for Mass Spectrometry 11, 1061-1064.

Cohen, B.A., Chyba, C.F., 2000. Racemization of meteoritic amino acids. Icarus 145, 272-281.

Collinson, M.E., Van Bergen, P.F., Scott, A.C., De Leeuw, J.W., 1994. The oil-generating potential of plants from coal and coal-bearing strata through time: a review with new evidence from Carboniferous plants. Geological Society, London, Special Publications 77, 31-70.

Cox, J.S., Seward, T.M., 2007. The hydrothermal reaction kinetics of aspartic acid. Geochimica Et Cosmochimica Acta 71, 797-820.

Damste, J.S.S., Rijpstra, W.I., Kockvandalen, A.C., Deleeuw, J.W., Schenck, P.A., 1989. Quenching of Labile Functionalized Lipids by Inorganic Sulfur Species - Evidence for the Formation of Sedimentary Organic Sulfur-Compounds at the Early Stages of Diagenesis. Geochimica Et Cosmochimica Acta 53, 1343-1355.

De Leeuw, J.W., Largeau, C., 1993. A review of macroomolecular organic compounds that comprise living organisms and their role in kerogen, coal and petroleum formation., in: Engel, M.H., Macko, S.A. (Eds.), Organic Geochemistry. Plenum Publishing Group, New York, pp. 23–72.

De Leeuw, J.W., Versteegh, G.J.M., van Bergen, P.F., 2006. Biomacromolecules of algae and plants and their fossil analogues. Plant Ecology 182, 209-233.

Derenne, S., Largeau, C., Berkaloff, C., Rousseau, B., Wilhelm, C., Hatcher, P.G., 1992a. Nonhydrolyzable Macromolecular Constituents from Outer Walls of Chlorella-Fusca and Nanochlorum-Eucaryotum. Phytochemistry 31, 1923-1929.

Derenne, S., Largeau, C., Casadevall, E., Berkaloff, C., 1989. Occurrence of a Resistant Bio-Polymer in the L-Race of Botryococcus-Braunii. Phytochemistry 28, 1137-1142.

Derenne, S., Largeau, C., Casadevall, E., Berkaloff, C., Rousseau, B., 1991. Chemical Evidence of Kerogen Formation in Source Rocks and Oil Shales Via Selective Preservation of Thin Resistant Outer Walls of Microalgae - Origin of Ultralaminae. Geochimica Et Cosmochimica Acta 55, 1041-1050.

Derenne, S., Largeau, C., Hatcher, P.G., 1992b. Structure of Chlorella-Fusca Algaenan - Relationships with Ultralaminae in Lacustrine Kerogens - Species-Dependent and Environment-Dependent Variations in the Composition of Fossil Ultralaminae. Organic Geochemistry 18, 417-422.

Derenne, S., Largeau, C., Hetenyi, M., BruknerWein, A., Connan, J., Lugardon, B., 1997. Chemical structure of the organic matter in a Pliocene maar-type shale: Implicated Botryococcus race strains and formation pathways. Geochimica Et

Cosmochimica Acta 61, 1879-1889.

Dote, Y., Sawayama, S., Inoue, S., Minowa, T., Yokoyama, S., 1994. Recovery of Liquid Fuel from Hydrocarbon-Rich Microalgae by Thermochemical Liquefaction. Fuel 73, 1855-1857.

Dria, K.J., Sachleben, J.R., Hatcher, P.G., 2002. Solid-state carbon-13 nuclear magnetic resonance of humic acids at high magnetic field strengths. Journal of Environmental Quality 31, 393-401.

Duan, P., Savage, P.E., 2011a. Catalytic treatment of crude algal bio-oil in supercritical water: optimization studies. Energy & Environmental Science 4, 1447-1456.

Duan, P.G., Savage, P.E., 2011b. Hydrothermal Liquefaction of a Microalga with Heterogeneous Catalysts. Industrial & Engineering Chemistry Research 50, 52-61.

Duan, P.G., Savage, P.E., 2011c. Upgrading of crude algal bio-oil in supercritical water. Bioresource Technology 102, 1899-1906.

Dubois, M., Gilles, K.A., Hamilton, J.K., Rebers, P.A., Smith, F., 1956. Colorimetric Method for Determination of Sugars and Related Substances. Analytical Chemistry 28, 350-356.

Earl, W.L., Vanderhart, D.L., 1981. Observations by High-Resolution C-13 Nuclear Magnetic-Resonance of Cellulose-I Related to Morphology and Crystal-Structure. Macromolecules 14, 570-574.

U.S. Energy Information Administration Congress. *Annual Coal Report 2012.* Washington, DC: 2013.

Elliott, D.C., 2007. Historical Developments in Hydroprocessing Bio-oils. Energy & Fuels 21, 1792-1815.

Elliott, D.C., Baker, E.G., 1989. Upgrading of biomass pyrolyzates. USA . p. 7 pp.

Fahim, M.A., Al-Sahhaf, T.A., Elkilani, A., 2009. Fundamentals of Petroleum Refining. Elsevier Science.

Fu, J., Klein, G.C., Smith, D.F., Kim, S., Rodgers, R.P., Hendrickson, C.L., Marshall, A.G., 2006. Comprehensive Compositional Analysis of Hydrotreated and Untreated Nitrogen-Concentrated Fractions from Syncrude Oil by Electron Ionization, Field Desorption Ionization, and Electrospray Ionization Ultrahigh-Resolution FT-ICR Mass Spectrometry. Energy & Fuels 20, 1235-1241.

Garcia-Moscoso, J.L., Obeid, W., Kumar, S., Hatcher, P.G., 2013. Flash hydrolysis of microalgae (Scenedesmus sp.) for protein extraction and production of biofuels intermediates. The Journal of Supercritical Fluids 82, 183-190.

Garcia Alba, L., Torri, C., Samorì, C., van der Spek, J., Fabbri, D., Kersten, S.R.A., Brilman, D.W.F., 2011. Hydrothermal Treatment (HTT) of Microalgae: Evaluation of the Process As Conversion Method in an Algae Biorefinery Concept. Energy & Fuels 26, 642-657.

Geiger, T., Clarke, S., 1987. Deamidation, Isomerization, and Racemization at Asparaginyl and Aspartyl Residues in Peptides - Succinimide-Linked Reactions That Contribute to Protein-Degradation. Journal of Biological Chemistry 262, 785-794.

Gelin, F., Boogers, I., Noordeloos, A.A.M., Damste, J.S.S., Hatcher, P.G., deLeeuw, J.W., 1996a. Novel, resistant microalgal polyethers: An important sink of organic carbon in the marine environment? Geochimica Et Cosmochimica Acta 60, 1275-

1280.

Gelin, F., Boogers, I., Noordeloos, A.A.M., Damste, J.S.S., Riegman, R., De Leeuw, J.W., 1997a. Resistant biomacromolecules in marine microalgae of the classes eustigmatophyceae and chlorophyceae: Geochemical implications. Organic Geochemistry 26, 659-675.

Gelin, F., Boogers, I., Noordeloos, A.A.M., Sinninghe Damste, J.S., Riegman, R., de Leeuw, J.W., 1997b. Resistant biomacromolecules in marine microalgae of the classes Eustigmatophyceae and Chlorophyceae: Geochemical implications. Organic Geochemistry 26, 659-675.

Gelin, F., Damste, J.S.S., Harrison, W.N., Reiss, C., Maxwell, J.R., DeLeeuw, J.W., 1996b. Variations in origin and composition of kerogen constituents as revealed by analytical pyrolysis of immature kerogens before and after desulphurization. Organic Geochemistry 24, 705-714.

Gelin, F., Volkman, J.K., deLeeuw, J.W., Damste, J.S.S., 1997c. Mid-chain hydroxy long-chain fatty acids in microalgae from the genus Nannochloropsis. Phytochemistry 45, 641-646.

Gelin, F., Volkman, J.K., Largeau, C., Derenne, S., Sinninghe Damsté, J.S., De Leeuw, J.W., 1999. Distribution of aliphatic, nonhydrolyzable biopolymers in marine microalgae. Organic Geochemistry 30, 147-159.

Goth, K., De Leeuw, J.W., Puttmann, W., Tegelaar, E.W., 1988. Origin of Messel Oil-Shale Kerogen. Nature 336, 759-761.

Griffin, R.C., Chamberlain, A.T., Hotz, G., Penkman, K.E.H., Collins, M.J., 2009. Age estimation of archaeological remains using amino acid racemization in dental enamel: A comparison of morphological, biochemical, and known ages-at-death. American Journal of Physical Anthropology 140, 244-252.

Hartman, B.E., Hatcher, P.G., 2014. Valuable Crude Oil from Hydrothermal Liquefaction of an Aliphatic Coal. Energy & Fuels 28, 7538-7551.

Hatcher, P.G., Clifford, D.J., 1997a. The organic geochemistry of coal: from plant materials to coal. Org. Geochem. 27, 251-274.

Hatcher, P.G., Clifford, D.J., 1997b. The organic geochemistry of coal: from plant materials to coal. Organic Geochemistry 27, 251-+.

Hatcher, P.G., Salmon, E., 2009. Process for the Selective Production of Hydrocarbon Based Fuels from Algae Utilizing Water at Subcritical Conditions. Old Dominion University Research Foundation, United States of America.

Hatcher, P.G., Spiker, E.C., Szeverenyi, N.M., Maciel, G.E., 1983. Selective Preservation and Origin of Petroleum-Forming Aquatic Kerogen. Nature 305, 498-501.

Higman, E.B., Schmeltz, I., Schlotzhauer, W.S., 1970. Products from the thermal degradation of some naturally occurring materials. Journal of Agricultural and Food Chemistry 18, 636-639.

Hill Bembenic, M.A., Burgess Clifford, C.E., 2013. Subcritical Water Reactions of Lignin-Related Model Compounds with Nitrogen, Hydrogen, Carbon Monoxide, and Carbon Dioxide Gases. Energy & Fuels 27, 6681-6694.

Ho, S.-H., Li, P.-J., Liu, C.-C., Chang, J.-S., 2013. Bioprocess development on microalgae-based CO2 fixation and bioethanol production using Scenedesmus obliquus CNW-N. Bioresource Technology 145, 142-149.

Hockaday, W.C., Purcell, J.M., Marshall, A.G., Baldock, J.A., Hatcher, P.G., 2009.

Electrospray and photoionization mass spectrometry for the characterization of organic matter in natural waters: a qualitative assessment. Limnology and Oceanography: Methods 7, 81-95.

Hoering, T.C., 1984. Thermal reactions of kerogen with added water, heavy water and pure organic substances. Organic Geochemistry 5, 267-278.

Holliday, R.L., King, J.W., List, G.R., 1997. Hydrolysis of vegetable oils in sub- and supercritical water. Industrial & Engineering Chemistry Research 36, 932-935.

Hughey, C.A., Rodgers, R.P., Marshall, A.G., Qian, K., Robbins, W.K., 2002. Identification of acidic NSO compounds in crude oils of different geochemical origins by negative ion electrospray Fourier transform ion cyclotron resonance mass spectrometry. Organic Geochemistry 33, 743-759.

Hwang, H.-I., Hartman, T.G., Ho, C.-T., 1995. Relative Reactivities of Amino Acids in the Formation of Pyridines, Pyrroles, and Oxazoles. Journal of Agricultural and Food Chemistry 43, 2917-2921.

Inoue, S., Dote, Y., Sawayama, S., Minowa, T., Ogi, T., Yokoyama, S.Y., 1994. Analysis of Oil Derived from Liquefaction of Botryococcus-Braunii. Biomass & Bioenergy 6, 269-274.

Izzo, H.V., Ho, C.T., 1993a. Effect of Residual Amide Content on Aroma Generation and Browning in Heated Gluten Glucose Model Systems. Journal of Agricultural and Food Chemistry 41, 2364-2367.

Izzo, H.V., Ho, C.T., 1993b. The Nonenzymatic Deamidation of Food Proteins during Processing and the Indication of Possible Protein Interactions. Abstracts of Papers of the American Chemical Society 205, 22-Agfd.

Jena, U., Das, K.C., Kastner, J.R., 2011. Effect of operating conditions of thermochemical liquefaction on biocrude production from Spirulina platensis. Bioresource Technology 102, 6221-6229.

Johnson, R.L., Schmidt-Rohr, K., 2014. Quantitative solid-state 13C NMR with signal enhancement by multiple cross polarization. Journal of Magnetic Resonance 239, 44-49.

Kabyemela, B.M., Adschiri, T., Malaluan, R.M., Arai, K., 1999. Glucose and fructose decomposition in subcritical and supercritical water: Detailed reaction pathway, mechanisms, and kinetics. Industrial & Engineering Chemistry Research 38, 2888-2895.

Kadouri, A., Derenne, S., Largeau, C., Casadevall, E., Berkaloff, C., 1988. Resistant Bio-Polymer in the Outer Walls of Botryococcus-Braunii, B-Race. Phytochemistry 27, 551-557.

Kamga, A.W., Behar, F., Hatcher, P.G., 2014. Quantitative Analysis of Long Chain Fatty Acids Present in a Type I Kerogen Using Electrospray Ionization Fourier Transform Ion Cyclotron Resonance Mass Spectrometry: Compared with BF3/MeOH Methylation/GC-FID. Journal of the American Society for Mass Spectrometry 25, 880-890.

Kawamura, K., Yukioka, M., 2001. Kinetics of the racemization of amino acids at 225-275 degrees C using a real-time monitoring method of hydrothermal reactions. Thermochimica Acta 375, 9-16.

Kharaka, Y.K., Carothers, W.W., Rosenbauer, R.J., 1983. Thermal Decarboxylation of Acetic-Acid - Implications for Origin of Natural-Gas. Geochimica Et

Cosmochimica Acta 47, 397-402.
Kim, S., Kramer, R.W., Hatcher, P.G., 2003. Graphical method for analysis of ultrahigh-resolution broadband mass spectra of natural organic matter, the van Krevelen diagram. Analytical Chemistry 75, 5336-5344.
King, J.W., Holliday, R.L., List, G.R., 1999. Hydrolysis of soybean oil in a subcritical water flow reactor. Green Chemistry 1, 261-264.
Kissin, Y.V., 1990. Catagenesis of light cycloalkanes in petroleum. Organic Geochemistry 15, 575-594.
Koch, B.P., Dittmar, T., 2006. From mass to structure: an aromaticity index for high-resolution mass data of natural organic matter. Rapid Communications in Mass Spectrometry 20, 926-932.
Kodner, R.B., Summons, R.E., Knoll, A.H., 2009. Phylogenetic investigation of the aliphatic, non-hydrolyzable biopolymer algaenan, with a focus on green algae. Organic Geochemistry 40, 854-862.
Kokinos, J.P., Eglinton, T.I., Goni, M.A., Boon, J.J., Martoglio, P.A., Anderson, D.M., 1998. Characterization of a highly resistant biomacromolecular material in the cell wall of a marine dinoflagellate resting cyst. Organic Geochemistry 28, 265-288.
Krevelen, D.W.v., Schuyer, J., 1957. Coal science; aspects of coal constitution. Elsevier Pub. Co., Amsterdam, Princeton N.J.
Kruse, A., Dinjus, E., 2007. Hot compressed water as reaction medium and reactant - Properties and synthesis reactions. Journal of Supercritical Fluids 39, 362-380.
Kuhlmann, B., Arnett, E.M., Siskin, M., 1994. Classical Organic Reactions in Pure Superheated Water. The Journal of Organic Chemistry 59, 3098-3101.
Kumar, S., Hablot, E., Moscoso, J.L.G., Obeid, W., Hatcher, P.G., DuQuette, B.M., Graiver, D., Narayan, R., Balan, V., 2014. Polyurethanes preparation using proteins obtained from microalgae. Journal of Materials Science 49, 7824-7833.
Lamer, M., 1957. The World Fertilizer Economy. Stanford University Press.
Largeau, C., Casadevall, E., Kadouri, A., Metzger, P., 1984. Formation of Botryococcus-derived kerogens—Comparative study of immature torbanites and of the extent alga Botryococcus braunii. Organic Geochemistry 6, 327-332.
Largeau, C., Derenne, S., Casadevall, E., Kadouri, A., Sellier, N., 1986. Pyrolysis of Immature Torbanite and of the Resistant Bio-Polymer (PRB A) Isolated from Extant Alga Botryococcus-Braunii - Mechanism of Formation and Structure of Torbanite. Organic Geochemistry 10, 1023-1032.
Larsen, G., Chilingar, G.V., 1967. Diagenesis in sediments. Elsevier, Amsterdam, London, New York etc.
Laurens, L.M.L., Dempster, T.A., Jones, H.D.T., Wolfrum, E.J., Van Wychen, S., McAllister, J.S.P., Rencenberger, M., Parchert, K.J., Gloe, L.M., 2012. Algal Biomass Constituent Analysis: Method Uncertainties and Investigation of the Underlying Measuring Chemistries. Analytical Chemistry 84, 1879-1887.
Lee, R.E., 2008. Phycology, 4th ed. Cambridge University Press, Cambridge, England ; New York.
Leif, R.N., Simoneit, B.R.T., 2000. The role of alkenes produced during hydrous pyrolysis of a shale. Organic Geochemistry 31, 1189-1208.
Levine, R.B., Sierra, C.O.S., Hockstad, R., Obeid, W., Hatcher, P.G., Savage, P.E., 2013.

The use of hydrothermal carbonization to recycle nutrients in algal biofuel production. Environmental Progress & Sustainable Energy 32, 962-975.

Lewan, M.D., 1985. Evaluation of petroleum generation by hydrous pyrolysis experimentation. PHILOSOPHICAL TRANSACTIONS OF THE ROYAL SOCIETY OF LONDON SERIES A-MATHEMATICAL AND PHYSICAL SCIENCES 315, 123-134.

Lewan, M.D., 1993. Hydrocarbon-Gas Generation from Different Kerogen Types Subjected to Hydrous Pyrolysis. Abstracts of Papers of the American Chemical Society 206, 32-Geoc.

Lewan, M.D., 1997. Experiments on the role of water in petroleum formation. Geochimica Et Cosmochimica Acta 61, 3691-3723.

Lewan, M.D., Winters, J.C., McDonald, J.H., 1979. Generation of Oil-Like Pyrolyzates from Organic-Rich Shales. Science 203, 897-899.

Li, J., Brill, T.B., 2002. Spectroscopy of Hydrothermal Reactions 20: Experimental and DFT Computational Comparison of Decarboxylation of Dicarboxylic Acids Connected by Single, Double, and Triple Bonds. The Journal of Physical Chemistry A 106, 9491-9498.

Li, J., Brill, T.B., 2003. Spectroscopy of hydrothermal reactions, part 26: Kinetics of decarboxylation of aliphatic amino acids and comparison with the rates of racemization. International Journal of Chemical Kinetics 35, 602-610.

Li, J., Wang, X.G., Klein, M.T., Brill, T.B., 2002. Spectroscopy of hydrothermal reactions, 19: pH and salt dependence of decarboxylation of alpha-alanine at 280-330 degrees C in an FT-IR spectroscopy flow reactor. International Journal of Chemical Kinetics 34, 271-277.

López Barreiro, D., Prins, W., Ronsse, F., Brilman, W., 2013. Hydrothermal liquefaction (HTL) of microalgae for biofuel production: State of the art review and future prospects. Biomass & Bioenergy 53, 113-127.

Makulla, A., 2000. Fatty acid composition of Scenedesmus obliquus: Correlation to dilution rates. Limnologica - Ecology and Management of Inland Waters 30, 162-168.

Mango, F.D., 1990. The origin of light cycloalkanes in petroleum. Geochimica Et Cosmochimica Acta 54, 23-27.

Marshall, A.G., Rodgers, R.P., 2008. Petroleomics: Chemistry of the underworld. Proceedings of the National Academy of Sciences of the United States of America 105, 18090-18095.

McCollom, T.M., Simoneit, B.R.T., Shock, E.L., 1999. Hydrous Pyrolysis of Polycyclic Aromatic Hydrocarbons and Implications for the Origin of PAH in Hydrothermal Petroleum. Energy & Fuels 13, 401-410.

McKee, G.A., Hatcher, P.G., 2010. Alkyl amides in two organic-rich anoxic sediments: A possible new abiotic route for N sequestration. Geochimica Et Cosmochimica Acta 74, 6436-6450.

McKinney, D.E., Bortiatynski, J.M., Carson, D.M., Clifford, D.J., DeLeeuw, J.W., Hatcher, P.G., 1996. Tetramethylammonium hydroxide (TMAH) thermochemolysis of the aliphatic biopolymer cutan: Insights into the chemical structure. Organic Geochemistry 24, 641-650.

Metzger, P., Casadevall, E., Pouet, M.J., Pouet, Y., 1985. Structures of Some

Botryococcenes - Branched Hydrocarbons from the B-Race of the Green-Alga Botryococcus-Braunii. Phytochemistry 24, 2995-3002.

Metzger, P., Largeau, C., 1994. A New-Type of Ether Lipid Comprising Phenolic Moieties in Botryococcus-Braunii - Chemical-Structure and Abundance, and Geochemical Implications. Organic Geochemistry 22, 801-814.

Metzger, P., Pouet, Y., Bischoff, R., Casadevall, E., 1993. An Aliphatic Polyaldehyde from Botryococcus-Braunii (a Race). Phytochemistry 32, 875-883.

Metzger, P., Rager, M.N., Largeau, C., 2007. Polyacetals based on polymethylsqualene diols, precursors of algaenan in Botryococcus braunii race B. Organic Geochemistry 38, 566-581.

Mills, V., Mcclain, H.K., 1949. Fat Hydrolysis. Industrial and Engineering Chemistry 41, 1982-1985.

Nagamori, M., Funazukuri, T., 2004. Glucose production by hydrolysis of starch under hydrothermal conditions. Journal of Chemical Technology and Biotechnology 79, 229-233.

Nguyen, R.T., Harvey, H.R., Zang, X., van Heemst, J.D.H., Hetenyi, M., Hatcher, P.G., 2003. Preservation of algaenan and proteinaceous material during the oxic decay of Botryococcus braunii as revealed by pyrolysis-gas chromatography/mass spectrometry and C-13 NMR spectroscopy. Organic Geochemistry 34, 483-497.

Nikonov, V.A., Senning, A., 1989. Sulfur Compounds In Hydrocarbon Pyrolysis. Routledge.

Oasmaa, A., Czernik, S., 1999. Fuel oil quality of biomass pyrolysis oils - State of the art for the end user. Energy & Fuels 13, 914-921.

Obeid, W., Salmon, E., Hatcher, P.G., 2014. The effect of different isolation procedures on algaenan molecular structure in Scenedesmus green algae. Organic Geochemistry 76, 259-269.

Pandey, A., Larroche, C., Ricke, S.C., Dussap, C.G., Gnansounou, E., 2011. Biofuels: Alternative Feedstocks and Conversion Processes. Elsevier Science.

Patil, T.A., Butala, D.N., Raghunathan, T.S., Shankar, H.S., 1988. Thermal Hydrolysis of Vegetable-Oils and Fats .1. Reaction-Kinetics. Industrial & Engineering Chemistry Research 27, 727-735.

Patil, V., Tran, K.-Q., Giselroed, H.R., 2008. Towards sustainable production of biofuels from microalgae. International Journal Of Molecular Sciences 9, 1188-1195.

Peters, K.E., Ramos, L.S., Zumberge, J.E., Valin, Z.C., Scotese, C.R., Gautier, D.L., 2007. Circum-Arctic petroleum systems identified using decision-tree chemometrics. Aapg Bulletin 91, 877-913.

Peters, K.E., Walters, C.C., Moldowan, J.M., 2005. The Biomarker Guide: Biomarkers and isotopes in petroleum systems and Earth history. Cambridge University Press.

Peterson, A.A., Vogel, F., Lachance, R.P., Froling, M., Antal, M.J., Jr., Tester, J.W., 2008. Thermochemical biofuel production in hydrothermal media: a review of sub- and supercritical water technologies. Energy Environ. Sci. 1, 32-65.

Philp, R.P., Calvin, M., 1976. Possible Origin for Insoluble Organic (Kerogen) Debris in Sediments from Insoluble Cell-Wall Materials of Algae and Bacteria. Nature 262, 134-136.

Poinar, H.N., Hoss, M., Bada, J.L., Paabo, S., 1996. Amino acid racemization and the preservation of ancient DNA. Science 272, 864-866.

Popper, Z.A., Tuohy, M.G., 2010. Beyond the Green: Understanding the Evolutionary Puzzle of Plant and Algal Cell Walls. Plant Physiology 153, 373-383.

Qian, K., Robbins, W.K., Hughey, C.A., Cooper, H.J., Rodgers, R.P., Marshall, A.G., 2001. Resolution and Identification of Elemental Compositions for More than 3000 Crude Acids in Heavy Petroleum by Negative-Ion Microelectrospray High-Field Fourier Transform Ion Cyclotron Resonance Mass Spectrometry. Energy & Fuels 15, 1505-1511.

Qian, Y.R., Engel, M.H., Macko, S.A., Carpenter, S., Deming, J.W., 1993. Kinetics of Peptide Hydrolysis and Amino-Acid Decomposition at High-Temperature. Geochimica Et Cosmochimica Acta 57, 3281-3293.

Quitain, A.T., Daimon, H., Fujie, K., Katoh, S., Moriyoshi, T., 2006. Microwave-assisted hydrothermal degradation of silk protein to amino acids. Industrial & Engineering Chemistry Research 45, 4471-4474.

Ritchie, P., Purves, C., 1947. Periodate lignins: their preparation and properties. Pulp and Paper Magazine of Canada 48, 74-82.

Rogalinski, T., Herrmann, S., Brunner, G., 2005. Production of amino acids from bovine serum albumin by continuous sub-critical water hydrolysis. The Journal of Supercritical Fluids 36, 49-58.

Rogalinski, T., Liu, K., Albrecht, T., Brunner, G., 2008. Hydrolysis kinetics of biopolymers in subcritical water. Journal of Supercritical Fluids 46, 335-341.

Ruble, T.E., Lewan, M.D., Philp, R.P., 2001. New insights on the Green River petroleum system in the Uinta basin from hydrous pyrolysis experiments. Aapg Bulletin 85, 1333-1371.

Ruble, T.E., Lewan, M.D., Philp, R.P., 2003. New insights on the Green River petroleum system in the Uinta basin from hydrous-pyrolysis experiments: reply. Aapg Bulletin 87, 1535-1541.

Sachleben, J.R., Chefetz, B., Deshmukh, A., Hatcher, P.G., 2004. Solid-state NMR characterization of pyrene - Cuticular matter interactions. Environmental Science & Technology 38, 4369-4376.

Salmon, E., Behar, F., Hatcher, P.G., 2011. Molecular characterization of Type I kerogen from the Green River Formation using advanced NMR techniques in combination with electrospray ionization/ultrahigh resolution mass spectrometry. Organic Geochemistry 42, 301-315.

Salmon, E., Behar, F., Lorant, F., Hatcher, P.G., Metzger, P., Marquaire, P.-M., 2009a. Thermal decomposition processes in algaenan of Botryococcus braunii race L. Part 1: Experimental data and structural evolution. Organic Geochemistry 40, 400-415.

Salmon, E., Behar, F., Lorant, F., Hatcher, P.G., Metzger, P., Marquaire, P.M., 2009b. Thermal decomposition processes in algaenan of Botryococcus braunii race L. Part 1: Experimental data and structural evolution. Organic Geochemistry 40, 400-415.

Sato, N., Quitain, A.T., Kang, K., Daimon, H., Fujie, K., 2004. Reaction Kinetics of Amino Acid Decomposition in High-Temperature and High-Pressure Water. Industrial & Engineering Chemistry Research 43, 3217-3222.

Savage, P.E., 1999. Organic chemical reactions in supercritical water. Chemical Reviews 99, 603-621.

Savage, P.E., 2012. Chemistry. Algae under pressure and in hot water. Science 338, 1039-1040.

Scheirs, J., 2000. Compositional and Failure Analysis of Polymers: A Practical Approach. Wiley.

Schenk, P.M., Thomas-Hall, S.R., Stephens, E., Marx, U.C., Mussgnug, J.H., Posten, C., Kruse, O., Hankamer, B., 2008. Second Generation Biofuels: High-Efficiency Microalgae for Biodiesel Production. Bioenergy Research 1, 20-43.

Schnitzer, M., Khan, S.U., 1972. Humic substances in the environment. M. Dekker, New York,.

Schouten, S., Moerkerken, P., Gelin, F., Baas, M., de Leeuw, J.W., Damste, J.S.S., 1998. Structural characterization of aliphatic, non-hydrolyzable biopolymers in freshwater algae and a leaf cuticle using ruthenium tetroxide degradation. Phytochemistry 49, 987-993.

Schroeder, R.A., Bada, J.L., 1976. A review of the geochemical applications of the amino acid racemization reaction. Earth-Science Reviews 12, 347-391.

Sleighter, R.L., McKee, G.A., Liu, Z., Hatcher, P.G., 2008. Naturally present fatty acids as internal calibrants for Fourier transform mass spectra of dissolved organic matter. Limnology and Oceanography:Methods 6, 246-253.

Smith, G.G., Blau, S.E., 1964. Decarboxylation .I. Kinetic Study of Vapor Phase Thermal Decarboxylation of 3-Butenoic Acid. Journal of Physical Chemistry 68, 1231-&.

Smith, G.G., Sivakua, T., 1983. Mechanism of the Racemization of Amino-Acids - Kinetics of Racemization of Arylglycines. Journal of Organic Chemistry 48, 627-634.

Sohn, M., Ho, C.T., 1995. Ammonia generation during thermal degradation of amino acids. Journal of Agricultural and Food Chemistry 43, 3001-3003.

Srokol, Z., Bouche, A.G., van Estrik, A., Strik, R.C.J., Maschmeyer, T., Peters, J.A., 2004. Hydrothermal upgrading of biomass to biofuel; studies on some monosaccharide model compounds. Carbohydrate Research 339, 1717-1726.

Staehelin, L.A., Pickettheaps, J.D., 1975. Ultrastructure of Scenedesmus (Chlorophyceae) .1. Species with Reticulate or Warty Type of Ornamental Layer. Journal of Phycology 11, 163-185.

Stanton, R.W., Warwick, P.D., Swanson, S.M., 2005. Tar yields from low-temperature carbonization of coal facies from the Powder River Basin, Wyoming, USA. International Journal of Coal Geology 63, 13-26.

Stenesh, J., 1998. Biochemistry. Plenum, New York.

Stubbins, A., Spencer, R.G.M., Chen, H., Hatcher, P.G., Mopper, K., Hernes, P.J., Mwamba, V.L., Mangangu, A.M., Wabakanghanzi, J.N., Six, J., 2010. Illuminated darkness: molecular signatures of Congo River dissolved organic matter and its photochemical alteration as revealed by ultrahigh precision mass spectrometry. Limnol. Oceanogr. 55, 1467-1477.

Sudasinghe, N., Dungan, B., Lammers, P., Albrecht, K., Elliott, D., Hallen, R., Schaub, T., 2014. High resolution FT-ICR mass spectral analysis of bio-oil and residual water soluble organics produced by hydrothermal liquefaction of the marine microalga Nannochloropsis salina. Fuel 119, 47-56.

Tegelaar, E.W., De Leeuw, J.W., Derenne, S., Largeau, C., 1989a. A reappraisal of kerogen formation. Geochimica Et Cosmochimica Acta 53, 3103-3106.

Tegelaar, E.W., De Leeuw, J.W., Derenne, S., Largeau, C., 1989b. A reappraisal of kerogen formation. Geochim. Cosmochim. Acta 53, 3103-3106.

Tegelaar, E.W., Matthezing, R.M., Jansen, J.B.H., Horsfield, B., De leeuw, J.W., 1989c. Possible Origin of Normal-Alkanes in High-Wax Crude Oils. Nature 342, 529-531.

Thomas, B.A., Meyen, S.V., 1984. A Reappraisal of the Lower Carboniferous Lepidophyte Eskdalia Kidston. Palaeontology 27, 707-718.

Tissot, B.P., Welte, D.H., 1984. Petroleum formation and occurrence, 2nd, rev. and enl. ed. Springer-Verlag, Berlin ; New York.

Torri, C., Alba, L.G., Samori, C., Fabbri, D., Brilman, D.W.F., 2012. Hydrothermal Treatment (HTT) of Microalgae: Detailed Molecular Characterization of HTT Oil in View of HTT Mechanism Elucidation. Energy & Fuels 26, 658-671.

Turner, J.W., Hartman, B.E., Hatcher, P.G., 2013. Structural characterization of suberan isolated from river birch (Betula nigra) bark. Organic Geochemistry 57, 41-53.

United States Congress, 110th Congress. *The energy independence and security act of 2007.* Washington, D.C.: Government printing office, 2007.

United States Navy, Congress. *The Department of the Navy's Energy Goals* 2009.

Vendeuvre, C., Ruiz-Guerrero, R., Bertoncini, F., Duval, L., Thiébaut, D., 2007. Chromatographie en phase gazeuse bidimensionnelle pour l'analyse détaillée des produits pétroliers. Oil & Gas Science and Technology - Rev. IFP 62, 43-55.

Versteegh, G.J.M., Blokker, P., 2004. Resistant macromolecules of extant and fossil microalgae. Phycological Research 52, 325-339.

Walter, W., Harke, H.P., Polchow, R., 1967. Behavior of glycine, alanine, α-aminobutyric acid, leucine, phenylalanine, and aspartic acid under hydrothermal conditions. Z. Naturforsch., B 22, 931-937.

Wang, Y., Poirier, R.A., 1994. Ab initio study on the thermal decarboxylation of but-3-enoic acid and its derivatives. Canadian Journal of Chemistry 72, 1338-1346.

Watanabe, M., Iida, T., Inomata, H., 2006. Decomposition of a long chain saturated fatty acid with some additives in hot compressed water. Energy Conversion and Management 47, 3344-3350.

Wildschut, J., Mahfud, F.H., Venderbosch, R.H., Heeres, H.J., 2009. Hydrotreatment of Fast Pyrolysis Oil Using Heterogeneous Noble-Metal Catalysts. Industrial & Engineering Chemistry Research 48, 10324-10334.

Wilkins, R.W.T., George, S.C., 2002. Coal as a source rock for oil: a review. International Journal of Coal Geology 50, 317-361.

Winters, J.C., Williams, J.A., Lewan, M.D., 1983. A laboratory study of petroleum generation by hydrous pyrolysis. Wiley, pp. 524-533.

Woo, K.-L., Kim, J.-I., 1999. New hydrolysis method for extremely small amount of lipids and capillary gas chromatographic analysis as N(O)-tert.-butyldimethylsilyl fatty acid derivatives compared with methyl ester derivatives. Journal of Chromatography A 862, 199-208.

Xu, L., Brilman, D.W.F., Withag, J.A.M., Brem, G., Kersten, S., 2011. Assessment of a dry and a wet route for the production of biofuels from microalgae: Energy balance analysis. Bioresource Technology 102, 5113-5122.

Zang, X., 2002. The Chemical Structure of Algaenan from Botryococcus Braunii Based on 13C NMR Spectroscopy, Pyrolysis Gas Chromatography-Mass Spectrometry,

and TMAH Thermochemolysis Gas Chromatography-Mass Spectrometry, Department of Chemistry. The Ohio State University, Columbus.

Zang, X., Nguyen, R.T., Harvey, H.R., Knicker, H., Hatcher, P.G., 2001. Preservation of proteinaceous material during the degradation of the green alga Botryococcus braunii: A solid-state 2D N-15 C-13 NMR spectroscopy study. Geochimica Et Cosmochimica Acta 65, 3299-3305.

Zelibor, J.L., Jr., Romankiw, L., Hatcher, P.G., Colwell, R.R., 1988. Comparative analysis of the chemical composition of mixed and pure cultures of green algae and their decomposed residues by carbon-13 nuclear magnetic resonance spectroscopy. Applied and Environmental Microbiology 54, 1051-1060.

Zhang, T., Zhang, L., Zhou, Y., Wei, Q., Chung, K.H., Zhao, S., Xu, C., Shi, Q., 2013. Transformation of Nitrogen Compounds in Deasphalted Oil Hydrotreating: Characterized by Electrospray Ionization Fourier Transform-Ion Cyclotron Resonance Mass Spectrometry. Energy & Fuels 27, 2952-2959.

Zhong, J., Sleighter, R.L., Salmon, E., McKee, G.A., Hatcher, P.G., 2011. Combining advanced NMR techniques with ultrahigh resolution mass spectrometry: A new strategy for molecular scale characterization of macromolecular components of soil and sedimentary organic matter. Organic Geochemistry 42, 903-916.

APPENDIX A

COPYRIGHT PERMISSIONS

Permissions for Figure 1 were obtained from Rightslink:

Thesis/Dissertation Reuse Request

Taylor & Francis is pleased to offer reuses of its content for a thesis or dissertation free of charge contingent on resubmission of permission request if work is published

Permissions for Table 1 were obtained from Rightslink:

Dear Mr. Wassim Obeid,

Thank you for placing your order through Copyright Clearance Center's RightsLink service. Royal Society of Chemistry has partnered with RightsLink to license its content. This notice is a confirmation that your order was successful.

Your order details and publisher terms and conditions are available by clicking the link below:
http://s100.copyright.com/CustomerAdmin/PLF.jsp?ref=20335b67-2c80-4e4b-9536-cc4a6ae2ad39

Order Details
Licensee: Wassim A Obeid
License Date: Nov 18, 2014
License Number: 3512100694704
Publication: Energy & Environmental Science
Title: Thermochemical biofuel production in hydrothermal media: A review of sub- and supercritical water technologies
Type Of Use: Thesis/Dissertation
Total: 0.00 USD

Permissions for Table 2 were obtained from Rightslink:

This is a License Agreement between Wassim A Obeid ("You") and Elsevier ("Elsevier") provided by Copyright Clearance Center ("CCC"). The license consists of your order details, the terms and conditions provided by Elsevier, and the payment terms and conditions.

All payments must be made in full to CCC. For payment instructions, please see information listed at the bottom of this form.

Supplier	Elsevier Limited The Boulevard,Langford Lane Kidlington,Oxford,OX5 1GB,UK
Registered Company Number	1982084
Customer name	Wassim A Obeid
Customer address	5610 Monroe pl Norfolk, VA 23508
License number	3542461097780
License date	Jan 05, 2015
Licensed content publisher	Elsevier
Licensed content publication	Elsevier Books
Licensed content title	Supercritical Fluid Science and Technology
Licensed content author	Gerd Brunner
Licensed content date	2014
Number of pages	115
Start Page	395
End Page	509
Type of Use	reuse in a thesis/dissertation
Portion	figures/tables/illustrations
Number of figures/tables/illustrations	1
Format	both print and electronic
Are you the author of this Elsevier chapter?	No
Will you be translating?	No
Original figure numbers	Table 8.8
Title of your thesis/dissertation	INVESTIGATION TO THE POTENTIAL FOR ALGAENAN TO PRODUCE HYDROCARBON BASED FUELS FROM ALGAE BY HYDROUS PYROLYSIS
Expected completion date	Jan 2015
Estimated size (number of pages)	

Permissions for Figures 2 and 3 were obtained from Rightslink:

This is a License Agreement between Wassim A Obeid ("You") and John Wiley and Sons ("John Wiley and Sons") provided by Copyright Clearance Center ("CCC"). The license consists of your order details, the terms and conditions provided by John Wiley and Sons, and the payment terms and conditions. All payments must be made in full to CCC. For payment instructions, please see information listed at the bottom of this form.

License Number	3525980275053
License date	Dec 11, 2014
Licensed content publisher	John Wiley and Sons
Licensed content publication	International Journal of Chemical Kinetics
Licensed content title	Spectroscopy of hydrothermal reactions, part 26: Kinetics of decarboxylation of aliphatic amino acids and comparison with the rates of racemization
Licensed copyright line	Copyright © 2003 Wiley Periodicals, Inc.
Licensed content author	Jun Li,Thomas B. Brill
Licensed content date	Sep 3, 2003
Start page	602
End page	610
Type of use	Dissertation/Thesis
Requestor type	University/Academic
Format	Print and electronic
Portion	Figure/table
Number of figures/tables	2
Original Wiley figure/table number(s)	Scheme 1 Scheme 2
Will you be translating?	No

Permissions for Figure 4 were obtained from Rightslink:

Title: Reaction Kinetics of Amino Acid Decomposition in High-Temperature and High-Pressure Water

Author: Nobuaki Sato, Armando T. Quitain, Kilyoon Kang, et al

Publication: Industrial & Engineering Chemistry Research

Publisher: American Chemical Society

Date: Jun 1, 2004

PERMISSION/LICENSE IS GRANTED FOR YOUR ORDER AT NO CHARGE

This type of permission/license, instead of the standard Terms & Conditions, is sent to you because no fee is being charged for your order. Please note the following:

- Permission is granted for your request in both print and electronic formats, and translations.
- If figures and/or tables were requested, they may be adapted or used in part.
- Please print this page for your records and send a copy of it to your publisher/graduate school.
- Appropriate credit for the requested material should be given as follows: "Reprinted (adapted) with permission from (COMPLETE REFERENCE CITATION). Copyright (YEAR) American Chemical Society." Insert appropriate information in place of the capitalized words.
- One-time permission is granted only for the use specified in your request. No additional uses are granted (such as derivative works or other editions). For any other uses, please submit a new request.

Permissions for table 4 were obtained from Rightslink:

This is a License Agreement between Wassim A Obeid ("You") and Elsevier ("Elsevier") provided by Copyright Clearance Center ("CCC"). The license consists of your order details, the terms and conditions provided by Elsevier, and the payment terms and conditions.

Supplier:

	Elsevier Limited The Boulevard,Langford Lane Kidlington,Oxford,OX5 1GB,UK
Registered Company Number	1982084
Customer name	Wassim A Obeid
License number	3540820920014
License date	Jan 02, 2015
Licensed content publisher	Elsevier
Licensed content publication	Organic Geochemistry
Licensed content title	Distribution of aliphatic, nonhydrolyzable biopolymers in marine microalgae
Licensed content date	March 1999
Licensed content volume number	30
Licensed content issue number	2-3
Number of pages	13
Start Page	147
End Page	159
Portion	figures/tables/illustrations
Number of figures/tables/illustrations	1
Format	both print and electronic
Are you the author of this Elsevier article?	No
Original figure numbers	Table 1
Title of your thesis/dissertation	INVESTIGATION TO THE POTENTIAL FOR ALGAENAN TO PRODUCE HYDROCARBON BASED FUELS FROM ALGAE BY HYDROUS PYROLYSIS

Permissions for Chapter 2 were obtained from Rightslink:

This is a License Agreement between Wassim A Obeid ("You") and Elsevier ("Elsevier") provided by Copyright Clearance Center ("CCC"). The license consists of your order details, the terms and conditions provided by Elsevier, and the payment terms and conditions.

Supplier	Elsevier Limited The Boulevard,Langford Lane Kidlington,Oxford,OX5 1GB,UK
Registered Company Number	1982084
Customer name	Wassim A Obeid
License number	3541040638367
License date	Jan 02, 2015
Licensed content publisher	Elsevier
Licensed content publication	Organic Geochemistry
Licensed content title	The effect of different isolation procedures on algaenan molecular structure in Scenedesmus green algae
Licensed content author	None
Licensed content date	November 2014
Licensed content volume number	76
Licensed content issue number	n/a
Number of pages	11
Start Page	259
End Page	269
Type of Use	reuse in a thesis/dissertation
Portion	full article
Format	both print and electronic
Are you the author of this Elsevier article?	Yes
Will you be translating?	No
Title of your thesis/dissertation	INVESTIGATION TO THE POTENTIAL FOR ALGAENAN TO PRODUCE HYDROCARBON BASED FUELS FROM ALGAE BY HYDROUS PYROLYSIS
Estimated size (number of pages)	200

APPENDIX B

MATLAB CODE

```
function data = MasterAtLargeBlankMod(fname);
```

```
% MasterAtLargeBlankMod is just the playing ground for new files
% fill in line numbers instead of #### before exporting

% PEAKSLABELS section was originally written by Elodie Salmon
% (esalmon@odu.edu) and later combined with the code for ease and
% streamlining
```

PEAKSLABELS SECTION

```
%This code add a label for each mass to define if the peaks are part of the
%blank (mass within 0.0005m/z), are salts (mass with a mass defect of
%0.4-0.99 up to 400m/z and 0.6-0.99 for 400-800) or 13C isotopologues (13C
%peak observed at 1.0034 mass unit higher than 12C peak and 13C peak
%intensity should be less than 50% of 12C peak intensity)

%How to run the code:
% save your mass list for your balnk in a file name Blank.txt (or change
%the name of the file in line ####)

%Data that can be changed:
%peak incertainty for the blank line,
%conditions to define salt peaks line #### and #### change ch1ML and Massdef
%Isotopologues:
%change 1.0034 to somethingelse line #### and the precision line ####
%change intensity ratio (now 0.5) line ####
%Format final xls file line 1####-####.


tic
dataML = load(fname);  %load mass list of your sample from a text data file
dataB = load('Blank.txt'); %load mass list of the blank from a text data file

ch1ML=dataML(:,1);    %m/z peak of the sample
PintML=dataML(:,2);     %peak area of the sample

ch1B=dataB(:,1);    %m/z peak of the Blank
PintB=dataB(:,2);     %peak area of the Blank
```

Find blank peaks

```
%Compare sample and blank mass:
Msam=repmat(ch1ML,1,size(dataB,1));
Mblank=repmat(ch1B', size(dataML,1),1);
diff=Msam-Mblank;
%Identify identical m/z:
[rowsamA,colA]=find(diff >= -0.0005 & diff <= 0.0005);
%Normalizing common peaks to remove blank
%A modified solvent subtraction method was implemented to remove
%solvent contamination peaks without removing real sample peaks.
%Common peaks observed between the sample peak list and the solvent
%peak list were compiled and normalized to the smallest solvent peak
%magnitude. The normalized solvent peaks magnitudes were subtracted
%from the normalized sample peak magnitudes yielding solvent free sample peak magnitudes.

PintMLcom = PintML(rowsamA); % intensity of the common sample peaks
[MinPintMLcom,RowMinIntMLcom] = min(PintMLcom); % minimum intensity of common sample peak
PintBcom = PintB(colA); % intensity of the common blank peaks
MinPintBcom =  PintBcom(RowMinIntMLcom); % intensity of the blank peak corresponding to
the smallest intensity of common peak in mass list

NormalizedBlankInt = PintBcom./MinPintBcom.*MinPintMLcom; % normalization of common peak
int to samllest common peak int in blank and sample
Subtracted = PintMLcom - NormalizedBlankInt;
[rowsamB,colB]= find((Subtracted./MinPintMLcom)>3); % finds NON-BLANK peaks (good)
PintML(rowsamA(rowsamB)) = Subtracted(rowsamB); % relpaces the old intensities of the
(NON-BLANK) with the normalized intensities

[rowsamblank,colC]=find((Subtracted./MinPintMLcom)<=3); % finds BLANK peaks (bad)

rowsamC = rowsamA(rowsamblank);

%formating output file
dataML1=[dataML zeros(size(dataML,1),4)];
%convert dataout from matrix to cell array:
dataout=num2cell(dataML1);
%Save blank peaks in output file
dataout(rowsamC,3)={'Blank'};
dataout(rowsamC,[4:5])=num2cell(dataB(colC,[1:2]));
```

Find salt peaks

```
%calculate mass defect of sample m/z
Massdef=ch1ML-fix(ch1ML);
[rowS1,colS1]=find(ch1ML<400 & Massdef>=0.4 & Massdef<=0.98);
[rowS2,colS2]=find(ch1ML>=400 &ch1ML<800 & Massdef>=0.6 & Massdef<=0.97);
rowS =[rowS1; rowS2];
%Save salt peaks in output file
dataout(rowS,3)={'Salt'};
```

Identify isotopic peaks

```
%identify all the 12C 13C by mass:
%1.0034-0.0008>=mass13C-mass12C>=1.0034+0.0008
M13C=repmat(ch1ML,1,size(ch1ML,1));
M12C=repmat(ch1ML', size(ch1ML,1),1);
isodiff=tril(M13C-M12C); % tril for delete all the upper value to the main diagonal of
the matrix
diffdiff=abs(1.0034-isodiff);
[valmin, rowmin]=min(diffdiff,[],1);
[rowi,col12C]=find(valmin<=0.0008 & rowmin>[1:length(rowmin)]);
row13Ctot=rowmin(col12C);
uniq=~ismember(row13Ctot,col12C);
row13C=row13Ctot(uniq);
col12C=col12C(uniq);
%Identify the C isotope by the intensity: int13C<=0.5*int12C
[i13C, coli]=find(PintML(row13C)<=0.5*PintML(col12C) & ch1ML(row13C)>ch1ML(col12C)&
PintML(row13C)./PintML(col12C)<1);
iso12C=col12C(i13C);
iso13C=row13C(i13C);
%Estimated carbon number for mass with 13C isotopologue identify
Cnr=PintML(iso13C)./PintML(iso12C);
for x=1:length(iso12C);
dataout(iso12C(x),6)={Cnr(x)*100};
end

%Save 13C peaks in output file
dataout(iso13C,3)={'13C'};
```

Statistics

```
% Total number of peaks between 200-1000m/z:
totp=find(ch1ML>=200 & ch1ML<=1000);
totpeak=size(totp,1);
% Total absolute intensity of the peaks between 200-1000m/z:
totint=sum(PintML(totp));
% Total % intensity of the peaks between 200-1000m/z:
percint=totint/totint*100;

% Number of Blank peaks identify in the sample:
nrbl=size(rowsamC,1);
% Total absolute intensity of blank peaks identify in the sample:
totintbl=sum(PintML(rowsamC));
% Total % intensity of blank peaks in the sample:
percintbl=totintbl/totint*100;

% Number of salt peaks identify in the sample:
nrst=size(rowS,1);
% Total absolute intensity of salt peaks identify in the sample:
totintst=sum(PintML(rowS));
% Total % intensity of salt peaks in the sample:
percintst=totintst/totint*100;
```

```
% Number of 13C peaks identify in the sample:
nriso=size(iso13C,2);
% Total absolute intensity of salt peaks identify in the sample:
totintiso=sum(PintML(iso13C));
% Total % intensity of salt peaks in the sample:
percintiso=totintiso/totint*100;

stat=[totpeak,totint,percint;nrbl,totintbl,percintbl;nrst,totintst,percintst;nriso,totint
iso,percintiso];
```

Finding the good peaks (added by wassim)

```
rowgood = [rowsamC; rowS1; rowS2; iso13C'];
I = ~ismember(1:size(ch1ML,1), rowgood);
DataG = [ ch1ML(I) PintML(I) ];
```

Save to xls file

```
title={'m/z', 'Intensity', 'Blank/salt/13C', 'bank mass', 'bank int','Estim C#'};
xlswrite([fname(1:end-4) '_labels'], title, 1, 'A1');
xlswrite([fname(1:end-4) '_labels'], dataout, 1, 'A2');
title2={'nr of peaks nr', 'abs intensity', '% total int'};
xlswrite([fname(1:end-4) '_labels'], title2, 1, 'I1');
xlswrite([fname(1:end-4) '_labels'], {'Total peaks(200-1000m/z)'}, 1, 'H2');
xlswrite([fname(1:end-4) '_labels'], {'Total blank peaks'}, 1, 'H3');
xlswrite([fname(1:end-4) '_labels'], {'Total salt peaks'}, 1, 'H4');
xlswrite([fname(1:end-4) '_labels'], {'Total 13C peaks'}, 1, 'H5');
xlswrite([fname(1:end-4) '_labels'], stat, 1, 'I2');
% added by wassim
xlswrite([fname(1:end-4) '_labels'], title(1:2), 2, 'A1');
xlswrite([fname(1:end-4) '_labels'], DataG , 2, 'A2');
fileID = fopen([fname(1:end-4) '_labels.txt'], 'w');
fprintf(fileID, '%.5f %.0f\r\n', DataG');
fclose(fileID);

%DataG = load(fname);  %load DataG file
%index=DataG(:,1);  %index indication consecutive peak m/z
ch1 = DataG(:,1);     %m/z peak
int = DataG(:,2);      %Intensity

% compute exact mass:
m12c = 12.000000000;
m1h = 1.007825032;
m14n = 14.003074007;
m16o = 15.994914622;
m32s = 31.9720707;
m23na = 22.9897697;
m31p = 30.9737615;
```

```
m35cl = 34.96885271;
melectron = 0.0005485799094622;

totint = sum(DataG(:,2));

% Define series cases (sc) of CnH2n-zOoNnSs (z,o,n,s)
%defining intervals for each variable
hm1nr = 5:100;
nnr = 0:10;
onr = 1:30;
snr = 0:10;
%nanr = 0:1;
pnr = 0:1;
%clnr = 0:1;
minc = 5;
ccalc = max(hm1nr)*m1h + max(nnr)*m14n + max(onr)*m16o +  max(snr)*m32s + max(pnr)*m31p;
% for minimum carbon calculation
%find the different cases:
r = size(ch1,1);
w = cell(r,1);


formc = combvec(minc,hm1nr,nnr,onr,snr,pnr);
% select formulas with integer DBE (CHNOS) S valency 2
% edit for different molecules
DBE = formc(1,:) - (formc(2,:)+1)./2 + formc(3,:)./2 + formc(6,:)./2 + 1;
locDBE = find(floor(DBE) == DBE & DBE>=0);
formca = formc(:,locDBE);
%formc(:,5)*m23na / formc(:,5)*m31p / formc(:,5)*m35cl
% create a matrix of the same size of DataG containing all the different
% combinations
exactm =
formca(1,:)*m12c+formca(2,:)*m1h+formca(3,:)*m14n+formca(4,:)*m16o+formca(5,:)*m32s+
formca(6,:)*m31p+melectron;
%add eventually nanr / clnr

for i = 1:r;
    maxc = floor(ch1(i)/m12c);
    ccalc2 = floor((ch1(i) - ccalc)/m12c);
    if ccalc2 <= minc;
        if maxc <= max(formca(1,:)) || maxc <= minc ;




        else
            minca = max(formca(1,:));
            formcb = combvec(minca + 1:maxc,hm1nr,nnr,onr,snr,pnr);

            % select formulas with integer DBE (CHNOS) S valency 2
            % edit for different molecules
            DBE2 = formcb(1,:) - (formcb(2,:)+1)./2 + formcb(3,:)./2 + formcb(6,:)./2 +
1;
```

```
            locDBE2 = find(floor(DBE2) == DBE2 & DBE2>=0);
            formcb2 = formcb(:,locDBE2);

            %formc(:,5)*m23na / formc(:,5)*m31p / formc(:,5)*m35cl
            % create a matrix of the same size of data containing all the different
            % combinations

            exactmb =
formcb2(1,:)*m12c+formcb2(2,:)*m1h+formcb2(3,:)*m14n+formcb2(4,:)*m16o+formcb2(5,:)*m32s+
formcb2(6,:)*m31p+melectron;

            %add eventually nanr / clnr
            formca = [formca formcb2];
            exactm = [exactm exactmb];
        end

    else
        minc2 = ccalc2;

        cminind = formca(1,:)>= minc2;

        formca = formca(:,cminind);
        exactm = exactm(:,cminind);

        if maxc <= max(formca(1,:)) || maxc <= minc ;




        else
            minca = max(formca(1,:));
            formcb = combvec(minca + 1:maxc,hm1nr,nnr,onr,snr,pnr);

            % select formulas with integer DBE (CHNOS) S valency 2
            % edit for different molecules
            DBE2 = formcb(1,:) - (formcb(2,:)+1)./2 + formcb(3,:)./2 + formcb(6,:)./2 +
1;
            locDBE2 = find(floor(DBE2) == DBE2 & DBE2>=0);
            formcb2 = formcb(:,locDBE2);

            %formc(:,5)*m23na / formc(:,5)*m31p / formc(:,5)*m35cl
            % create a matrix of the same size of data containing all the different
            % combinations

            exactmb =
formcb2(1,:)*m12c+formcb2(2,:)*m1h+formcb2(3,:)*m14n+formcb2(4,:)*m16o+formcb2(5,:)*m32s+
formcb2(6,:)*m31p+melectron;

            %add eventually nanr / clnr
            formca = [formca formcb2];
            exactm = [exactm exactmb];
        end
```

```
    end

    diff = ch1(i)-exactm;
    error =(diff./exactm)*10^6;
    %Identify identical m/z:

    colsam = find(error >= -1 & error <= 1);
    A = repmat(size(colsam,2),1,size(colsam,2))'; % A is number of possibilities

    B = repmat(ch1(i),1,size(colsam,2))'; % B is m/z from instrument

    C = repmat(int(i),1,size(colsam,2))'; % C is Peak area

    D = formca(:,colsam)'; % D identifies correct formulas

    E = exactm(colsam)'; % E is exact mass of each formula

    F = error(colsam)'; % F is error on each formula
    w{i,1} = [ A B C D E F ];




    % Select exact mass that fit into the mass spectrum range -180-1500 m/z
    %minch1 = min(ch1(i))-1;
    %maxch1 = max(ch1(i))+1;
    %locmsrange = find(exactm>=minch1 & exactm<=maxch1);
    %formc3 = formc2(:,locmsrange);
    %exactm2 = exactm(locmsrange);



end


% not assigned masses
emptycell = cellfun('isempty',w);
notass = ch1(emptycell);

wmat = cell2mat(w);
wmat = [wmat(:,1:5) (wmat(:,5)+1) wmat(:,6:end)];

% Formula rules

C = wmat(:,4);
Hm1 = wmat(:,5);
H = wmat(:,6);
N = wmat(:,7);
```

```
O = wmat(:,8);
S = wmat(:,9);
P = wmat(:,10);

    % Nitrogen rule
    %nominalm = round(wmat(:,2));
    %Nruleind =
(((mod(nominalm,2)==0)&(mod(N,2)==0))|((mod(nominalm,2)~=0)&(mod(N,2)~=0)));

    % Define cases
    szCompounds = size(wmat);
    nCases      = 13;
    bad         = zeros([szCompounds(1),nCases]);

    bad(:,1) = O./C >= 1.2;
    bad(:,2) = (H)./C >= 2.25;
    bad(:,3) = (H)./C <=.3;
    bad(:,4) = Hm1 > ((2.*C)+ 2);
    bad(:,5) = N./O >1;  % does not work for amino acids arginine, lycine, and histadine
    bad(:,6) = N./C >= 0.5;
    bad(:,7) = O > (C+2);
    bad(:,8) = S./C >= 0.2;
    bad(:,9) = (S+P)./C > 0.2;
    bad(:,10) = P./C >= 0.1;
    bad(:,11) = O < 4.*P;
    bad(:,12) = (N + 4.*P + 4.*S) > O;  %assuming all phosphorous is phosphate, all
sulphur is sulphate (from HPLC analysis) and nitrogen is in protein/nitrate
     %bad(:,12) = Nruleind;

    databad = wmat(any(bad')',:);
    datagood = wmat(~any(bad')',:);

zztop = size(datagood,1);
y = cell(zztop,1);
for j = 1:zztop;

%Identify identical m/z:

    U = find(datagood(:,2)== datagood(j,2));
    R = size(U,1);
    y{j,1} = [ R ];
end
ymat = cell2mat(y);
% Output 1 Identified formulas
title=;

if ~isempty(wmat)
    xlswrite([fname(1:end-4) '_out'], title, 1, 'A1');
    xlswrite([fname(1:end-4) '_out'], wmat, 1, 'A2');
else
    disp('No identified formulas')
end
```

```
% Output 2 Non Identified
if ~isempty(notass)
    xlswrite([fname(1:end-4) '_notass'], notass, 1, 'A2');
else
    disp('No non identified peaks')
end

% Output 3 Identified formulas after reducing
if ~isempty(datagood)
    title={'m/z', 'Intensity', 'C', 'H-1', 'H', 'N', 'O', 'S','P', 'exact mass',
'error','possibilities'};
    xlswrite([fname(1:end-4) '_out_reduced'], title, 1, 'A1');
    xlswrite([fname(1:end-4) '_out_reduced'], [datagood(:,2:end) ymat], 1, 'A2');
else
    disp('No identified formulas after reducing')
end
% Output 4 Identified eliminated formulas after reducing
if ~isempty(databad)
    title={'m/z', 'Intensity', 'C', 'H-1', 'H', 'N', 'O', 'S','P', 'exact mass',
'error'};
    xlswrite([fname(1:end-4) '_out_elim'], title, 1, 'A1');
    xlswrite([fname(1:end-4) '_out_elim'], databad(:,2:end), 1, 'A2');
else
    disp('No eliminated formulas after reducing')
end

toc



% Series
datagood2 = [datagood(:,2:end) ymat];

ch1=datagood2(:,1);    %m/z peak
c=datagood2(:,3);      %carbon
hm1=datagood2(:,4);    %hydrogen minus 1
h=datagood2(:,5);      % hydrogen
n=datagood2(:,6);      %nitrogen
o=datagood2(:,7);      %oxygen
s=datagood2(:,8);      %sulfur
p=datagood2(:,9);     %phosporus
posib=datagood(:,11); %# of possibilities

%na=DataG(:,11);     %Sodium Na
%ch2=DataG(:,12);   %m/z individual compound, Exact mass
%stdev2=DataG(:,13);%Error(ppm)
%hp1=DataG(:,8);      %h+1
%NM=DataG(:,15)       %nominal mass
%KMD=DataG(:,16)      %kendrick mass diffect
%osurc=DataG(:,17)    %O/C ratio
%hsurc=DataG(:,9);    %H/C ratio
%dbe=DataG(:,10);      %DBE
%nsurc=DataG(:,20)    %N/C ratio
```

```
%ssurc=DataG(:,21)    %S/C ratio


%hp1= h + 1;                  %H+1
%ch2KM= ch2.*(14/14.01565);   %Kendrick mass for CH2
%NM= fix(ch2KM);              %Nominal mass of the Kendrick mass
%KMD=ch2KM-NM;                %Kendrick mass defect

%osurc= o./c;                 %O/C ratio
%hsurc= hp1./c;               %H/C ratio
%dbe= (2.*c + 2 - (h+1) + n + p)./2;%double bonds equivalent
%nsurc= n./c;                 %N/C ratio
%ssurc= s./c;                 %S/C ratio
%psurc= p./c;                 %P/C ratio

%DataG = [DataG hp1 NM KMD osurc hsurc dbe nsurc ssurc];
%DataG(isnan(DataG)) = 0; % convert NaN into 0


% Define cases CHONS
szCompounds = size(datagood2);
nCases      = 6;
bad2thebone         = zeros([szCompounds(1),nCases]);

bad2thebone(:,1) = c == 0;
bad2thebone(:,2) = h == 0;
bad2thebone(:,3) = o == 0;
bad2thebone(:,4) = n == 0;
bad2thebone(:,5) = s == 0;
bad2thebone(:,6) = p ~= 0;
databad1=datagood2(any(bad2thebone')',:);
data1=datagood2(~any(bad2thebone')',:);
L{1,1} = 'CHONS';
therock1 = repmat(L,size(data1,1),1);

% Define cases CHON
szCompounds = size(datagood2);
nCases      = 6;
bad2thebone         = zeros([szCompounds(1),nCases]);

bad2thebone(:,1) = c == 0;
bad2thebone(:,2) = h == 0;
bad2thebone(:,3) = o == 0;
bad2thebone(:,4) = n == 0;
bad2thebone(:,5) = s ~= 0;
bad2thebone(:,6) = p ~= 0;
databad2=datagood2(any(bad2thebone')',:);
data2=datagood2(~any(bad2thebone')',:);
L{1,1} = 'CHON';
therock2 = repmat(L,size(data2,1),1);

% Define cases CHOS
szCompounds = size(datagood2);
```

```
nCases      = 6;
bad2thebone         = zeros([szCompounds(1),nCases]);

bad2thebone(:,1) = c == 0;
bad2thebone(:,2) = h == 0;
bad2thebone(:,3) = o == 0;
bad2thebone(:,4) = n ~= 0;
bad2thebone(:,5) = s == 0;
bad2thebone(:,6) = p ~= 0;
databad3=datagood2(any(bad2thebone')',:);
data3=datagood2(~any(bad2thebone')',:);
L{1,1} = 'CHOS';
therock3 = repmat(L,size(data3,1),1);

% Define cases CHNS
szCompounds = size(datagood2);
nCases      = 6;
bad2thebone         = zeros([szCompounds(1),nCases]);

bad2thebone(:,1) = c == 0;
bad2thebone(:,2) = h == 0;
bad2thebone(:,3) = o ~= 0;
bad2thebone(:,4) = n == 0;
bad2thebone(:,5) = s == 0;
bad2thebone(:,6) = p ~= 0;
databad4=datagood2(any(bad2thebone')',:);
data4=datagood2(~any(bad2thebone')',:);
L{1,1} = 'CHNS';
therock4 = repmat(L,size(data4,1),1);

% Define cases CHO
szCompounds = size(datagood2);
nCases      = 6;
bad2thebone         = zeros([szCompounds(1),nCases]);

bad2thebone(:,1) = c == 0;
bad2thebone(:,2) = h == 0;
bad2thebone(:,3) = o == 0;
bad2thebone(:,4) = n ~= 0;
bad2thebone(:,5) = s ~= 0;
bad2thebone(:,6) = p ~= 0;
databad5=datagood2(any(bad2thebone')',:);
data5=datagood2(~any(bad2thebone')',:);
L{1,1} = 'CHO1';
therock5 = repmat(L,size(data5,1),1);

% Define cases CHN
szCompounds = size(datagood2);
nCases      = 6;
bad2thebone         = zeros([szCompounds(1),nCases]);

bad2thebone(:,1) = c == 0;
bad2thebone(:,2) = h == 0;
```

```
bad2thebone(:,3) = o ~= 0;
bad2thebone(:,4) = n == 0;
bad2thebone(:,5) = s ~= 0;
bad2thebone(:,6) = p ~= 0;
databad6=datagood2(any(bad2thebone')',:);
data6=datagood2(~any(bad2thebone')',:);
L{1,1} = 'CHN';
therock6 = repmat(L,size(data6,1),1);

% Define cases CHS
szCompounds = size(datagood2);
nCases      = 6;
bad2thebone         = zeros([szCompounds(1),nCases]);

bad2thebone(:,1) = c == 0;
bad2thebone(:,2) = h == 0;
bad2thebone(:,3) = o ~= 0;
bad2thebone(:,4) = n ~= 0;
bad2thebone(:,5) = s == 0;
bad2thebone(:,6) = p ~= 0;
databad7=datagood2(any(bad2thebone')',:);
data7=datagood2(~any(bad2thebone')',:);
L{1,1} = 'CHS';
therock7 = repmat(L,size(data7,1),1);

% Define cases CH
szCompounds = size(datagood2);
nCases      = 6;
bad2thebone         = zeros([szCompounds(1),nCases]);

bad2thebone(:,1) = c == 0;
bad2thebone(:,2) = h == 0;
bad2thebone(:,3) = o ~= 0;
bad2thebone(:,4) = n ~= 0;
bad2thebone(:,5) = s ~= 0;
bad2thebone(:,6) = p ~= 0;
databad8=datagood2(any(bad2thebone')',:);
data8=datagood2(~any(bad2thebone')',:);
L{1,1} = 'CH';
therock8 = repmat(L,size(data8,1),1);

% Define cases CHONSP
szCompounds = size(datagood2);
nCases      = 6;
bad2thebone         = zeros([szCompounds(1),nCases]);

bad2thebone(:,1) = c == 0;
bad2thebone(:,2) = h == 0;
bad2thebone(:,3) = o == 0;
bad2thebone(:,4) = n == 0;
bad2thebone(:,5) = s == 0;
bad2thebone(:,6) = p == 0;
databad9=datagood2(any(bad2thebone')',:);
```

```
data9=datagood2(~any(bad2thebone')',:);
L{1,1} = 'CHONSP';
therock9 = repmat(L,size(data9,1),1);

% Define cases CHONP
szCompounds = size(datagood2);
nCases      = 6;
bad2thebone         = zeros([szCompounds(1),nCases]);

bad2thebone(:,1) = c == 0;
bad2thebone(:,2) = h == 0;
bad2thebone(:,3) = o == 0;
bad2thebone(:,4) = n == 0;
bad2thebone(:,5) = s ~= 0;
bad2thebone(:,6) = p == 0;
databad10=datagood2(any(bad2thebone')',:);
data10=datagood2(~any(bad2thebone')',:);
L{1,1} = 'CHONP';
therock10 = repmat(L,size(data10,1),1);

% Define cases CHOSP
szCompounds = size(datagood2);
nCases      = 6;
bad2thebone         = zeros([szCompounds(1),nCases]);

bad2thebone(:,1) = c == 0;
bad2thebone(:,2) = h == 0;
bad2thebone(:,3) = o == 0;
bad2thebone(:,4) = n ~= 0;
bad2thebone(:,5) = s == 0;
bad2thebone(:,6) = p == 0;
databad11=datagood2(any(bad2thebone')',:);
data11=datagood2(~any(bad2thebone')',:);
L{1,1} = 'CHOSP';
therock11 = repmat(L,size(data11,1),1);

% Define cases CHOP
szCompounds = size(datagood2);
nCases      = 6;
bad2thebone         = zeros([szCompounds(1),nCases]);

bad2thebone(:,1) = c == 0;
bad2thebone(:,2) = h == 0;
bad2thebone(:,3) = o == 0;
bad2thebone(:,4) = n ~= 0;
bad2thebone(:,5) = s ~= 0;
bad2thebone(:,6) = p == 0;
databad12=datagood2(any(bad2thebone')',:);
data12=datagood2(~any(bad2thebone')',:);
L{1,1} = 'CHOP';
therock12 = repmat(L,size(data12,1),1);
```

Formation of the final XLS files

```
title={'Type', 'm/z', 'PeakInt', 'C', 'H-1', 'H', 'N', 'O', 'S', 'P','exact
mass','error','possibilities'};

if ~isempty(data1)
xlswrite([fname(1:end-4) '_reduced_sorted'], data1, 'CHONS', 'B2');
xlswrite([fname(1:end-4) '_reduced_sorted'], title, 'CHONS', 'A1');
xlswrite([fname(1:end-4) '_reduced_sorted'], therock1, 'CHONS', 'A2');
xlswrite([fname(1:end-4) '_reduced_sorted'], size(data1,1), 'CHONS', 'M1');
else
end
if ~isempty(data2)
xlswrite([fname(1:end-4) '_reduced_sorted'], data2, 'CHON', 'B2');
xlswrite([fname(1:end-4) '_reduced_sorted'], title, 'CHON', 'A1');
xlswrite([fname(1:end-4) '_reduced_sorted'], therock2, 'CHON', 'A2');
xlswrite([fname(1:end-4) '_reduced_sorted'], size(data2,1), 'CHON', 'M1');
else
end
if ~isempty(data3)
xlswrite([fname(1:end-4) '_reduced_sorted'], data3, 'CHOS', 'B2');
xlswrite([fname(1:end-4) '_reduced_sorted'], title, 'CHOS', 'A1');
xlswrite([fname(1:end-4) '_reduced_sorted'], therock3, 'CHOS', 'A2');
xlswrite([fname(1:end-4) '_reduced_sorted'], size(data3,1), 'CHOS', 'M1');
else
end
if ~isempty(data4)
xlswrite([fname(1:end-4) '_reduced_sorted'], data4, 'CHNS', 'B2');
xlswrite([fname(1:end-4) '_reduced_sorted'], title, 'CHNS', 'A1');
xlswrite([fname(1:end-4) '_reduced_sorted'], therock4, 'CHNS', 'A2');
xlswrite([fname(1:end-4) '_reduced_sorted'], size(data4,1), 'CHNS', 'M1');
else
end
if ~isempty(data5)
xlswrite([fname(1:end-4) '_reduced_sorted'], data5, 'CHO', 'B2');
xlswrite([fname(1:end-4) '_reduced_sorted'], title, 'CHO', 'A1');
xlswrite([fname(1:end-4) '_reduced_sorted'], therock5, 'CHO', 'A2');
xlswrite([fname(1:end-4) '_reduced_sorted'], size(data5,1), 'CHO', 'M1');
else
end
if ~isempty(data6)
xlswrite([fname(1:end-4) '_reduced_sorted'], data6, 'CHN', 'B2');
xlswrite([fname(1:end-4) '_reduced_sorted'], title, 'CHN', 'A1');
xlswrite([fname(1:end-4) '_reduced_sorted'], therock6, 'CHN', 'A2');
xlswrite([fname(1:end-4) '_reduced_sorted'], size(data6,1), 'CHN', 'M1');
else
end
if ~isempty(data7)
xlswrite([fname(1:end-4) '_reduced_sorted'], data7, 'CHS', 'B2');
xlswrite([fname(1:end-4) '_reduced_sorted'], title, 'CHS', 'A1');
xlswrite([fname(1:end-4) '_reduced_sorted'], therock7, 'CHS', 'A2');
xlswrite([fname(1:end-4) '_reduced_sorted'], size(data7,1), 'CHS', 'M1');
else
end
if ~isempty(data8)
```

```
xlswrite([fname(1:end-4) '_reduced_sorted'], data8, 'CH', 'B2');
xlswrite([fname(1:end-4) '_reduced_sorted'], title, 'CH', 'A1');
xlswrite([fname(1:end-4) '_reduced_sorted'], therock8, 'CH', 'A2');
xlswrite([fname(1:end-4) '_reduced_sorted'], size(data8,1), 'CH', 'M1');
else
end
if ~isempty(data9)
xlswrite([fname(1:end-4) '_reduced_sorted'], data9, 'CHONSP', 'B2');
xlswrite([fname(1:end-4) '_reduced_sorted'], title, 'CHONSP', 'A1');
xlswrite([fname(1:end-4) '_reduced_sorted'], therock9, 'CHONSP', 'A2');
xlswrite([fname(1:end-4) '_reduced_sorted'], size(data9,1), 'CHONSP', 'M1');
else
end
if ~isempty(data10)
xlswrite([fname(1:end-4) '_reduced_sorted'], data10, 'CHONP', 'B2');
xlswrite([fname(1:end-4) '_reduced_sorted'], title, 'CHONP', 'A1');
xlswrite([fname(1:end-4) '_reduced_sorted'], therock10, 'CHONP', 'A2');
xlswrite([fname(1:end-4) '_reduced_sorted'], size(data10,1), 'CHONP', 'M1');
else
end
if ~isempty(data11)
xlswrite([fname(1:end-4) '_reduced_sorted'], data11, 'CHOSP', 'B2');
xlswrite([fname(1:end-4) '_reduced_sorted'], title, 'CHOSP', 'A1');
xlswrite([fname(1:end-4) '_reduced_sorted'], therock11, 'CHOSP', 'A2');
xlswrite([fname(1:end-4) '_reduced_sorted'], size(data11,1), 'CHOSP', 'M1');
else
end
if ~isempty(data12)
xlswrite([fname(1:end-4) '_reduced_sorted'], data12, 'CHOP', 'B2');
xlswrite([fname(1:end-4) '_reduced_sorted'], title, 'CHOP', 'A1');
xlswrite([fname(1:end-4) '_reduced_sorted'], therock12, 'CHOP', 'A2');
xlswrite([fname(1:end-4) '_reduced_sorted'], size(data12,1), 'CHOP', 'M1');
else
end

datall = [data1;data2;data3;data4;data5;data6;data7;data8;data9;data10;data11;data12];
steveaustin =
[therock1;therock2;therock3;therock4;therock5;therock6;therock7;therock8;therock9;therock
10;therock11;therock12];
xlswrite([fname(1:end-4) '_reduced_sorted'], datall, 'All', 'B2');
xlswrite([fname(1:end-4) '_reduced_sorted'], title, 'All', 'A1');
xlswrite([fname(1:end-4) '_reduced_sorted'], steveaustin, 'All', 'A2');

% write the statistics sheet

%title2={'Type', 'm/z', 'PeakInt', 'RelPeakInt', 'C', 'H-1', 'H', 'N', 'O', 'S', 'P',
'exact mass', 'error', 'possibilities', 'O/C', 'H/C', 'DBE', 'DBE/C', 'AImod', 'O/Cw',
'H/Cw', 'DBEw', 'DBE/Cw', 'm/zw', 'C#w'};

%inttot = sum(datall(:,3));
%intrel = datall(:,3)./inttot;
%OtoC = datall(:,7)./datall(:,4);
%HtoC = datall(:,5)
```

```
toc
```

```
end
```

Published with MATLAB® R2014a

APPENDIX A

ENERGY RETURN ON INVESTMENT

I made a few assumptions in the calculations to be consistent with industrial operations: 1) the HP operation is up scaled; 2) the algae-to-water ratio is increased ; and 4) the reactor is well insulated. (Xu et al., 2011)

Preliminary Material Balance
Material Balance (wt basis): Input 5 kg Dry Algae/Algaenan
Water: Algae = 4:1

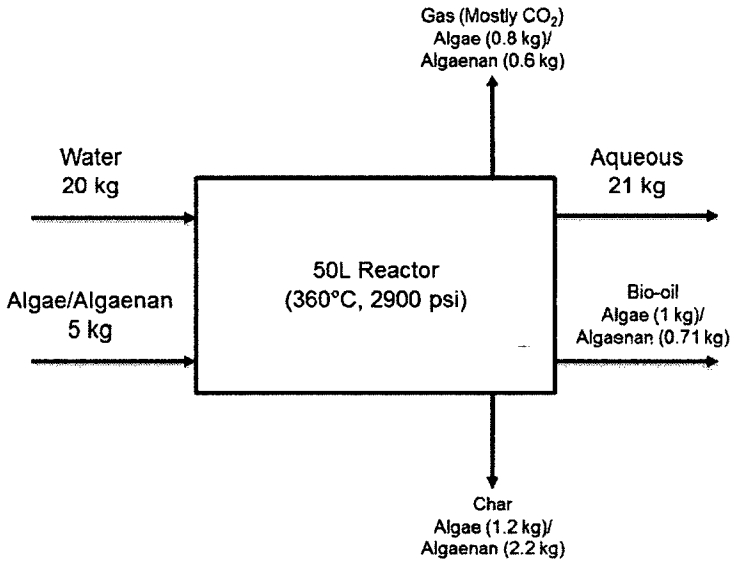

Energy Balance:

All energy values are for Sensible Heat

Water Enthalpy at 360°C, 2900 psi : 1.78 kJ/kg
Heat capacity of Bio-oil is ~1.8 kJ /(kg·K)
Enthalpy of CO_2 is 0.54 MJ/kg at 360°C
Char heat capacity 0.001MJ/ (kg·K)

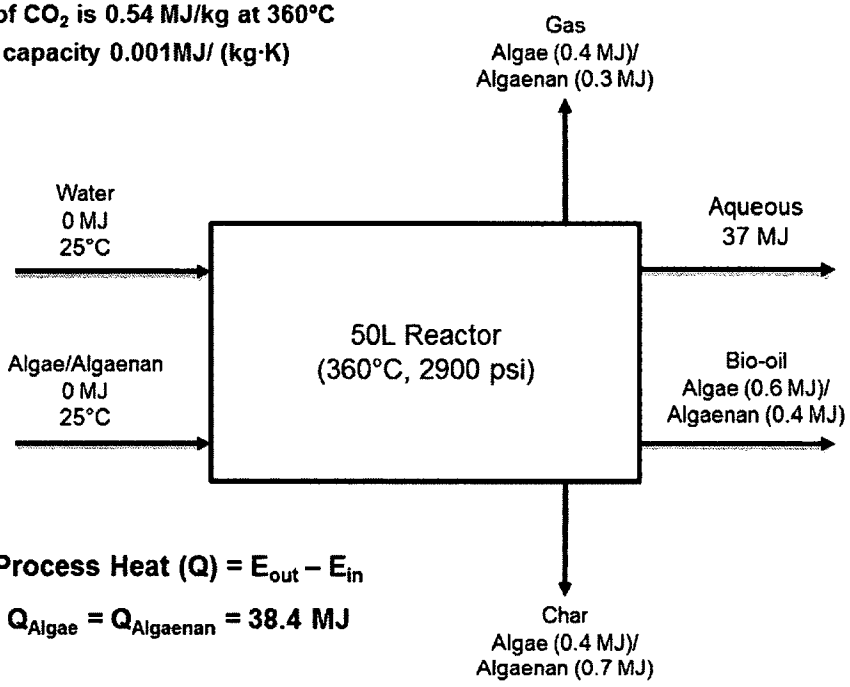

Process Heat (Q) = $E_{out} - E_{in}$

$Q_{Algae} = Q_{Algaenan} = 38.4$ MJ

Fossil Energy Ratio (FER)

The performance indicators considered here is the overall energy balance with fossil energy ratio (FER) i.e ratio of higher heating value (HHV) of bio-oil to the process energy required

$$FER = \frac{HHV_{biofuel}}{E_{input}} \left[\frac{GJ\ products}{GJ\ fossil\ enery\ input}\right]$$

Heating Value of Algae-oil: 37 MJ/kg
Heating Value of Algaenan-oil: 41 MJ/kg
Process heat (Q) = 38.4 MJ

Process	FER(Algae)	FER(Algaenan)
No Waste heat recovery	0.96	1.07
25% Waste Heat Recovery	1.28	1.42
50% Waste Heat Recovery	1.92	2.14
75% Waste Heat Recovery	3.85	4.27

VITA

WASSIM ADEL OBEID

Department of Chemistry and Biochemistry

Old Dominion University

Norfolk, VA 23529

EDUCATION

Jan. 2009 – Mar. 2015	Old Dominion University (ODU), Norfolk VA, USA Doctorate of philosophy in Chemistry
Sept. 2004 – Jul. 2008	American University of Beirut (AUB), Beirut, Lebanon Bachelor of Sciences Degree in Chemistry

SELECTED PUBLICATIONS

Obeid, W.; Salmon, E.; Lewan, M.D.; Hatcher, P.G.; "Hydrous pyrolysis of Scenedesmus algae and algaenan-like residue." *Organic Geochemistry,* 2015.

Obeid, W.; Salmon, E.; Hatcher, P.G. "The effect of different isolation procedures on algaenan molecular structure in Scenedesmus green algae." *Organic Geochemistry,* Volume 76, November 2014.

Kumar, S.; Hablot, E.; Garcia, L. J.; Obeid, W.; Hatcher, P. G.; DuQuette, B. M.; Graiver, D.; Narayan, R.; Balan, V. "Polyurethanes preparation using proteins obtained from microalgae." *Journal of Materials Science,* 2014.

Levine, R. B.; Sierra, C. O.; Hockstad, R.; Obeid, W.; Hatcher, P. G.; Savage, P. E. "The use of hydrothermal carbonization to recycle nutrients in algal biofuel production." *Environmental Progress and Sustainable Energy,* Volume 32, Issue 4, December 2013.

Obeid, W., Hatcher, P.G. "Conversion of brown coal to hydrocarbon based oil by hydrothermal liquefaction at subcritical conditions." Proceedings to the 13th International Conference on Coal Science & Technology, October 2013.

Garcia, L. J.; Obeid, W.; Kumar, S.; Hatcher, P.G. "Flash Hydrolysis of Microalgae (*Scenedesmus sp.*) for Protein Extraction and Production of Biofuels Intermediates." *Journal of supercritical fluid,* Volume 82, October 2013.

AWARDS

Spring 2012	Outstanding Chemistry Teacher Assistant of the Year
Fall 2009 – Spring 2011	Dominion Scholar Fellowship